JYU DISSERTATIONS 693

Vasco Fachada

Intramyocellular Lipid Metabolism in Health, Diet and Exercise

A Focus on Lipid Droplets and the Perilipin Protein Family

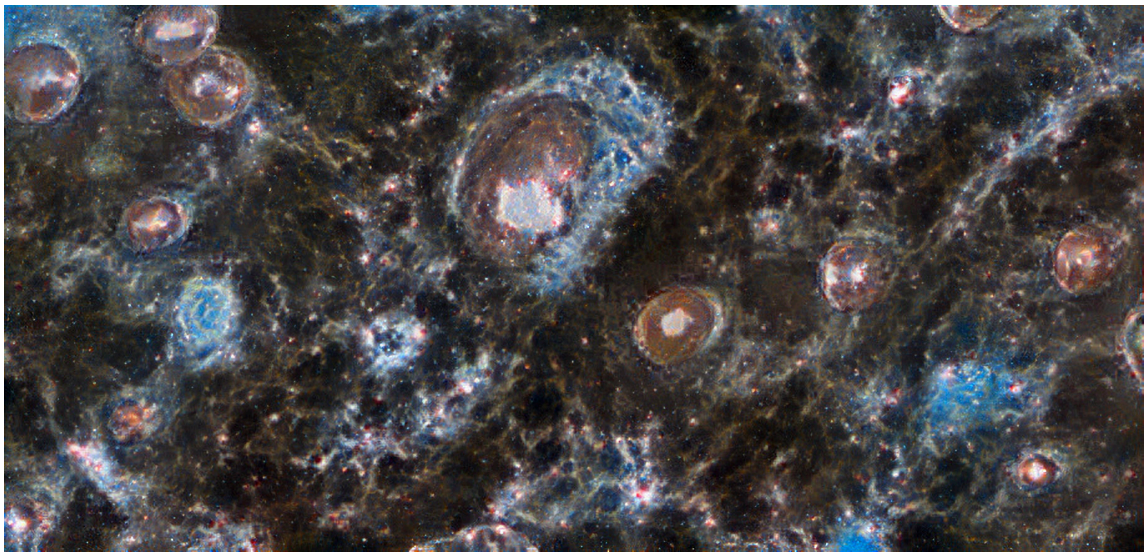

UNIVERSITY OF JYVÄSKYLÄ
FACULTY OF SPORT AND
HEALTH SCIENCES

JYU DISSERTATIONS 693

Vasco Fachada

Intramyocellular Lipid Metabolism in Health, Diet and Exercise

A Focus on Lipid Droplets and the Perilipin Protein Family

Esitetään Jyväskylän yliopiston liikuntatieteellisen tiedekunnan suostumuksella
julkisesti tarkastettavaksi yliopiston Liikunta-rakennuksen auditoriossa L304
lokakuun 13. päivänä 2023 kello 11.45.

Academic dissertation to be publicly discussed, by permission of
the Faculty of Sport and Health Sciences of the University of Jyväskylä,
in building Liikunta, auditorium L304, on October 13, 2023, at 11.45 a.m.

JYVÄSKYLÄN YLIOPISTO
UNIVERSITY OF JYVÄSKYLÄ

JYVÄSKYLÄ 2023

Editors
Simon Walker
Faculty of Sport and Health Sciences, University of Jyväskylä
Timo Hautala
Open Science Centre, University of Jyväskylä

Cover: An AI generation from the images in page 3.

ISBN 978-951-39-9733-5 (PDF)
URN:ISBN:978-951-39-9733-5
ISSN 2489-9003

Permanent link to this publication: http://urn.fi/URN:ISBN:978-951-39-9733-5

Chaos is just Order yet to be deciphered.

José Saramago

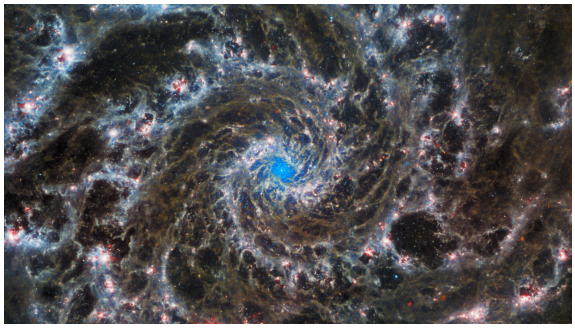

Phantom Galaxy
James Webb Telescope
NASA, ESA, CSA

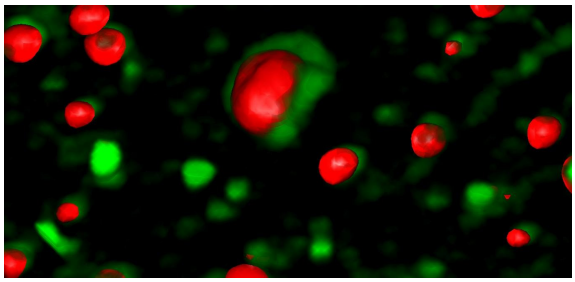

Lipid droplets (red) & perilipin 5 (green)
Olympus FV1000 microscope
Vasco Fachada

ABSTRACT

Fachada, Vasco
Intramyocellular Lipid Metabolism in Health, Diet and Exercise: A Focus on Lipid Droplets and the Perilipin Protein Family
Jyväskylä: University of Jyväskylä, 2023, 90 p. (+included articles)
(JYU Dissertations
ISSN 2489-9003; 639)
ISBN 978-951-39-9733-5 (PDF)

This doctoral study investigated the role of perilipins (PLINs) in skeletal muscle lipid metabolism and their association with intramyocellular lipid droplets (LDs) in relation to health, exercise and and nutrition. Using diverse study models including human subjects, *in vitro* experiments, and advanced image analysis techniques, the study aimed to explore the effects of insulin resistance, physical activity, and branched-chain amino acid (BCAA) availability on PLIN coating of LDs and its implications for muscle phenotype. The results revealed that individuals with unhealthier skeletal muscle phenotypes exhibited deficient PLIN coating of LDs, particularly in the inner regions of glycolytic fibertypes. These findings were further validated in glycolytic myotubes subjected to BCAA deprivation, which also displayed reduced PLIN coating together with reduced LD turnover indicators. On the contrary, physical activity and balanced BCAA availability were associated with enhanced LD coating, which can provide protection against intramyocellular lipotoxicity. Moreover, the study uncovered the involvement of PLINs in various cellular processes within and between organelles, emphasizing the significance of their functional role beyond LD association. Notably, it was observed that PLIN5 translocated to the nuclei following muscle contractions, suggesting its potential contribution to transcriptional pathways. In conclusion, this study highlights the crucial role of PLIN physiology in skeletal muscle lipid metabolism and overall muscle health. Appropriate physical activity and nutrition were found to positively impact muscle health by facilitating proper association of PLINs with intramyocellular LDs and engaging in diverse cellular functions. The study suggests that targeting the PLIN coating of LDs could hold therapeutic potential for metabolic diseases. Future research directions include further investigation of the different PLIN members, such as PLIN3 and PLIN4, and exploring the nature of a putative intramyocellular lipid network. Additionally, understanding the mechanisms underlying PLIN translocation to nuclei following muscle contractions opens up new avenues for studying the involvement of PLINs in transcriptional pathways related to energy metabolism.

Keywords: perilipins, insulin resistance, skeletal muscle, physical activity, lipotoxicity, BCAA, lipid droplets, myotubes, PGC-1α

TIIVISTELMÄ (ABSTRACT IN FINNISH)

Fachada, Vasco
Terveyden, ruokavalion ja liikunnan vaikutukset lihassolun lipidimetaboliaan: painopisteenä lipidipisarat ja perilipiiniproteiinit
Jyväskylä: University of Jyväskylä, 2023, 90 s. (+artikkelit)
(JYU Dissertations
ISSN 2489-9003; 693)
ISBN 978-951-39-9733-5 (PDF)

Tässä väitöstutkimuksessa tutkittiin rasvapisaroiden ja niiden pintaproteiinien perilipiinien roolia luurankolihaksen rasva-aineenvaihdunnassa sekä liikunnan ja ravitsemuksen vaikutuksia. Tutkimuksessa analysoitiin näytteitä ihmistutkimuksista sekä *in vitro*-solukokeista käyttäen kehittyneitä mikroskooppitekniikoita. Tutkimuksen tavoitteena oli tutkia insuliiniresistenssin, fyysisen aktiivisuuden ja haaraketjuisten aminohappojen (BCAA) saatavuuden vaikutuksia rasvapisaroiden perilipiineihin ja lihaksen ilmiasuun. Tulokset osoittivat, että yksilöillä, joilla oli normaalista poikkeava luurankolihaksen ilmiasu, rasvapisaroiden perilipiinirakenne oli puutteellinen erityisesti nopeiden glykolyyttisten lihassolujen sisäosissa. Nämä havainnot validoitiin edelleen in *vitro*-solukokeilla glykolyyttisissä myotuubeissa, joilta poistettiin BCAA:t. Tämä aiheutti perilipiinipinnoitteen vähentymisen rasvapisaroiden vaihdunnan vähentyneiden indikaattorien ohella. Sen sijaan, fyysinen aktiivisuus ja tasapainoinen BCAA:n saatavuus liittyivät parempaan rasvapisaroiden pinnan perilipiinirakenteeseen, mikä tarjoaa suojaa solunsisäistä lipotoksisuutta vastaan. Lisäksi tutkimuksessa paljastui perilipiinien osallistuminen erilaisiin soluprosesseihin organellien välillä, mikä korostaa niiden toiminnallisuutta rasvapisararoolin lisäksi. Erityisesti havaittiin, että perilipiini 5 proteiini siirtyi lihastumiin lihassupistusten jälkeen, viitaten sen mahdolliseen tehtävään geenien ilmenemisen säätelyssä. Yhteenvetona voidaan todeta periliipiineillä olevan merkittävä rooli luurankolihaksen rasva-aineenvaihdunnassa ja lihaksen terveydessä. Fyysisen aktiivisuuden ja ravitsemuksen havaittiin vaikuttavan myönteisesti lihasten terveyteen edistämällä perilipiinien vuorovaikutusta solunsisäisten rasvapisaroiden kanssa niiden osallistumista. Tutkimus viittaa siihen, että rasvapisaroiden periliipini-päällysteen muokkaamisella voisi olla terapeuttista potentiaalia aineenvaihduntasairauksien hoidossa. Tulevissa tutkimuksissa tulisi selvittää myös muiden perilipiinien, kuten perilipiini 3 ja 4 roolia sekä solunsisäisen lipidiverkoston rakennetta. Lisäksi lihassupistusten aiheuttaman perilipiinien tumaan siirtymisen mekanismien ymmärtäminen avaa mahdollisuuksia tutkia perilipiinien osallistumista energia-aineenvaihduntaa säätelevien geenien ilmenemiseen.

Avainsanat: perilipiinit, insuliiniresistenssi, luustolihakset, fyysinen aktiivisuus, lipotoksisuus, BCAA, rasvapisarat, myotuubit, PGC-1α

Author

Vasco Fachada, MSc
Faculty of Sport and Health Sciences
NeuroMuscular Research Center
University of Jyväskylä
Jyväskylä, Finland

Supervisors

Associate Professor Juha Hulmi, PhD
Faculty of Sport and Health Sciences
NeuroMuscular Research Center
University of Jyväskylä
Jyväskylä, Finland

Associate Professor Riikka Kivelä, PhD
Faculty of Sport and Health Sciences
NeuroMuscular Research Center
University of Jyväskylä
Jyväskylä, Finland

Professor Emeritus Heikki Kainulainen, PhD
Faculty of Sport and Health Sciences
NeuroMuscular Research Center
University of Jyväskylä
Jyväskylä, Finland

Reviewers

Chris Shaw, PhD
Senior Lecturer in Exercise Physiology
Faculty of Health
School of Exercise & Nutrition Sciences
Deakin University
Melbourne, Victoria, Australia

Sam Shepherd, PhD
Lecturer in Sport & Exercise Nutrition
Faculty of Science
School of Sport & Exercise Sciences
Liverpool John Moores University
Liverpool, United Kingdom

Opponent

Heikki Koistinen, MD, PhD
Senior Clinical Instructor, Docent
Department of Medicine, University of Helsinki
Helsinki University Hospital
Minerva Foundation Institute for Medical Research
Helsinki, Finland

ACKNOWLEDGEMENTS

The primary research conducted for this thesis took place at the University of Jyväskylä, namely at the Faculty of Sport and Health Sciences. I would like to express my gratitude to the Faculty for granting me access to excellent resources and skilled personnel to collaborate with. Additionally, I acknowledge the Faculty of Mathematics and Science for granting access to their imaging facilities during the earlier stages of my work. The financial support for my work was received from different sources at different times, mainly I would like to acknowledge the grant given by the Fundação para a Ciência e Tecnologia, followed by other support originating from Ellen ja Artturi Nyyssösen säätiö, the Association of Researchers and Teachers of Jyväskylä, and several individual research projects from our Faculty.

I wish to express a warm word of acknowledgment towards Professor Heikki Kyrölainen, who I know since the the times of my Master degree seminars. Since then until today, you have always been supportive, interested and helping in my progress as a PhD candidate. In tough periods, the constant positive attitude, plus the words and acts of encouragement can go a long way, and yours definitely helped me going through the finish line.

Supervising is a determining endeavor in doctoral studies, and for this reason I would like to thank a number of people. A word of appreciation must be given to Professors Varpu Marjomäki and Urho Kujala for early consultation and data sharing, respectively. I wish to thank Professor Riikka Kivelä for your thorough revisions of my texts and for your very pragmatic advising during regular office visits. A critical component for the completion of my doctoral work needs to be credited to Professor Juha Hulmi. Since long before you became my supervisor, either in the lab or in beach volley, you always advised me on how to value my time and how excessive perfectionism can easily disable productivity. I was only able to understand and manage that important balance when you became my supervisor, through your 'surgical' and healthy pressure during the several stepping stones of my later doctoral path. Finally, no one word alone would suffice to express my gratitude towards Professor Heikki Kainulainen, my first and main supervisor. I remember very clearly knocking on your door to introduce myself and ask for a topic for my MSc. thesis that could involve microscopy, you were able to immediately hook my attention with the *athlete paradox* and some mysterious *lipid droplets*. From this point onward you have always tried to support my research either with funding originating from different projects of yours, but mainly by believing in me and in my ability to complete this journey. Your role was vital, not only in supporting me directly, but also in shielding my image from the outside. For all this, a big thank you, Heikki.

Guidance is not limited to supervisors, and there can be different kinds of mentors. To truly employ the scientific method one has to not only master specific technical skills, but also understand the principles of logic and Science itself, two aspects that can only materialize with countless hours of practice and discus-

sion. To this respect I would like to acknowledge two co-authors who are at the center of honing my scientific skills, both the technical and philosophical ones. First I would like to thank Paavo Rahkila for being my main mentor during the initial stages of my research, with you I learned the wet lab skills necessary to collect all my histological data, from cryosectioning, immunohistochemistry, culture of isolated myofibers, confocal microscopy to an introduction to Image J. It was also with you that I first practiced and understood the methodological principles of repeatability and reproducibility, I am truly thankful for all this, Paavo. Secondly, I wish to acknowledge the role of by brother Dr. Nuno Fachada, mainly in introducing me to the dry lab skills that I later realized were the core of my PhD work. I remember your advice during early stages when I asked you to co-develop TopoCell as a GUI and user-friendly application, to which you replied: 'ok man, but coding for 'user-friendliness' is a lot of work in exchange for loss of functionality, instead, you would be much better off if you learn how to code your own functions'. After a few years of ignoring your advice, I finally came to terms with the idea and developed a taste for coding, with much of your teachings, from which point my research just exponentiated, not only in output, but also in depth and quality. Without learning how to code I would have never been able to analyze so many images and literally millions of lipid droplets. A warm thanks, Nuno, for giving me only the first 'fish' and immediately teaching me 'how to fish'.

I wish to acknowledge the colleagues on whose papers I have co-authored along. The work I have done together with with Dr. Juha Ahtiainen, Dr. Tuuli Nissinen, Dr. Jaakko Hentilä and Dr. Hanna Juppi, were determinant in validating the tools developed to complete my PhD. To the same effect, despite no publications, I would like to thank the opportunity to develop image analysis applications with Dr. Juulia Lautaoja, Dr. Mika Silvennoinen, Dr. Sanna Lensu, Dr. Satu Pekkala and Elina Mäkinen. I am also thankful to Dr. Tuomas Turpeinen for initiating me in and developing the image analysis methodology, being very important to my first article.

A warm acknowledgement needs to be given to Dr. Mika Silvennoinen and to Dr. Sira Karvinen, my first and most influential co-workers with whom I shared an office and a research group for several years. Sira, I have always seen you as the highest professional standard one could aim at, your organizational skills have motivated me, and together with the crucial contribution in my second paper, made a small light finally shine at the end of a long tunnel. Mika, you were the person I shared a working space for the longest time, we have partied together and shared all sort of thoughts and stories, your early friendship was made of meaningful work and life advice, and to culminate all of it, your leadership and output in the BCAA project was absolutely decisive for my two last papers.

I want to thank all the colleagues and lab technicians that made my work easier. Thank you Leena Tulla, Maarit Lehti, Hanne Tähti, Jouni Tukiainen, Petri Tynkkynen, Emilia Kerttunen and Sakari Mäntyselkä. Special thanks to Ulla Sahinaho for the immense lab work for my last paper. A cheerful thanks to Mervi

Matero for being a friend, chatting about life every once in a while and for letting me 'steal' her charger every other day. Finally, thank you Katja Pylkkänen, Minna Herpola, Paivi Saari and Tiina Ahonen for the administrative assistance. I would also wish to thank the reviewers of my dissertation, Dr. Sam Shepherd and Dr. Chris Shaw, for their constructive and valuable comments. I also want to thank Professor Heikki Koistinen for accepting the invitation to come to Jyväskylä and to be my opponent.

I want to thank all my closer friends in Jyväskylä who helped give excitement to life during the toughest years of my PhD. Aapo, Braulio, Ella, Emilia, Jean, Masa to name a few. A kind acknowledgment to Anna Kavoura for meaningful chats and advice during the darkest times. When I was considering to quit my PhD., you brilliantly hinted me that 'then you should quit, and it's really ok to do so', something that immediately triggered me to refuse the idea and fight back towards this moment. Likewise, for me it is important to thank all my Judo and BJJ families, who helped give meaning to life, your influence and friendships inspired me to impact the world positively, regardless of any number of surgeries on the way.

Finally, I wish to thank my whole family for being supportive of my situation and understanding my physical absence from important family events. I want to express an endless feeling of gratitude towards my parents, not only for your direct influence in me becoming a physiologist, but also in my education as person, carrying the warm values of love, kindness and respect, but also in the life teachings of logic, rationality and critical thinking. O que de vós absorvi, foi e continuará a ser importante no meu caminho e no meu impacto no mundo.

ORIGINAL PUBLICATIONS AND AUTHOR CONTRIBUTION

This dissertation is based on the following original research articles that are referred by their Roman numerals in the text:

I Fachada, V., Rahkila, P., Fachada, N., Turpeinen, T., Kujala, U.M., Kainulainen, H. (2022). Enlarged PLIN5-uncoated lipid droplets in inner regions of skeletal muscle type II fibers associate with type 2 diabetes. *Acta Histochemica* 124(3), 151869.

II Karvinen, S.*, Fachada, V.*, Sahinaho, U.M., Pekkala, S., Lautaoja, J.H., Mäntyselkä, S., Permi, P., Hulmi, J.J., Silvennoinen, M., Kainulainen, H. (2022). Branched-Chain amino acid deprivation decreases lipid oxidation and lipogenesis in C2C12 myotubes. *Metabolites* 12(4), 328.

III Fachada, V., Silvennoinen, M., Sahinaho, U.M., Rahkila, P., Kivelä, R., Hulmi, J.J., Kujala, U.M., Kainulainen, H. (2023). Effects of long-term physical activity and BCAA availability on the subcellular associations between intramyocellular lipids, perilipins and PGC-1α. *International Journal of Molecular Sciences* 24(5), 4282.

The studies included in this dissertation were planned by me and Heikki Kainulainen (I, II, III), together with Urho Kujala (I, III), Mika Silvennoinen (II, III), Juha Hulmi (II, III), Riikka Kivelä (III) and Paavo Rahkila (I). Together with the latter, I conceptualized the software to deal with the required tasks (I), and also participated in its development together with Nuno Fachada and Tuomas Turpeinen (I). Histological work was mostly carried by me (I, II, III), with assistance from Paavo Rahkila (I, II) and Ulla-Sahinaho (II). Widefield and confocal microscopy were conducted mostly by me (I, II, III) with help from Paavo Rahkila (III). Coding for image processing, image analysis, big data analysis together with data visualization were also preformed by me (I, II, III). I had the main responsibility of writing articles I and III, and I wrote article II together with Sira Karvinen, as indicated by asterisks (*) in the list above.

FIGURES

TABLES

ABBREVIATIONS

all-LDs All detected lipid droplets
ANOVA1 One-way analysis of variance
ANOVA2 Two-way analysis of variance
ATGL Adipose triglyceride lipase
BCAA Branched-chain amino acids
BF Blocking buffer: BSA in study I and GS in studies II and III
BSA Bovine serum albumin
col-LDs Lipid droplets colocalized with PLIN5
CS Citrate synthase
DAG Diacylglycerol
DGAT2 Diacylglycerol O-acyltransferase
EPS Electrical pulse stimulation
FAs Fatty acids, mostly used to refer to free, or unesterified fatty acids
GLUT4 Glucose transporter type 4
GS Goat serum
HSL Hormone-sensitive lipase
ICA Intensity correlation analysis
IMCL Intramyocellular lipids
IMTG Intramyocellular triglycerides
LDs Lipid droplets
LTPA Leisure time physical activity
MAG Monoacylglycerol
PGC-1α Peroxisome proliferator-activated receptor gamma coactivator 1-alpha
PLIN2 Perilipin 2
PLIN3 Perilipin 3
PLIN5 Perilipin 5
PLINs Perilipin protein family
TAG Triacylglycerol
unc-LDs Lipid droplets uncoated with PLIN5

CONTENTS

1 INTRODUCTION

Lipids are ubiquitous molecules and are believed to have played a crucial role in abiogenesis (Goodpaster et al. 2001; Rimmer et al. 2018). According to the 'lipid world' hypothesis, liposomes were the first self-assembling and replicating structures to emerge on Earth, even before RNA (Subbotin & Fiksel 2023). They became an essential component of living organisms and play vital roles in various biological processes, including cell membrane formation, energy storage, and cell signaling (Akie & Cooper 2015; Gemmink et al. 2016; Halama et al. 2016). Today liposomes exist in virtually every cell type of every organism, often receiving the name of lipid droplets or LDs (Figure 1).

Most liposomes are spherical structures composed of lipid bilayers that have the ability to encapsulate a hydrophobic compartment. They can form spontaneously in aqueous environments and are considered a probable precursor to the first cells (Cavalier-Smith 2001; Hanczyc et al. 2003). While the most well-known function of liposomes relates to their role as a cell membrane, they are also involved in the formation of organelles such as mitochondria, peroxisomes or the endoplasmic reticulum (Casares et al. 2019; Hanczyc et al. 2003).

However, not all liposomes are made of bilayers. For example, lipid droplets and lipoproteins are a special kind of liposome made up of a phospholipid monolayer. The former are lipid-rich organelles found in many cell types, including adipocytes, hepatocytes, and myocytes, serving as a primary storage site for fatty acids and energy (Bartz et al. 2007; Listenberger et al. 2003; Pressly et al. 2022; Zadoorian et al. 2023). While they are crucial for cellular metabolism, LDs can also be a source of toxicity to cells if their metabolism is dysregulated, leading to a pathophysiological state known as lipotoxicity (Unger et al. 2010).

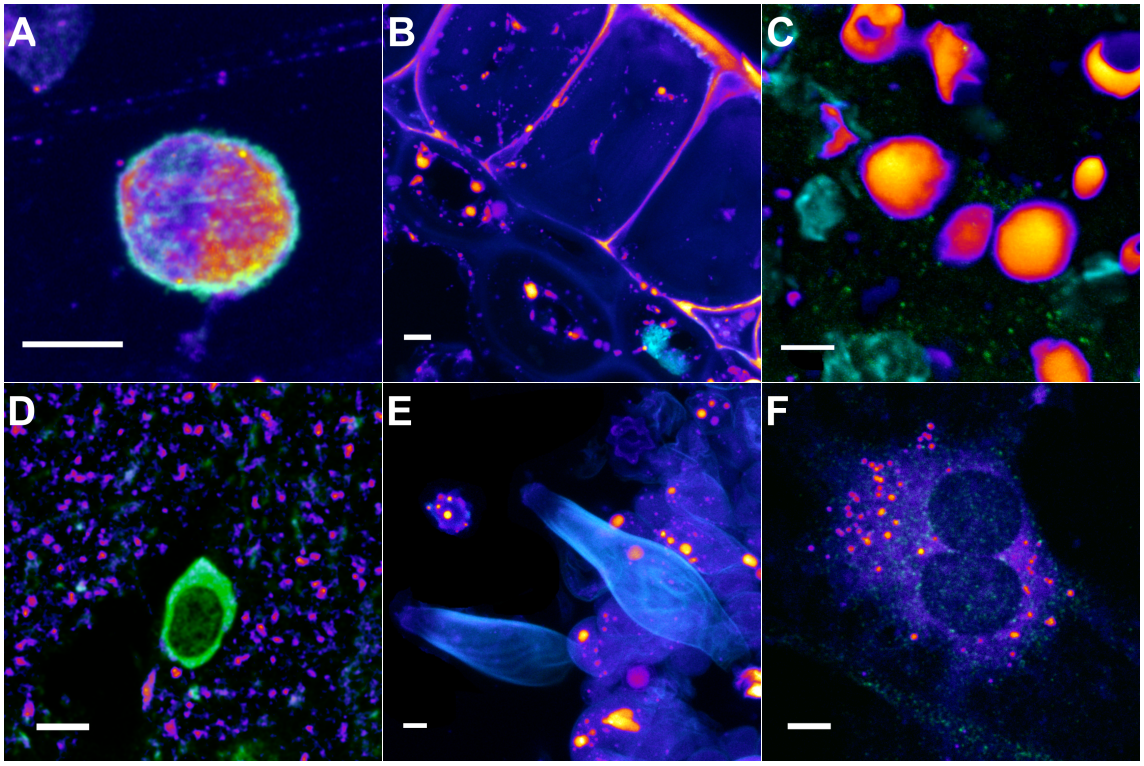

FIGURE 1 Intracellular liposomes in different cells and lifeforms, often organizing as lipid droplets. Here stained as neutral lipids, ranging from dark purple (low concentrations) to bright orange (high concentrations). A) Human erythrocyte, cyan is actin cytoskeleton; B) Plant (*Pinus mugo*) epidermal and hypodermal cells, cyan are nuclei; C) Mouse (*Mus musculus*) liver, cyan are nuclei, green is PLIN5; D) Rat (*Rattus norvegicus*) striatum, green are D1 positive neurons; E) Mushroom (*Inocybe asterospora*) hymenium with basidia, cystidia and ejected spore, cyan is autofluorescence; F) Rat (*Rattus norvegicus*) fibroblasts, green is PLIN5. Bars = 5 µm.

Lipotoxicity occurs when cells accumulate excess lipids that cannot be effectively utilized, leading to cellular dysfunction and damage. This phenomenon is often observed in metabolic disorders such as obesity, type 2 diabetes, and non-alcoholic fatty liver disease (Pressly et al. 2022; Wree et al. 2013; Zadoorian et al. 2023). These disorders are prevalent in western countries, and their treatment imposes a significant economic burden on healthcare systems worldwide (Gustafson et al. 2007).

This dissertation focuses on glycerolipids, which are a type of lipid that contains a glycerol backbone and one or more fatty acid chains. Glycerolipids are the primary constituents of LDs, and their metabolism is critical for maintaining cellular homeostasis (Listenberger et al. 2003; Zadoorian et al. 2023). This is remarkably true in the skeletal muscle, given its large volume and high lipid turnover rate (Kenney et al. 2021; Seibert et al. 2020). The perilipin protein family members (PLINs) are central agents in regulating LDs and glycerolipids, keeping the skeletal muscle lipid metabolism at equilibrium (MacPherson & Peters 2015).

Nevertheless, the study of skeletal muscle lipid metabolism must not be

segregated from the complete and holistic metabolic essence. A prime example of this is the crosstalk with energy metabolism and branched-chain amino acid (BCAA) metabolism (Kainulainen et al. 2013). In this regard, metabolic phenotypes are not merely defined by the individual genotype and can be significantly impacted by human behavior, namely through nutrition and exercise (Goodpaster et al. 2001).

As the cardinal aim, the present work proposes to investigate the distribution of LDs and PLINs within muscle cells and their relationship with other organelles such as the nucleus and the sarcolemma. As a secondary objective, sizeable efforts are steered towards the connection between the muscle lipid, energy and BCAA metabolisms. These grounds were studied across contrasting metabolic, nutritional and physical activity statuses. The chosen approach in this dissertation is largely based on pattern recognition and comprehension, as it is believed that characterizing and understanding patterns in cellular events can provide insight into metabolic status and disease development (Murphy 2010; Xu et al. 2020; Zheng et al. 2011).

In summary, this dissertation aims to provide insight into the allocation patterns of LDs and related markers, together with their association with other organelles within cells, particularly in muscle cells, to gain a better understanding of cellular lipid metabolism and its dysregulation in metabolic disorders.

2 LITERATURE REVIEW

2.1 Skeletal muscle lipid metabolism

Being such prevailing molecules, lipids are also harbored within muscle cells (Machann et al. 2004; Malenfant et al. 2001; Moro et al. 2008; Shaw et al. 2008). As the largest organ in the human body, skeletal muscle plays a major part in metabolizing nutrients and other compounds (Pedersen 2013). This becomes more evident when acknowledging the high energy demands of skeletal muscle (Kenney et al. 2021). In respect to lipids, these are the source of one of the three macronutrients, necessary to make all cells function. Although the immediately obvious role lipids play in myofibers is as an energy fuel (Kenney et al. 2021; Seibert et al. 2020), this group of molecules have a wide array of other critical functions within the skeletal muscle cell and organ as a whole. Such additional roles range from cell mechanical protection and structural integrity via sarcolemma and other membranal complexes, signaling pathways related to inflammation or vesicle trafficking (Morales et al. 2017; Seibert et al. 2020; Zehmer et al. 2009).

Moreover, the overall relevance of skeletal muscle lipid metabolism is highlighted by its connection with several health implications (Le Lay & Dugail 2009; Morales et al. 2017) and a close interplay with energy metabolism as well as BCAA metabolism (Hatazawa et al. 2014; Sjögren et al. 2021).

2.1.1 Extracellular lipid sources

Lipids reach myofibers via blood circulation, to where they can be introduced from either ingestion or from the adipose tissue. If ingested, lipids start being broken down by saliva in the mouth, though most of their digestion happens in the small intestine (Silverthorn 2010). Once in the blood, lipids circulate mostly as lipoproteins, which are essentially esterified fatty acids into glycerol, which together with cholesterol are enveloped by a phospholipid monolayer embedded with regulating proteins (Maughan et al. 1997; Silverthorn 2010).

When these circulating lipids reach the capillaries contiguous to myofibers,

specific enzymes released from the endothelium can hydrolyze lipoproteins into simpler free fatty acids (FA), releasing them into the plasma. Then, these simplified albumin-bound FAs can enter skeletal muscle cells assisted by protein channels and transporters (Goldberg et al. 2021; Maughan et al. 1997; Silverthorn 2010; Su & Abumrad 2009).

2.1.2 Intramyocellular lipids and terminology

Now that the intramyocellular space has been reached, it is important to define a few lipid-related terms. Starting with the FAs that just entered the cell, these are relatively simple molecules, which will be, eventually, directly utilized by the cell to carry numerous vital functions, such as β-oxidation at the mitochondria and consequential ATP production. Like the term suggests, these are molecules with an acidic signature (Gunstone & Harwood 2007; Voet et al. 2016).

Another possible fate of FAs is esterification by binding glycerol molecules, thus generating glycerolipids, the most referred one being triacylglycerol (TAG). The latter is composed of one glycerol molecule bound to three FAs, and no longer has an acidic profile, but a neutral one (Gunstone & Harwood 2007; Voet et al. 2016). When TAG is discussed inside muscle fibers, the term *intramycellular triglycerides* (IMTG) is often applied (Badin et al. 2013; Coen et al. 2009; Moro et al. 2008; Watt 2009).

Although a commonly used term, including in this dissertation, intramyocellular lipids (IMCL) is arguably the most controversial or ambiguous one. Interpreted literally, it should refer to all lipids present within the myocite, including FAs, phospholipids, cholesterol, TAG and so on. However, IMCL has often been used throughout the literature to refer to those lipids with a neutral charge, such as diacyglycerol (DAG), monoacyglycerol (MAG) and cholesterol, but mainly to TAG, i.e., the neutral lipids which reside inside the muscle cell (Chow et al. 2017; Gemmink et al. 2016, 2021; Stokie et al. 2023).

2.1.3 Lipid droplets & cell architecture

The main container of TAG in muscle cells – or IMTG – is the LD, a very popular term in the field. It is sometimes used interchangeably with IMCL, although in this dissertation those two terms are not considered synonyms. Here, the term LD is reserved for neutral lipid aggregates of subglobose shapes. On the contrary, IMCL are used to refer to neutral lipids in general, which are targeted by stains like Bodipy or LD540, and not necessarily to lipids organized within any kind of subglobose organelle (see section 6.2 for related discussion).

In the particular case of skeletal muscle, most of the intracellular LDs visbile with light microscopy are well under 1 µm in diameter, rarely reaching 2 µm, and localize just adjacent to myofibrils and its sheeting sarcoplasmic reticulum (Bosma 2016; Koh et al. 2017; Walther & Farese 2012), as illustrated in Figure 2.

Given the tightly packed architecture and the contractile properties of muscle fibers (Kenney et al. 2021), LD morphology and distribution are under the

influence of both biochemical and biomechanical dynamics (Prats et al. 2006).

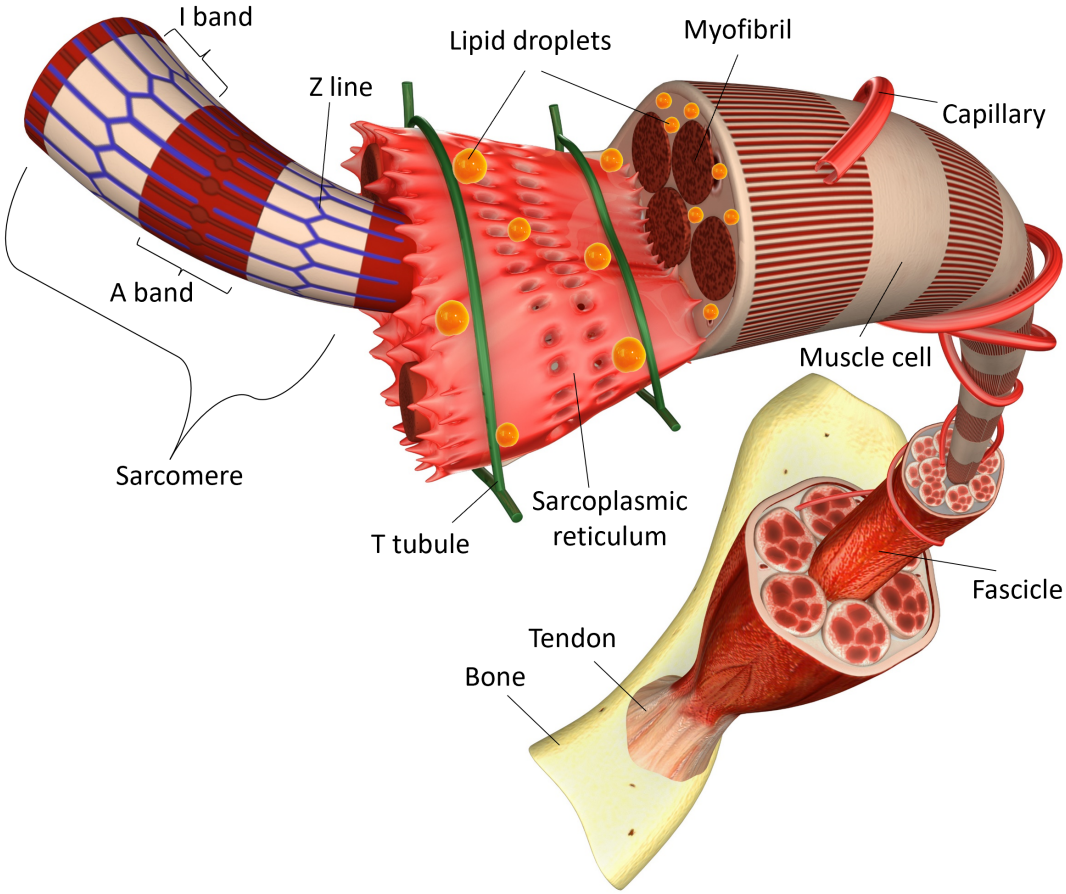

FIGURE 2 Architecture of the skeletal muscle, from bone to protein filaments. The structures in the illustration are not to scale.

2.1.4 Lipid turnover & LD regulation by the perilipin protein family

The LD is a dynamic organelle involved in the storage and utilization of lipids in cells (Welte 2015). It is composed of a neutral lipid core surrounded by a phospholipid monolayer and associated proteins (Figure 3). The most abundant neutral lipid in LDs is TAG, with smaller amounts of cholesterol and DAG (Murphy 2012; Wilfling et al. 2014).

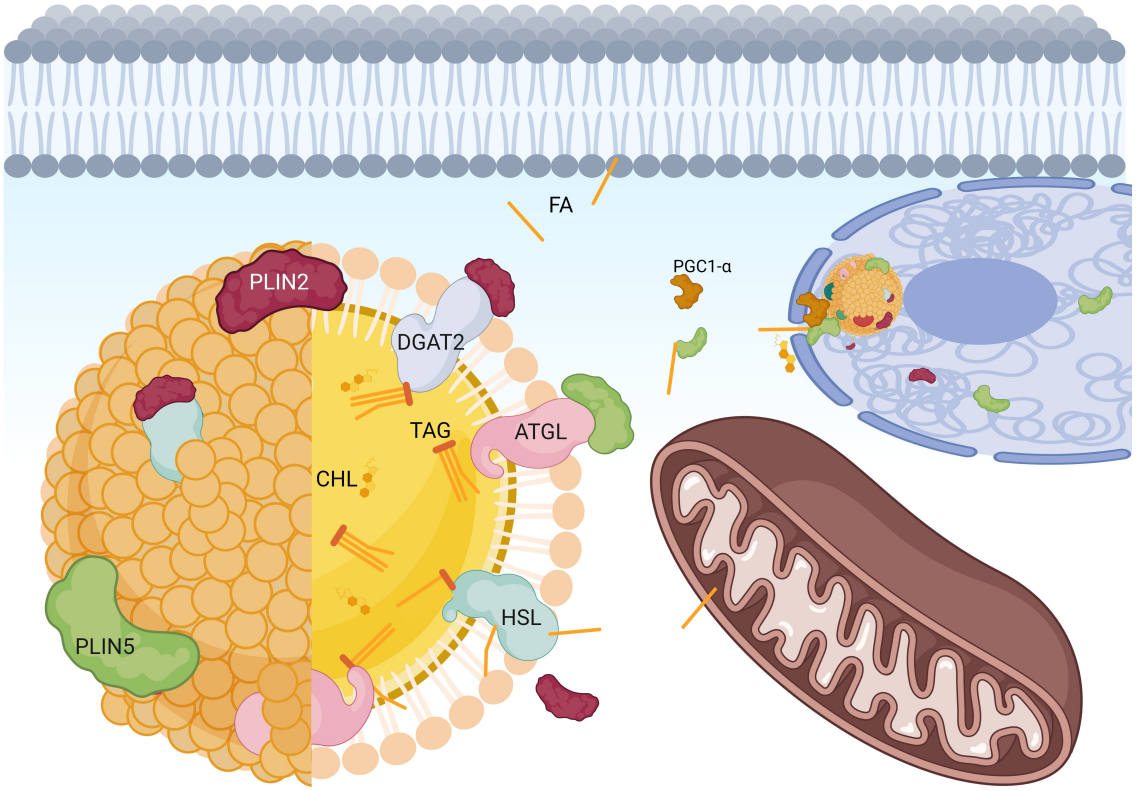

FIGURE 3 Simplified illustration of LD composition and main regulating interactions of PLINs. While FAs flow to and from the phospholipid-monolayered LD before used by mitochondria, the LD is metabolized by enzymes like ATGL or HSL, which in turn are regulated by PLINs. Some PLINs seem to have a nuclear role.

This organelle plays a crucial role in the energy metabolism by providing FAs – hydrolyzed from TAG –, as a source of acetyl coenzyme A for the Krebs cycle in mitochondria, and ultimately producing the ATP required for contraction and other cellular functions (Bosma 2016; Kenney et al. 2021; Maughan et al. 1997; Morales et al. 2017). Simultaneously, LDs are the first stop for freshly endocytosed FAs (Kanaley et al. 2009; Su & Abumrad 2009).

The regulation of LDs involves several enzymes, including hydrolyzing enzymes – such as hormone-sensitive lipase (HSL) or adipose triglyceride lipase (ATGL) – and esterifying enzymes such as diacylglycerol O-acyltransferase 2 (DGAT2) (Krahmer et al. 2009). These enzymes play a critical role in controlling the size and number of LDs in cells. Many of these enzymes are regulated by post-translational modifications and complex interactions with other proteins (Krahmer et al. 2009; Wilfling et al. 2014).

Central to such regulation are the PLIN proteins, formerly known as PAT proteins (Greenberg et al. 1991; MacPherson & Peters 2015). The PLINs are primarily located on the surface of LDs, where they interact with other LD-associated proteins and enzymes involved in lipid metabolism, regulating their access to lipid stores (Granneman et al. 2009). They can, for instance, inhibit lipolysis by interacting with ATGL, HSL and some of their co-activators (Granneman

et al. 2011; Sztalryd & Brasaemle 2017). In skeletal muscle, all isoforms but PLIN1 seem to be present, whereas PLIN2 and PLIN5 are the more prominent, particularly in fine tuning LD hydrolysis (Daemen et al. 2018b; MacPherson & Peters 2015), and therefore will be under focus in this review.

Starting with PLIN2 – also known as adipophilin and ADRP, amongst other names – it is a ubiquitous isoform throughout the different tissues and, at the same time, the most expressed PLIN in skeletal muscle (MacPherson & Peters 2015; Shaw et al. 2009; Shepherd et al. 2012, 2013). Accordingly, PLIN2 seems to replace the function of other PLINs in different tissues and therefore it is likely a more generalistic or unspecialized isoform (MacPherson & Peters 2015). This fact is perhaps reflected by the ability to bind and interact with both lipases and esterification enzymes, thus participating actively in both lipolysis and lipogenesis (MacPherson & Peters 2015; Stone et al. 2009; Wang et al. 2011).

Very close to PLIN2 in its RNA sequence, there is PLIN5, an isoform mainly expressed in highly oxidative tissues, such as skeletal muscle and also known as OXPAT, MLDP, or LSDP5 (MacPherson & Peters 2015; Shepherd et al. 2012, 2013; Wolins et al. 2006). It seems to behave very similarly to PLIN2 in the capacity to inhibit lipases, LD hydrolysis and consequently promoting LD growth (Daemen et al. 2018b; MacPherson & Peters 2015). However, unlike PLIN2, PLIN5 is not reported to interact with DGAT2 (Stone et al. 2009) and there are studies connecting PLIN5 with increased oxidative capacity, TAG hydrolysis and LD enrichment with high energy TAG (Billecke et al. 2015; Bosma et al. 2012b; Peters et al. 2012; Whytock et al. 2018). Taken together, this suggests PLIN5 plays a specialized role in skeletal muscle, where it has the ability to quickly restrict or activate the lipolytic status of LDs (Wolins & Mittendorfer 2018; Zhang et al. 2022).

However, the roles of PLIN-LD dynamics expand beyond providing FAs to mitochondria. For instance, they have been shown to translocate to nuclei and directly influence transcriptional events (Cinato et al. 2023; Farese & Walther 2016). One such event, for instance, is the activation of peroxisome proliferator-activated receptor gamma coactivator 1-alpha (PGC-1α) and consequentially, mitochondrial biogenesis (Gallardo-Montejano et al. 2016; Seibert et al. 2020).

In conclusion, LDs are dynamic organelles involved with – but not limited to – lipid turnover. The regulation of LDs is complex and involves several proteins, including the PLINs. Both LDs and PLINs have a role in energy metabolism, lipid turnover and intramyocellular signaling in general. A simplified illustration of the LD dynamics in the muscle cell can be seen in Figure 3.

2.1.5 Link between lipid, energy and BCAA metabolisms

The connection between the lipid and energy metabolisms also extends to the BCAA metabolism, as muscle BCAA are an important source of IMTG (Nye et al. 2008). The latter occurs through glyceroneogenesis, a crucial metabolic pathway in facilitating the production of glycerol 3-phosphate or TAG from sources other than glucose. In this process, pyruvate, alanine, glutamine, and various substances derived from the Krebs cycle serve as precursors for glycerol 3-phosphate.

Glyceroneogenesis not only produces lipids for utilization in other metabolic pathways but also maintains cytosolic lipid levels by re-esterifying FAs to form triglycerides (Kainulainen et al. 2013; Nye et al. 2008). Highlighting this, there is the fact that unlike other amino acids that can be processed by the liver, BCAAs are mainly broken down in skeletal muscle (Kainulainen et al. 2013; Lerin et al. 2016). Importantly, PGC-1α constitutes a critical link between the lipid and BCAA metabolisms in skeletal muscle, as it plays a role in activating the latter through multiple nuclear receptors (Hatazawa et al. 2018; Sjögren et al. 2021). The relevance of PGC-1α is further emphasized by correlating with glucose transporter type 4 (GLUT4) and insulin sensitivity in skeletal muscle (Al-Khalili et al. 2006).

Additionally, poor BCAA metabolism in skeletal muscle has been linked to impaired lipid metabolism and insulin resistance (Lerin et al. 2016), while exercise has been shown to affect muscle BCAA metabolism (Leskinen et al. 2010). For instance, the high expression of genes involved in BCAA degradation and FA metabolism in skeletal muscle is linked to high endurance capacity in rats (Kivela et al. 2010). Likewise, an under-regulated amino acid catabolism impairs exercise metabolism and reduces endurance capacity in mice (She et al. 2010). Furthermore, it has been demonstrated that acute exercise stimulus activates the primary pathways of BCAA oxidation (Kasperek et al. 1985; Xu et al. 2001).

Despite this, research establishing a connection between intramyocellular BCAA and PLINs is scarce, at best. It is therefore essential to investigate the effects of BCAA availability on the LD-PLIN regulation, as this could potentially reveal crucial dynamics underlying several aspects of metabolic health.

2.2 Intramyocellular lipids & metabolic health

2.2.1 The *athlete paradox*

The interest in the study of IMCL, particularly LDs, exploded with the paradigm shift initiated by the so-called *athlete paradox* (Daemen et al. 2018a; Goodpaster et al. 2001; Russell 2004; van Loon et al. 2004a; Wolins & Mittendorfer 2018). By comparing obese and type 2 diabetic individuals against healthy controls, it was thought that insulin resistance correlated linearly with increased IMCL (Falholt et al. 1988; Standl et al. 1980). However, when researchers decided to look into athletes – particularly endurance oriented, but not limited to (Shepherd et al. 2014) – they were surprised by the even higher content of IMCL in these individuals (Goodpaster et al. 2001). It became evident that the relationship between insulin resistance and IMCL content was not a linear one (Figure 4). The necessary conclusion was that skeletal muscle insulin resistance was not simply determined by the amount of IMCL, and the number of research questions multiplied from there (Daemen et al. 2018a; Goodpaster et al. 2001; Russell 2004; van Loon et al. 2004a).

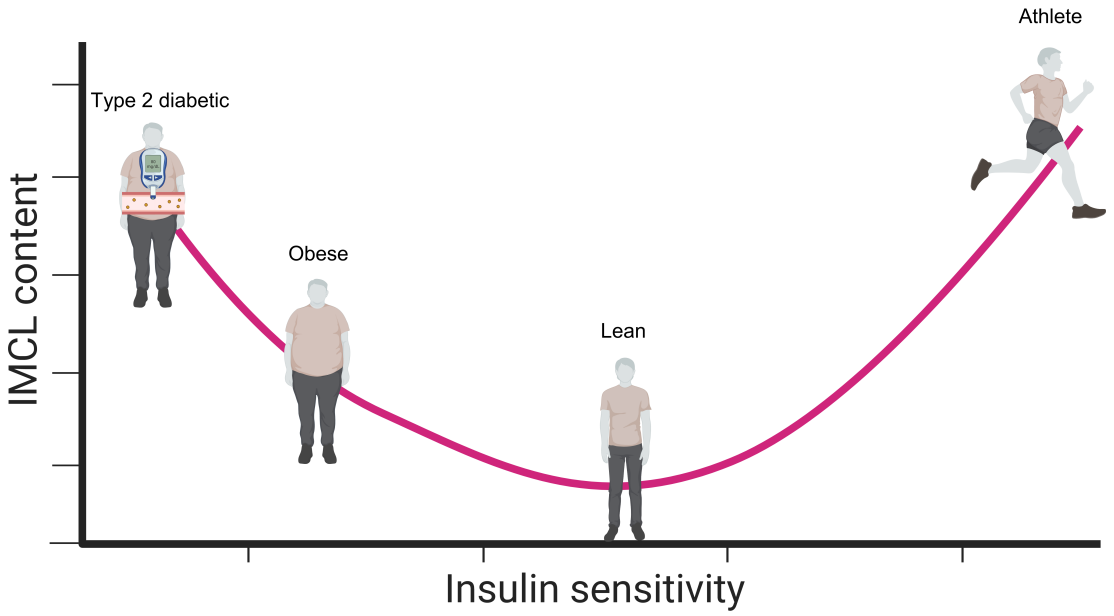

FIGURE 4 The *athlete paradox*. Insulin-resistant individuals, such as type 2 diabetic represented on the left side of the plot, show increased IMCL content when compared to insulin sensitive controls, in the center of the plot. However, paradoxically athletes show even higher contents of IMCL, despite elevated insulin sensitivity.

One of the questions emerging from the athlete paradox concerns the location of LDs and its metabolic implications, both in terms of cell type, as well as in terms of subcellular localization (Nielsen et al. 2010; van Loon & Goodpaster 2006; van Loon et al. 2004b). However, studies focusing on this matter are relatively scarce and occasionally inconsistent in their results, especially in human skeletal muscle (Daemen et al. 2018b). The present dissertation proposes to contribute novel insights to this field of knowledge.

2.2.2 Lipotoxicity and metabolic disorders

The main metabolic disorder connected to the study of intramyocellular LDs is insulin resistance (Bouzakri et al. 2005; Daemen et al. 2018a; Goodpaster et al. 2001; Pressly et al. 2022; Russell 2004; van Loon et al. 2004a; Zadoorian et al. 2023), the rationale being the disruption of the insulin-signaling pathway, specifically through inhibition of insulin receptor substrates (IRS). These signaling cascades initiated by specific ceramides – and possibly DAG to some degree – ultimately result in impaired translocation of GLUT4 towards the sarcolemma (Figure 5), consequently leading to hyperglycemia due to decreased glucose uptake by cells (Chaurasia & Summers 2015; Daemen et al. 2018b; Ebeling et al. 1998; Koistinen

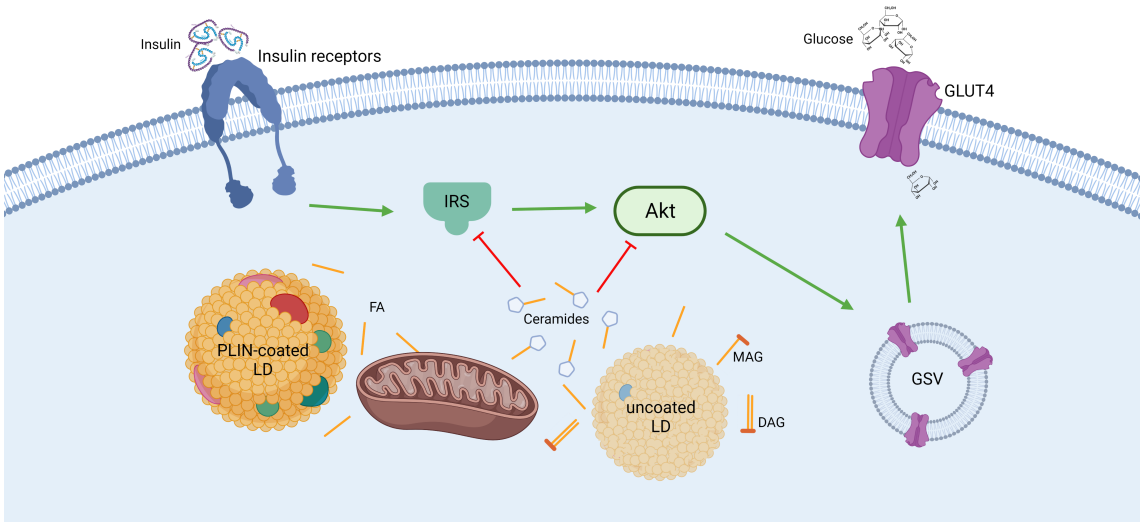

FIGURE 5 Simplified model of lipotoxic influence of LDs in skeletal muscle and consequent insulin resistance. Specific types of ceramides inhibit IRS and/or Akt, ultimately preventing GLUT4 storage vesicles (GSV) from translocating to the sarcolemma.

& Zierath 2002; Machann et al. 2004; Park & Seo 2020; Perreault et al. 2018; Summers et al. 1998; Watt 2009). Such ceramides seem to originate from inefficient mitochondrial β-oxidation, which, together with FA transportation and hydrolysis within LDs, has been demonstrated to be impaired in insulin-resistant individuals (Ahmed et al. 2021; Blaak 2005; Blaak et al. 2000; Listenberger et al. 2003; Moro et al. 2008; Scott et al. 2016). Proportionally, ceramide levels are shown to be higher in insulin-resistant individuals (Adams et al. 2004; Amati et al. 2011).
The ramifications of excess intramyocellular ceramides for metabolic disorders are not limited to insulin resistance. Some schools of thought consider cancer to be a metabolic disorder (Coller 2014) and, in fact, ceramides are connected to the induction of apoptosis in muscle cells and ultimately cancer if unaddressed physiologically (Hsieh et al. 2014; Pierucci et al. 2021). Interestingly, cancer patients have been demonstrated to have increasing intramyocellular LDs as cachexia progresses (Stephens et al. 2011). To summarize, the effects that dysfunctions of skeletal muscle lipid metabolism can have on metabolic health cannot be ignored, particularly with regard to LDs and their regulation.

2.2.3 The LD-PLIN dynamics in health, nutrition and exercise

As discussed in section 2.1.4, LDs are often coated by PLINs, a family of proteins with several roles in managing the fate of intracellular lipids. In C2C12 muscle cells, PLIN2 has been associated with both the formation of LDs and the improvement of insulin sensitivity (Bosma et al. 2012a). Likewise, PLIN2 seems to be expressed more in the muscle of insulin-sensitive populations (Amati et al. 2011; Minnaard et al. 2009; Shepherd et al. 2013) and in insulin-resistant individ-

uals when undergoing treatment, thus improving their insulin sensitivity (Bosma et al. 2012a). Similarly to PLIN2, trained endurance individuals have increased levels of PLIN5 expression in both fiber types when compared to untrained BMI-matched participants (Shaw et al. 2020). Importantly, PLIN5 deletion causes insulin resistance in skeletal muscle and it is suggested to protect this organ against lipotoxicity (Laurens et al. 2016; Mason et al. 2014).

In general, both PLIN2 and PLIN5 seem to follow IMCL levels, which is highly influenced by nutrition (MacPherson & Peters 2015; Minnaard et al. 2009; Peters et al. 2012; Shepherd et al. 2013). In mice, for instance, high fat feeding results in increased muscle PLIN5 mRNA expression and protein content, while PLIN2 responses were similar, but seemed bolstered by exercise (Rinnankoski-Tuikka et al. 2014). The concentrations of IMCL appear to be mainly driven by circulating FA, as the replenishment of depleted IMCL (e.g. by exercise) happens pretty quickly in all fiber types after FA ingestion (Daemen et al. 2018b; Phielix et al. 2012). The same phenomenon – and extended to PLIN2 expression – can be observed in C2C12 cells when supplemented with FAs (Bosma et al. 2012a). Larger LDs can also be the result of fasting, as long as these droplets are coated with PLIN5. The latter is especially true in insulin sensitive individuals, reinforcing the protective role of PLIN5 against lipotoxicity discussed above (Daemen et al. 2018b; Gemmink et al. 2016). It is worth mentioning that not all calories are made equal, and some specific diets (e.g. one including resveratrol) seem to have benefits similar to exercise, with the strongest response for IMCL and PLIN5 happening in type I fibers (Daemen et al. 2018b; Timmers et al. 2011).

Curiously, the usage of IMCL with exercise may be interconnected with nutrition, as FA pre-loading increases significantly IMCL utilization during exercise, especially in trained individuals. Naturally, IMCL utilization also depends on increasing exercise duration (Daemen et al. 2018b; Stokie et al. 2023). Regarding the effects of short-term exercise on PLIN2 and PLIN5, there are sufficient studies showing their increased mRNA expression or protein content, especially in type I fibers (Rinnankoski-Tuikka et al. 2014; Shaw et al. 2012; Shepherd et al. 2013, 2017). As stated in section 2.2.1, athletes have the highest concentrations of IMCL, however exercise does not seem to lead to increased IMCL in every case. Insulin-resistant groups tend to show conflicting results, with no clear increase or decrease in IMCL with exercise, despite a known improvement in insulin sensitivity, oxidative capacity and increased contact between LDs and mitochondria (Daemen et al. 2018b; Devries et al. 2013; Shepherd et al. 2017; Tarnopolsky et al. 2007). Some of the existing contradictions might be due to a lack of truly longitudinal studies on the topic of physical activity, LDs and PLINs. The latter equally applies with regard to LD coating, wherein there are fewer studies investigating the effects of exercise, especially long-term, and it is not clear that there are significant differences in LD coating by PLINs (Shepherd et al. 2013).

Despite the lack of studies, there are good studies alluding to the relationship between exercise and LD coating by PLINs. Some research has interestingly demonstrated that LDs coated with PLINs tend to be depleted after exercise, contrarily to those LDs which are uncoated (Shepherd et al. 2012, 2013). Still, and

despite the current model pointing to PLIN5 as protective against lipotoxicity, its coating of LDs has been considered insufficient in explaining insulin sensitivity (Gemmink et al. 2018). At this point is worth acknowledging that although this thesis focuses on PLIN2 and PLIN5, nutrition and and physical activity also have an impact on the muscle PLIN3 and PLIN4 isoforms (Pourteymour et al. 2015; Shepherd et al. 2017; Whytock et al. 2020).

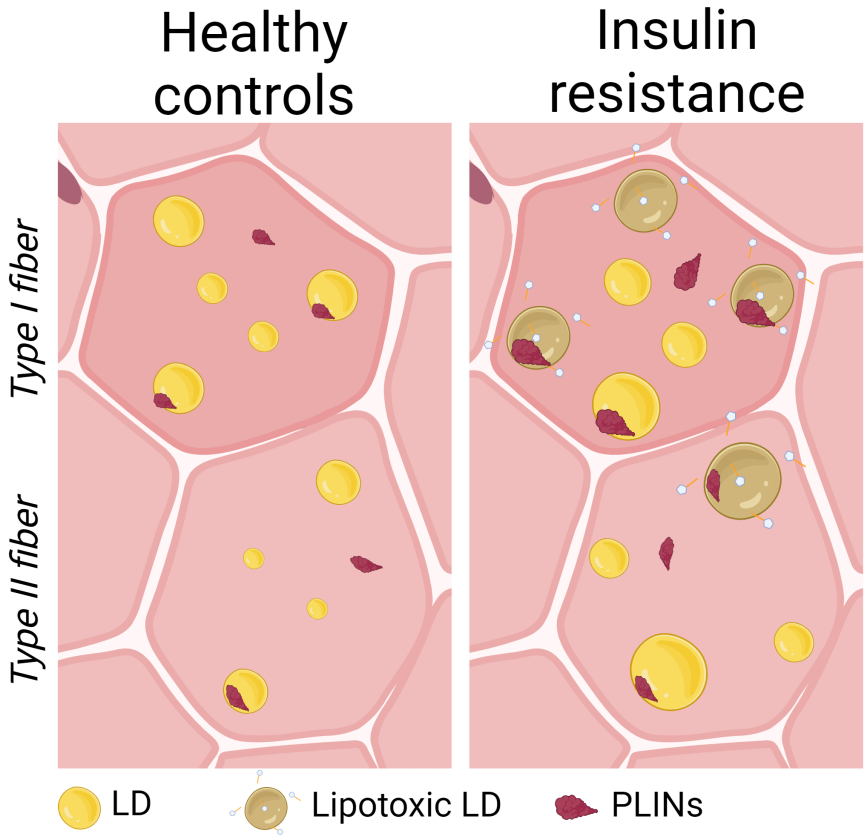

FIGURE 6 Illustration of the current model characterizing intramyocellular lipotoxic IMCL. Increased subsarcolemmal IMCL correlates with insulin resistance, especially in type I fibers.

Studies on LD distribution are not abundant, but the most well-established models state that insulin-resistant participants have higher IMCL contents and larger LDs in subsarcolemmal regions, especially in type I fibers (Figure 6). The LDs in these regions seem to be metabolically more accessible and mutable, thus being more quickly normalized towards physiological levels after exercise (Bucher et al. 2014; Devries et al. 2013; Li et al. 2014; Nielsen et al. 2010). However, such preferential usage between subsarcolemmal and intermyofibrillar LDs may depend on the specific muscle involved, type of exercise and algorithm defining the different subcellular regions (Koh et al. 2017; Stokie et al. 2023). Notably, recent research has shown that subsarcolemmal LDs are differently composed than LDs in inner regions of fibers, remarkably in being more saturated and correlating with insulin resistance (Daemen et al. 2020; Kahn et al. 2021). However, the great majority of

studies focusing on LD subcellular distribution do not investigate the differential LD coating by PLIN proteins.

In summary, there is a gap in the literature connecting metabolic health with the combined importance of subcellular localization and PLIN association of LDs. This dissertation proposes to test the hypothesis that the subcellular localization of coated IMCL is as critical to understand as are the isolated questions of localization and PLIN association. In addition, this work explores the extent to which the latter events are predetermined by genetics and influenced by behaviors related to nutrition and exercise.

3 AIMS OF THE STUDY

The aim of this dissertation was to better understand how intramyocellular LDs and the perilipin protein family contribute to the health and efficiency of skeletal muscle lipid metabolism. For good measure, the connection between LD, PLINs and the BCAA metabolism is also investigated. Since it is already known that these agents are affected by physical activity and nutrition, these were investigated in different human and cell models. The approach chosen to investigate this matter was mostly pattern-based with careful high-throughput measurements of cellular and subcellular localization, colocalization, density and size of LDs, PLINs and other targeted markers with roles in the lipid and energy metabolisms. Additionally, other standard molecular approaches were implemented in order to complement the morphological observations and skeletal muscle lipid metabolism in general.

The specific aims were as follows:

1. Expand on known topography of LD coating by PLIN5 in skeletal muscle of type 2 diabetic, obese and lean individuals.

   Hypothesis: Different metabolic profiled individuals reveal additional differences in LD coating by PLIN5. Different-sized LDs in different regions of the muscle cell reveal different coating patterns previously unknown.

2. Establish the profile of LDs and PLIN proteins in human twin pairs with contrasting long-termed lifestyles.

   Hypothesis: Inactive twins have higher IMCL content accompanied by different PLIN protein association. Even though PLIN levels are associated with systemic fat in literature, less relative percentage of this protein properly targets and is associated with LDs in inactive twins.

3. Study lipogenesis and lipolysis *in vitro*, involving LDs, PLINs and PGC1-α during exercise and BCAA supplementation. Further investigate PLIN proteins as regulatory factors in the lipid and BCAA metabolisms in skeletal muscle.

   Hypothesis: Exercise and BCAA supplementation alter lipid turnover, together with PLIN concentration and IMCL coating profile. The roles of PLINs beyond regulation of lipolysis and lipogenesis are expanded, showing novel patterns of associations with PGC1-α in different compartments of cells.

4 MATERIALS AND METHODS

4.1 Experimental designs

4.1.1 Insulin resistant humans (I)

Twenty-five physically inactive male participants were grouped depending on their health status and body mass index (BMI). Seven healthy individuals (BMI $\leq$30 kg $\cdot$ m^{-2} or body fat percentage 10-20%) formed the control group (HC). The obese group (OB) was composed of 8 non-diabetic obese men (BMI >30 kg $\cdot$ m^{-2}). Finally, the diabetic group (T2D) consisted of 10 participants clinically diagnosed with type 2 diabetes (Table 1). Prior to collecting the muscle biopsy, subjects refrained from exercising for 48 h. The skin area was shaved and cooled with ice for 10 min before local the anaesthetic was injected (Lidocain 20 mg $\cdot$ mL^{-1} concentration of adrenalin). Biopsies were taken with a Bergström needle from the *vastus lateralis* muscle. The samples were covered with Tissue-Tek and frozen immediately in isopentane cooled with liquid nitrogen, then stored at -80°C until further analyses.

TABLE 1 Group characteristics in study I. Mean $\pm$ SEM. **$p < 0.01$ using a Kruskal-Wallis H test. Pairwise post hoc significance ($p < 0.05$) is denoted with letters *a* to *c*, from highest to lowest value.

Variable	**Controls** (HC) n=7	**Diabetic** (T2D) n=10	**Obese** (OB) n=8
Age (years)	56.4 ± 2.8	52.7 ± 2.2	51.9 ± 3.2
Body weight (kg)**	78.4 ± 2.4^{c}	112.0 ± 7.1^{a}	99.6 ± 5.4^{b}
BMI (kg$\cdot$m^{-2})**	25.8 ± 0.4^{b}	34.0 ± 1.6^{a}	32.3 ± 1.0^{a}
Body fat (%)**	19.9 ± 1.1^{b}	29.2 ± 1.4^{a}	30.7 ± 1.8^{a}
Triglycerides (mmol $\cdot$ L^{-1})**	1.4 ± 0.2^{b}	2.8 ± 0.7^{a}	1.8 ± 0.4^{b}
Blood glucose (mmol $\cdot$ L^{-1})**	5.1 ± 0.2^{b}	8.0 ± 1.3^{a}	5.1 ± 0.6^{b}
VO_2 max (mL $\cdot$ min $\cdot$ kg^{-2})**	30.7 ± 1.5^{b}	23.0 ± 1.8^{a}	28.6 ± 2.1^{b}

4.1.2 Physical activity discordant twin pairs (III)

A total of 4 pairs of same-sex twins (2 male and 2 female) with discordant leisure time physical activity (LTPA) were identified from the Finnish Twin Cohort (Table 2). Discordance was based on a questionnaire relating to leisure activity and physical activity. It should be noted that the active twins' average LTPA score (13.8), corresponds to 1 h of running per day, for more than three decades. Conversely, the inactive twins were not sedentary and endured basic levels of physical activity. Participants were instructed not to exercise heavily before their laboratory visits. Muscle biopsies were taken after an overnight fast between 8 am and 10 am and in a similar fashion as in section 4.1.1.

TABLE 2 Characteristics of twin pairs. Mean ± SEM. $^{**}p < 0.001$ with T-Test

	Inactive	**Active**
Number of participants	n=4	n=4
LTPA (MET-hours $\cdot$day^{-1})**	2.9 ± 1.4	13.8 ± 1.0
Age (years)	58.0 ± 2.9	58.0 ± 2.9
VO_2 max (mL $\cdot$ min $\cdot$ kg^{-2})	30.2 ± 1.4	32.8 ± 1.8
Body weight (kg)	71.5 ± 3.4	69.8 ± 5.1
BMI (kg $\cdot$ m^{-2})	25.0 ± 0.6	24.6 ± 1.1
Body fat (%)	24.1 ± 2.9	20.2 ± 3.3
Triglycerides (mmol $\cdot$ L^{-1})	0.9 ± 0.2	1.0 ± 0.3

4.1.3 Electrically stimulated & BCAA treated myotubes (II, III)

Murine C2C12 myoblasts (American Type Culture Collection, ATCC, Manassas, VA, USA) were kept in high glucose-containing Dulbecco's Modified Eagle growth medium (GM) (4.5 g $\cdot$ L^{-1}, DMEM, #BE12-614F, Lonza, Basel, Switzerland) enriched with 10% (v/v) fetal bovine serum (FBS, #10270, Gibco, Rockville, MD, USA), 100 U $\cdot$ mL^{-1} penicillin, 100 µg $\cdot$ mL^{-1} streptomycin (P/S, #15140, Gibco) and 2 mM L-glutamine (#17-605E, Lonza). The cells were seeded on 6-well plates (NunclonTM Delta; Thermo Fisher Scientific, Waltham, MA, USA) until 95-100% confluence was reached. The myoblasts were then rinsed with phosphate-buffered saline (PBS, pH 7.4), and the GM was replaced by differentiation medium (DM) containing high glucose DMEM, 2% (v/v) horse serum (HS, 12449C, Sigma-Aldrich, St. Luis, MO, USA), 100 U $\cdot$ mL^{-1} and 100 µg $\cdot$ mL^{-1} P/S and 2 mM L-glutamine to promote differentiation into myotubes. The DM was replaced on alternate days. Mycoplasma contaminations were negative after cell screening, following the manufacturer's instructions (MycoSPY Master Mix Test Kit, M020, Biontex, München, Germany). The following experiments were duplicatedly conducted on days 5-6 after differentiation.

The myotubes on 6-well plates were acquainted to 0.1 mM oleic acid and 1 mM L-carnitine in normal BCAA DM on day 4 post differentiation. On the next day, the electrodes were placed directly into the wells. The electrical pulse stimulation (EPS) was applied to the cells (1 Hz, 2 ms, 12 V) using a C-Pace pulse generator (C-Pace EM, IonOptix, Milton, MA, USA) for 24 h at 37°C. Then, EPS

was paused after 22 h and target BCAA concentrations were employed to investigate the interactive effects of EPS and BCAA treatments.

The BCAA experiments were carried out for 2 h at 37°C in high-glucose BCAA-free DM (4.5 $g \cdot L^{-1}$, BioConcept, 1-26S289-I, Allschwill, Switzerland). The utilized BCAA concentrations were as follows: 1) cells deprived 0.0 ($mmol \cdot L^{-1}$) of any BCAAs (No BCAA); 2) cells supplemented with 0.8 $mmol \cdot L^{-1}$ of every (Normal BCAA); and 3) cells supplemented with 2.8 $mmol \cdot L^{-1}$ of every BCAA (High BCAA). A resume of the C2C12 study setup can be seen in Table 3.

TABLE 3 Study setup for studying combined effects of EPS and BCAA on C2C12 myotubes. Arrows represent measurements equally performed under EPS conditions.

BCAA concentration	**Rest**	**EPS**
No BCAA (0.0 $mmol \cdot L^{-1}$**)**	Metabolite analysis (II)	→
	Total protein content & citrate synthase (II)	→
	Lipogenesis & Lipid oxidation (II)	→
	Lipid droplet microscopy (II, III)	→
	PLIN2; PLIN5 & PGC-1α microscopy (IIII)	→
	Intensity correlation analysis (III)	→
	Myotube compartmental analysis (cytosol vs. nuclei) (III)	→
	Protein content & mRNA expression (III)	
Normal BCAA (0.8 $mmol \cdot L^{-1}$**)**	Metabolite analysis (II)	→
	Total protein content & citrate synthase (II)	→
	Lipogenesis & Lipid oxidation (II)	→
	Lipid droplet microscopy (II, III)	→
	PLIN2; PLIN5 & PGC-1α microscopy (IIII)	→
	Intensity correlation analysis (III)	→
	Myotube compartmental analysis (cytosol vs. nuclei) (III)	→
	Protein content & mRNA expression (III)	
High BCAA (2.8 $mmol \cdot L^{-1}$**)**	Metabolite analysis (II)	→
	Total protein content & citrate synthase (II)	→
	Lipogenesis & Lipid oxidation (II)	→

4.2 Lipid oxidation & Lipogenesis in C2C12 myotubes (II)

Succinctly, myotubes cultivated in normal BCAA conditions 0.8 $mmol \cdot L^{-1}$) were first acclimatized to dissolved and albumin-complexed 0.1 mM oleic acid (#O3008, Sigma-Aldrich, St. Luis, MO, USA) and 1 mM L-carnitine (C0158, Sigma-Aldrich) in DM on the day 4 post differentiation. The following day, the myotubes were rinsed with PBS and incubated in the oxidation medium containing BCAA-free medium, 0.1 mM oleic acid, 2% (v/v) horse serum, 100 $U \cdot mL^{-1}$ penicillin, 100 $\mu g \cdot mL^{-1}$ streptomycin and 2 mM L-glutamine, 1 mM L-carnitine and 1 $\mu Ci \cdot mL^{-1}$ 9,10-[^{3}H(N)] oleic acid 24 ($Ci \cdot mmol^{-1}$, NET289005MC, PerkinElmer, Boston, MA, USA). The radiolabeled oleic acid was omitted from the negative controls.

4.2.1 Lipogenesis

Lipogenesis was assessed by using ^{3}H-acetate to track lipids as described previously in more detail (Akie & Cooper 2015). To examine the impact of BCAA deprivation or supplementation on lipogenesis, myotubes were washed with PBS and then placed in DM with various BCAA concentrations (see Table 3) on the fifth day after differentiation. To stimulate lipogenesis, 10 µM sodium acetate and 0.5 µCi ^{3}H-acetate were added per well, and myotubes were incubated in the lipogenesis medium at 37°C for 16 h. After the incubation period, cells were washed with PBS and scraped into 0.1 M HCl. An aliquot of the lysate was reserved for total protein content analysis. The lipids were extracted using a mixture of chloroform and methanol, and the samples were centrifuged before the lower phases were transferred to scintillation vials (Akie & Cooper 2015). The amount of radioactivity incorporated into the cellular lipids was measured using scintillation counting and expressed relative to the normal BCAA group.

4.2.2 Lipid oxidation

The lipid oxidation experiment was carried out as previously described (Lautaoja et al. 2021). Target BCAA concentrations (see Table 3) were applied during the 2 h at 37°C to investigate the effect of BCAA deprivation or supplementation on lipid oxidation. After the lipid oxidation experiment, the myotubes were washed with PBS and harvested into PBS-0.1% PBS-Triton X-100 for analysis of total protein content and enzyme activity. The media and PBS were run through Dowex OH resin ion-exchange columns (pH 7.1 · 8-200, Cat no. 217425, Sigma Aldrich). In order to elute the $^{3}H_2O$ produced and released by the myotubes to the media, deionized H_2O was employed. The radioactivity was analyzed as disintegrations per minute (DPM). The scintillation counting technique was used to determine the radioactivity in $^{3}H_2O$ that was integrated with Optiphase HiSafe 3 scintillation cocktail (Cat no. 1200.437, PerkinElmer) using the Tri-Carb 2910 TR Liquid Scintillation Analyzer (PerkinElmer). The outcome was stated in DPM per well. The findings of lipid oxidation were normalized to the BCAA group that was normal.

4.2.3 Nuclear magnetic resonance (NMR) spectroscopy

The lipid oxidation experiment involved collecting and preparing both the cell lysates and experiment media for ^{1}H-NMR analysis. The process of analysis and data interpretation was explained in detail previously (Lautaoja et al. 2021). In short, cold methanol was mixed with media from three wells and cells were scraped into a mixture of aqueous methanol-chloroform. After being lyophilized, the resultant supernatants were reconstituted. An AVANCE III HD NMR spectrometer (Bruker Company, MA, USA) with a cryogenically cooled ^{1}H, ^{13}C, and ^{15}N triple-resonance probe head was used to acquire all of the NMR spectra. The software Chenomx 8.6 was used to evaluate the data (Edmonton, AB, Canada).

4.2.4 Enzyme activity & total protein content

The total protein content was measured using the Bicinchoninic Acid Protein Assay Kit from Pierce Biotechnology (Rockford, IL, USA), while citrate synthase (CS) activity was analyzed using the #CS0720 kit from Sigma-Aldrich. An automated Indiko analyzer from Thermo Fisher Scientific (Vantaa, Finland) was used to perform the analysis following the manufacturers' protocols.

4.3 Western blotting (III)

Briefly, the myotubes were harvested and 10 µg of total protein per samples were loaded on 4%–20% Criterion TGX Stain-Free protein gels (#5678094, Bio-Rad Laboratories, Hercules, CA, USA) before being separated by SDS-PAGE.

To visualize proteins using stain-free technology, the gels were activated and the proteins were transferred to the PVDF membranes. The membranes were then blocked with Intercept Blocking Buffer (#927-70001, LI-COR, Lincoln, NE, USA) followed by overnight incubation at 4°C with primary antibody (PGC-1α, 1:10000, ab191838, Abcam, Cambridge, UK) in Intercept Blocking Buffer diluted (v:v, 1:1) with 0.1% Tween-20 in Tris-buffered saline (TBS).

Membranes were finally incubated with the horseradish peroxidase-conjugated secondary IgG antibody (anti-Rabbit, 1:40000) (Jackson ImmunoResearch Laboratories, West Grove, PA, USA) in Intercept Blocking Buffer diluted (v:v, 1:1) with TBS-0.1% Tween 20. Enhanced chemiluminescence (SuperSignal west femto maximum sensitivity substrate; Pierce Biotechnology, Rockford, IL, USA) and ChemiDoc MP device (Bio-Rad Laboratories) were together used for protein visualization. Stain free (75-250 kDA area of the lanes) was used as a loading control and for the normalization of the results.

4.4 mRNA arrays (III)

Briefly, Trizol-reagent (Invitrogen, Carlsbad, CA, USA) was used to isolate total RNA from the twin muscle biopsies, which were homogenized on FastPrep FP120 apparatus (MP Biomedicals, Illkirch, France). An Illumina RNA amplification kit (Ambion, Austin, TX, USA) was used to obtain biotinlabeled cRNA from 500 ng of total RNA.

Hybridizations to Illumina HumanWG-6 v3.0 Expression BeadChips (Illumina Inc., San Diego, CA, USA) containing probes for *PLIN2* and *PLIN5*, were performed by the Finnish DNA Microarray Center at Turku Center for Biotechnology according to the Illumina BeadStation 500x manual. Hybridized probes were detected with Cyanin-3-streptavidin 1 ($\mu g \cdot mL^{-1}$, Amersham Biosciences, GE Healthcare, Uppsala, Sweden) using Illumina BeadArray Reader (Illumina

Inc.) and BeadStudio v3 software (Illumina Inc.). More details can be found in the work by Leskinen et al. 2010.

The gene expression data and the raw data sets for skeletal muscle have been deposited in the *GEO* database (https://www.ncbi.nlm.nih.gov/geo/query/acc.cgi?acc=GSE20319, accessed on January 5th, 2023).

4.5 Histology (I, II, III)

4.5.1 Sample preparation

Muscle biopsies were cut (5 µm in study I and 8 µm in study III) in a cryostat at -25°C (Leica CM 3000, Germany). Sections were collected onto 13 mm round coverslips. For the myotube experiments, 6-well plates were used containing three 13 mm round coverslips in each well. Measurements were made from 18 coverslips for every experimental group. After the 24 h of EPS, the plates were removed from the incubator and the medium was aspirated.

4.5.2 Fixation, blocking & permeabilization

After the previous steps, all coverslips were immediately fixed in 4% paraformaldehyde for 15 min at room temperature (RT), followed by a $3 \cdot 5$ min wash in PBS. The samples were then incubated for 30 min in blocking buffer (BF; 3% bovine serum albumin (BSA) in study I and 10% goat serum (GS) in studies II and III) in PBS with 0.05% saponin (PBSap) for 30 min at RT. To remove excess serum, a quick 10 seconds wash with PBSap took place before antibody incubation.

4.5.3 Immunohistochemistry (I, III)

Primary antibodies were diluted in 1% BF-PBSap and incubated for 1 h at RT. A $3 \cdot 10$ min wash in PBSap ensued before incubating the secondary antibodies for 1 h at RT. Excess antibody was removed with another $3 \cdot 10$ min wash in PBSap. Cross reactivity was successfully ruled out by carefully controlling every antibody combination. Finally, non-immuno stains were incubated for 30 min and consequently washed $2 \cdot 10$ s with PBS. Active stirring and smooth rocking were a constant in order to grant even staining. Every dye and marker is represented in Table 4.
Every coverslip was mounted on microscopy slides using Mowiol with 2.5% DABCO (Sigma-Aldrich) and left to dry for 24 h in the dark at 4°C. Imaging took place within 48 h after mounting.

TABLE 4 Combination of histochemical markers for each study. *Repeated secondary antibodies over different primary antibodies were incubated in different coverslips.

study	protocol step	product (manufacturer)	host/target	dilution or [concentration]
Diabetic humans (study I)	primary antibodies	M4276 (Sigma, USA)	mouse/fast myosin	1:50
		GP31 (Progen, USA)	guinea pig/PLIN5	1:200
	secondary antibodies	AlexaFluor AMCA (JacksonImmunoResearch, USA)	goat/mouse	1:50
		AlexaFluor 594 (JacksonImmunoResearch, USA)	goat/guinea pig	1:50
	other stains	LipidTOX™ Green (Molecular Probes, USA)	—/neutral lipids	1:100
Twin humans (study III)	primary antibodies	PA1-066 (Thermo Fisher Scientific, USA)	rabbit/Caveolin3	$[2\mu g \cdot mL^{-1}]$
		A4.951 (DSHB, USA)	mouse/slow myosin	$[2\mu g \cdot mL^{-1}]$
		GP47 (Progen, USA)	guinea pig/PLIN2	1:200
		GP31 (Progen, USA)	guinea pig/PLIN5	1:200
	secondary antibodies	Alexa Fluor 405 (JacksonImmunoResearch, USA)	goat/rabbit	1:200
		Alexa Fluor 594 (JacksonImmunoResearch, USA)	goat/mouse	1:200
		Alexa Fluor 488 (JacksonImmunoResearch, USA)	goat/guinea pig*	1:200
		Alexa Fluor 488 (JacksonImmunoResearch, USA)	goat/guinea pig*	1:200
	other stains	LD540 (University of Jyväskylä, Finland)	—/neutral lipids	$[0.1\mu g \cdot mL^{-1}]$
C2C12 myotubes (studies II & III)	primary antibodies	MF-20 (DSHB, USA)	mouse/sarcomere	$[5\mu g \cdot mL^{-1}]$
		GP31 (Progen, USA)	guinea pig/PLIN5	1:200
		ab52356 (Abcam, USA)	rabbit/PLIN2	$[5\mu g \cdot mL^{-1}]$
		ab191838 (Abcam, USA)	rabbit/PGC-1α	$[5\mu g \cdot mL^{-1}]$
	secondary antibodies	Alexa Fluor 647 (Thermo Fisher Scientific, USA)	donkey/mouse	1:200
		Alexa Fluor 488 (Thermo Fisher Scientific, USA)	goat/guinea pig	1:200
		Alexa Fluor 594 (Thermo Fisher Scientific, USA)	donkey/rabbit*	1:200
		Alexa Fluor 594 (Thermo Fisher Scientific, USA)	donkey/rabbit*	1:200
	other stains	LD540 (University of Jyväskylä, Finland)	—/neutral lipids	$[0.1\mu g \cdot mL^{-1}]$
		DAPI (Thermo Fisher Scientific, USA)	—/nuclei	$[5\mu g \cdot mL^{-1}]$

4.6 Microscopy (I, II, III)

4.6.1 Instruments

For study I, widefield data was collected with an BX50 BXFLA microscope (Olympus, Japan) and a ColorViewIII camera (Soft Imaging Systems, Germany), through a FLUAR 40×/0.7 objective (Olympus, Japan). The secondary antibody conjugates were excited with a mercury lamp, via U-MWB, U-MWU and MWG excitation cubes.

For studies II and III, confocal data was collected with a LSM700 microscope (Zeiss, Germany), using a 20×/0.8 (Twin study) and a 63×/1.4 oil (C2C12 studies) Plan-Apochromat objectives (Zeiss, Germany). The selected antibody conjugates were excited with 405 nm, 488 nm, 555 nm or 639 nm laser lines.

4.6.2 Acquisition & controls

For each channel in study I, fluorescence data was acquired as gray signal via the software *AnalySIS 5.0* (Soft Imaging Systems, Germany). Mild exposure time and a dimming filter were used to decrease bleed-through to negligible levels.

Confocal images in studies II and III were acquired with the *ZEN black* software (Zeiss, Germany). Voxel size was set to 0.31 µm · 0.31 µm · 2.4 µm in the Twin study and 0.1 µm · 0.1 µm · 1.0 µm in the C2C12 studies. Any potential bleed through was completely ruled out by single track imaging and secondary

dichroic mirror configuration for each channel separately. In all cases, control samples incubated solely with secondary antibodies were used to set background values.

4.7 Batch processing & analyses (I, II, III)

4.7.1 Denoising & Deconvolution

All collected images were subject to linear denoising with soft background subtraction before deconvolution. Applying the *Richards & Wolf 3D optical model* with *PSF Generator* (Kirshner et al. 2013) in *Fiji* (Schindelin et al. 2012), a theoretical point spread function was created separately for each wavelength in each dataset and respective voxel size. Deconvolution was achieved by applying the *Richardson & Lucy* algorithm with the *DeconvolutionLab2* plugin (Sage et al. 2017) in *Fiji* (Schindelin et al. 2012). Additionally and in conjunction with the previous, 0.5 µm TetraSpeck microbeads (Molecular Probes, USA) were imaged for particle size calibration and validation.

4.7.2 Segmentation & Classification

In study I, given a high number of low quality samples, intact myofibers were pre selected with the aid of a Cadboy drawing tablet (NGS technologies, China). Fiber types were classified either as type I or type II depending on a thresholded value for the stained fast myosin. Additionally, every LD (all-LDs) was further classified as coated (col-LDs) or uncoated (unc-LDs) by PLIN5, after performing colocalization analysis in *Fiji* (see 4.7.4). Segmentation, classification and measurements of cells and intracellular particles were performed with *TopoCell*, an *ImageJ* plugin developed for this study (Fachada et al. 2012).

In studies II and III, cell segmentation was achieved in *Fiji* by a machine learning approach in teaching the computer how to recognize C2C12 myotubes and human myofiber sarcolemma, using *Trainable Weka Segmentation* (Arganda-Carreras et al. 2017). By the same means, myotube nuclei and cytosol were also classified for later analysis.

4.7.3 Intracellular particle density

In study I the intracellular density of the studied markers was measured as area fraction, i.e., dividing the total area of the binarized marker particles by the cross sectional area of the cell, expressed as percentage. Additionally, the same method was implemented in study II in order to count the number of individual lipid droplets. For studies II and III, intracellular density of each studied marker was measured directly as the mean non-binarized signal after denoising and deconvolution.

4.7.4 Intensity correlation analysis

The non-random colocalization between pixel intensity of different channels was assessed through intensity correlation analysis (ICA), implemented accordingly to Costes et al. (Costes et al. 2004), using *Coloc 2* (ImageJ.net 2018) in *Fiji*.

In the case of study I, ICA was performed in order to generate col-LDs from IMCL and PLIN5 signals, and from there deduce unc-LDs. The main objective being the comparison of the size and distribution of binarized col-LDs and unc-LDs between study groups. On the other hand, in study III, ICA was used to more closely compare the degree the level of association between the studied markers amongst the study groups.

4.7.5 Subcellular localization

In study I, using *TopoCell* (Fachada et al. 2012) in *ImageJ*, individual intramyocellular particles were measured for their size and subcellular coordinates after binarized. Each particle coordinate was then measured against the closest point of the sarcolemma of its respective cell, generating a distance value for each particle. All *ImageJ* routines coded for this purposes can be found online (https://github.com/seiryoku-zenyo/Diabetic-study, accessed on March 1st, 2023).

However, in study III, the approach was slightly different. While in human twin data the intracellular signal was only differentially measured between fiber types, in myotubes every marker was measured separately from the cytosol and the nuclei. The *Fiji* routines coded for this purpose can also be found online (https://github.com/seiryoku-zenyo/twinC2C12-studies, accessed on March 1st, 2023).

4.8 Data analysis (I, II, III)

4.8.1 Data crunching

The 'comma-separated values' generated with *Fiji* were then imported and cleaned as working dataframes in the *pandas* (pandas development team 2020) in *Pyhton 3.9.0*.

For the diabetic human study (I), values from each single particle analyzed were averaged into cellular values, followed by further averaging by fiber type into a final participant mean value. Thus, human participants configured the statistical cases as seen in Table 1 for the box blot figures. For particle intracellular localization in function of their size, from each fiber type and particle type, 500 LDs per participant were drawn at random into a pool representing each group, and then 3000 LDs were drawn at random from each pool.

In the twin human dataset (III), given the very low number of participants,

individual muscle fibers composed the statistical cases (Table 2). Since there were no segmented particle measurements, no averaging was required. Finally, outliers were identified and removed via z-score (2 standard deviations).

Concerning the C2C12 myotubes (II, III), from each coverslip, the two closest values per variable were averaged. Then from each well, the mean values from the two closest coverslips were also averaged. To control for batch variability, all values were normalized against the control group (Normal BCAA | Rest). Outliers were equally processed as in the twin dataset above.

4.8.2 Statistics

Concerning the diabetic dataset (study I), group and fiber type differences were investigated by a two-way analysis of variance (ANOVA2), while post-hoc evaluation was carried through Mann-Whitney U tests. Lastly, correlation analyses were conducted by Spearman's rank correlation coefficient. The significance levels were set for $p < 0.05$ and $p < 0.01$.

In study III, group or fiber type comparisons were performed using either the Mann-Whitney U-test or the t-test, depending on the data distribution. The effect of interaction was tested using ANOVA2. The ICA between different markers was tested using the Manders split coefficient test. In the twin human dataset, due to the large number of myofibers, the levels of significance were set to $p < 0.01$ and $p < 0.001$. For the C2C12 data, significance levels were set to $p < 0.05$ and $p < 0.01$.

Relatively to study II, if normality criteria were met, differences between groups were assessed using one-way analysis of variance (ANOVA1) followed by independent-samples t-test. If the normality criterion was not met, the Kruskal-Wallis test followed by the Mann-Whitney U test was used to assess differences between groups. Levels of significance were set to $p < 0.05$, $p < 0.01$ and $p < 0.001$.

In all studies, the Shapiro-Wilk test and histogram analysis were used to determine normality. All variable sets prepared in *pandas* dataframes were statistically analyzed with the *SciPy* and *statsmodels* modules in *Python 3.9.0* (Seabold & Perktold 2010; Virtanen et al. 2020).

4.8.3 Visualization

Boxes in the boxplot figures depict interquartile ranges and medians, while whiskers represent the 95% confidence interval, unless stated otherwise. The dots within the boxes represent statistical cases. The significant main effects tested by ANOVA1, ANOVA2 or Kruskal-Wallis test are depicted by the # symbol, while the significant interacting effects between variables are depicted with the & symbol. The significant effects measured by t-student, Mann-Whitney U and Spearman's ρ tests are depicted with the * symbol. Double or triple symbols signify reaching the established significance levels.

In study I, the intracellular distribution of differently sized particles was

probabilistically visualized by density kernel estimation (KDE), see sections 4.8.1 and 5.1.4. The Spearman's ρ was visualized by line charts where the shaded areas represent bootstrapped 95% confidence intervals for the fitted regressions (5.1.5). Data visualization in every publication was produced with *seaborn* and *matplotlib* in *Python 3.9.0* (Hunter 2007; Waskom & the seaborn development team 2020).

5 RESULTS

5.1 Lipid droplets and PLIN5 coating in insulin resistance (I)

5.1.1 Increased PLIN5-uncoated IMCL in insulin resistant type II fibers

There were no discernible changes between the groups in the proportion of total LDs (all-LDs), despite the tendency of increasing IMCL in T2D and OB. Nonetheless, type I fibers had a substantially greater all-LDs proportion when compared to type II fibers among groups, as expected ($p < 0.05$). As shown in Figure 7a, these fiber type changes were primarily caused by variations within the HC and T2D groups ($p = 0.02$ and $p = 0.032$, respectively).

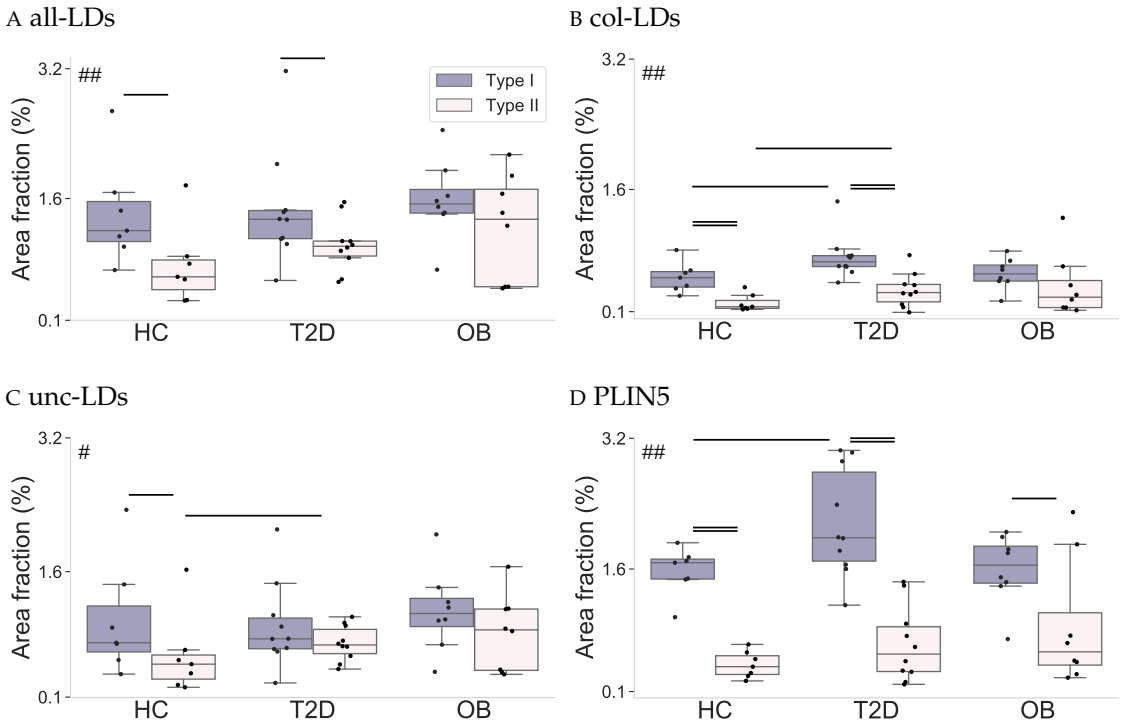

FIGURE 7 Area fraction for a) all-LDs; b) col-LDs; c) unc-LDs and d) PLIN5. Fiber type differences by ANOVA2 denoted with #($p < 0.05$) and ##($p < 0.01$). Post hoc statistical significance is denoted with horizontal bars ($p < 0.05$) or double horizontal bars ($p < 0.01$).

With respect to the area fraction of uncoated LDs (unc-LD), HC retained differences between fiber type ($p = 0.048$), whereas T2D lost these differences ($p = 0.240$). As a result, as seen in Figure 7c, type II fibers in T2D exhibited a significantly higher unc-LD fraction than the same fiber type in HC (P = 0.044). This phenomenon can be observed in representative Figure 8.

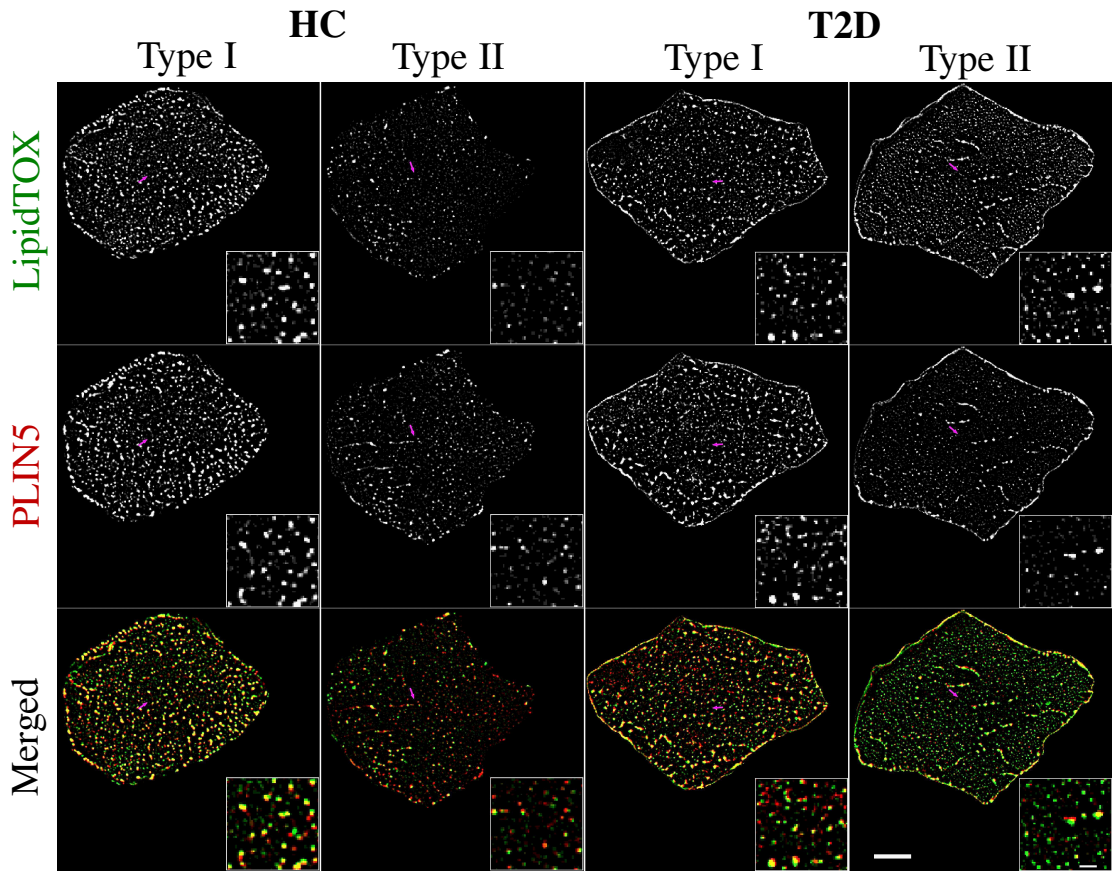

FIGURE 8 Representative image of IMCL and PLIN5 in different fiber types of diabetic vs. lean participants. Note greener type II fibers in T2D, depicting increased IMCL (green) unattended by PLIN5 (red). Small boxes correspond to the area pointed by magenta arrows. Large bar = 10 µm; small bar = 2 µm.

More overtly than all-LD, significant differences in PLIN5 area fraction were found between fiber types throughout all groups ($p < 0.001$) and within each group ($p = 0.001$ for HC, $p < 0.001$ for T2D and $p = 0.041$ for OB), as seen in Figure 7d. The increase in PLIN5 area fraction in type I fibers was particularly pronounced in T2D, and post-hoc revealed significantly higher values when compared to the same fiber type in HC ($p = 0.029$). Interestingly, the same PLIN5 area fraction increase in type I fibers in T2D vs. HC was not observed in type II fibers ($p = 0.200$).

In addition to the higher PLIN5 area fraction in type I fibers, T2D also showed a significantly higher percentage of colocalized (col-LD) than HC in both fiber types ($p = 0.014$ for type I fibers and $p = 0.036$ for type II fibers). See Figure 7b.

5.1.2 Uncoated droplets are larger in diabetic type II fibers

Regarding the size of LDs, notable variations in the diameter of LDs in all groups were observed ($p = 0.008$), particularly in type II muscle fibers ($p = 0.021$). The data presented in Figure 9a indicates that these differences are mainly due to the

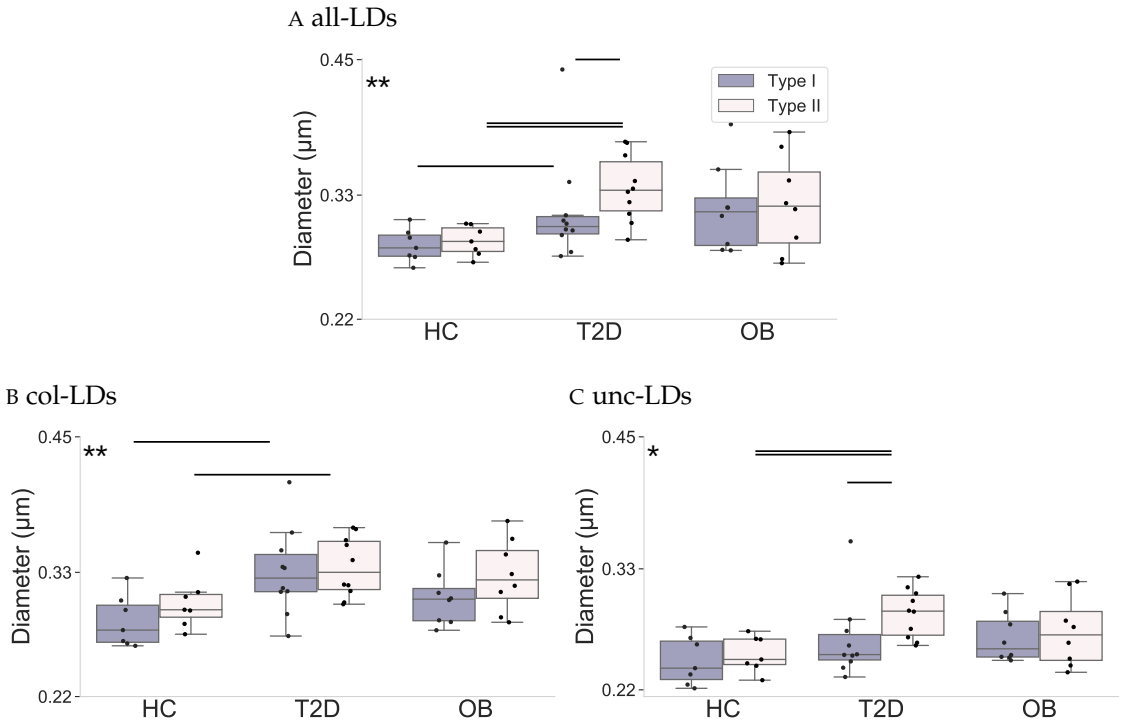

FIGURE 9 Size of a) all-LDs; b) col-LDs and c) unc-LDs. Group differences by ANOVA2 denoted with *($p < 0.05$) and **($p < 0.01$). Post hoc statistical significance is denoted with horizontal bars ($p < 0.05$) or double horizontal bars ($p < 0.01$).

larger size of LDs in T2D when compared to HC individuals, with a significance level of $p = 0.029$ for type I fibers and $p = 0.001$ for type II fibers.

Although ANOVA2 did not reveal any differences in fiber type among all groups, T2D individuals were discovered to have significantly larger LDs in type II muscle fibers compared to type I fibers ($p = 0.027$). Interestingly, the differences in LD size appear to arise from unc-LDs ($p = 0.070$) rather than col-LDs, as shown in Figure 9b-c, where the differences between fiber types vanish ($p = 0.760$).

In all groups, it was observed that the size of col-LDs was greater than that of unc-LDs in both types of fibers, as anticipated ($p < 0.010$).

5.1.3 Uncoated droplets lay deep inside diabetic type II fibers

Although there were no significant differences between groups ($p = 0.120$) or fiber types ($p = 0.300$) with ANOVA2, the HC group tended to have LDs that were closer to the sarcolemma, as demonstrated in Figure 10a. Interestingly, HC type II fibers had significantly closer LDs to the sarcolemma than type I fibers $p = 0.027$. In addition, HC type II fibers had LDs that were significantly closer to the sarcolemma than the same fiber type in T2D individuals ($p = 0.018$), which indicates a difference in the internalization of LDs between the two groups. This observation seems to originate from unc-LDs, as shown in Figure 10c.

It is noteworthy that ANOVA2 did reveal that PLIN5 was significantly closer to the sarcolemma in type II fibers ($p = 0.032$), although it did not detect any significant differences between groups ($p = 0.070$), as illustrated in Fig-

ure 10d.

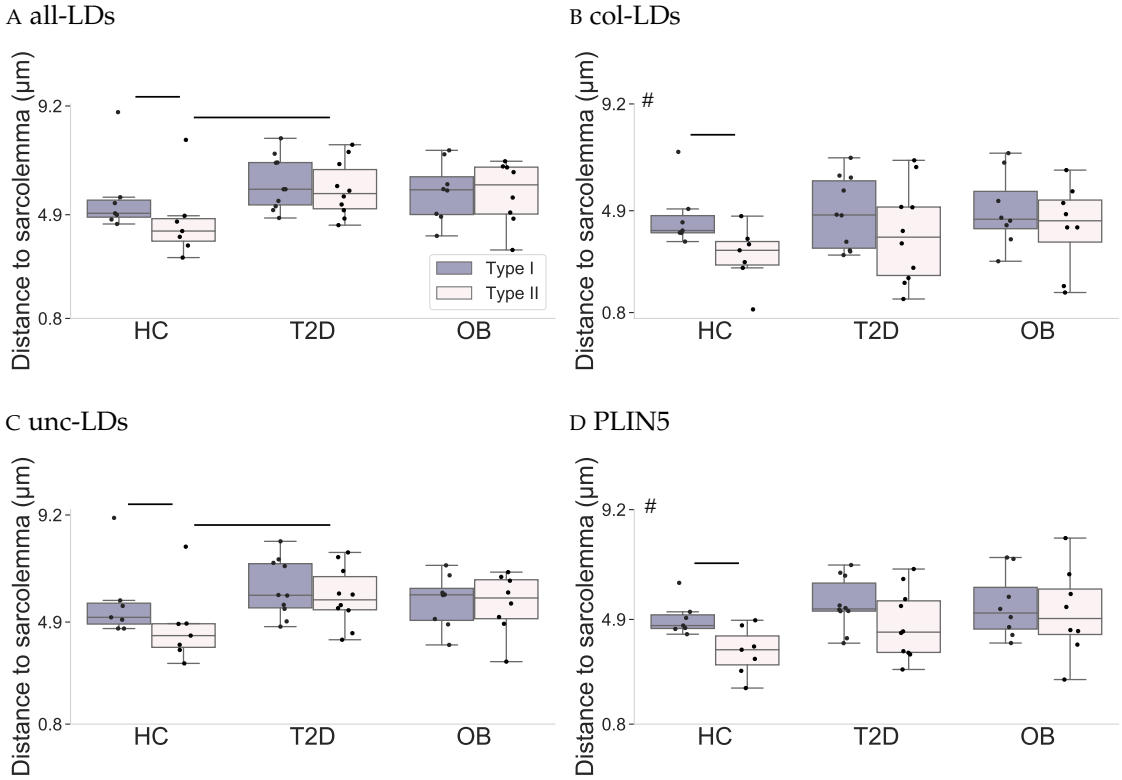

FIGURE 10 Distance to sarcolemma of a) all-LDs; b) col-LDs; c) unc-LDs and d) PLIN5. Fiber type differences by ANOVA2 denoted with #($p < 0.05$). Post hoc statistical significance is denoted with horizontal bars ($p < 0.05$).

5.1.4 Larger and deepest LDs in diabetic type II fibers are left uncoated

After observing the increased percentage and size of unc-LDs in the deeper subcellular regions of type II fibers in T2D individuals, it was decided to investigate this relationship further. To do so, a bivariate kernel density estimation was plotted for the diameter and subcellular location of LDs (Figure 11). The analysis revealed a distinct sub-population of enlarged unc-LDs in inner regions of type II fibers only in T2D, as illustrated in Figure 11b.

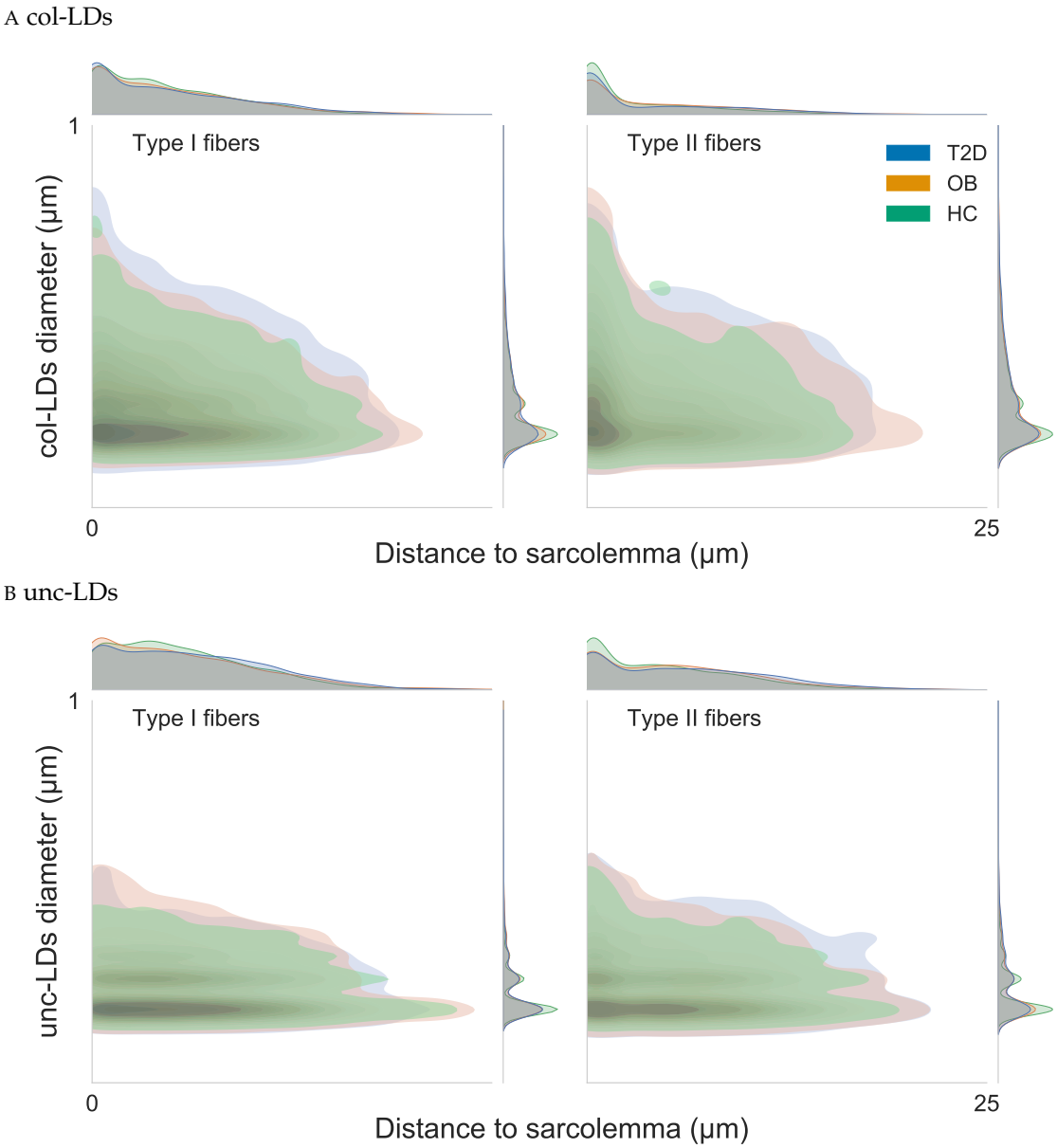

FIGURE 11 Large lipid droplets uncoated from PLIN5 in inner parts of diabetic type II fibers. The plots depict the bivariate kernel density estimation between diameter and distance to sarcolemma of a) colocalized lipid droplets (col-LDs) and b) uncoated lipid droplets (unc-LDs). From each fiber type and particle type, 500 LDs per subject were randomly selected into a pool representing each group, then from each pool, 3000 LDs were randomly selected to generate the present figure.

Interestingly, in all groups and fiber types, the largest LDs were consistently found close to the sarcolemma and associated with PLIN5. This pattern was particularly evident in type II fibers, where a relatively low density col-LDs was observed in the inner regions of the cells, as shown in Figure 11a.

5.1.5 PLIN5 coated LDs correlate with VO_2max

Finally, it is worth reporting that a strong correlation (ρ= 0.760, $p = 0.011$) was found between unc-LDs in type II fibers and VO_2max, but this was observed only in T2D individuals, as shown in Figure 12b.

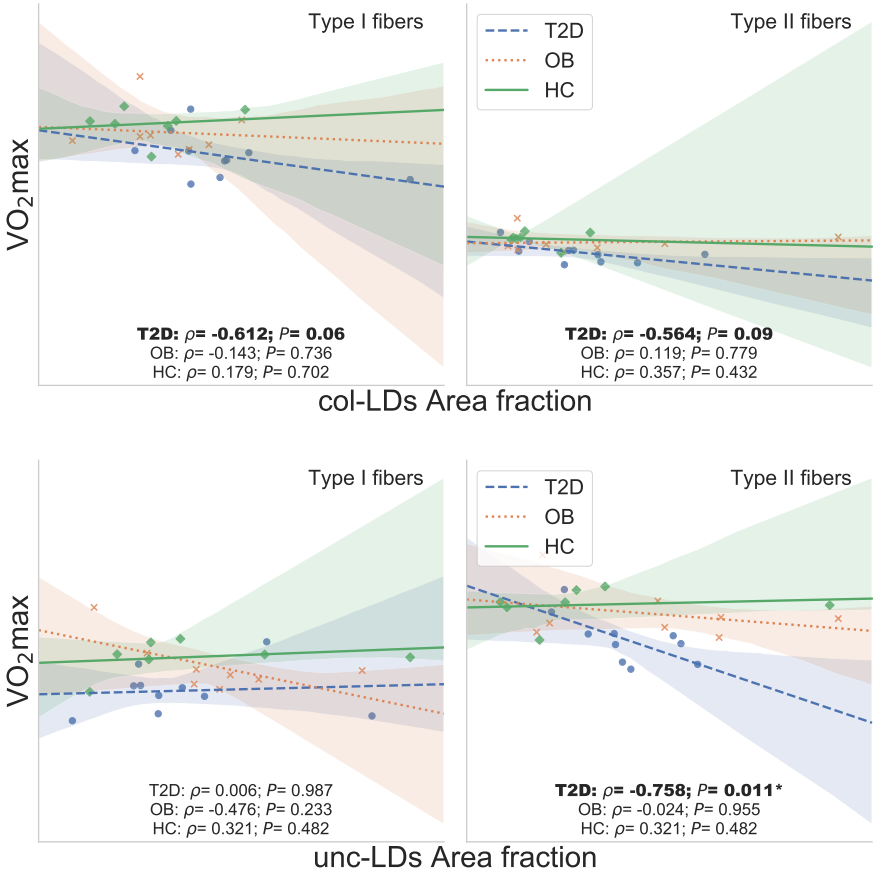

FIGURE 12 Uncoated LDs significantly correlate with lower VO_2 max only in diabetic type II fibers. Plot shows the linear association between VO_2 max and area fraction of a) colocalized lipid droplets (col-LDs) and b) uncoated lipid droplets (unc-LDs). Shaded areas show bootstrapped 95% confidence intervals for the fitted regressions. Bold signifies $|\rho| > 0.5$; *$p < 0.05$.

5.2 Intramyocellular lipids, PLIN2 and PLIN5 in long-term physical activity (III)

The twin pairs with discordant physical activity provided an excellent model to investigate the effects of long-life physical activity regardless of the genetic background. Below the reader can read specifically the effects on IMCL, PLIN2, PLIN5 and their associations in different fiber types.

5.2.1 Type I Fibers in active Twins exhibit higher levels of IMCL

Regarding the twin participants described in Table 2, type I fibers showed more IMCL than type II fibers, which was expected and confirmed by Figure 13A-C with statistical significance ($p < 0.001$). Notably, physically active twins had more IMCL in their type I fibers compared to their inactive twin ($p < 0.001$, Figure 13B-C), but there was no difference in type II fibers due to LTPA. Active twins also had a significant difference in IMCL between fiber types ($p < 0.001$), which was not observed in inactive twins ($p = 0.064$), as shown in Figure 13C.

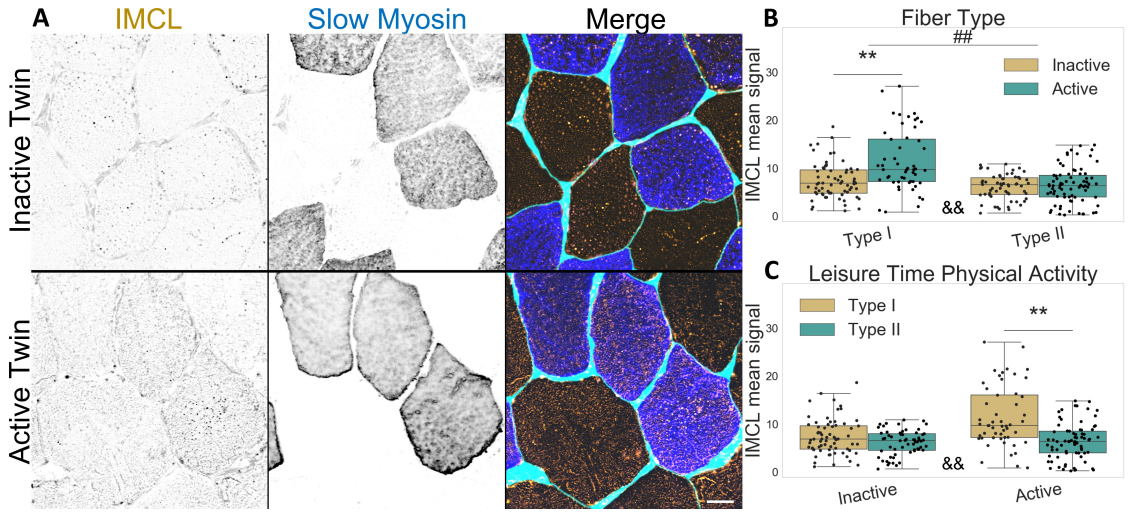

FIGURE 13 IMCL mean signal intensity between twin pairs. (**A**) representative image showing differences between groups. Gray level indicates signal, cyan indicates segmented sarcolemma. Note the active twin type I fibers with higher IMCL signal; Bar = 20 µm; (**B**) fiber type as main effect, with LTPA combined; (**C**) LTPA main effect, with fiber type combined; main effect differences denoted with **##** ($p < 0.001$); combined group differences denoted with ****** ($p < 0.001$); interacting effect between fiber type and LTPA denoted with **&&** ($p < 0.001$). Dots in **B** and **C** represent individual muscle fibers.

As anticipated, IMCL associated with PLIN5 was significantly higher in type I fibers than in type II fibers ($p = 0.001$, Figure 14A-B), with no differences observed between twin pairs (Figure 14B-C). Lastly, both PLIN5 mRNA levels and PLIN5 confocal mean signal remained unchanged between twin pairs (III).

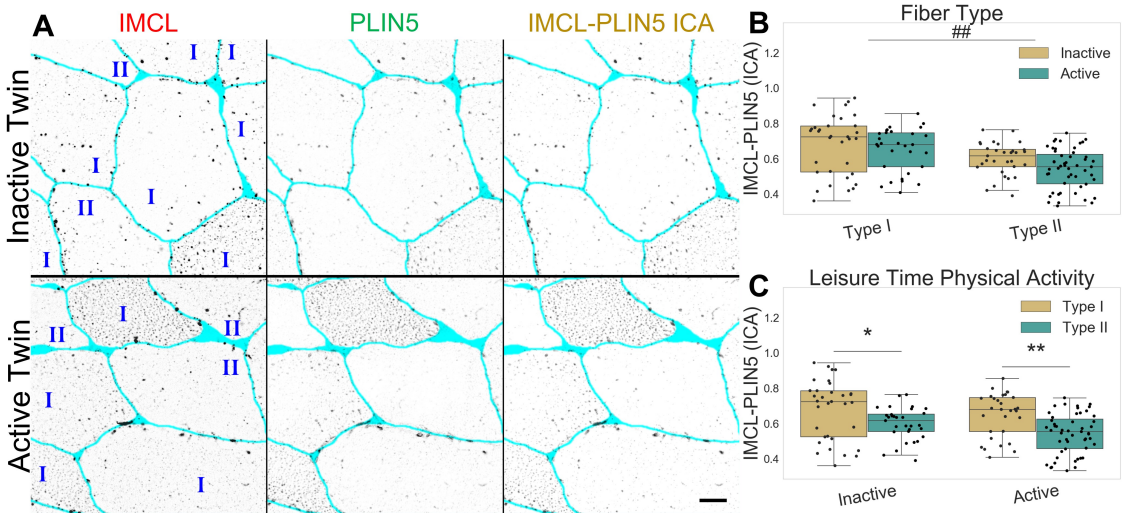

FIGURE 14 IMCL-PLIN5 intensity correlation analysis in twin pairs. (**A**) representative image showing differences between groups. Gray level indicates signal, cyan indicates segmented sarcolemma. Bar = 20 µm; (**B**) fiber type as main effect, with LTPA combined; (**C**) LTPA main effect, with fiber type combined. Main effect differences denoted with **##** ($p < 0.001$). Combined group differences denoted with * ($p < 0.01$) and ** ($p < 0.001$). Dots in **B** and **C** represent individual muscle fibers.

5.2.2 Inactive twins with decreased IMCL-PLIN2 association

The twin pairs who are not physically active exhibit a reduced association between IMCL and PLIN2 ($p = 0.008$), primarily due to a substantial decrease in type II fibers ($p < 0.001$, Figure 15A-C). Despite no disparities in PLIN2 mean signal or PLIN2 mRNA levels between fiber types or physical activity levels (III). Together, this indicates that PLIN2's ability to target IMCL is distinctly restricted in type II fibers of inactive twins.

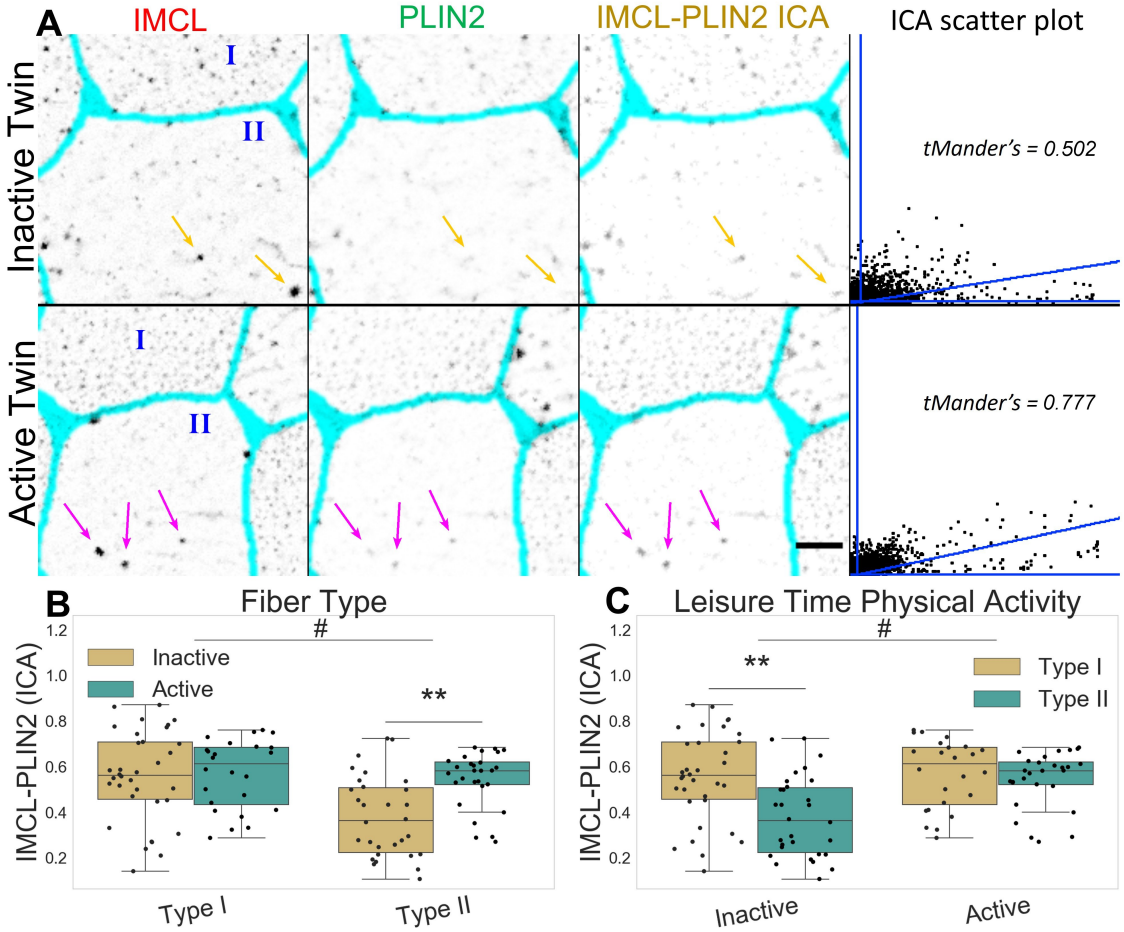

FIGURE 15 IMCL-PLIN2 intensity correlation analysis in twin pairs. (**A**) representative image showing differences between groups. Gray level indicates marker signal, cyan indicates segmented sarcolemma. Note active twin type II fiber with high intensity IMCL significantly colocalized by PLIN2 (magenta arrows), unlike the inactive twin (orange arrows). Bar = 10 µm. Scatter plot is relative to the arrowed type II fiber; (**B**) fiber type as main effect, with LTPA combined; (**C**) LTPA as main effect, with fiber type combined, main effect differences denoted with **#** ($p < 0.010$); combined group differences denoted with ** ($p < 0.001$). Dots in **B** and **C** represent individual muscle fibers.

5.3 Effects of amino acids and muscle contractions in myotubes (II, III)

In order to complement the observations made from the human studies, it was decided to investigate the impacts of EPS-derived muscle contractions and BCAA availability in C2C12 myotubes.

More concretely, the objective was to assess the combined effects that BCAA and EPS have in myotube lipid metabolism, focusing on IMCL turnover, subcellular localization and association with other key participants in the energy and

BCAA metabolisms, such as PLIN2, PLIN5 and PGC-1α.

5.3.1 BCAA deprivation decreases BCAA degradation products, total protein and citrate synthase enzyme activity (II)

To verify that our cell culture medium without BCAAs contained very low levels of BCAAs, and that adding normal levels of BCAAs led to substantially higher levels of both BCAAs and their degradation products, NMR-based metabolomics were conducted on the C2C12 cells and their cell media (Table 5). Our findings confirmed that myotubes cultured with No BCAA had lower levels of both pooled and individual BCAAs than myotubes cultured with Normal BCAA ($p = 0.004$, Table 5). Moreover, the cell culture media of myotubes cultured without BCAAs had lower levels of both pooled and individual BCAAs, as well as lower pooled BCAA degradation products than myotubes cultured with BCAAs, indicating reduced BCAA degradation in cells treated with the no BCAA medium ($p = 0.014$, Table 5).

TABLE 5 Metabolites measured via ^{1}H-NMR spectroscopy both within the cells and in the culture media (μM). Data is presented as mean (SEM). Metabolites with significant p-values are marked with *.

	Metabolite (μM)	**No BCAA control**	**No BCAA EPS**	**Normal BCAA control**	**Normal BCAA EPS**	**p (BCAA)**	**p (EPS)**
Myotubes (n=3/group)	Pooled BCAAs*	6.6(3.8)	14.0(8.1)	213.9(123.5)	275.8(159.2)	0.004*	0.749
	Isoleucine*	2.0(1.2)	4.4(2.6)	75.7(43.7)	97.4(56.2)	0.004*	0.749
	Leucine*	2.3(1.3)	4.7(2.7)	66.0(38.1)	85.4(49.3)	0.004*	0.749
	Valine*	2.3(1.3)	4.8(2.8)	72.2(41.7)	93.0(53.7)	0.004*	0.749
	Pooled BCAA degradation products	0.0(0.0)	0.0(0.0)	2.2(1.3)	2.1(1.2)	0.140	0.902
	Isobutyrate	0.0(0.0)	0.0(0.0)	0.3(0.2)	0.3(0.2)	0.138	1.000
	Isovalerate	0.0(0.0)	0.0(0.0)	0.9(0.5)	0.7(0.4)	0.140	0.902
	2-Methylbutvrate	0.0(0.0)	0.0(0.0)	1.0(0.6)	1.1(0.7)	0.140	0.902
Cell media (n=2-3/group)	Pooled BCAAs*	23.4(16.5)	36.9(26.1)	1717.3(1214.3)	1789.0(1032.9)	0.014*	0.806
	Isoleucine*	8.2(5.8)	12.7(9.0)	629.1(444.8)	646.0(372.9)	0.014*	0.806
	Leucine*	6.8(4.8)	10.9(7.7)	475.5(336.2)	509.5(294.1)	0.014*	0.806
	Valine*	8.4(6.0)	13.3(9.4)	612.8(433.3)	633.6(365.8)	0.014*	1.000
	Pooled BCAA degradation products*	6.6(4.6)	10.6(7.5)	46.9(33.2)	46.8(27.0)	0.014*	1.000
	Isobutyrate	0.7(0.5)	0.7(0.5)	3.6(2.5)	2.1(1.2)	0.121	1.000
	Isovalerate	1.2(0.8)	1.1(0.7)	10.2(7.2)	6.8(4.0)	0.121	1.000
	2-Ketoisovalerate	0.8(0.6)	1.5(1.1)	3.5(2.5)	5.1(2.9)	0.348	0.184
	2-Methylbutyrate	1.3(0.9)	1.3(0.9)	10.3(7.3)	5.5(3.2)	0.121	1.000
	3-Methyl-2-oxovalerate	1.5(1.1)	3.3(2.3)	9.3(6.6)	13.5(7.8)	0.355	0.127
	2-Oxoisocaproate	1.1(0.8)	2.7(1.9)	10.0(7.1)	13.8(8.0)	0.355	0.275

The effects of BCCA were additionally investigated for total protein contents and CS activity (Figure 16). When compared to both Normal | BCCA and High | BCAA, the deprivation of BCAA resulted in significant decrease of total protein content and CS activity (Figure 16A-B). Interestingly, such impacts seem to originate mostly from isoleucine (Figure 16C-D).

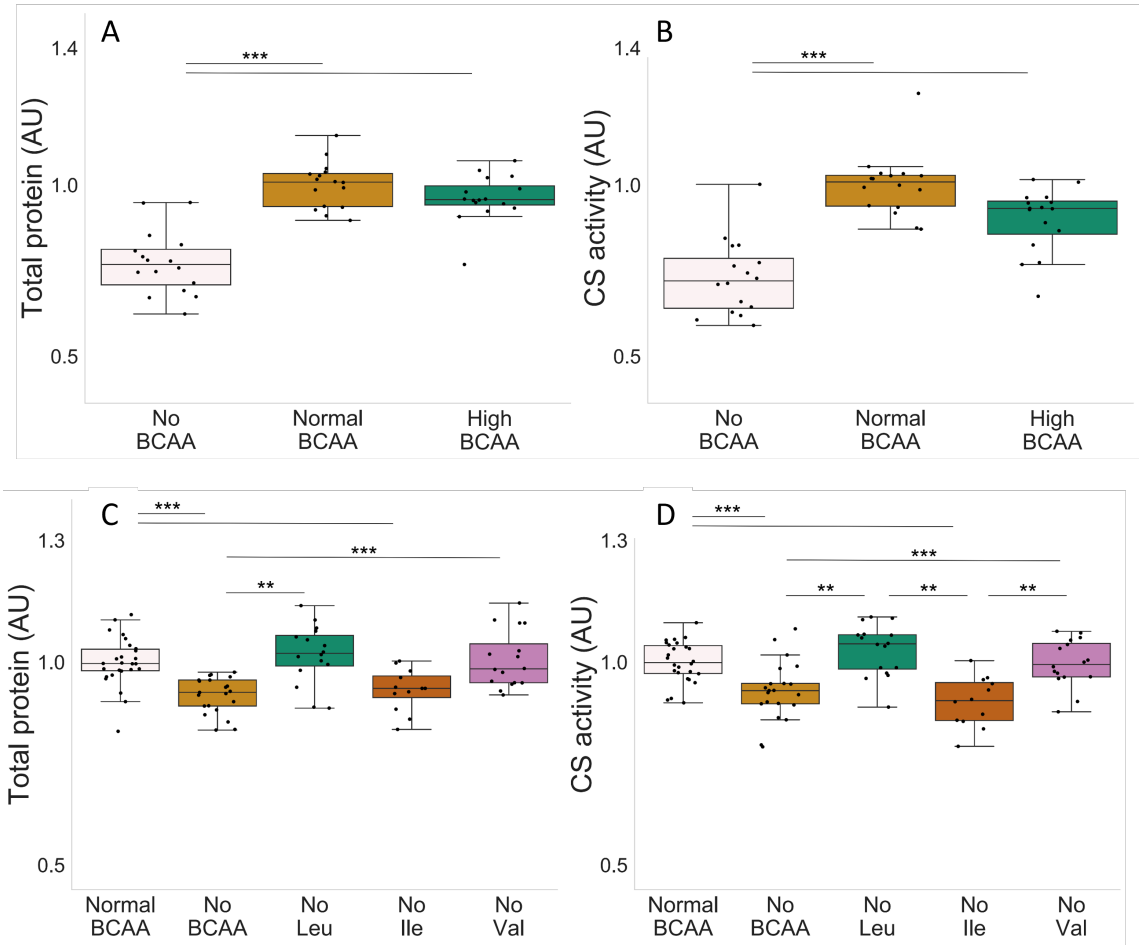

FIGURE 16 Effects of all BCAAs on total protein content (**A**) and CS activity (**B**). Effects of individual BCAAs on total protein content (**C**) and CS activity (**D**). * ($p < 0.050$), ** ($p < 0.010$), *** ($p < 0.001$).

5.3.2 BCAA deprivation hampers lipogenesis and lipid oxidation (II)

The lipid oxidation experiments evaluated the ideal BCAA supplementation using the three distinct BCAA concentrations explained in 4.1.3 and resumed in Table 3. The concentration of $0.8\text{mmol} \cdot \text{L}^{-1}$ resulted in the most significant lipid oxidation among the three concentrations tested (Figure 17A, $p < 0.001$). Consequently, it was named Normal BCAA and it was selected as the reference level for the lipid oxidation tests. Both Normal BCAA and High BCAA resulted in more significant lipogenesis than the absence of BCAA (Figure 17B, $p = 0.021$). As there was no notable difference between Normal and High BCAA supplementation ($p = 0.093$), the same concentration as utilized in the oxidation experiment was selected as the control level for the lipogenesis experiment.

In addition to the effects of all BCAAs combined, individual BCAA were also tested in lipogenesis and lipid oxidation. The removal of leucine ($p = 0.046$) and isoleucine ($p < 0.001$), but not valine ($p = 0.070$), was found to reduce lipid oxidation. Furthermore, lipid oxidation was diminished even further in the isoleucine deprivation group when compared to the groups that experienced

leucine and valine deprivation ($p = 0.004$, as illustrated in Figure 17C). In the myotubes, the absence of all BCAAs resulted in decreased lipogenesis ($p < 0.001$) as demonstrated in Figure 17D when compared to the presence of normal BCAA. Similarly, when a single BCAA was eliminated at a time (valine, leucine, or isoleucine), lipogenesis decreased compared to normal BCAA ($p < 0.001$); however, the decrease was not as substantial as when all BCAAs were absent (no Leu, no Ile, or no Val compared with no BCAA, $p = 0.003$).

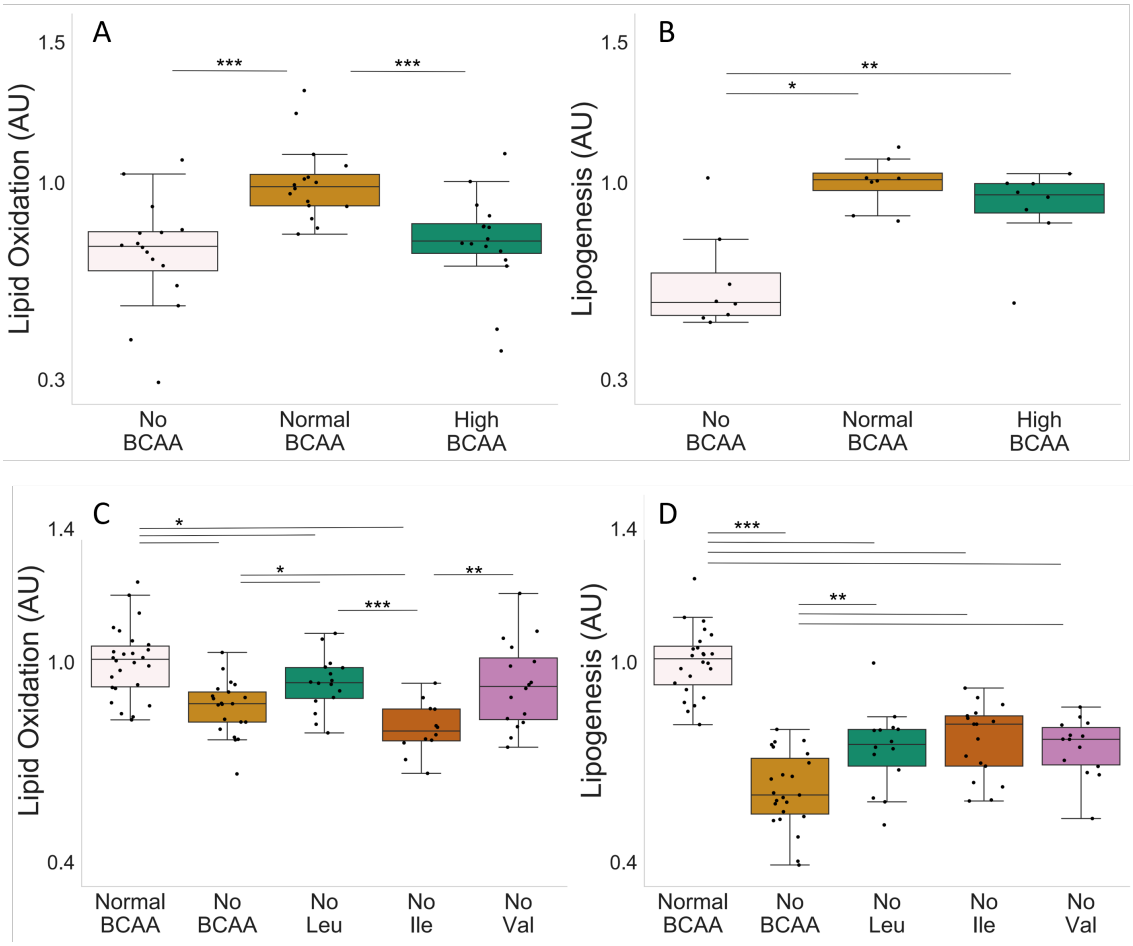

FIGURE 17 Lipid oxidation (**A**) and lipogenesis (**B**) in C2C12 cells with different BCAA levels. Lipid oxidation (**C**) and lipogenesis (**D**) in C2C12 deprived from different individual BCAAs. * ($p < 0.050$), ** ($p < 0.010$), *** ($p < 0.001$).

Figure 18 displays the results of experiments examining the effects of supplementing the three levels of BCAA with and without EPS. The data indicates that EPS reduced lipid oxidation regardless of BCAA levels, with a significant effect observed ($p = 0.023$, Figure 18A-B). Interestingly, only when combined with EPS, high BCAA levels reduced lipid oxidation ($p = 0.032$). The deprivation of BCAA reduced lipogenesis in both control ($p = 0.002$) and EPS-treated ($p = 0.022$) myotubes, as seen in Figure 18C.

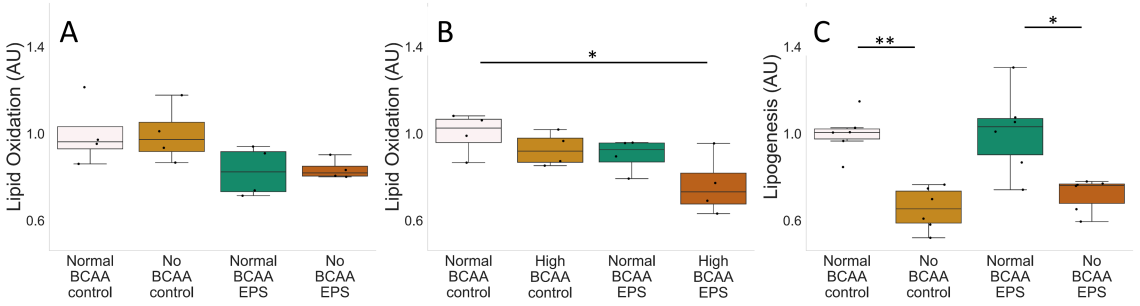

FIGURE 18 Lipid oxidation, BCAA deprivation and EPS in C2C12 cells with Normal (**A**) and High (**B**) BCAA levels; and lipogenesis with BCAA deprivation and EPS (**C**). * ($p < 0.050$), ** ($p < 0.010$).

5.3.3 Subcellular outline of IMCL, PLINs and PGC-1α (III)

Afterwards, PGC-1α's association with IMCL and PLIN5 was investigated in different compartments of myotubes, as it plays a crucial role in regulating energy metabolism and interacts with PLIN5 in the nucleus. The compartmental analysis demonstrated a substantial distinction ($p < 0.001$) in the signals between cytosolic and nuclear markers in myotubes. IMCL and PLIN5 had the highest nuclear signals, while only a small portion of PLIN2 was detected above the background ($p < 0.001$) and sometimes in a particle-like pattern (Figure 19A-B).

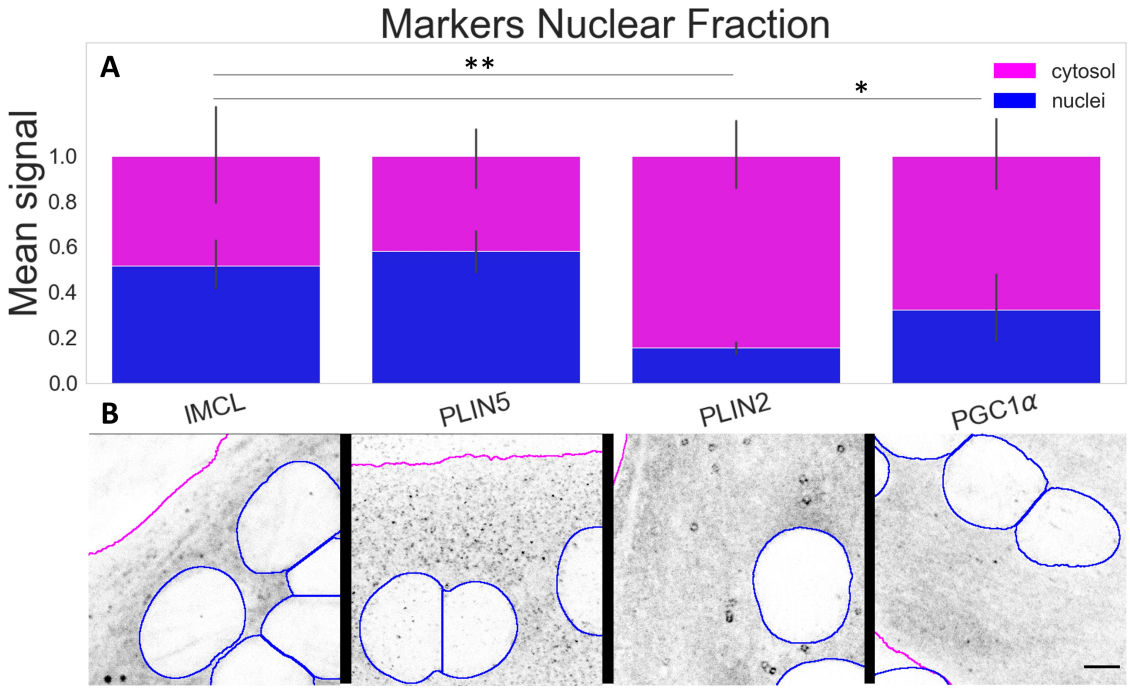

FIGURE 19 Marker signal comparison between myotube compartments. (**A**) proportion of nuclear signal (blue bars) in relation to cytosolic signal (full bars). Data normalized to the cytosolic reference and measured from the control group (Normal BCAA | Rest). Differences between nuclear fractions of IMCL versus remaining markers * ($p < 0.05$) and ** ($p < 0.001$). Whiskers signify standard deviation; (**B**) representative images of respective markers. Gray is signal, blue are limits of segmented nuclei, magenta are limits of segmented myotubes. Bar = 5 µm.

5.3.4 Dissociation of PLIN2 from IMCL due to BCAA deprivation (III)

Most of the signal for both IMCL and PLIN2 appeared to be diffused in the C2C12 myotubes, although there were occasional semi-spherical IMCL aggregates visible as LDs. Additionally, PLIN2 aggregates were common and often observed as dotted ring structures surrounding the LDs (as shown in Figure 20A).

Apart from exercise and muscle fiber type, BCAA can also have an impact on IMCL metabolism, which may interact with muscle contraction. Respectively, this dissertation' results demonstrated a decrease in the cytosolic association between PLIN2 and IMCL after BCAA deprivation ($p = 0.028$, Figure S2), particularly following EPS ($p = 0.048$, Figure 20B). In the absence of BCAA and with EPS, an increase in the association of PLIN2 and PLIN5 inside the nuclei was observed ($p = 0.030$), and this was dependent on each other ($p = 0.033$, Figure 20C).

These events were not influenced by the overall PLIN2 signal, which remained unchanged after both EPS and BCAA deprivation (III).

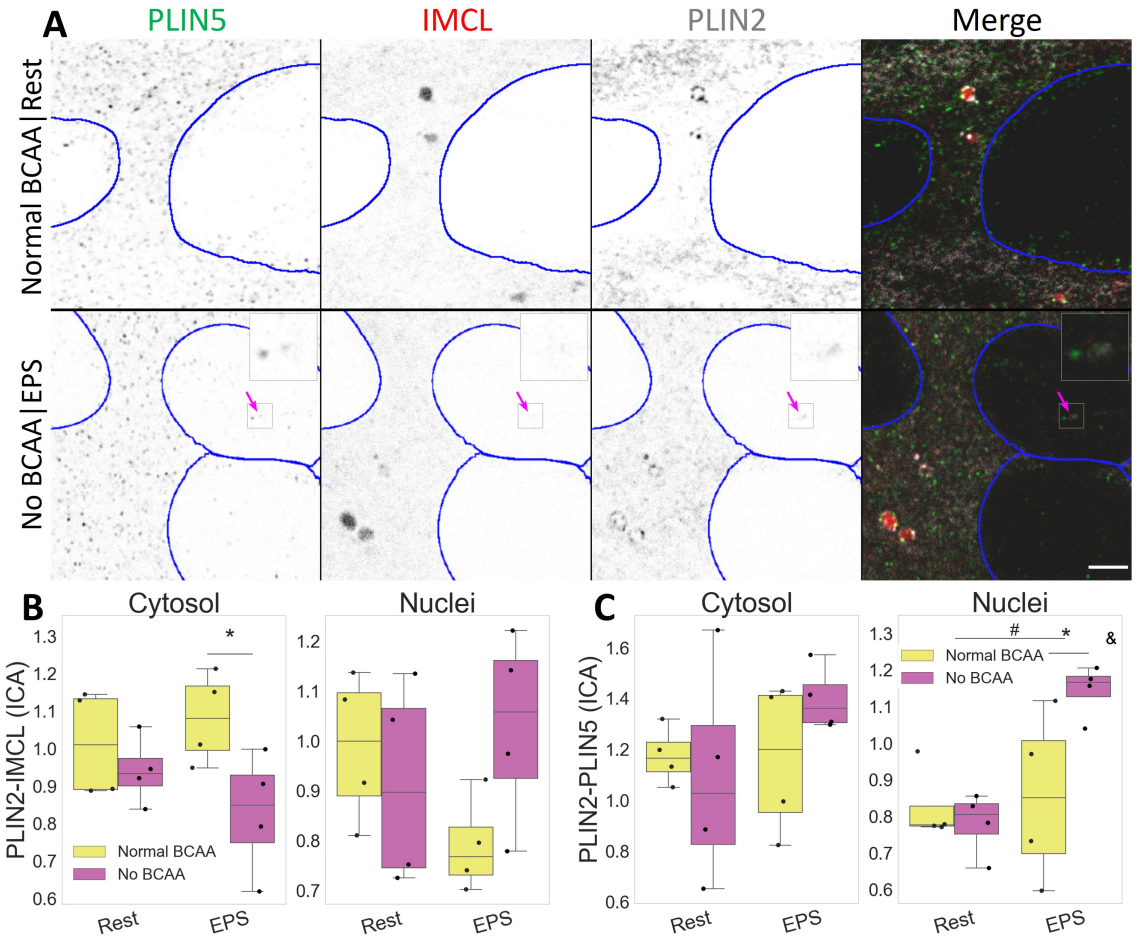

FIGURE 20 Compartmental PLIN2 association with IMCL and PLIN5 after EPS and BCAA deprivation. (**A**) representative image. Note a more diffused PLIN2 pattern after BCAA deprivation and PLIN2-PLIN5 association in nuclei after EPS (pink arrow). Gray is signal, blue are limits of segmented nuclei. Bar = 3 µm; (**B**) colocalization via intensity correlation analysis (ICA) between PLIN2 and IMCL; (**C**) colocalization via intensity correlation analysis (ICA) between PLIN2 and PLIN5. Main effect differences denoted with **#** ($p < 0.05$). Combined group differences denoted with * ($p < 0.05$); interacting effect between fiber type and LTPA denoted with **&** ($p < 0.05$).

5.3.5 Translocation of PLIN5 to nuclei following stimulation, increasing its association to IMCL and PGC-1α (III)

The signal for PLIN5 appeared mostly as numerous punctate structures and was often located next to or overlapping with other markers. On the other hand, PGC-1α showed mostly a scattered signal, occasionally gathering in variously shaped clusters, and frequently co-occurring with IMCL (as shown in Figure 21A).

Importantly, the signal of PLIN5 increased in nuclei after EPS ($p = 0.033$ as shown in Figure 21B), where its association with IMCL increased significantly ($p = 0.019$, Figure 21D). Moreover, under normal BCAA and EPS conditions, the association of nuclear PLIN5 with PGC-1α increased even further and in a highly

significant manner ($p = 0.009$, Figure 21E).

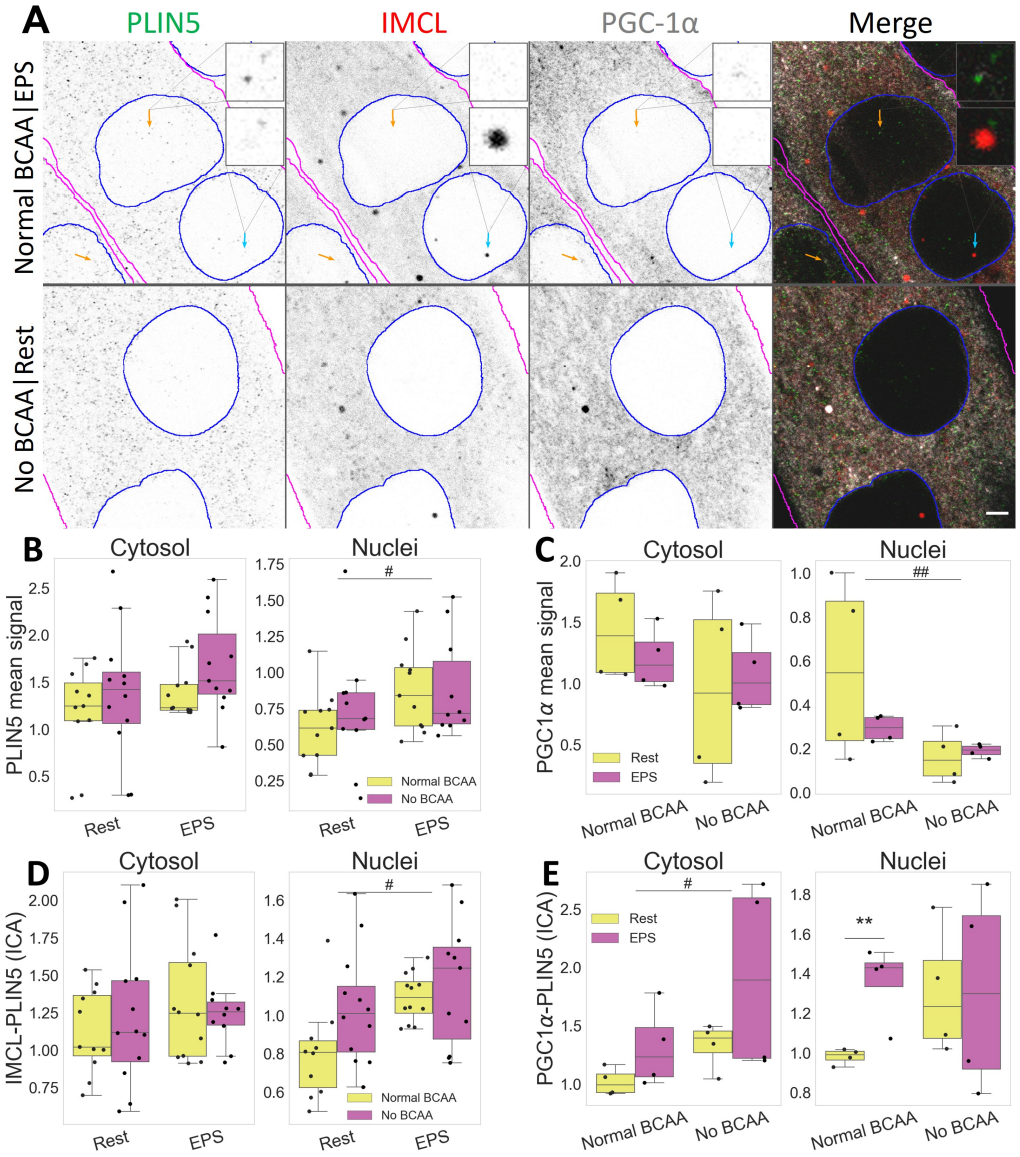

FIGURE 21 Compartmental association and distribution of PLIN5, IMCL and PGC-1α after EPS and BCAA deprivation. A) Representative image. Note more abundant PLIN5 in nuclei after EPS, with stronger association with PGC-1α (orange arrows) and IMCL (cyan arrow). Gray is signal, blue are limits of segmented nuclei, magenta are limits of segmented myotubes. Bar = 3 µm; B) PLIN5 signal intensity in different compartments; C) PGC-1α signal intensity in different compartments; D) ICA between IMCL and PLIN5 in different compartments; E) ICA between PGC-1α and PLIN5 in different compartments. Main effect differences denoted with #($p < .05$). Combined group differences denoted with *($p < .05$). Dots in B-E represent averaged coverslip values. Data normalized to the control group reference (Normal BCAA | Rest).

6 DISCUSSION

This dissertation investigated the relationship between metabolic health, physical activity and skeletal muscle lipid metabolism. More specifically, it focused on how intramyocellular lipids and their key regulators – the PLIN proteins – behave in insulin resistance, physical activity and BCAA supplementation.

The main finding was that healthier metabolic phenotypes and behaviors – characterized by adequate physical activity and nutrition – are associated with specific patterns of IMCL distribution and coating by PLIN proteins, namely with robust coating by PLIN2 and PLIN5 and a reduced presence in type II fibers. Furthermore, such appropriate coating of IMCL by PLINs seems to be promoted by adequate BCAA availability and metabolic efficiency, both correlated to a balanced IMCL turnover.

Additionally, this study further expands the knowledge on IMCL-PLINs dynamics beyond their known cytosolic roles related to energy metabolism and mitochondrial function. Specifically, both IMCL and PLINs may interact with transcription factor activators related to cell respiration and indeed translocate to nuclei upon contraction.

6.1 Intramyocellular lipids in different models (I, III)

In order to better understand the skeletal muscle lipid metabolism, IMCL were studied in two different human models plus in C2C12 cells. Although the terms *IMCL* and *skeletal muscle* are repeatedly used within these studies – and the literature in general – it is important to recognize that these and other models are mere approximations of each other. In other words, these lipids may not necessarily behave and respond in the same way to different stimuli in different models.

On one hand, the organisms themselves may often differ between each other, and that alone forcibly means that the results might not be directly comparable. For instance, it is known that mouse skeletal muscle, unlike human skeletal muscle, expresses the IIb isoform, resulting in the presence of type IIb fibers, with

specific mechanical and molecular properties (Andruchov et al. 2004).

Not only may species differ throughout the literature, but different muscle groups often add to the difficulty in comparing results between studies. Often IMCL and PLIN are compared between different muscles (e.g. *gastrocnemius* vs. *vastus lateralis*), adding one more layer of potential error in interpretations (Schrauwen-Hinderling et al. 2006). Despite this, the human studies in this dissertation both looked at the *vastus lateralis* muscle cross-sections (Figure 22A).

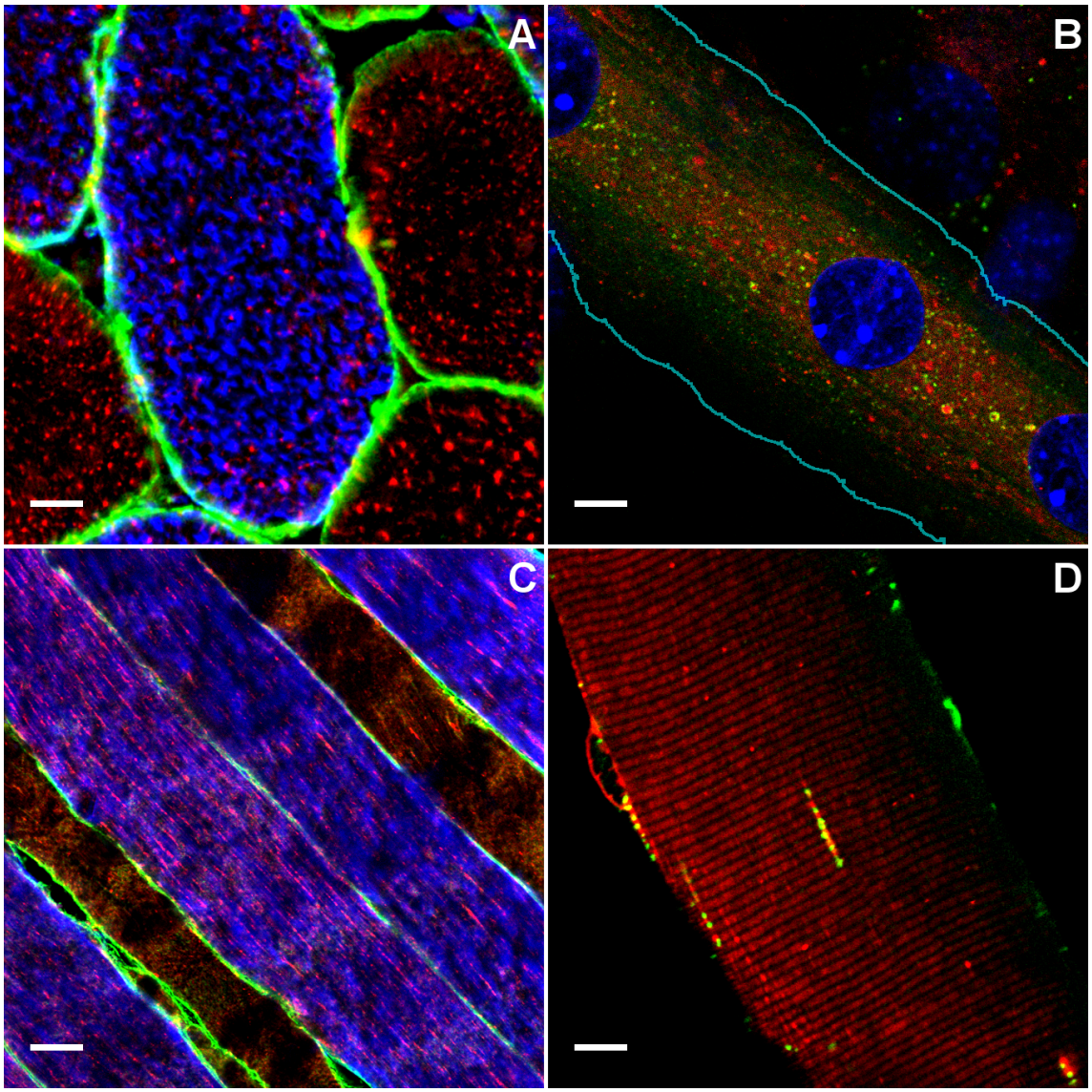

FIGURE 22 Different IMCL study models in fluorescence microscopy. A) Cross-sections (Human vastus lateralis, red: IMCL, green: sarcolemma, blue: fast myosin); B) Cultured myotubes (C2C12, red: IMCL, green: PLIN2, blue: nuclei, cyan: edge of segmented myotube); C) Longitudinal sections (Human vastus lateralis, red: IMCL, green: sarcolemma, blue: slow myosin); D) Isolated fibers (Rat EDL, red: IMCL, green: Golgi). Bars = 10 µm.

Besides cross-sections, another way to microscopically study IMCL, though less common, is longitudinally, either from muscle biopsies (Figure 22C) or from dis-

sected myofibers (Figure 22D). The choice between these two options can easily produce results which can be hard to compare and can certainly convey different information. For instance, only occasionally can large LDs be seen to organize in chain-like patterns, spanning a large portion of the cross sectional area. However, in longitudinal views LDs are very frequently organized in chain-patterns running along the myofibrils (Bosma 2016), as seen in Figure 22C. For this doctoral program, longitudinal data from C2C12 myotubes were studied in more depth (Figure 22B).

Despite being equally longitudinal in orientation, myotube studies can be difficult to directly compare against isolated myofibers or longitudinal sections. Even if differentiated and contracting, C2C12 myotubes are hardly striated and consequently have different physical and physiological properties when compared to tissue or dissected fibers (Figure 22B).

6.2 Different approaches in studying IMCL and LDs through microscopy

When studying LDs and IMCL microscopically, it is important to understand and define the terms at play (see section 2.1.2). The concept of intramyocellular LDs itself can be cumbersome and rather subjective to delimit. The term LD is extensively used in the study of IMCL and is typically treated as a subspherical and isolated structure (Daemen et al. 2018b), see Figure 23A-B. However, reality may be more complex than that. During the period of my PhD candidacy, several terabytes worth of IMCL micrographs were produced and inspected in different types of samples. The immediate contrast with most of the literature was the fact that, in skeletal muscle, neutral lipids rarely organize in purely isolated globose LDs. On the contrary, these LDs often seemed part of a web-like continuum, embedding the whole cell and manifesting in larger and brighter depots (Figure 23D), something that is seldom reported in literature (Howald et al. 2002).

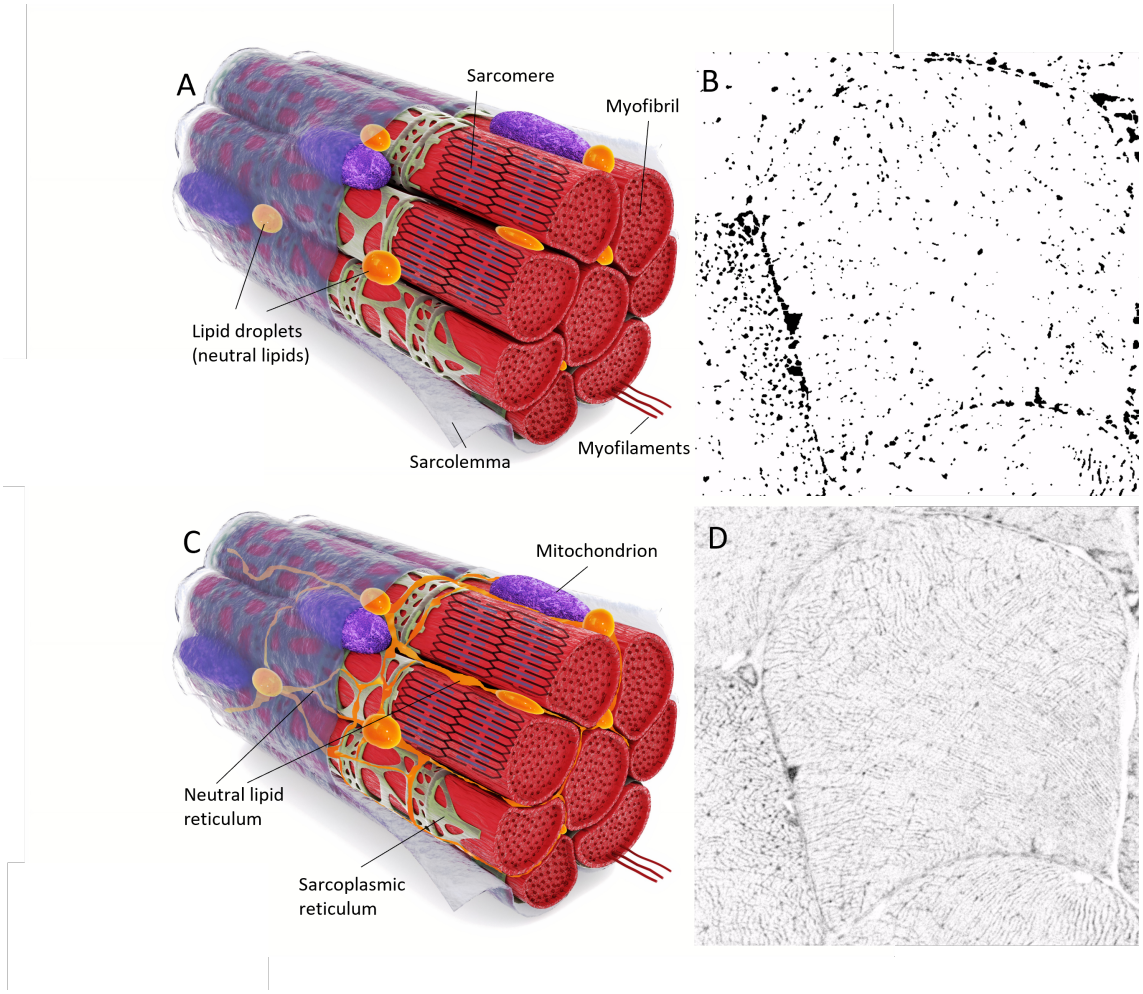

FIGURE 23 Neutral lipids versus LDs. Depending on the pre-processing of light microscopy data (B- threshold segmentation, D- gray signal), different structures may be measured (A- larger LDs; C- neutral lipids in general).

It is conceivable that intramyocellular LDs are just larger aggregates – or depots – of a large and interconnected structure of lipids, and eventually serving as a network of signaling molecules. Whether such a reticulated structure stands alone or integrates fatty membrane structures of the myocyte, such as the sarcoplasmic reticulum (Figure 23C), remains to be fully understood. Interestingly, PLIN5 has been recently demonstrated to interact with the sarcoplasmic reticulum, potentiating cardiac contractility via Ca^{2+} signaling (Cinato et al. 2023), strengthening the hypothesis of a neutral lipid continuum.

Either way, it is important to keep in mind that, frequently, LDs are arbitrarily segmented through image thresholding before being studied, and much of the dimmer signal from the reticulated network or lower background is left out from analyses. Every study should take this in consideration, as neutral lipids, TAG and even PLINs (if also thresholded) with relevant roles may be excluded unintendedly.

In the present studies it was decided to approach the term LD as a thresholded/binarized structure, while the term IMCL is understood as whole signal

left after denoising and deconvolution, including larger subspherical droplets, reticulum-like structures and general diffused intracellular signal. Both approaches are useful and informative, and should be chosen depending on the original research question (Figure 23).

6.3 Lipids to where they belong

The collective psyque of many cultures still sees fats from a rather negative lens, associating it to wrong nutritional behaviors and poor aesthetics (Brewis & Wutich 2012; Cramer & Steinwert 1998; Orbach 2005; Roddy et al. 2011). Researchers however, have added more resolution to this topic throughout the years, namely by categorizing the quality of different types of fat. Nevertheless, the paradigm may still be focusing excessively in the *bad fats versus good fats* perspective (Asrih & Jornayvaz 2014; DiNicolantonio & O'Keefe 2017; Hapala et al. 2011; McClain et al. 2007; Russell et al. 2003).

By now, the reader would have realized that this doctoral dissertation focuses on muscle fats as either detrimental or beneficial depending on their cellular and subcellular location, in combination with proper targeting by the PLIN protein family. As such, throughout the following subsections, I will present the arguments supporting the hypothesis wherein IMCL can become and remain the most harmful if accumulated deep within glycolytic myocytes.

6.3.1 Inadequacy of glycolytic myocytes in managing lipids

It is well established that glycolytic fibers are less oxygenated by capillaries, have fewer mitochondria than oxidative fibers and therefore its ability to oxidize lipids is diminished (Ingjer 1979; Picard et al. 2012; Tan et al. 2018). Moreover, type II fibers are ill equipped for FA endocytosis and transportation (Bonen et al. 1998). Interestingly, in insulin resistance the ability to internalize FAs can be increased to abnormal levels, while mitochondrial respiration remains severely reduced (Bonen et al. 2004; Mogensen et al. 2007).

Correspondingly, study I revealed that when compared to controls, T2D participants have increased concentrations of LDs in type II fibers (Figure 24), something that has been equally observed by other groups (Daemen et al. 2018a; Koh et al. 2018). In short, LDs and their derivatives are not necessarily harmful, but in tissues and cells not prepared to process them, they could become pathophysiologic.

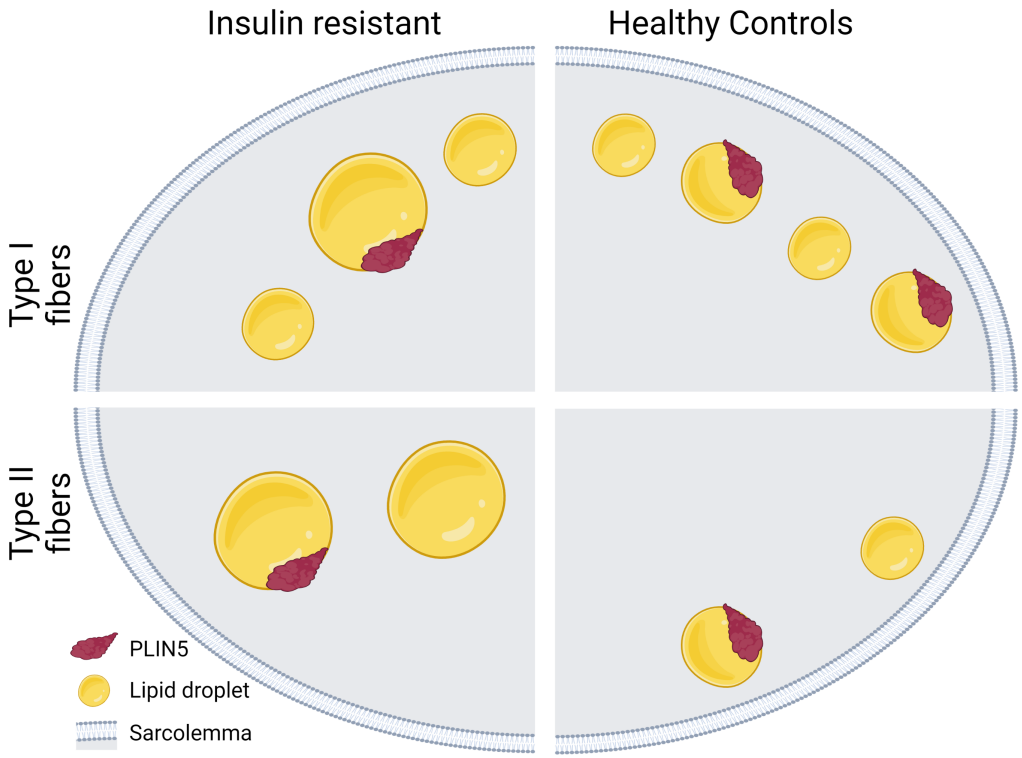

FIGURE 24 Graphical summary of study I. Insulin resistant individuals have a significant portion of large and uncoated LDs in inner regions of type II fibers. The illustration refers to *vastus lateralis* muscle

6.3.2 Accessibility of LDs helps determine metabolic health

Study I (see section 5.1) has not only shown that T2D participants have larger intramyocellular LDs when compared to lean controls, but also that a significant portion of these LDs is uncoated by PLIN5 in the inner regions of type II fibers, establishing a novel result in the field (Figure 24). Indeed, the current model suggests that PLIN5 plays a role in protecting the myocyte against insulin resistance by coating LDs and preventing the release of lipotoxic molecules from this organelle (Gemmink et al. 2016; MacPherson & Peters 2015; Mason et al. 2014).

However, it is often discussed in the literature that peripheral – or subsarcolemmal – LDs are likely the major initiator of lipotoxic events leading to insulin resistance, especially in type I fibers (Bucher et al. 2014; Daemen et al. 2020; Devries et al. 2013; Kahn et al. 2021; Li et al. 2014; Nielsen et al. 2010). This may be so. By being closer to the extracellular space and the source of lipids, oxygen, mitochondria and protein transporters, it is expected that these droplets are more readily assembled, expanded, shrunk or depleted. Consequently, these peripheral LDs may also release lipotoxic molecules at significantly higher rates when compared to intermyofibrillar LDs. By the same token, they are demonstratedly the first droplets to reacquire a healthy insulin sensitive phenotype after exercise interventions (Bucher et al. 2014; Devries et al. 2013; Li et al. 2014; Nielsen et al.

2010; Shepherd et al. 2017).

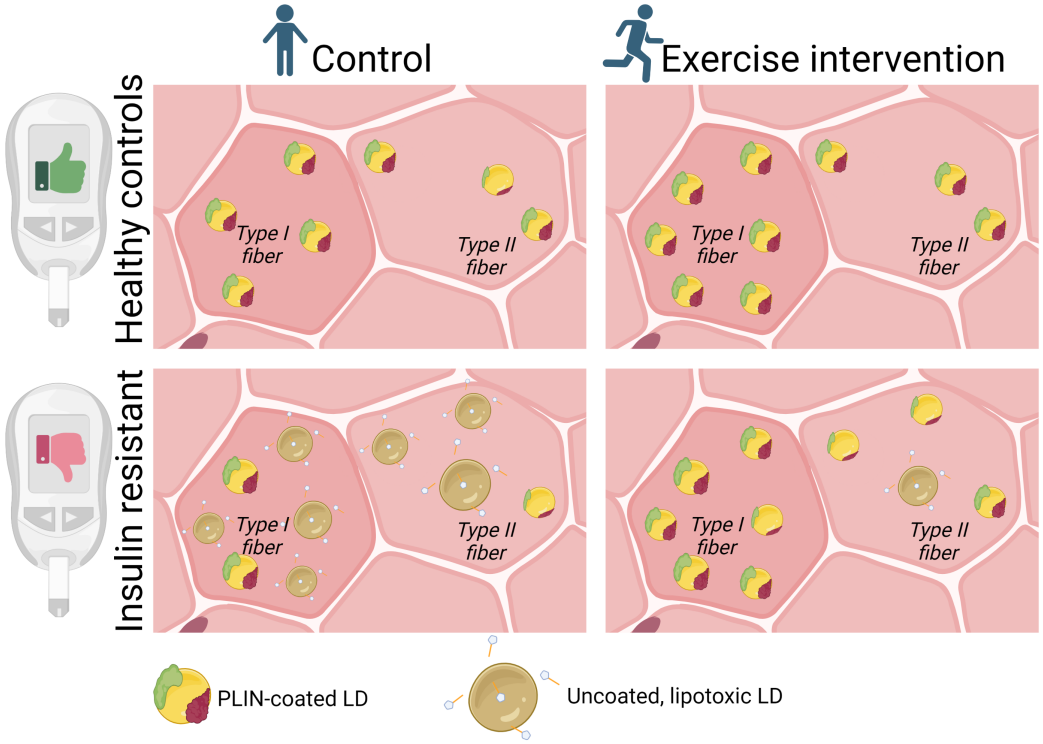

FIGURE 25 Proposed model hypothesis. Subsarcolemmal LDs in type I fibers as main lipotoxicity initiator and as main responders to exercise interventions. intermyofibrillar LDs in type II fibers as persistent lipotoxic agents, poor responders to exercise interventions.

The research question arising from study I relates to the role and impact of those distantly internalized intermyofibrillar LDs, harder to access by regulating proteins, including the insulin-sensitizing PLINs (Figure 24). The findings of this doctoral dissertation suggest that internalized, large and uncoated LDs in glycolytic fibers of T2D individuals, do in fact characterize the insulin resistant phenotype and may continue to contribute for lipotoxicity, even after the initial benefits that exercise interventions bring to peripheral LDs (Figure 25).

Ultimately, this study adds resolution to the body of evidence linking the inadequacy of excessive and unregulated intramyocellular LDs in type II fibers and the skeletal muscle insulin-resistance phenotype. Whether the model hypothesis proposed in Figure 25 represents reality, is something that will require future research to determine. Nonetheless, the remaining discussions relative to those from studies II & III do seem supportive, or at least compatible, with the aforementioned hypothesis.

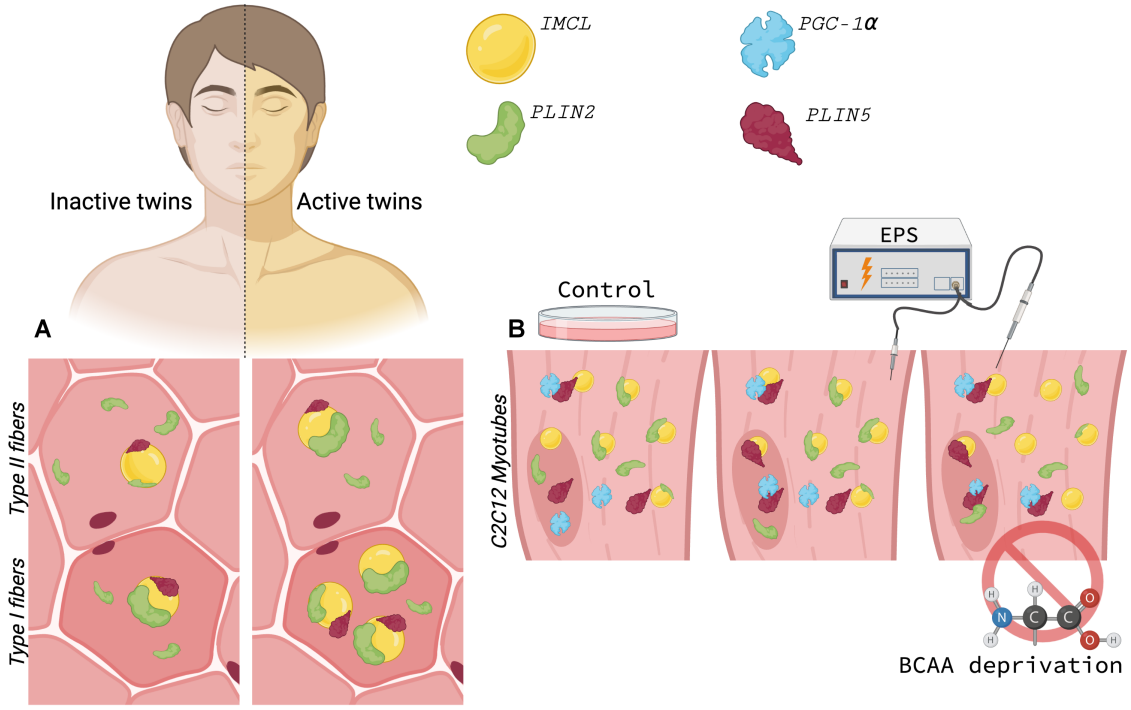

FIGURE 26 Graphical summary of study III. A) Active twins have higher concentrations of IMCL in type I fibers and improved PLIN2 coating in type II fibers; B) EPS induced contractions promote PLIN5 translocation towards nuclei, further associating with LDs and PGC-1α. BCAA deprivation leads to LD uncoating by PLIN2 as well as PGC-1α diminishment in nuclei.

6.4 Long-term physical activity improves IMCL-PLIN profile regardless of genotype

One of the observations of study III was that LTPA alone can produce an athlete phenotype, that is, it leads to increased IMCL levels in comparison to controls, especially in type I fibers (Figure 26). This conclusion is relevant as it was the first time it was demonstrated that the athlete paradox could be achieved via LTPA and regardless of the individual's genetic background.
The twins labeled as 'inactive' were not sedentary or unhealthy individuals, yet, in comparison to the 'active' group, the contrasts in IMCL profile were clear and not limited to IMCL concentrations. Another major difference observed was the significantly improved IMCL coating by PLIN2 in type II fibers of the active twins (Figure 26). Correspondingly, as cited in the literature review (see 2.2.3), IMCL coating by PLIN2 is also associated with insulin sensitivity.

Altogether, the fact that LTPA promotes better coating of IMCL in type II fibers and that insulin resistance is associated with large portions of uncoated IMCL in the same fiber type (Figure 24), further indicates that unattended LDs in less oxidative muscle may be pathophysiological and that short-term exercise

may not be enough to revert such a profile (Figure 25).

6.5 BCAA availability linked to healthy IMCL phenotypes

A dysregulated BCCA metabolism is often connected to impaired lipid oxidation and consequent insulin resistance, wherein emphasis is usually given to excess BCAA availability (Connor et al. 2010; Lerin et al. 2016; Newgard et al. 2009). In study II not only excess BCAA supplementation reduced lipid oxidation in myotubes, but BCAA deprivation produced the same result (section 5.3.2), something that has been equally observed in previous research (Estrada-Alcalde et al. 2017). Moreover, study II demonstrated that BCAA deprivation also led to decreased lipogenesis (section 5.3.2). The previous hypothesis by Kainulainen et al. (2013) is supported by these findings, indicating that both lipid oxidation and lipogenesis would be disrupted by BCAA deprivation. The disturbances of glyceroneogenesis, lipid oxidation and lipogenensis could be speculated to have a direct impact in lipotoxic signaling, ultimately promoting insulin resistance.

Returning to the topic of PLIN2 coating, study III revealed that BCAA deprivation led to a dissociation between IMCL and this PLIN member in myotubes (see section 5.3.4). As introduced in 2.1.4, IMCL coating by PLIN2 is linked to insulin sensitivity through improved regulation of lipogenic and lipolytic enzymes on the surface of LDs. This might explain the outcome of study II, where in the same samples, BCAA deprivation resulted in decreased lipid oxidation, decreased lipogenesis, as well as reduced CS activity (see 5.3.2). Together, study II and III suggest that proper intake of BCAA may be necessary for a healthy IMCL profile, namely by adequate PLIN2 coating and consequent balanced LD turnover.

However, BCAA deprivation resulted in no equivalent results when it comes to PLIN5 (Figure 21), possibly reflecting a more adaptive and resistant role of this PLIN member in comparison to PLIN2, compensating for the latter during the typically more demanding stimuli of skeletal muscle.

6.6 LDs beyond energy sources

As briefly mentioned in section 2.1.4, LDs play several intracellular roles beyond serving as energy reservoirs, from membrane trafficking, inflammation and immune response pathways, to mRNA transcription (Cruz et al. 2020; Henne et al. 2018; Pereira-Dutra et al. 2019; Welte 2015).

Concerning transcription and still related to energy metabolism, it has been shown that the phosphorylation of PLIN5 and its lipid-bound translocation to nuclei, promote the activation of PGC-1α through the disinhibition of Sirtuin 1 (Gallardo-Montejano et al. 2016; Najt et al. 2020). This event seems to be trig-

gered by catecholamines and fasting, and therefore, it was hypothesized that exercise could elicit a comparable reaction (Gallardo-Montejano et al. 2016). Findings from study III substantiate this hypothesis, as it newly demonstrated that EPS leads to the enrichment of PLIN5 in myotube nuclei, forming additional associations with PGC-1α (under normal BCAA) and LDs (Figure 26).

Irrespective of EPS, a significant decrease in nuclear PGC-1α was observed following BCAA deprivation (Figure 26). This suggests that the role of PGC-1α as a promoter of mitochondrial biogenesis is hindered under these conditions. These findings align with the reduced lipid oxidation and lipogenesis resulting from the same BCAA deprivation (5.3.2), as previously hypothesized (Kainulainen et al. 2013).

Taken together, this thesis further contributes to the field of knowledge involving LDs-PLINs and transcriptional events. Namely by demonstrating that LDs and PLIN5 may be key players in contraction-induced mitochondrial biogenesis.

6.7 Strengths and limitations

One of the strengths of this doctoral work lies in the utilization of different study models, namely two human and one *in vitro*. Insulin resistant humans in study I provided a classical model already extensively studied in the field of intramyocellular LDs and PLINs. With this setup it was primarily possible to validate the methodology by replicating comparable results with the known literature. Only then were the novel pattern recognition results produced, specifically the identification of large and uncoated LDs in inner regions of diabetic type II fibers. The second human setup – the twins with discordant physical activity in study III – provided an important and unstudied model in this field, allowing for the first time a glimpse of the effects of life-long physical activity on IMCL and PLINs, while controlling for genetic background. Finally, the C2C12 myotube model in studies II and III brought the ability to investigate the combined effects of EPS and BCAA availability on the subcellular arrangement of IMCL, PLINs and PGC-1α.

However, it is in the C2C12 model where one of the limitations of this dissertation can be found, concretely in the fact that this cell line may bear too little resemblance to muscle tissue, especially to type I fibers. Thus, C2C12 myotubes may be a sub-optimal model in the study of oxidative responses and lipid utilization (Brown et al. 2012; Son et al. 2019). On the flip side, these myotubes proved to be a good glycolytic study model. In study II, for instance, there was indeed a poor lipolytic response to EPS, triggering no changes in lipogenesis or IMCL content together with a decrease in lipid oxidation (5.3.2). This indicates a rather glycolytic response to EPS, something indeed previously observed from the exact same setup (Lautaoja et al. 2021).

Other limitations worth noting concern the twin setup in study III, explicitly the low number of participants which ultimately did not allow an in-depth con-

trol for variables like gender or zygosity. On the other hand, the strength comes from the twin model, quite powerful in itself (Kujala et al. 2013) and from the several hundreds of glycolytic and oxidative myocytes compared between active and inactive twin pairs (see 5.2).

As mentioned earlier, the main approach during this work was based on microscopy. Although the robust image analyses involving deconvolution, machine learning segmentation or ICA can be a strength in these studies, it is also true that without complementary methodologies, the meaningfulness of a single approach may be compromised. To that effect, studies II and III pose a considerable enhancement in comparison to study I and contribute to a better overall picture of the studied phenomena. Nevertheless, even within microscopy, neither of our studies involved electron microscopy nor live imaging, therefore terms such as *association* or *translocation*, respectively, should be interpreted with caution. On the other hand, the latter methods lack the ability to easily scan large areas of samples stained for multiple markers, as it was the case with five markers for C2C12 myotubes in study III.

In a nutshell, the main strength and the main limitation of the present work simultaneously relate to the methodological focus, that is, microscopy and image analysis. If on the one hand such focus risks overinterpreting the data and missing the big picture, then, on the other, hand it allows a deeper examination of unexplored phenomena. The necessary conclusion is that both the broad approach together with the in-depth one should be equally invested in.

6.8 Future directions

Arguably, the main open question raised by this doctoral study relates to the PLIN coating of LDs in glycolytic muscle fibers (studies I and III). As discussed in 6.3, when researching skeletal muscle lipotoxicity, a significant effort has been directed to LDs from subcellular areas where they most abound, that is, the subsarcolemmal region of type I fibers. Therefore, a logical path forward would be to first corroborate the observations made here, and then investigate the practical impacts of having IMCL dissociated from PLINs in intermyofibrillar regions of type II fibers. Is this just a coincidental correlation towards the unhealthier phenotypes, without any causation or physiological significance? Can it be merely diagnostical? Or perhaps, is it indeed causational and could eventually become a target for future therapeutic strategies? The model hypothesis proposed in Figure 25 should be tested. These are questions raised in this dissertation that should be pursued in future research.

Regarding the role of PLINs and LDs as partakers in transcriptional pathways, the proverbial surface has only recently been scratched. On the one side, it seems clear that PLIN5 is required to chaperone FAs towards myonuclei in order to promote PGC-1α activation and consequent mitochondrial biogenesis (Gallardo-Montejano et al. 2016; Najt et al. 2020). On the other side, it is not clear

if LD proximity is required for this process, or if it needs to occur only within the nuclei. Study III contributed to this field of knowledge by demonstrating that contractions indeed lead to nuclear enrichment by PLIN5 and its association with both PGC-1α and LDs (Figure 26). Additionally, BCAA deprivation led to an increased association between PLIN5 and PGC-1α in the cytosol while leading to nuclear depletion of the latter (Figure 26). The exact reasons for these events are unclear. It is evident that there is still much to be learned about the role of PLIN5 – and other PLINs too – in regulating transcription factors related to the energy metabolism, both in the cytosol and in the nuclei. It is thus foreseeable that this research direction will receive escalating attention in the years ahead.

Concerning the nature of the perilipin family, the publications produced during the PhD period approached solely PLIN2 and PLIN5, the most prominent and well studied PLIN members in skeletal muscle (Daemen et al. 2018b; MacPherson & Peters 2015). Thus, it is legitimate to pose questions regarding the role of other less notable PLINs present in this tissue, such as PLIN3 and PLIN4. The differential tasks of each PLIN are still a rather obscure topic, with little known about the degree of overlapping, compensating ability or distinctive nuances of each member in skeletal muscle metabolism. This should certainly prompt research efforts in the near future.

Finally, as shortly debated in section 6.2, there may be meaningful discoveries to be made concerning IMCL as a neutral lipid network, hypothetically yielding physical routes for signaling pathways. Understanding this network, of which LDs would be a part, could prove to be crucial in further disclosing the mechanisms connecting intramyocellular LD dynamics and metabolic diseases. For instance, it could add resolution to the process involving the interaction between PLINs and the sarcoplasmic reticulum, also discussed in section 6.2. Moreover, it could help explain how large droplets form and remain uncoated in inner regions of type II fibers in diabetic individuals.

7 MAIN FINDINGS AND CONCLUSIONS

1. When compared to healthy and active, insulin resistant and less active human skeletal muscle phenotypes show poorer PLIN coating of LDs, particularly in the inner regions of more glycolytic fiber types. Decreased PLIN coating further extends to glycolytic myotubes when deprived of BCAA. (I, III)

2. Physical activity can promote better coating of LDs, which is known to protect against intramyocellular lipotoxicity. Similar effects can be enhanced by balanced BCAA availability and an efficient BCAA metabolism. Conversely, BCAA deprivation decreases both lipogenesis and lipolysis in myotubes. (II, III)

3. PLINs are not mere LD proteins and seem to participate in several cellular roles between and inside different organelles. Plus, the PLIN profile of LDs is more critical than LD size or abundance. Cellular and subcellular localization of LDs may also define myocyte health, depending on their LD coating profile. (I, II, III)

In conclusion, appropriate physical activity and nutrition exert positive effects on health and skeletal muscle lipid metabolism through functional PLIN physiology, namely via adequate association with intramyocellular lipid droplets and by participating in further cellular roles.

REFERENCES

Adams, I., John M., Pratipanawatr, T., Berria, R., Wang, E., DeFronzo, R. A., Sullards, M. C., & Mandarino, L. J. (2004). Ceramide Content Is Increased in Skeletal Muscle From Obese Insulin-Resistant Humans. *Diabetes*, *53*(1), 25–31. https://doi.org/10.2337/diabetes.53.1.25

Ahmed, B., Sultana, R., & Greene, M. W. (2021). Adipose tissue and insulin resistance in obese. *Biomedicine& Pharmacotherapy*, *137*, 111315. https://doi.org/https://doi.org/10.1016/j.biopha.2021.111315

Akie, T. E., & Cooper, M. P. (2015). Determination of fatty acid oxidation and lipogenesis in mouse primary hepatocytes. *JoVE (Journal of Visualized Experiments)*, (102), e52982.

Al-Khalili, L., Bouzakri, K., Glund, S., Lönnqvist, F., Koistinen, H. A., & Krook, A. (2006). Signaling Specificity of Interleukin-6 Action on Glucose and Lipid Metabolism in Skeletal Muscle. *Molecular Endocrinology*, *20*(12), 3364–3375. https://doi.org/10.1210/me.2005-0490

Amati, F., Dubé, J. J., Alvarez-Carnero, E., Edreira, M. M., Chomentowski, P., Coen, P. M., Switzer, G. E., Bickel, P. E., Stefanovic-Racic, M., Toledo, F. G., & Goodpaster, B. H. (2011). Skeletal Muscle Triglycerides, Diacylglycerols, and Ceramides in Insulin Resistance: Another Paradox in Endurance-Trained Athletes? *Diabetes*, *60*(10), 2588–2597. https://doi.org/10.2337/db10-1221

Andruchov, O., Andruchova, O., Wang, Y., & Galler, S. (2004). Kinetic properties of myosin heavy chain isoforms in mouse skeletal muscle: Comparison with rat, rabbit, and human and correlation with amino acid sequence. *American Journal of Physiology-Cell Physiology*, *287*(6), C1725–C1732. https://doi.org/10.1152/ajpcell.00255.2004

Arganda-Carreras, I., Kaynig, V., Rueden, C., Eliceiri, K. W., Schindelin, J., Cardona, A., & Sebastian Seung, H. (2017). Trainable Weka Segmentation: a machine learning tool for microscopy pixel classification. *Bioinformatics*, *33*(15), 2424–2426. https://doi.org/10.1093/bioinformatics/btx180

Asrih, M., & Jornayvaz, F. R. (2014). Diets and nonalcoholic fatty liver disease: The good and the bad. *Clinical Nutrition*, *33*(2), 186–190. https://doi.org/10.1016/j.clnu.2013.11.003

Badin, P.-M., Langin, D., & Moro, C. (2013). Dynamics of skeletal muscle lipid pools. *Trends in Endocrinology & Metabolism*, *24*(12), 607–615. https://doi.org/https://doi.org/10.1016/j.tem.2013.08.001

Bartz, R., Li, W.-H., Venables, B., Zehmer, J. K., Roth, M. R., Welti, R., Anderson, R. G., Liu, P., & Chapman, K. D. (2007). Lipidomics reveals that adiposomes store ether lipids and mediate phospholipid traffic. *Journal of lipid research*, *48*(4), 837–847. https://doi.org/10.1194/jlr.M600413-JLR200

Billecke, N., Bosma, M., Rock, W., Fleissner, F., Best, G., Schrauwen, P., Kersten, S., Bonn, M., Hesselink, M. K. C., & Parekh, S. H. (2015). Perilipin 5 mediated

lipid droplet remodelling revealed by coherent Raman imaging. *Integrative Biology*, *7*(4), 467–476. https://doi.org/10.1039/c4ib00271g

Blaak, E. E. (2005). Metabolic fluxes in skeletal muscle in relation to obesity and insulin resistance [Childhood Obesity]. *Best Practice& Research Clinical Endocrinology& Metabolism*, *19*(3), 391–403. https://doi.org/https://doi.org/10.1016/j.beem.2005.04.001

Blaak, E. E., Wagenmakers, A. J. M., Glatz, J. F. C., Wolffenbuttel, B. H. R., Kemerink, G. J., Langenberg, C. J. M., Heidendal, G. A. K., & Saris, W. H. M. (2000). Plasma ffa utilization and fatty acid-binding protein content are diminished in type 2 diabetic muscle [PMID: 10893334]. *American Journal of Physiology-Endocrinology and Metabolism*, *279*(1), E146–E154. https://doi.org/10.1152/ajpendo.2000.279.1.E146

Bonen, A., Luiken, J., Liu, S., Dyck, D., Kiens, B., Kristiansen, S., Turcotte, L., Van Der Vusse, G., & Glatz, J. (1998). Palmitate transport and fatty acid transporters in red and white muscles. *American Journal of Physiology-Endocrinology And Metabolism*, *275*(3), E471–E478. https://doi.org/10.1152/ajpendo.1998.275.3.E471

Bonen, A., Parolin, M. L., Steinberg, G. R., Calles-Escandon, J., Tandon, N. N., Glatz, J. F., Luiken, J. J., Heigenhauser, G. J., & Dyck, D. J. (2004). Triacylglycerol accumulation in human obesity and type 2 diabetes is associated with increased rates of skeletal muscle fatty acid transport and increased sarcolemmal fat/cd36. *The FASEB Journal*, *18*(10), 1144–1146. https://doi.org/10.1096/fj.03-1065fje

Bosma, M. (2016). Lipid droplet dynamics in skeletal muscle [The Biology of Lipid Droplets]. *Experimental Cell Research*, *340*(2), 180–186. https://doi.org/10.1016/j.yexcr.2015.10.023

Bosma, M., Hesselink, M. K., Sparks, L. M., Timmers, S., Ferraz, M. J., Mattijssen, F., van Beurden, D., Schaart, G., de Baets, M. H., Verheyen, F. K., et al. (2012a). Perilipin 2 improves insulin sensitivity in skeletal muscle despite elevated intramuscular lipid levels. *Diabetes*, *61*(11), 2679–2690. https://doi.org/10.2337/db11-1402

Bosma, M., Minnaard, R., Sparks, L. M., Schaart, G., Losen, M., De Baets, M. H., Duimel, H., Kersten, S., Bickel, P. E., Schrauwen, P., et al. (2012b). The lipid droplet coat protein perilipin 5 also localizes to muscle mitochondria. *Histochemistry and cell biology*, *137*, 205–216. https://doi.org/10.1007/s00418-011-0888-x

Bouzakri, K., Koistinen, H. A., & Zierath, J. R. (2005). Molecular mechanisms of skeletal muscle insulin resistance in type 2 diabetes. *Current diabetes reviews*, *1*(2), 167–174. https://doi.org/10.2174/1573399054022785

Brewis, A. A., & Wutich, A. (2012). Explicit versus implicit fat-stigma. *American Journal of Human Biology*, *24*(3), 332–338. https://doi.org/10.1002/ajhb.22233

Brown, D. M., Parr, T., & Brameld, J. M. (2012). Myosin heavy chain mrna isoforms are expressed in two distinct cohorts during c2c12 myogenesis. *Jour-*

nal of muscle research and cell motility, *32*(6), 383–390. https://doi.org/10.1007/s10974-011-9267-4

Bucher, J., Krüsi, M., Zueger, T., Ith, M., Stettler, C., Diem, P., Boesch, C., Kreis, R., & Christ, E. (2014). The effect of a single 2 h bout of aerobic exercise on ectopic lipids in skeletal muscle, liver and the myocardium. *Diabetologia*, *57*, 1001–1005. https://doi.org/10.1007/s00125-014-3193-0

Casares, D., Escribá, P. V., & Rosselló, C. A. (2019). Membrane lipid composition: Effect on membrane and organelle structure, function and compartmentalization and therapeutic avenues. *International Journal of Molecular Sciences*, *20*(9), 2167. https://doi.org/10.3390/ijms20092167

Cavalier-Smith, T. (2001). Obcells as proto-organisms: Membrane heredity, lithophosphorylation, and the origins of the genetic code, the first cells, and photosynthesis. *Journal of Molecular Evolution*, *53*, 555–595. https://doi.org/10.1007/s002390010245

Chaurasia, B., & Summers, S. A. (2015). Ceramides – lipotoxic inducers of metabolic disorders. *Trends in Endocrinology& Metabolism*, *26*(10), 538–550. https://doi.org/https://doi.org/10.1016/j.tem.2015.07.006

Chow, L. S., Mashek, D. G., Wang, Q., Shepherd, S. O., Goodpaster, B. H., & Dubé, J. J. (2017). Effect of acute physiological free fatty acid elevation in the context of hyperinsulinemia on fiber type-specific imcl accumulation [PMID: 28450549]. *Journal of Applied Physiology*, *123*(1), 71–78. https://doi.org/10.1152/japplphysiol.00209.2017

Cinato, M., Mardani, I., Miljanovic, A., Drevinge, C., Laudette, M., Bollano, E., Henricsson, M., Tolö, J., Thorbrügge, M. B., Levin, M., et al. (2023). Cardiac plin5 interacts with serca2 and promotes calcium handling and cardiomyocyte contractility. *Life Science Alliance*, *6*(4). https://doi.org/10.26508/lsa.202201690

Coen, P. M., Dubé, J. J., Amati, F., Stefanovic-Racic, M., Ferrell, R. E., Toledo, F. G., & Goodpaster, B. H. (2009). Insulin resistance is associated with higher intramyocellular triglycerides in type i but not type ii myocytes concomitant with higher ceramide content. *Diabetes*.

Coller, H. A. (2014). Is cancer a metabolic disease? *The American Journal of Pathology*, *184*(1), 4–17. https://doi.org/https://doi.org/10.1016/j.ajpath.2013.07.035

Connor, S. C., Hansen, M. K., Corner, A., Smith, R. F., & Ryan, T. E. (2010). Integration of metabolomics and transcriptomics data to aid biomarker discovery in type 2 diabetes. *Molecular BioSystems*, *6*(5), 909–921. https://doi.org/10.1039/B914182K

Costes, S. V., Daelemans, D., Cho, E. H., Dobbin, Z., Pavlakis, G., & Lockett, S. (2004). Automatic and quantitative measurement of protein-protein colocalization in live cells. *Biophysical journal*, *86*(6), 3993–4003. https://doi.org/10.1529/biophysj.103.038422

Cramer, P., & Steinwert, T. (1998). Thin is good, fat is bad: How early does it begin? *Journal of Applied Developmental Psychology*, *19*(3), 429–451. https://doi.org/10.1016/S0193-3973(99)80049-5

Cruz, A. L., Barreto, E. d. A., Fazolini, N. P., Viola, J. P., & Bozza, P. T. (2020). Lipid droplets: Platforms with multiple functions in cancer hallmarks. *Cell death & disease*, *11*(2), 105. https://doi.org/10.1038/s41419-020-2297-3

Daemen, S., Gemmink, A., Brouwers, B., Meex, R. C., Huntjens, P. R., Schaart, G., Moonen-Kornips, E., Jörgensen, J., Hoeks, J., Schrauwen, P., & Hesselink, M. K. (2018a). Distinct lipid droplet characteristics and distribution unmask the apparent contradiction of the athlete's paradox. *Molecular Metabolism*, *17*, 71–81. https://doi.org/https://doi.org/10.1016/j.molmet.2018.08.004

Daemen, S., Gemmink, A., Paul, A., Billecke, N., Rieger, K., Parekh, S. H., & Hesselink, M. K. (2020). Label-free cars microscopy reveals similar triacylglycerol acyl chain length and saturation in myocellular lipid droplets of athletes and individuals with type 2 diabetes. *Diabetologia*, *63*(12), 2654–2664. https://doi.org/10.1007/s00125-020-05266-6

Daemen, S., van Polanen, N., Hesselink, M. K. C., Suarez, R. K., & Hoppeler, H. H. (2018b). The effect of diet and exercise on lipid droplet dynamics in human muscle tissue [jeb167015]. *Journal of Experimental Biology*, *221*(Suppl1). https://doi.org/10.1242/jeb.167015

Devries, M. C., Samjoo, I. A., Hamadeh, M. J., McCready, C., Raha, S., Watt, M. J., Steinberg, G. R., & Tarnopolsky, M. A. (2013). Endurance Training Modulates Intramyocellular Lipid Compartmentalization and Morphology in Skeletal Muscle of Lean and Obese Women. *The Journal of Clinical Endocrinology & Metabolism*, *98*(12), 4852–4862. https://doi.org/10.1210/jc.2013-2044

DiNicolantonio, J. J., & O'Keefe, J. H. (2017). Good fats versus bad fats: A comparison of fatty acids in the promotion of insulin resistance, inflammation, and obesity. *Missouri medicine*, *114*(4), 303.

Ebeling, P., Koistinen, H. A., & Koivisto, V. A. (1998). Insulin-independent glucose transport regulates insulin sensitivity. *FEBS Letters*, *436*(3), 301–303. https://doi.org/10.1016/S0014-5793(98)01149-1

Estrada-Alcalde, I., Tenorio-Guzman, M. R., Tovar, A. R., Salinas-Rubio, D., Torre-Villalvazo, I., Torres, N., & Noriega, L. G. (2017). Metabolic fate of branched-chain amino acids during adipogenesis, in adipocytes from obese mice and c2c12 myotubes. *Journal of Cellular Biochemistry*, *118*(4), 808–818. https://doi.org/10.1002/jcb.25755

Fachada, V., Fachada, N., Turpeinen, T., Rahkila, P., Rosa, A., & Kainulainen, H. (2012). Topocell – an image analysis tool to study intracellular topography. *The FASEB Journal*, *26*(S1), 578.2–578.2. https://doi.org/10.1096/fasebj.26.1_supplement.578.2

Falholt, K., Jensen, I., Jensen, S. L., Mortensen, H., Vølund, A., Heding, L., Petersen, P. N., & Falholt, W. (1988). Carbohydrate and lipid metabolism of skeletal muscle in type 2 diabetic patients. *Diabetic Medicine*, *5*(1), 27–31. https://doi.org/10.1111/j.1464-5491.1988.tb00936.x

Farese, J., Robert V., & Walther, T. C. (2016). Lipid droplets go nuclear. *Journal of Cell Biology*, *212*(1), 7–8. https://doi.org/10.1083/jcb.201512056

Gallardo-Montejano, V. I., Saxena, G., Kusminski, C. M., Yang, C., McAfee, J. L., Hahner, L., Hoch, K., Dubinsky, W., Narkar, V. A., & Bickel, P. E. (2016). Nuclear perilipin 5 integrates lipid droplet lipolysis with pgc-1α/sirt1-dependent transcriptional regulation of mitochondrial function. *Nature communications*, *7*(1), 1–14. https://doi.org/10.1038/ncomms12723

Gemmink, A., Bosma, M., Kuijpers, H. J., Hoeks, J., Schaart, G., van Zandvoort, M. A., Schrauwen, P., & Hesselink, M. K. (2016). Decoration of intramyocellular lipid droplets with plin5 modulates fasting-induced insulin resistance and lipotoxicity in humans. *Diabetologia*, *59*(5), 1040–1048. https://doi.org/10.1007/s00125-016-3865-z

Gemmink, A., Daemen, S., Brouwers, B., Hoeks, J., Schaart, G., Knoops, K., Schrauwen, P., & Hesselink, M. K. (2021). Decoration of myocellular lipid droplets with perilipins as a marker for in vivo lipid droplet dynamics: A super-resolution microscopy study in trained athletes and insulin resistant individuals. *Biochimica et Biophysica Acta (BBA) - Molecular and Cell Biology of Lipids*, *1866*(2), 158852. https://doi.org/10.1016/j.bbalip.2020.158852

Gemmink, A., Daemen, S., Brouwers, B., Huntjens, P. R., Schaart, G., Moonen-Kornips, E., Jörgensen, J., Hoeks, J., Schrauwen, P., & Hesselink, M. K. C. (2018). Dissociation of intramyocellular lipid storage and insulin resistance in trained athletes and type 2 diabetes patients; involvement of perilipin 5? *The Journal of Physiology*, *596*(5), 857–868. https://doi.org/10.1113/JP275182

Goldberg, I. J., Cabodevilla, A. G., Samovski, D., Cifarelli, V., Basu, D., & Abumrad, N. A. (2021). Lipolytic enzymes and free fatty acids at the endothelial interface. *Atherosclerosis*, *329*, 1–8. https://doi.org/https://doi.org/10.1016/j.atherosclerosis.2021.05.018

Goodpaster, B. H., He, J., Watkins, S., & Kelley, D. E. (2001). Skeletal Muscle Lipid Content and Insulin Resistance: Evidence for a Paradox in Endurance-Trained Athletes. *The Journal of Clinical Endocrinology & Metabolism*, *86*(12), 5755–5761. https://doi.org/10.1210/jcem.86.12.8075

Granneman, J. G., Moore, H.-P. H., Mottillo, E. P., & Zhu, Z. (2009). Functional interactions between mldp (lsdp5) and abhd5 in the control of intracellular lipid accumulation. *Journal of Biological Chemistry*, *284*(5), 3049–3057. https://doi.org/10.1074/jbc.M808251200

Granneman, J. G., Moore, H.-P. H., Mottillo, E. P., Zhu, Z., & Zhou, L. (2011). Interactions of perilipin-5 (plin5) with adipose triglyceride lipase. *Journal of Biological Chemistry*, *286*(7), 5126–5135.

Greenberg, A. S., Egan, J. J., Wek, S. A., Garty, N. B., Blanchette-Mackie, E. J., & Londos, C. (1991). Perilipin, a major hormonally regulated adipocyte-specific phosphoprotein associated with the periphery of lipid storage droplets. *Journal of Biological Chemistry*, *266*(17), 11341–11346. https://doi.org/10.1016/S0021-9258(18)99168-4

Gunstone, F. D., & Harwood, J. L. (2007). *The lipid handbook with cd-rom*. CRC press.

Gustafson, B., Hammarstedt, A., Andersson, C. X., & Smith, U. (2007). Inflamed adipose tissue. *Arteriosclerosis, Thrombosis, and Vascular Biology*, *27*(11), 2276–2283. https://doi.org/10.1161/ATVBAHA.107.147835

Halama, A., Horsch, M., Kastenmüller, G., Möller, G., Kumar, P., Prehn, C., Laumen, H., Hauner, H., Hrabě de Angelis, M., Beckers, J., Suhre, K., & Adamski, J. (2016). Metabolic switch during adipogenesis: From branched chain amino acid catabolism to lipid synthesis [Applications of Metabolomics]. *Archives of Biochemistry and Biophysics*, *589*, 93–107. https://doi.org/10.1016/j.abb.2015.09.013

Hanczyc, M. M., Fujikawa, S. M., & Szostak, J. W. (2003). Experimental models of primitive cellular compartments: Encapsulation, growth, and division. *Science*, *302*(5645), 618–622. https://doi.org/10.1126/science.1089904

Hapala, I., Marza, E., & Ferreira, T. (2011). Is fat so bad? modulation of endoplasmic reticulum stress by lipid droplet formation. *Biology of the Cell*, *103*(6), 271–285. https://doi.org/10.1042/BC20100144

Hatazawa, Y., Qian, K., Gong, D.-W., & Kamei, Y. (2018). Pgc-1α regulates alanine metabolism in muscle cells. *PLOS ONE*, *13*(1), 1–13. https://doi.org/10.1371/journal.pone.0190904

Hatazawa, Y., Tadaishi, M., Nagaike, Y., Morita, A., Ogawa, Y., Ezaki, O., Takai-Igarashi, T., Kitaura, Y., Shimomura, Y., Kamei, Y., & Miura, S. (2014). Pgc-1α-mediated branched-chain amino acid metabolism in the skeletal muscle. *PLOS ONE*, *9*(3), 1–10. https://doi.org/10.1371/journal.pone.0091006

Henne, W. M., Reese, M. L., & Goodman, J. M. (2018). The assembly of lipid droplets and their roles in challenged cells. *The EMBO Journal*, *37*(12), e98947. https://doi.org/10.15252/embj.201898947

Howald, H., Boesch, C., Kreis, R., Matter, S., Billeter, R., Essén-Gustavsson, B., & Hoppeler, H. H. (2002). Content of intramyocellular lipids derived by electron microscopy, biochemical assays, and (1)h-mr spectroscopy. *Journal of applied physiology*, *92 6*, 2264–72. https://doi.org/10.1152/JAPPLPHYSIOL.01174.2001

Hsieh, C.-T., Chuang, J.-H., Yang, W.-C., Yin, Y., & Lin, Y. (2014). Ceramide inhibits insulin-stimulated akt phosphorylation through activation of rheb/mtorc1/s6k signaling in skeletal muscle. *Cellular Signalling*, *26*(7), 1400–1408. https://doi.org/https://doi.org/10.1016/j.cellsig.2014.03.004

Hunter, J. D. (2007). Matplotlib: A 2d graphics environment. *Computing in Science & Engineering*, *9*(3), 90–95. https://doi.org/10.1109/MCSE.2007.55

ImageJ.net. (2018). Coloc 2 3.0.5 [Accessed: 2023-03-08].

Ingjer, F. (1979). Capillary supply and mitochondrial content of different skeletal muscle fiber types in untrained and endurance-trained men. a histochemical and ultrastructural study. *European journal of applied physiology and occupational physiology*, *40*, 197–209. https://doi.org/10.1007/BF00426942

Kahn, D., Perreault, L., Macias, E., Zarini, S., Newsom, S. A., Strauss, A., Kerege, A., Harrison, K., Snell-Bergeon, J., & Bergman, B. C. (2021). Subcellular localisation and composition of intramuscular triacylglycerol influence in-

sulin sensitivity in humans. *Diabetologia*, *64*, 168–180. https://doi.org/10.1007/s00125-020-05315-0

Kainulainen, H., Hulmi, J. J., & Kujala, U. M. (2013). Potential role of branched-chain amino acid catabolism in regulating fat oxidation. *Exercise and sport sciences reviews*, *41*(4), 194–200. https://doi.org/10.1097/JES.0b013e3182a4e6b6

Kanaley, J. A., Shadid, S., Sheehan, M. T., Guo, Z., & Jensen, M. D. (2009). Relationship between plasma free fatty acid, intramyocellular triglycerides and long-chain acylcarnitines in resting humans. *The Journal of Physiology*, *587*(24), 5939–5950. https://doi.org/https://doi.org/10.1113/jphysiol.2009.180695

Kasperek, G. J., Dohm, G. L., & Snider, R. D. (1985). Activation of branched-chain keto acid dehydrogenase by exercise [PMID: 3970232]. *American Journal of Physiology-Regulatory, Integrative and Comparative Physiology*, *248*(2), R166–R171. https://doi.org/10.1152/ajpregu.1985.248.2.R166

Kenney, W. L., Wilmore, J. H., & Costill, D. L. (2021). *Physiology of sport and exercise*. Human kinetics.

Kirshner, H., Aguet, F., Sage, D., & Unser, M. (2013). 3-d psf fitting for fluorescence microscopy: Implementation and localization application. *Journal of Microscopy*, *249*(1), 13–25. https://doi.org/https://doi.org/10.1111/j.1365-2818.2012.03675.x

Kivela, R., Silvennoinen, M., Lehti, M., Rinnankoski-Tuikka, R., Purhonen, T., Ketola, T., Pullinen, K., Vuento, M., Mutanen, N., Sartor, M. A., Reunanen, H., Koch, L. G., Britton, S. L., & Kainulainen, H. (2010). Gene expression centroids that link with low intrinsic aerobic exercise capacity and complex disease risk. *The FASEB Journal*, *24*(11), 4565–4574. https://doi.org/10.1096/fj.10-157313

Koh, H.-C. E., Nielsen, J., Saltin, B., Holmberg, H.-C., & Ørtenblad, N. (2017). Pronounced limb and fibre type differences in subcellular lipid droplet content and distribution in elite skiers before and after exhaustive exercise. *The Journal of Physiology*, *595*(17), 5781–5795. https://doi.org/10.1113/JP274462

Koh, H.-C. E., Ørtenblad, N., Winding, K. M., Hellsten, Y., Mortensen, S. P., & Nielsen, J. (2018). High-intensity interval, but not endurance, training induces muscle fiber type-specific subsarcolemmal lipid droplet size reduction in type 2 diabetic patients. *American Journal of Physiology-Endocrinology and Metabolism*, *315*(5), E872–E884.

Koistinen, H. A., & Zierath, J. (2002). Regulation of glucose transport in human skeletal muscle. *Annals of medicine*, *34*(6), 410–418. https://doi.org/10.1080/078538902321012351

Krahmer, N., Guo, Y., Farese, R. V., & Walther, T. C. (2009). Snapshot. *Cell*, *139*(5), 1024–1024.e1. https://doi.org/10.1016/j.cell.2009.11.023

Kujala, U. M., Mäkinen, V.-P., Heinonen, I., Soininen, P., Kangas, A. J., Leskinen, T. H., Rahkila, P., Würtz, P., Kovanen, V., Cheng, S., Sipilä, S., Hirvensalo, M., Telama, R., Tammelin, T., Savolainen, M. J., Pouta, A., O'Reilly, P. F.,

Mäntyselkä, P., Viikari, J., … Ala-Korpela, M. (2013). Long-term leisure-time physical activity and serum metabolome. *Circulation*, *127*(3), 340–348. https://doi.org/10.1161/CIRCULATIONAHA.112.105551

Laurens, C., Bourlier, V., Mairal, A., Louche, K., Badin, P.-M., Mouisel, E., Montagner, A., Marette, A., Tremblay, A., Weisnagel, J. S., et al. (2016). Perilipin 5 fine-tunes lipid oxidation to metabolic demand and protects against lipotoxicity in skeletal muscle. *Scientific reports*, *6*(1), 38310. https://doi.org/10.1038/srep38310

Lautaoja, J. H., M. O'Connell, T., Mäntyselkä, S., Peräkylä, J., Kainulainen, H., Pekkala, S., Permi, P., & Hulmi, J. J. (2021). Higher glucose availability augments the metabolic responses of the c2c12 myotubes to exercise-like electrical pulse stimulation [PMID: 34181491]. *American Journal of Physiology-Endocrinology and Metabolism*, *321*(2), E229–E245. https://doi.org/10.1152/ajpendo.00133.2021

Le Lay, S., & Dugail, I. (2009). Connecting lipid droplet biology and the metabolic syndrome. *Progress in lipid research*, *48*(3-4), 191–195.

Lerin, C., Goldfine, A. B., Boes, T., Liu, M., Kasif, S., Dreyfuss, J. M., De Sousa-Coelho, A. L., Daher, G., Manoli, I., Sysol, J. R., Isganaitis, E., Jessen, N., Goodyear, L. J., Beebe, K., Gall, W., Venditti, C. P., & Patti, M.-E. (2016). Defects in muscle branched-chain amino acid oxidation contribute to impaired lipid metabolism. *Molecular Metabolism*, *5*(10), 926–936. https://doi.org/10.1016/j.molmet.2016.08.001

Leskinen, T., Rinnankoski-Tuikka, R., Rintala, M., Seppänen-Laakso, T., Pöllänen, E., Alen, M., Sipilä, S., Kaprio, J., Kovanen, V., Rahkila, P., Orešič, M., Kainulainen, H., & Kujala, U. M. (2010). Differences in muscle and adipose tissue gene expression and cardio-metabolic risk factors in the members of physical activity discordant twin pairs. *PLOS ONE*, *5*(9), 1–9. https://doi.org/10.1371/journal.pone.0012609

Li, Y., Lee, S., Langleite, T., Norheim, F., Pourteymour, S., Jensen, J., Stadheim, H. K., Storås, T. H., Davanger, S., Gulseth, H. L., Birkeland, K. I., Drevon, C. A., & Holen, T. (2014). Subsarcolemmal lipid droplet responses to a combined endurance and strength exercise intervention. *Physiological Reports*, *2*(11), e12187. https://doi.org/10.14814/phy2.12187

Listenberger, L. L., Han, X., Lewis, S. E., Cases, S., Farese Jr, R. V., Ory, D. S., & Schaffer, J. E. (2003). Triglyceride accumulation protects against fatty acid-induced lipotoxicity. *Proceedings of the National Academy of Sciences*, *100*(6), 3077–3082. https://doi.org/10.1073/pnas.0630588100

Machann, J., Häring, H., Schick, F., & Stumvoll, M. (2004). Intramyocellular lipids and insulin resistance. *Diabetes, Obesity and Metabolism*, *6*(4), 239–248.

MacPherson, R. E., & Peters, S. J. (2015). Piecing together the puzzle of perilipin proteins and skeletal muscle lipolysis. *Applied Physiology, Nutrition, and Metabolism*, *40*(7), 641–651. https://doi.org/10.1139/apnm-2014-0485

Malenfant, P., Joanisse, D., Theriault, R., Goodpaster, B., Kelley, D., & Simoneau, J. (2001). Fat content in individual muscle fibers of lean and obese subjects. *International journal of obesity*, *25*(9), 1316–1321.

Mason, R. R., Mokhtar, R., Matzaris, M., Selathurai, A., Kowalski, G. M., Mokbel, N., Meikle, P. J., Bruce, C. R., & Watt, M. J. (2014). Plin5 deletion remodels intracellular lipid composition and causes insulin resistance in muscle. *Molecular metabolism*, *3*(6), 652–663.

Maughan, R. J., Gleeson, M., & Greenhaff, P. L. (1997). *Biochemistry of exercise and training*. Oxford medical publications.

McClain, C. J., Barve, S., & Deaciuc, I. (2007). Good fat/bad fat. *Hepatology*, *45*(6), 1343–1346. https://doi.org/10.1002/hep.21788

Minnaard, R., Schrauwen, P., Schaart, G., Jorgensen, J. A., Lenaers, E., Mensink, M., & Hesselink, M. K. (2009). Adipocyte differentiation-related protein and oxpat in rat and human skeletal muscle: Involvement in lipid accumulation and type 2 diabetes mellitus. *The Journal of Clinical Endocrinology & Metabolism*, *94*(10), 4077–4085.

Mogensen, M., Sahlin, K., Fernström, M., Glintborg, D., Vind, B. F., Beck-Nielsen, H., & Højlund, K. (2007). Mitochondrial Respiration Is Decreased in Skeletal Muscle of Patients With Type 2 Diabetes. *Diabetes*, *56*(6), 1592–1599. https://doi.org/10.2337/db06-0981

Morales, P. E., Bucarey, J. L., & Espinosa, A. (2017). Muscle lipid metabolism: Role of lipid droplets and perilipins. *Journal of diabetes research*, *2017*. https://doi.org/10.1155/2017/1789395

Moro, C., Bajpeyi, S., & Smith, S. R. (2008). Determinants of intramyocellular triglyceride turnover: Implications for insulin sensitivity. *American Journal of Physiology-Endocrinology and Metabolism*, *294*(2), E203–E213. https://doi.org/10.1152/ajpendo.00624.2007

Murphy, D. J. (2012). The dynamic roles of intracellular lipid droplets: From archaea to mammals. *Protoplasma*, *249*, 541–585. https://doi.org/10.1007/s00709-011-0329-7

Murphy, R. F. (2010). Communicating subcellular distributions. *Cytometry Part A*, *77*(7), 686–692. https://doi.org/10.1002/cyto.a.20933

Najt, C. P., Khan, S. A., Heden, T. D., Witthuhn, B. A., Perez, M., Heier, J. L., Mead, L. E., Franklin, M. P., Karanja, K. K., Graham, M. J., Mashek, M. T., Bernlohr, D. A., Parker, L., Chow, L. S., & Mashek, D. G. (2020). Lipid droplet-derived monounsaturated fatty acids traffic via plin5 to allosterically activate sirt1. *Molecular Cell*, *77*(4), 810–824.e8. https://doi.org/10.1016/j.molcel.2019.12.003

Newgard, C. B., An, J., Bain, J. R., Muehlbauer, M. J., Stevens, R. D., Lien, L. F., Haqq, A. M., Shah, S. H., Arlotto, M., Slentz, C. A., Rochon, J., Gallup, D., Ilkayeva, O., Wenner, B. R., Yancy, W. S., Eisenson, H., Musante, G., Surwit, R. S., Millington, D. S., … Svetkey, L. P. (2009). A branched-chain amino acid-related metabolic signature that differentiates obese and lean humans and contributes to insulin resistance. *Cell Metabolism*, *9*(4), 311–326. https://doi.org/10.1016/j.cmet.2009.02.002

Nielsen, J., Mogensen, M., Vind, B. F., Sahlin, K., Højlund, K., Schrøder, H. D., & Ørtenblad, N. (2010). Increased subsarcolemmal lipids in type 2 diabetes: Effect of training on localization of lipids, mitochondria, and glyco-

gen in sedentary human skeletal muscle. *American Journal of Physiology-Endocrinology and Metabolism*, *298*(3), E706–E713.

Nye, C. K., Hanson, R. W., & Kalhan, S. C. (2008). Glyceroneogenesis is the dominant pathway for triglyceride glycerol synthesis in vivo in the rat. *Journal of Biological Chemistry*, *283*(41), 27565–27574. https://doi.org/10.1074/jbc.M804393200

Orbach, S. (2005). Commentary: There is a public health crisis—its not fat on the body but fat in the mind and the fat of profits. *International Journal of Epidemiology*, *35*(1), 67–69. https://doi.org/10.1093/ije/dyi256

pandas development team, T. (2020). Pandas-dev/pandas: Pandas. https://doi.org/10.5281/zenodo.3509134

Park, S. S., & Seo, Y.-K. (2020). Excess accumulation of lipid impairs insulin sensitivity in skeletal muscle. *International Journal of Molecular Sciences*, *21*(6), 1949. https://doi.org/10.3390/ijms21061949

Pedersen, B. K. (2013). Muscle as a secretory organ. In *Comprehensive physiology* (pp. 1337–1362). John Wiley & Sons, Ltd. https://doi.org/10.1002/cphy.c120033

Pereira-Dutra, F. S., Teixeira, L., de Souza Costa, M. F., & Bozza, P. T. (2019). Fat, fight, and beyond: The multiple roles of lipid droplets in infections and inflammation. *Journal of Leukocyte Biology*, *106*(3), 563–580. https://doi.org/10.1002/JLB.4MR0119-035R

Perreault, L., Newsom, S. A., Strauss, A., Kerege, A., Kahn, D. E., Harrison, K. A., Snell-Bergeon, J. K., Nemkov, T., D'Alessandro, A., Jackman, M. R., MacLean, P. S., & Bergman, B. C. (2018). Intracellular localization of diacylglycerols and sphingolipids influences insulin sensitivity and mitochondrial function in human skeletal muscle. *JCI Insight*, *3*(3). https://doi.org/10.1172/jci.insight.96805

Peters, S. J., Samjoo, I. A., Devries, M. C., Stevic, I., Robertshaw, H. A., & Tarnopolsky, M. A. (2012). Perilipin family (plin) proteins in human skeletal muscle: The effect of sex, obesity, and endurance training. *Applied Physiology, Nutrition, and Metabolism*, *37*(4), 724–735. https://doi.org/10.1139/h2012-059

Phielix, E., Meex, R., Ouwens, D. M., Sparks, L., Hoeks, J., Schaart, G., Moonen-Kornips, E., Hesselink, M. K., & Schrauwen, P. (2012). High Oxidative Capacity Due to Chronic Exercise Training Attenuates Lipid-Induced Insulin Resistance. *Diabetes*, *61*(10), 2472–2478. https://doi.org/10.2337/db11-1832

Picard, M., Hepple, R. T., & Burelle, Y. (2012). Mitochondrial functional specialization in glycolytic and oxidative muscle fibers: Tailoring the organelle for optimal function. *American Journal of Physiology-Cell Physiology*, *302*(4), C629–C641. https://doi.org/10.1152/ajpcell.00368.2011

Pierucci, F., Frati, A., Battistini, C., Penna, F., Costelli, P., & Meacci, E. (2021). Control of skeletal muscle atrophy associated to cancer or corticosteroids by ceramide kinase. *Cancers*, *13*(13). https://doi.org/10.3390/cancers13133285

Pourteymour, S., Lee, S., Langleite, T. M., Eckardt, K., Hjorth, M., Bindesbøll, C., Dalen, K. T., Birkeland, K. I., Drevon, C. A., Holen, T., & Norheim, F. (2015).

Perilipin 4 in human skeletal muscle: Localization and effect of physical activity. *Physiological Reports*, *3*(8), e12481. https://doi.org/https://doi.org/10.14814/phy2.12481

Prats, C., Donsmark, M., Qvortrup, K., Londos, C., Sztalryd, C., Holm, C., Galbo, H., & Ploug, T. (2006). Decrease in intramuscular lipid droplets and translocation of hsl in response to muscle contraction and epinephrine. *Journal of lipid research*, *47*(11), 2392–2399. https://doi.org/10.1194/jlr.M600247-JLR200

Pressly, J. D., Gurumani, M. Z., Varona Santos, J. T., Fornoni, A., Merscher, S., & Al-Ali, H. (2022). Adaptive and maladaptive roles of lipid droplets in health and disease. *American Journal of Physiology-Cell Physiology*, *322*(3), C468–C481. https://doi.org/10.1152/ajpcell.00239.2021

Rimmer, P. B., Xu, J., Thompson, S. J., Gillen, E., Sutherland, J. D., & Queloz, D. (2018). The origin of rna precursors on exoplanets. *Science Advances*, *4*(8), eaar3302. https://doi.org/10.1126/sciadv.aar3302

Rinnankoski-Tuikka, R., Hulmi, J. J., Torvinen, S., Silvennoinen, M., Lehti, M., Kivelä, R., Reunanen, H., Kujala, U. M., & Kainulainen, H. (2014). Lipid droplet-associated proteins in high-fat fed mice with the effects of voluntary running and diet change. *Metabolism*, *63*(8), 1031–1040. https://doi.org/10.1016/j.metabol.2014.05.010

Roddy, S., Stewart, I., & Barnes-Holmes, D. (2011). Facial reactions reveal that slim is good but fat is not bad: Implicit and explicit measures of body-size bias. *European Journal of Social Psychology*, *41*(6), 688–694. https://doi.org/10.1002/ejsp.839

Russell, A. P., Gastaldi, G., Bobbioni-Harsch, E., Arboit, P., Gobelet, C., Dériaz, O., Golay, A., Witztum, J. L., & Giacobino, J.-P. (2003). Lipid peroxidation in skeletal muscle of obese as compared to endurance-trained humans: A case of good vs. bad lipids? *FEBS Letters*, *551*(1-3), 104–106. https://doi.org/10.1016/S0014-5793(03)00875-5

Russell, A. (2004). Lipotoxicity: The obese and endurance-trained paradox. *International Journal of Obesity*, *28*(4), S66–S71. https://doi.org/10.1038/sj.ijo.0802859

Sage, D., Donati, L., Soulez, F., Fortun, D., Schmit, G., Seitz, A., Guiet, R., Vonesch, C., & Unser, M. (2017). Deconvolutionlab2: An open-source software for deconvolution microscopy. *Methods*, *115*, 28–41. https://doi.org/10.1016/j.ymeth.2016.12.015

Schindelin, J., Arganda-Carreras, I., Frise, E., Kaynig, V., Longair, M., Pietzsch, T., Preibisch, S., Rueden, C., Saalfeld, S., Schmid, B., et al. (2012). Fiji: An open-source platform for biological-image analysis. *Nature methods*, *9*(7), 676–682. https://doi.org/10.1038/nmeth.2019

Schrauwen-Hinderling, V. B., Hesselink, M. K., Schrauwen, P., & Kooi, M. E. (2006). Intramyocellular lipid content in human skeletal muscle. *Obesity*, *14*(3), 357–367. https://doi.org/10.1038/oby.2006.47

Scott, L. J., Erdos, M. R., Huyghe, J. R., Welch, R. P., Beck, A. T., Wolford, B. N., Chines, P. S., Didion, J. P., Narisu, N., Stringham, H. M., Koistinen, H. A.,

et al. (2016). The genetic regulatory signature of type 2 diabetes in human skeletal muscle. *Nature communications*, *7*(1), 11764. https://doi.org/10.1038/ncomms11764

Seabold, S., & Perktold, J. (2010). Statsmodels: Econometric and statistical modeling with python. *9th Python in Science Conference*.

Seibert, J. T., Najt, C. P., Heden, T. D., Mashek, D. G., & Chow, L. S. (2020). Muscle lipid droplets: Cellular signaling to exercise physiology and beyond. *Trends in Endocrinology & Metabolism*, *31*(12), 928–938. https://doi.org/10.1016/j.tem.2020.08.002

Shaw, C. S., Shepherd, S. O., Wagenmakers, A. J. M., Hansen, D., Dendale, P., & van Loon, L. J. C. (2012). Prolonged exercise training increases intramuscular lipid content and perilipin 2 expression in type i muscle fibers of patients with type 2 diabetes. *American Journal of Physiology-Endocrinology and Metabolism*, *303*(9), E1158–E1165. https://doi.org/10.1152/ajpendo.00272.2012

Shaw, C. S., Jones, D. A., & Wagenmakers, A. J. (2008). Network distribution of mitochondria and lipid droplets in human muscle fibres. *Histochemistry and cell biology*, *129*(1), 65–72.

Shaw, C. S., Sherlock, M., Stewart, P. M., & Wagenmakers, A. J. (2009). Adipophilin distribution and colocalisation with lipid droplets in skeletal muscle. *Histochemistry and cell biology*, *131*(5), 575–581.

Shaw, C. S., Swinton, C., Morales-Scholz, M. G., McRae, N., Erftemeyer, T., Aldous, A., Murphy, R. M., & Howlett, K. F. (2020). Impact of exercise training status on the fiber type-specific abundance of proteins regulating intramuscular lipid metabolism. *Journal of Applied Physiology*, *128*(2), 379–389.

She, P., Zhou, Y., Zhang, Z., Griffin, K., Gowda, K., & Lynch, C. J. (2010). Disruption of bcaa metabolism in mice impairs exercise metabolism and endurance [PMID: 20133434]. *Journal of Applied Physiology*, *108*(4), 941–949. https://doi.org/10.1152/japplphysiol.01248.2009

Shepherd, S. O., Cocks, M., Tipton, K. D., Ranasinghe, A. M., Barker, T. A., Burniston, J. G., Wagenmakers, A. J. M., & Shaw, C. S. (2012). Preferential utilization of perilipin 2-associated intramuscular triglycerides during 1 h of moderate-intensity endurance-type exercise. *Experimental Physiology*, *97*(8), 970–980. https://doi.org/https://doi.org/10.1113/expphysiol.2012.064592

Shepherd, S. O., Cocks, M., Tipton, K. D., Ranasinghe, A. M., Barker, T. A., Burniston, J. G., Wagenmakers, A. J. M., & Shaw, C. S. (2013). Sprint interval and traditional endurance training increase net intramuscular triglyceride breakdown and expression of perilipin 2 and 5. *The Journal of Physiology*, *591*(3), 657–675. https://doi.org/10.1113/jphysiol.2012.240952

Shepherd, S. O., Cocks, M., Tipton, K. D., Witard, O. C., Ranasinghe, A. M., Barker, T. A., Wagenmakers, A. J. M., & Shaw, C. S. (2014). Resistance training increases skeletal muscle oxidative capacity and net intramuscular triglyceride breakdown in type i and ii fibres of sedentary males. *Ex-*

perimental Physiology, *99*(6), 894–908. https://doi.org/https://doi.org/10.1113/expphysiol.2014.078014

Shepherd, S., Cocks, M., Meikle, P., Mellett, N., Ranasinghe, A., Barker, T., Wagenmakers, A., & Shaw, C. (2017). Lipid droplet remodelling and reduced muscle ceramides following sprint interval and moderate-intensity continuous exercise training in obese males. *International journal of obesity*, *41*(12), 1745–1754. https://doi.org/10.1038/ijo.2017.170

Silverthorn, U. (2010). Human physiology: An integrated approach by dee. *San Fransico: Pearson Benjamin Cummings*, 598–601.

Sjögren, R. J., Rizo-Roca, D., Chibalin, A. V., Chorell, E., Furrer, R., Katayama, S., Harada, J., Karlsson, H. K., Handschin, C., Moritz, T., et al. (2021). Branched-chain amino acid metabolism is regulated by errα in primary human myotubes and is further impaired by glucose loading in type 2 diabetes. *Diabetologia*, *64*(9), 2077–2091. https://doi.org/10.1007/s00125-021-05481-9

Son, Y. H., Lee, S.-M., Lee, S. H., Yoon, J. H., Kang, J. S., Yang, Y. R., & Kwon, K.-S. (2019). Comparative molecular analysis of endurance exercise in vivo with electrically stimulated in vitro myotube contraction [PMID: 31622160]. *Journal of Applied Physiology*, *127*(6), 1742–1753. https://doi.org/10.1152/japplphysiol.00091.2019

Standl, E., Lotz, N., Dexel, T., Janka, H. .-., & Kolb, H. (1980). Muscle triglycerides in diabetic subjects: Effect of insulin deficiency and exercise. *Diabetologia*, *18*, 463–469. https://doi.org/10.1007/BF00261702

Stephens, N. A., Skipworth, R. J., MacDonald, A. J., Greig, C. A., Ross, J. A., & Fearon, K. C. (2011). Intramyocellular lipid droplets increase with progression of cachexia in cancer patients. *Journal of cachexia, sarcopenia and muscle*, *2*, 111–117. https://doi.org/10.1007/s13539-011-0030-x

Stokie, J. R., Abbott, G., Howlett, K. F., Hamilton, D. L., & Shaw, C. S. (2023). Intramuscular lipid utilisation during exercise: A systematic review, meta-analysis and meta-regression. *Journal of Applied Physiology*. https://doi.org/10.1152/japplphysiol.00637.2021

Stone, S. J., Levin, M. C., Zhou, P., Han, J., Walther, T. C., & Farese, R. V. (2009). The endoplasmic reticulum enzyme dgat2 is found in mitochondria-associated membranes and has a mitochondrial targeting signal that promotes its association with mitochondria. *Journal of Biological Chemistry*, *284*(8), 5352–5361. https://doi.org/10.1074/jbc.M805768200

Su, X., & Abumrad, N. A. (2009). Cellular fatty acid uptake: A pathway under construction. *Trends in Endocrinology & Metabolism*, *20*(2), 72–77. https://doi.org/10.1016/j.tem.2008.11.001

Subbotin, V., & Fiksel, G. (2023). Exploring the lipid world hypothesis: A novel scenario of self-sustained darwinian evolution of the liposomes. *Astrobiology*. https://doi.org/10.1089/ast.2021.0161

Summers, S. A., Garza, L. A., Zhou, H., & Birnbaum, M. J. (1998). Regulation of insulin-stimulated glucose transporter glut4 translocation and akt kinase

activity by ceramide. *Molecular and Cellular Biology*, *18*(9), 5457–5464. https://doi.org/10.1128/MCB.18.9.5457

Sztalryd, C., & Brasaemle, D. L. (2017). The perilipin family of lipid droplet proteins: Gatekeepers of intracellular lipolysis [Recent Advances in Lipid Droplet Biology]. *Biochimica et Biophysica Acta (BBA) - Molecular and Cell Biology of Lipids*, *1862*(10, Part B), 1221–1232. https://doi.org/10.1016/j.bbalip.2017.07.009

Tan, R., Nederveen, J. P., Gillen, J. B., Joanisse, S., Parise, G., Tarnopolsky, M. A., & Gibala, M. J. (2018). Skeletal muscle fiber-type-specific changes in markers of capillary and mitochondrial content after low-volume interval training in overweight women. *Physiological Reports*, *6*(5), e13597. https://doi.org/10.14814/phy2.13597

Tarnopolsky, M. A., Rennie, C. D., Robertshaw, H. A., Fedak-Tarnopolsky, S. N., Devries, M. C., & Hamadeh, M. J. (2007). Influence of endurance exercise training and sex on intramyocellular lipid and mitochondrial ultrastructure, substrate use, and mitochondrial enzyme activity. *American Journal of Physiology-Regulatory, Integrative and Comparative Physiology*, *292*(3), R1271–R1278. https://doi.org/10.1152/ajpregu.00472.2006

Timmers, S., Konings, E., Bilet, L., Houtkooper, R. H., van de Weijer, T., Goossens, G. H., Hoeks, J., van der Krieken, S., Ryu, D., Kersten, S., Moonen-Kornips, E., Hesselink, M. K., Kunz, I., Schrauwen-Hinderling, V. B., Blaak, E. E., Auwerx, J., & Schrauwen, P. (2011). Calorie restriction-like effects of 30 days of resveratrol supplementation on energy metabolism and metabolic profile in obese humans. *Cell Metabolism*, *14*(5), 612–622. https://doi.org/https://doi.org/10.1016/j.cmet.2011.10.002

Unger, R. H., Clark, G. O., Scherer, P. E., & Orci, L. (2010). Lipid homeostasis, lipotoxicity and the metabolic syndrome [Lipotoxicity]. *Biochimica et Biophysica Acta (BBA) - Molecular and Cell Biology of Lipids*, *1801*(3), 209–214. https://doi.org/10.1016/j.bbalip.2009.10.006

van Loon, L. J. C., Koopman, R., Manders, R., van der Weegen, W., van Kranenburg, G. P., & Keizer, H. A. (2004a). Intramyocellular lipid content in type 2 diabetes patients compared with overweight sedentary men and highly trained endurance athletes [PMID: 15165998]. *American Journal of Physiology-Endocrinology and Metabolism*, *287*(3), E558–E565. https://doi.org/10.1152/ajpendo.00464.2003

van Loon, L. J., & Goodpaster, B. H. (2006). Increased intramuscular lipid storage in the insulin-resistant and endurance-trained state. *Pflügers Archiv*, *451*(5), 606–616.

van Loon, L. J., Koopman, R., Manders, R., van der Weegen, W., van Kranenburg, G. P., & Keizer, H. A. (2004b). Intramyocellular lipid content in type 2 diabetes patients compared with overweight sedentary men and highly trained endurance athletes. *American Journal of Physiology-Endocrinology And Metabolism*, *287*(3), E558–E565.

Virtanen, P., Gommers, R., Oliphant, T. E., Haberland, M., Reddy, T., Cournapeau, D., Burovski, E., Peterson, P., Weckesser, W., Bright, J., van der Walt, S. J.,

Brett, M., Wilson, J., Millman, K. J., Mayorov, N., Nelson, A. R. J., Jones, E., Kern, R., Larson, E., ... SciPy 1.0 Contributors. (2020). SciPy 1.0: Fundamental Algorithms for Scientific Computing in Python. *Nature Methods*, *17*, 261–272. https://doi.org/10.1038/s41592-019-0686-2

Voet, D., Voet, J. G., & Pratt, C. W. (2016). *Fundamentals of biochemistry: Life at the molecular level*. John Wiley & Sons.

Walther, T. C., & Farese, R. V. (2012). Lipid droplets and cellular lipid metabolism [PMID: 22524315]. *Annual Review of Biochemistry*, *81*(1), 687–714. https://doi.org/10.1146/annurev-biochem-061009-102430

Wang, H., Bell, M., Sreenevasan, U., Hu, H., Liu, J., Dalen, K., Londos, C., Yamaguchi, T., Rizzo, M. A., Coleman, R., et al. (2011). Unique regulation of adipose triglyceride lipase (atgl) by perilipin 5, a lipid droplet-associated protein. *Journal of Biological Chemistry*, *286*(18), 15707–15715.

Waskom, M., & the seaborn development team. (2020). *Mwaskom/seaborn* (Version latest). Zenodo. https://doi.org/10.5281/zenodo.592845

Watt, M. J. (2009). Storing up trouble: Does accumulation of intramyocellular triglyceride protect skeletal muscle from insulin resistance? *Clinical and Experimental Pharmacology and Physiology*, *36*(1), 5–11.

Welte, M. (2015). Expanding roles for lipid droplets. *Current biology*, *25*(11), R470–R481. https://doi.org/10.1016/j.cub.2015.04.004

Whytock, K. L., Parry, S. A., Turner, M. C., Woods, R. M., James, L. J., Ferguson, R. A., Ståhlman, M., Borén, J., Strauss, J. A., Cocks, M., Wagenmakers, A. J. M., Hulston, C. J., & Shepherd, S. O. (2020). A 7-day high-fat, high-calorie diet induces fibre-specific increases in intramuscular triglyceride and perilipin protein expression in human skeletal muscle. *The Journal of Physiology*, *598*(6), 1151–1167. https://doi.org/https://doi.org/10.1113/JP279129

Whytock, K., Shepherd, S., Wagenmakers, A., & Strauss, J. (2018). Hormone sensitive lipase preferentially redistributes to perilipin-5 lipid droplets in human skeletal muscle during moderate-intensity exercise. *Journal of Physiology*. https://doi.org/10.1113/JP275502

Wilfling, F., Haas, J. T., Walther, T. C., & Farese Jr, R. V. (2014). Lipid droplet biogenesis. *Current opinion in cell biology*, *29*, 39–45. https://doi.org/10.1016/j.ceb.2014.03.008

Wolins, N. E., & Mittendorfer, B. (2018). The athlete's paradoxpat. *The Journal of Physiology*, *596*(5), 755–756. https://doi.org/10.1113/JP275505

Wolins, N. E., Quaynor, B. K., Skinner, J. R., Tzekov, A., Croce, M. A., Gropler, M. C., Varma, V., Yao-Borengasser, A., Rasouli, N., Kern, P. A., et al. (2006). Oxpat/pat-1 is a ppar-induced lipid droplet protein that promotes fatty acid utilization. *Diabetes*, *55*(12), 3418–3428.

Wree, A., Broderick, L., Canbay, A., Hoffman, H. M., & Feldstein, A. E. (2013). From nafld to nash to cirrhosis—new insights into disease mechanisms. *Nature reviews Gastroenterology & hepatology*, *10*(11), 627–636. https://doi.org/10.1038/nrgastro.2013.149

Xu, M., Nagasaki, M., Obayashi, M., Sato, Y., Tamura, T., & Shimomura, Y. (2001). Mechanism of activation of branched-chain α-keto acid dehydrogenase complex by exercise. *Biochemical and Biophysical Research Communications*, *287*(3), 752–756. https://doi.org/10.1006/bbrc.2001.5647

Xu, Y.-Y., Shen, H.-B., & Murphy, R. F. (2020). Learning complex subcellular distribution patterns of proteins via analysis of immunohistochemistry images. *Bioinformatics*, *36*(6), 1908–1914. https://doi.org/10.1093/bioinformatics/btz844

Zadoorian, A., Du, X., & Yang, H. (2023). Lipid droplet biogenesis and functions in health and disease. *Nature Reviews Endocrinology*, 1–17. https://doi.org/10.1038/s41574-023-00845-0

Zehmer, J. K., Huang, Y., Peng, G., Pu, J., Anderson, R. G. W., & Liu, P. (2009). A role for lipid droplets in inter-membrane lipid traffic. *PROTEOMICS*, *9*(4), 914–921. https://doi.org/https://doi.org/10.1002/pmic.200800584

Zhang, X., Xu, W., Xu, R., Wang, Z., Zhang, X., Wang, P., Peng, K., Li, M., Li, J., Tan, Y., et al. (2022). Plin5 bidirectionally regulates lipid metabolism in oxidative tissues. *Oxidative Medicine and Cellular Longevity*, *2022*. https://doi.org/10.1155/2022/4594956

Zheng, N., Tsai, H. N., Zhang, X., Shedden, K., & Rosania, G. R. (2011). The subcellular distribution of small molecules: A meta-analysis. *Molecular pharmaceutics*, *8*(5), 1611–1618. https://doi.org/10.1021/mp200093z

ORIGINAL PUBLICATIONS

I

ENLARGED PLIN5-UNCOATED LIPID DROPLETS IN INNER REGIONS OF SKELETAL MUSCLE TYPE II FIBERS ASSOCIATE WITH TYPE 2 DIABETES

by

Fachada, V., Rahkila, P., Fachada, N., Turpeinen, T., Kujala, U.M., Kainulainen, H (2022)

Acta Histochemica 124(3), 151869.

https://doi.org/10.1016/j.acthis.2022.151869

.

Acta Histochemica 124 (2022) 151869

Contents lists available at ScienceDirect

Acta Histochemica

journal homepage: www.elsevier.com/locate/acthis

Enlarged PLIN5-uncoated lipid droplets in inner regions of skeletal muscle type II fibers associate with type 2 diabetes

Vasco Fachada [a,*], Paavo Rahkila [a], Nuno Fachada [b], Tuomas Turpeinen [c], Urho M. Kujala [a], Heikki Kainulainen [a]

[a] Faculty of Sport and Health Sciences, NeuroMuscular Research Center, University of Jyvaskyla, Rautpohjankatu 8, Jyvaskyla 40014, Finland
[b] Lusofona University, COPELABS, Lisboa 1749-024, Portugal
[c] Department of Physics, University of Jyvaskyla, Jyvaskyla 40014, Finland

ARTICLE INFO

Keywords:
Lipid droplets
PLIN5
Type II diabetes
Skeletal muscle
Insulin resistance
Fiber type

ABSTRACT

Skeletal muscle physiology remains of paramount importance in understanding insulin resistance. Due to its high lipid turnover rates, regulation of intramyocellular lipid droplets (LDs) is a key factor. Perilipin 5 (PLIN5) is one of the most critical agents in such regulation, being often referred as a protector against lipotoxicity and consequent skeletal muscle insulin resistance. We examined area fraction, size, subcellular localization and PLIN5 association of LDs in two fiber types of type 2 diabetic (T2D), obese (OB) and healthy (HC) individuals by means of fluorescence microscopy and image analysis. We found that T2D type II fibers have a significant sub-population of large and internalized LDs, uncoated by PLIN5. Based on this novel result, additional hypotheses for the pathophysiology of skeletal muscle insulin resistance are formulated, together with future research directions.

1. Introduction

Skeletal muscle is a specialized tissue with particular importance in mammalian physiology, from energy turnover to a wide range of signaling pathways and consequent metabolic and health implications, such as insulin resistance (Coen et al., 2009; Goodpaster and Wolf, 2004; LeLay and Dugail, 2009; Machann et al., 2004). In the past two decades, the understanding of such roles has been strengthened by the uprising study of lipid droplets (LDs) as a key role player in cell signaling, including its relationship to insulin resistance. Initially it was thought this relationship was linear, where increased intramyocellular lipid content (IMCL) translated directly into elevated insulin resistance. Later, however, the so called *atlhete's paradox* demonstrated that extremely insulin sensitive individuals, such as endurance athletes, had even higher IMCL than type 2 diabetic patients (Goodpaster et al., 2001; Van Loon et al., 2004; van Loon and Goodpaster, 2006; Moro et al., 2008). Such data shifted research from quantitative towards more qualitative facets of IMCL regulation, namely lipotoxicity, i.e., the hypothesis that byproducts from inefficient IMCL lipolysis could trigger insulin resistance signaling (Russell, 2004).

One of the hot topics became the Perilipin (PLIN) family, a group of proteins directly involved in LDs turnover by often coating these organelles and regulating the access of enzymes and related co-activators (Bickel et al., 2009; MacPherson and Peters, 2015; Minnaard et al., 2009). One of the PLIN members, PLIN5, is known to express significantly in highly oxidative tissues, as skeletal muscle (Wolins et al., 2006). Given PLIN5′s significant participation in IMCL physiology, it has become one of the central agents in the study of skeletal muscle insulin resistance, namely by its function in protecting against lipotoxicity (Mason and Watt, 2015; Gemmink et al., 2016). Moreover, together with fiber typing, subcellular localization of IMCL has also been studied in relation to insulin resistance and muscle oxidative capacity (Nielsen et al., 2010; Shaw et al., 2008, 2009, 2020; Koh et al., 2018).

Nevertheless, we believe that LDs sub-populations have yet to be fully identified, namely concerning the relationship between their size, subcellular localization and PLIN5 association. We hence hypothesized that the relationship between intramyocellular LDs and PLIN5 in different fiber types would reveal hidden profile differences between

Abbreviations: LDs, lipid droplets; all-LDs, all lipid droplets; col-LDs, colocalized lipid droplets; unc-LDs, uncoated lipid droplets; HC, healthy controls; OB, obese; T2D, type II diabetic; IMCL, intramyocellular lipids; PLIN5, perilipin 5.

* Corresponding author.
E-mail address: vasco.fachada@jyu.fi (V. Fachada).

https://doi.org/10.1016/j.acthis.2022.151869
Received 19 October 2021; Received in revised form 3 February 2022; Accepted 12 February 2022
Available online 24 February 2022

healthy and insulin resistant individuals. Thus, we analyzed microscope images of human skeletal muscle of type 2 diabetic (T2D), obese (OB) and healthy control (HC) human subjects. We explored two different fiber types for area fraction, size and subcellular localization of LDs, PLIN5 and their colocalization. Subtle key differences in skeletal muscle lipid profile were found between the studied groups and novel observations were made concerning IMCL and its relationship with PLIN5 in different fiber types.

2. Methods

2.1. Subjects

Twenty-five physically inactive male individuals were divided into three groups according to their health status and weight. Seven healthy, non-diabetic subjects (BMI $\leq$ 30 kg.m^{-2} or body fat percentage 10–20%) were included in the HC. The obese group consisted of 8 non-diabetic obese subjects (BMI $>$ 30 kg.m^{-2}). The type II diabetic group consisted of 10 subjects clinically diagnosed with type 2 diabetes (Table 1). Most individuals in T2D were medicated against insulin resistance and/or high blood pressure. Written informed consent and health questionnaires were obtained from all volunteers before starting any measurements. The study plan was approved by the ethical committee of the University of Jyväskylä.

Blood samples were collected from the brachial artery after overnight fasting. All blood variables were measured in plasma by standard enzymatic methods using Roche Diagnostic's reagents with an automated analyzer (Roche Modular P800, Roche Diagnostics GmbH, Germany).

Maximal oxygen consumption (VO_2 max) was measured in a graded bicycle test. Respiratory gases were measured by open-circuit spirometry (Oxycon Pro Jæger, Germany). The test was carried until subjects wanted to stop, or when heart rate, blood pressure or oxygen consumption started decreasing. The maximal oxygen consumption was considered as the highest 30 s average of oxygen consumption in relative value (mL.min^{-1}.kg^{-1}).

Prior to collecting the muscle biopsy, subjects refrained from physical exercise for 48 h. Before taking the biopsy the skin area was shaved and cooled with ice for ten minutes before local the anesthetic was injected (Lidocain 20 mg.mL^{-1} c. adrenalin). The biopsy was performed with a Bergström needle from the vastus lateralis muscle approximately 15 cm above the patella tendon and 2 cm away from the fascia. The samples were covered with Tissue-Tek and frozen immediately in isopentane cooled with liquid nitrogen, then finally stored at − 80°C until further analyses.

2.2. Histology and imaging

Five micrometer cross sections were cut in a cryostat at − 25°C (Leica CM 3000, Germany). Sections were collected in 13 mm round coverslips and immediately fixed in 4% paraformaldehyde for 15 min at room temperature (RT).

Table 1
Group characteristics. Mean ± SEM. ** $P < 0.01$ using a Kruskal-Wallis H test. Pairwise post hoc significance ($P < 0.05$) is denoted with letters *a* to *c*, from highest to lowest value.

n	Controls (HC) 7	Diabetic (T2D) 10	Obese (OB) 8
Age (years)	56.4 ± 2.8	52.7 ± 2.2	51.9 ± 3.2
Body weight (kg)**	78.4 ± 2.4^{c}	112.0 ± 7.1^{a}	99.6 ± 5.4^{b}
BMI (kg.m^{-2})**	25.8 ± 0.4^{b}	34.0 ± 1.6^{a}	32.3 ± 1.0^{a}
Fat percentage (%)**	19.9 ± 1.1^{b}	29.2 ± 1.4^{a}	30.7 ± 1.8^{a}
Tryglycerides (mmol.L^{-1})**	1.4 ± 0.2^{b}	2.8 ± 0.7^{a}	1.8 ± 0.4^{b}
Blood glucose (mmol.L^{-1})**	5.1 ± 0.2^{b}	8.0 ± 1.3^{a}	5.1 ± 0.6^{b}
VO_2 max (mL.min^{-1}.kg^{-1})**	30.7 ± 1.5^{b}	23.0 ± 1.8^{a}	28.6 ± 2.1^{b}

After washing for 3×5 minutes with phosphate buffer saline (PBS), the sections were blocked with 3% bovine serum albumin (BSA) for 30 min and then washed briefly with PBS. Primary antibodies were diluted in 1% BSA and incubated for 1 h in at RT, using GP31 (Progen, Germany) against PLIN5 diluted 1–200 and M4276 (Sigma, USA) against fast myosin heavy chain diluted 1–50.

Next, the samples were washed for 3×15 min with PBS, before incubating with the secondary antibodies in 1% BSA for 1 h in dark RT, using anti guinea pig IgG AlexaFluor 594 (JacksonImmunoResearch, USA) diluted 1–50 together with anti mouse IgG AlexaFluor AMCA (JacksonImmunoResearch, USA) diluted 1–50. A 3×10 min PBS washing followed. Up to this point, all steps were performed with 0.05% saponin. Lipid droplets were then stained with LipidTOX™ Green (FITS, Molecular Probes), using a 1–100 dilution in PBS for 30 min in dark RT. Excess dye was removed with 2×10 seconds brief PBS wash right before mounting.

Slides were mounted using Mowiol with 2.5% DABCO (Sigma-Aldrich) and left to dry for at least 1 h in the dark at 4°C.

Raw data collection was achieved with a BX50 BXFLA (Olympus, Japan), coupled to ColorViewIII camera (Soft Imaging Systems), through a 40x/0.75NA objective. Fluorophores were excited with a mercury lamp, through U-MWU, U-MWB and MWG excitation cubes. Controlled with the software AnalySIS 5.0 (Soft Imaging Systems), fluorescent signal was gray-scale recorded for each channel. Fig. 1a-c represents raw data prior to any image processing.

2.3. Image processing and variable assessment

Fluorescent 0.5 μm microspheres (TetraSpeck, Molecular Probes) were used for particle size calibration and exclusion of diffracted signal as illustrated in Fig. 1D-I. Prior to analyses, all images were denoised and deconvoluted in *ImageJ* (Schneider et al., 2012) using a theoretical point spread function separately for each channel.

From each cross section, all intact and artifact-free skeletal muscle fibers were selected, and then carefully segmented (HC = 88 ± 20; T2D = 32 ± 7 and OB = 41 ± 9. Mean ± SE). Cells were classified into either type I or type II fibers, according to the detected and thresholded signal of fast myosin per cell area (cutoff value = 500). For each cell, every binarized particle (Fig. 1F) was measured in *ImageJ*. Size and subcellular localization of each of these particles was assessed in different fiber types. These variables were measured from the total number of detected LDs (all-LDs), PLIN5, the LDs associating with PLIN5 (col-LDs), and for the LDs uncoated with PLIN5 (unc-LDs). The association between PLIN5 and LDs was determined by colocalization (Costes et al., 2004) and performed as previously (Nissinen et al., 2021).

2.4. Data analysis

Unless stated otherwise, significance between the three groups (marked with *) and fiber types (marked with #) was assessed with two-way analysis of variance (ANOVA2). For post hoc analysis to compare fiber type differences between each group or any variable between two given groups, Mann-Whitney U test was performed. Normality was assessed with Shapiro-Wilk test and histogram inspection. Boxes in the boxplot figures depict interquartile ranges and medians, while whisquers represent the 95% confidence interval. Correlation analyses were carried with Spearman's ρ. Statistical significance levels were set at $P < 0.05$ and $P < 0.01$. Data crunching, statistics and visualization were performed in *Python*, with the packages *NumPy* (Harris et al., 2020), *pandas* (Anon, 2020), *SciPy* (Virtanen et al., 2020), *statsmodels* (Seabold and Perktold, 2010), *seaborn* (Waskom, 2020) and *matplotlib* (Hunter, 2007), respectively. All *ImageJ* and *Python* routines can be found at https://github.com/seiryoku-zenyo/Diabetic-study.

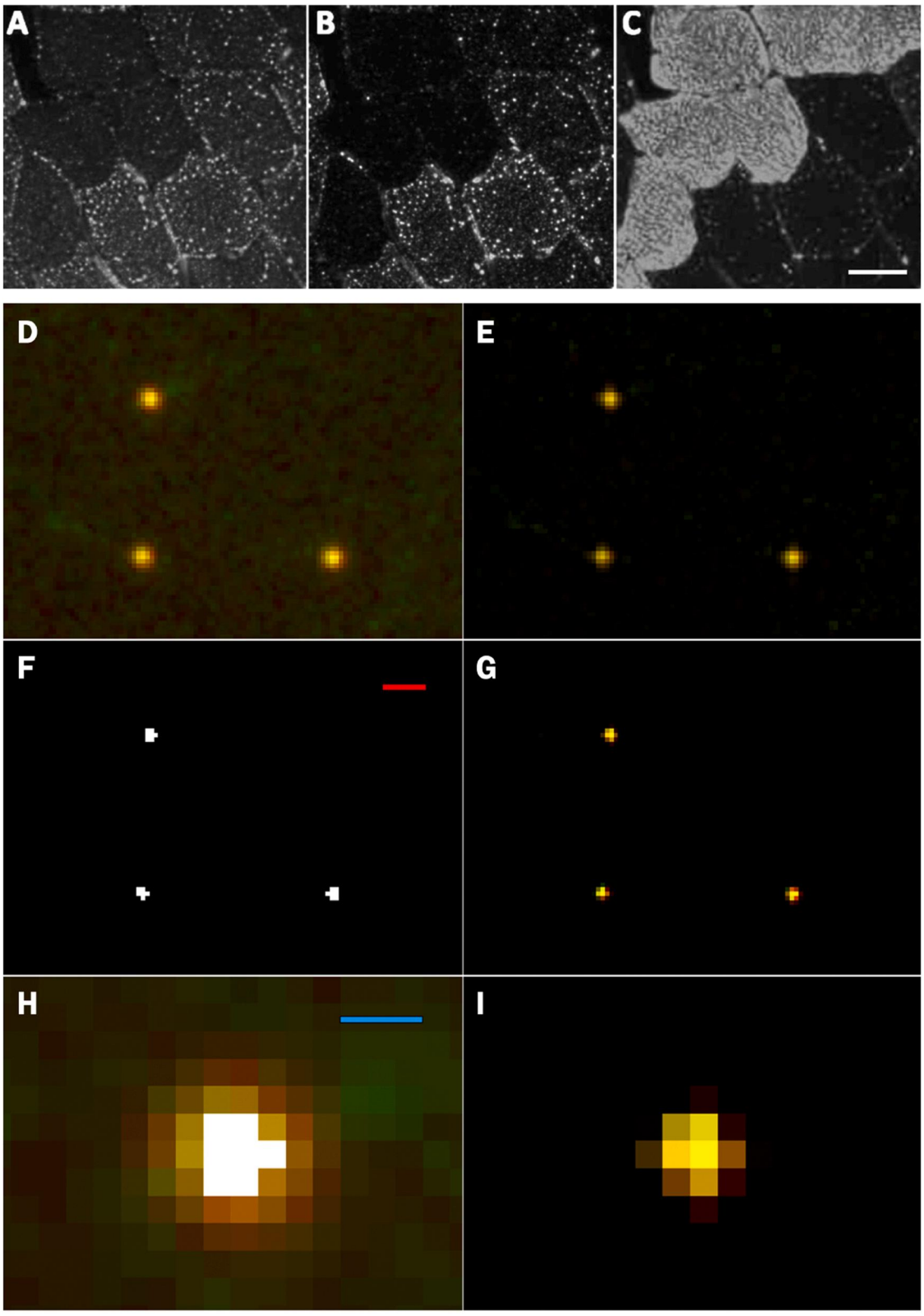

Fig. 1. Microscope data calibration. A): LipidTOX. B): PLIN5. C): Fast myosin. D): Raw imaged 0.5 μm microspheres. E): Denoising of D. F): Binarization ("Otsu" threshold) of G. G) Deconvolution (Richardson-Lucy) of E. H): Cropping of upper left microsphere, binarized data (F) overlayed on raw data (D). I): Cropping of deconvoluted upper left microsphere (G). White bar in C = 40 μm, red bar in F = 2 μm, blue bar in H = 0.5 μm.

3. Results

3.1. Area fraction

Despite the visible tendency of increased IMCL in T2D and OB, no significant differences between groups were detected in all-LDs fraction. Nonetheless, amongst groups and as expected, type I fibers showed significantly higher all-LDs fraction when compared to type II fibers ($P = 0.05$). Such fiber type differences were mainly driven by differences within the HC and T2D groups ($P = 0.02$ and $P = 0.032$, respectively), as seen in Fig. 2a.

Interestingly, however, concerning unc-LDs area fraction, HC retained fiber type differences ($P = 0.048$), while T2D lost these differences ($P = 0.24$). Consequently, type II fibers of T2D showed significantly higher unc-LD area fraction than the same fiber type in HC ($P = 0.044$) as seen in Fig. 2c.

More clearly than in all-LDs, we found significant differences in PLIN5 area fraction between fiber types amongst groups ($P = 1.01e^{-9}$) and within every group ($P = 0.001$ for HC, $P = 1e^{-4}$ for T2D and $P = 0.041$ for OB), as seen in Fig. 2d. The increased PLIN5 area fraction in type I fibers was especially evident in T2D, where post hoc revealed significantly higher values versus the same fiber type in HC ($P = 0.029$). It is interesting to note that the same increased PLIN5 area fraction in Type I fibers of T2D versus HC, was not observed between type II fibers of both groups ($P = 0.20$).

In addition to higher PLIN5 area fraction in type I fibers, T2D also showed significantly higher fraction of col-LDs than HC in both fiber types ($P = 0.014$ for type I fibers and $P = 0.036$ for type II fibers) as seen in Fig. 2b.

3.2. LD diameter

In terms of LD size, we found significant differences in the diameter of all-LDs between groups ($P = 0.008$), especially in type II fibers ($P = 0.021$). As summarized by Fig. 3a, these differences were mainly driven by larger all-LDs in T2D versus HC ($P = 0.029$ for type I fibers and $P = 0.001$ for type II fibers).

Although ANOVA2 showed no fiber type differences amongst all groups, we did find that T2D alone had significantly larger all-LDs in type II fibers in comparison to type I fibers ($P = 0.027$). Interestingly, these differences in LD size seem to originate from unc-LDs ($P = 0.027$) and not from col-LDs, where differences between fiber types disappear ($P = 0.76$), as presented in Fig. 3b-c.

As expected, col-LDs were significantly larger than unc-LDs in both fiber types of all groups ($P < 0.01$).

3.3. Subcellular localization

The HC group showed a tendency for all-LDs being closer to the sarcolemma as seen in Fig. 4a, albeit no differences with ANOVA2 between groups ($P = 0.12$) or fiber types ($P = 0.3$). Unlike the other groups however, HC showed closer all-LDs to sarcolemma in type II fibers when compared to type I ($P = 0.027$). Interestingly, HC type II fibers revealed significantly closer all-LDs to the sarcolemma versus the same fiber type in T2D ($P = 0.018$). Again, the internalized nature of all-LDs seem to originate from unc-LDs (Fig. 4c).

It is worth noting that ANOVA2 did show PLIN5 to be significantly closer to the sarcolemma in type II fibers ($P = 0.032$), albeit not detecting significant differences between groups ($P = 0.07$), as highlighted in Fig. 4d.

3.4. Diameter versus localization

Given the increased fraction and size of unc-LDs, together with its deeper subcellular localization in type II fibers of T2D, we decided to further investigate such relationship.

By plotting a bivariate kernel density estimation between the diameter and subcellular location of LDs, we observed that T2D has a substantial sub-population of enlarged unc-LDs in inner regions of type II fibers only (Fig. 5b).

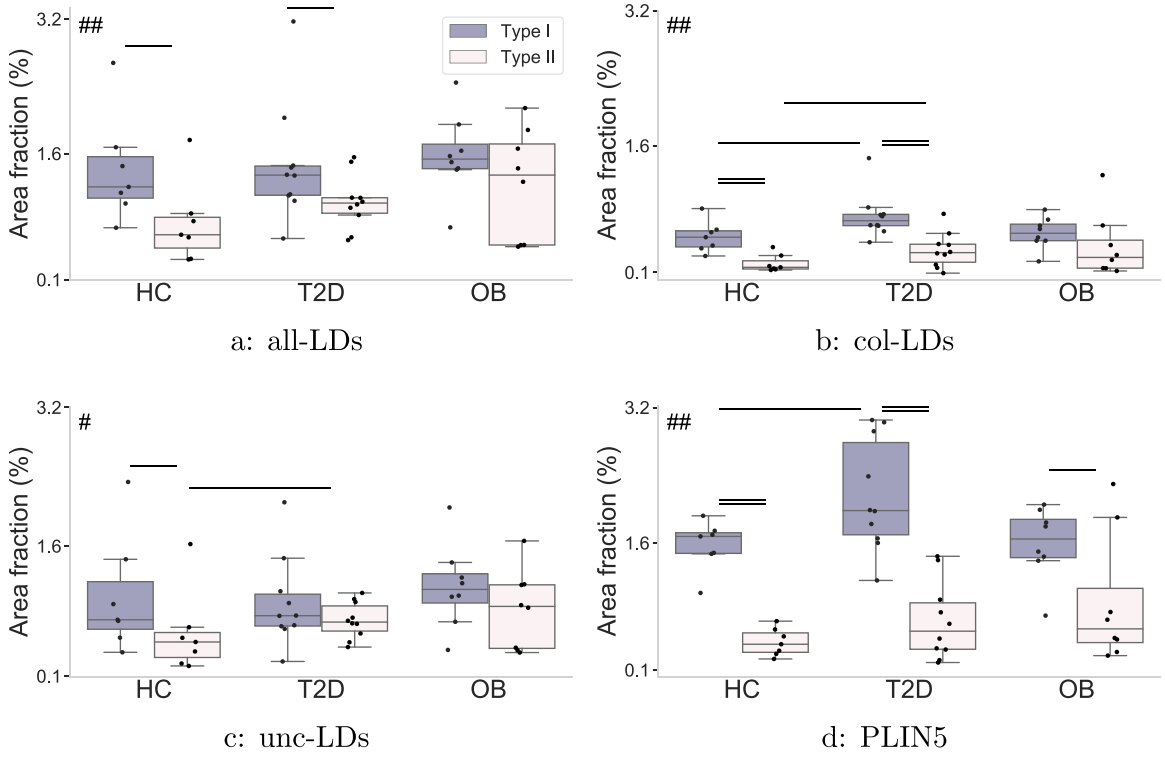

Fig. 2. Area fraction for a) all-LDs; b) col-LDs; c) unc-LDs and d) PLIN5. Fiber type differences by ANOVA2 denoted with #($P < 0.05$) and ##($P < 0.01$). Post hoc statistical significance is denoted with horizontal bars ($P < 0.05$) or double horizontal bars ($P < 0.01$).

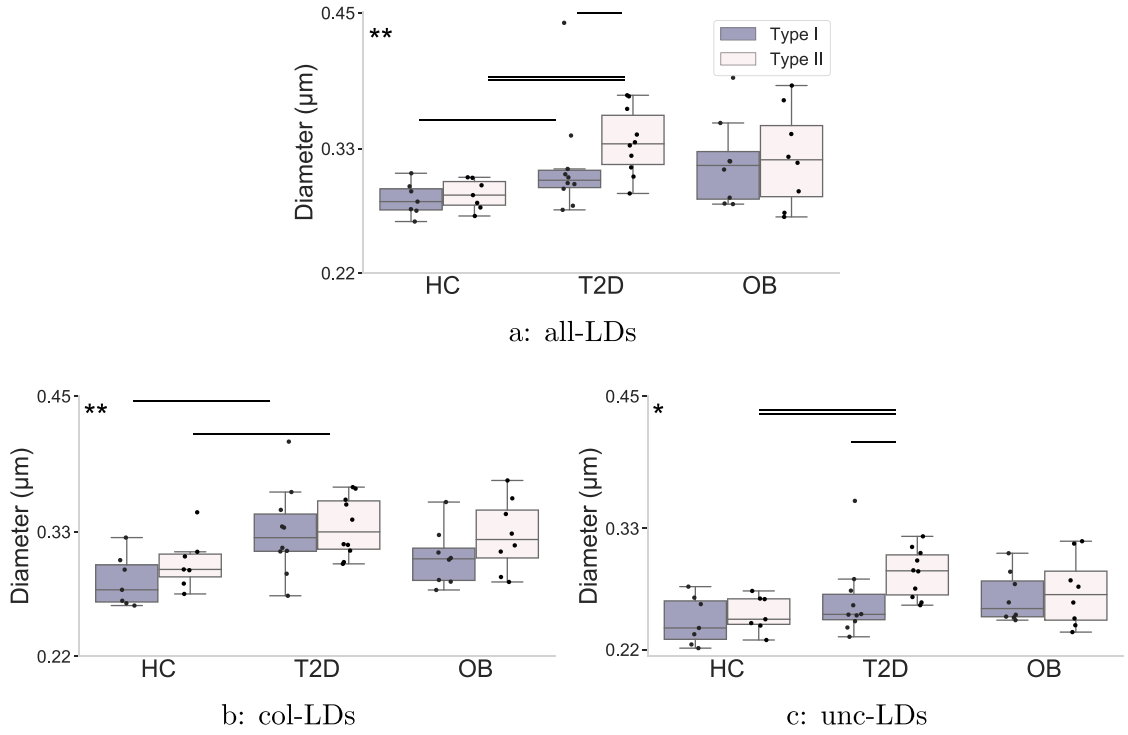

Fig. 3. Size of a) all-LDs; b) col-LDs and c) unc-LDs. Group differences by ANOVA2 denoted with * ($P < 0.05$) and **($P < 0.01$). Post hoc statistical significance is denoted with horizontal bars ($P < 0.05$) or double horizontal bars ($P < 0.01$).

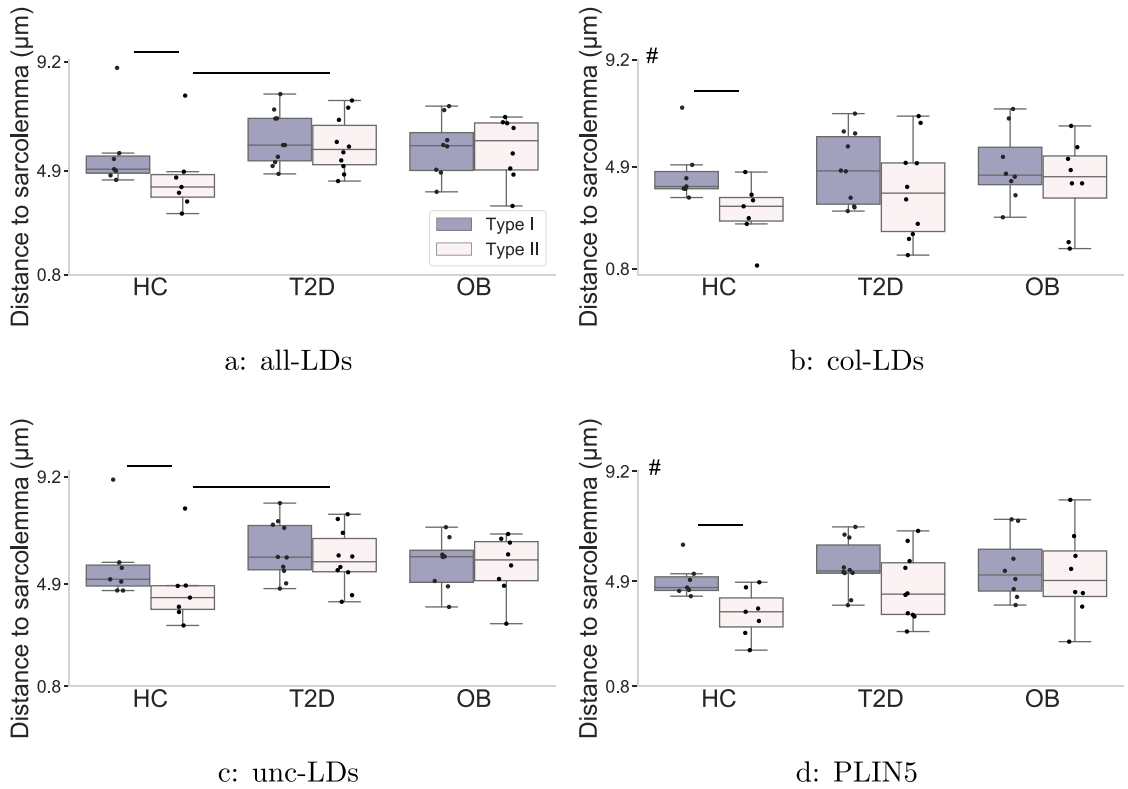

Fig. 4. Distance to sarcolemma of a) all-LDs; b) col-LDs; c) unc-LDs and d) PLIN5. Fiber type differences by ANOVA2 denoted with #($P < 0.05$). Post hoc statistical significance is denoted with horizontal bars ($P < 0.05$).

In all groups and fiber types, the largest LDs could be found associating with PLIN5 and close to the sarcolemma. This was more evident in type II fibers, where we found a relatively low density (light tones) of col-LDs in inner regions of the cells (Fig. 5a).

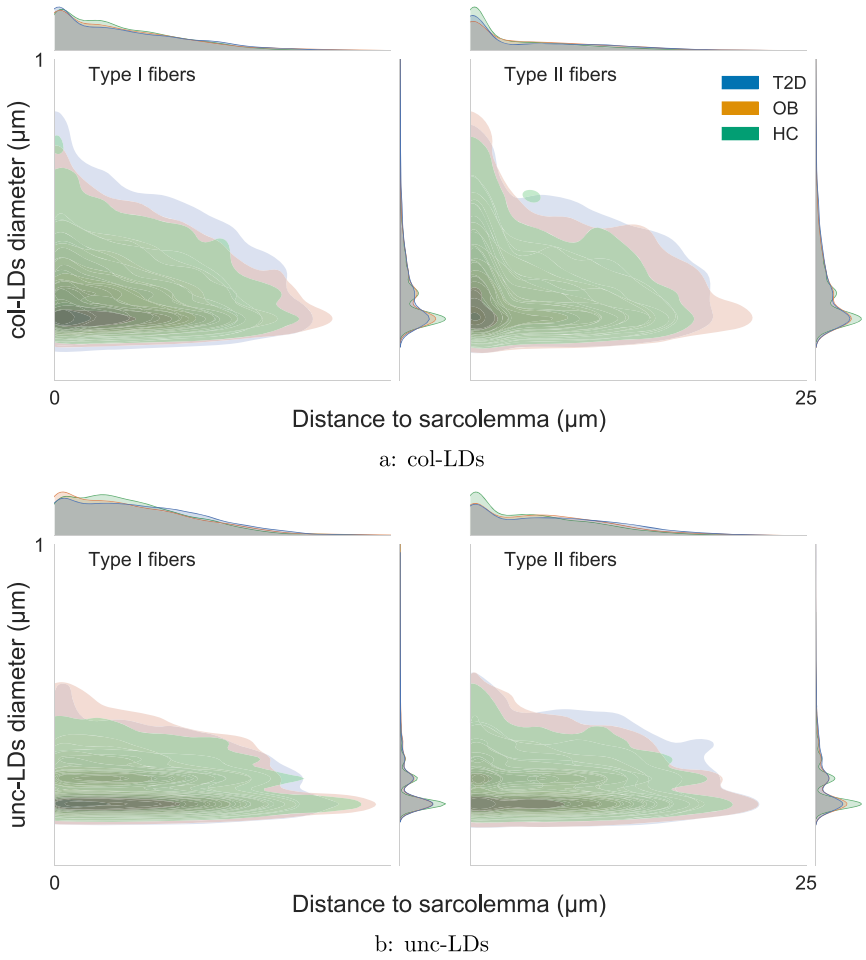

Fig. 5. Bivariate kernel density estimation between diameter and distance to sarcolemma of a) col-LDs and b) unc-LDs. From each fiber type and particle type, 500 LDs per subject were randomly selected into a pool representing each group, then from each pool, 3000 LDs were randomly selected to generate the present figure.

3.5. Correlations

We observed a mild positive correlation between the diameter of unc-LDs and blood glucose levels in T2D only, albeit without reaching significance and with no fiber type differences ($\rho = 0.56$, $P = 0.093$ for type I fibers and $\rho = 0.51$, $P = 0.13$ for type II fibers) as seen in Supplement A.1.

Furthermore, we found strong negative correlations between fat percentage and PLIN5 area fraction in HC only (Fig. 6 b), especially in type I fibers (P= 0.002), where PLIN5 abounds.

Interestingly, when testing against VO_2 max, we found a strong and significant correlation ($\rho = 0.76$, $P = 0.01$) for unc-LDs in type II fibers of T2D only (Fig. 7b).

4. Discussion

4.1. Overview

In this study we examined IMCL, namely area fraction, subcellular localization and size of LDs in different fiber types of obese, type II diabetic and healthy individuals. Additionally, we looked at the association of each of these LDs with PLIN5 across the groups. Amongst the three distinct profiles, T2D and HC were, as expected, the more contrasting ones.

Our main findings were that T2D have increased IMCL uncoated with PLIN5 in type II fibers, mainly in the form of larger LDs in inner regions of the cells. Unlike HC, T2D does not show a decreased area fraction of unc-LDs in type II fibers in comparison to type I fibers (Fig. 2c). This seems to originate from significantly larger unc-LDs, which indeed, were larger in type II than in type I fibers of T2D (Fig. 3c). In normal physiological conditions, type II fibers are expected to have a lower amount of IMCL, as they are known to have a lower oxidative capacity when compared to type I fibers (Malenfant et al., 2001). Possible physiological impacts of this phenomenon remain to be shown.

Equally expected Shaw et al. (2020), is the significantly increased PLIN5 area fraction in type I versus type II fibers, which we observed in every group. In fact, this partially explains the increased col-LDs area fraction in type I fibers of all groups (Fig. 2b and d). It is known that PLIN5 is a responder to increased IMCL in oxidative tissues like skeletal muscle type I fibers. It seems to have a role in protecting muscle against lipotoxicity, by translocating towards IMCL and thus regulating the access of lipases and co-activators, consequently decreasing, if necessary, the rate of triacylglycerol hydrolysis (MacPherson and Peters, 2015). This mechanism has been suggested as a putative role PLIN5 has in attenuating lipid induced insulin resistance in skeletal muscle (Gemmink et al., 2016). Additionally, PLIN5 deletion has been shown to lead to insulin resistance (Mason et al., 2014b, 2014a). Curiously enough, we have observed a mild positive correlation between PLIN5 area fraction and fat percentage in T2D and OB, while HC showed a clearer but negative correlation ($\rho = -0.94$, $P = 0.002$ for type I fibers and $\rho = 0.78$, $P = 0.041$ for type II fibers) as seen in Fig. 6b and Fig. 7.

We were therefore startled, that despite PLIN5′s increased area fraction in type I fibers of T2D, it did not seem equally or sufficiently present in type II fibers of the same group in order to coat the increased IMCL in that same fiber type. This is represented in Fig. 8, where the most impacting contrast between HC and T2D appears to be in type II

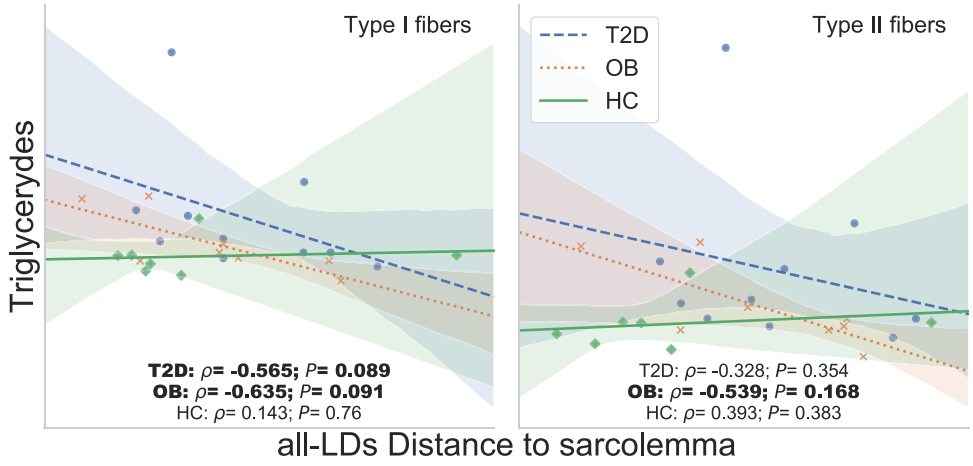

a: All-LDs distance to sarcolemma vs. Triglycerides

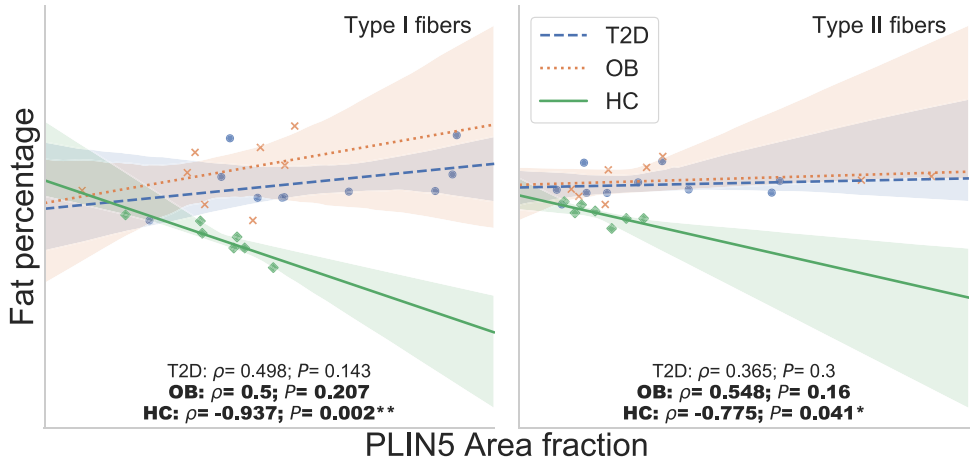

b: PLIN5 area fraction vs. Fat percentage

Fig. 6. Linear association with systemic lipids. Between a) Triglycerides and all-LDs distance to sarcolemma; b) PLIN5 area fraction and Fat percentage. Shaded areas show bootstrapped 95% confidence intervals for the fitted regressions. Bold signifies $|\rho| > 0.5$; * $P < 0.05$; ** $P < 0.01$.

fibers, precisely by showing increased amounts of IMCL relatively devoid of PLIN5. Given that PLIN5 area fraction and distance to sarcolemma are not different in T2D type II fibers in comparison to HC, it seems likely that the internalized unc-LDs originate from excess IMCL in general rather than from a diminished presence of PLIN5.

4.2. LD size

We observed that not only all-LDs are larger in T2D than in HC, but also that the largest droplets in both fiber types are coated with PLIN5 (Fig. 3b and Fig. 5a). In accordance, while this manuscript was being prepared, another group has observed that the largest LDs were more extensively coated with PLIN5 in T2D versus athletes (Gemmink et al., 2021). Like in our study, others have observed larger LDs in type II versus type I fibers within T2D, as well as in T2D versus healthy individuals (Koh et al., 2018; Daemen et al., 2018). However, as far as we know, this is the first study demonstrating that a notable portion of these larger droplets in type II fibers is not coated with PLIN5 in T2D, which is clearly contrasting with HC and therefore, likely not physiological (Fig. 3c).

It is important to reinforce the notion that large col-LDs are metabolically active IMCL, which by being close to the cell membrane, are close to higher densities of mitochondria, enzymes and chaperones, and consequently, more actively hydrolyzing tryacylglycerol into fatty acids or, depending on cell needs, esterifying incoming fatty acids into triacylglycerol. It is therefore, not too surprising that col-LDs tend to be larger. This begs the question, what is the role or impact of enlarged unc-LDs?

4.3. Localization of large unc-LDs in type II fibers

We measured the distance of each lipid droplet towards the sarcolemma and found that HC, in average, have more peripheral IMCL in type II than in type I fibers (Fig. 4a). This is somewhat expectable, as type II fibers are less equipped to internalize and process fatty acids (Bonen et al., 1998). Additionally, we observed that not only T2D did not reveal the same fiber type differences as HC, but actually showed type II fibers with more internalized IMCL than the same fiber type in HC (Fig. 4). Previous research as shown that increased IMCL in T2D and OB individuals is at least partially explained by an increased ability to transport and internalize fatty acids (Bonen et al., 2004).

Subcellular localization of IMCL has been studied in similar populations before, and while some studies might have shown concurring results to ours (Van Loon et al., 2004), the relationship between the localization of different sub-populations of LDs and insulin resistance seems far from fully understood. For instance, by means of electron microscopy, type 2 diabetic individuals were shown to possess higher relative amounts of subsarcolemmal IMCL, which in turn, correlated to

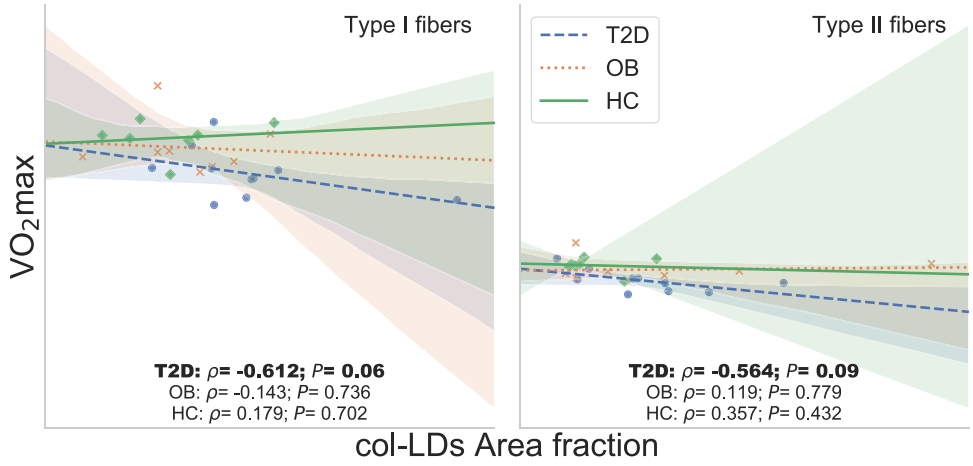

a: col-LDs diameter vs. VO_2 max

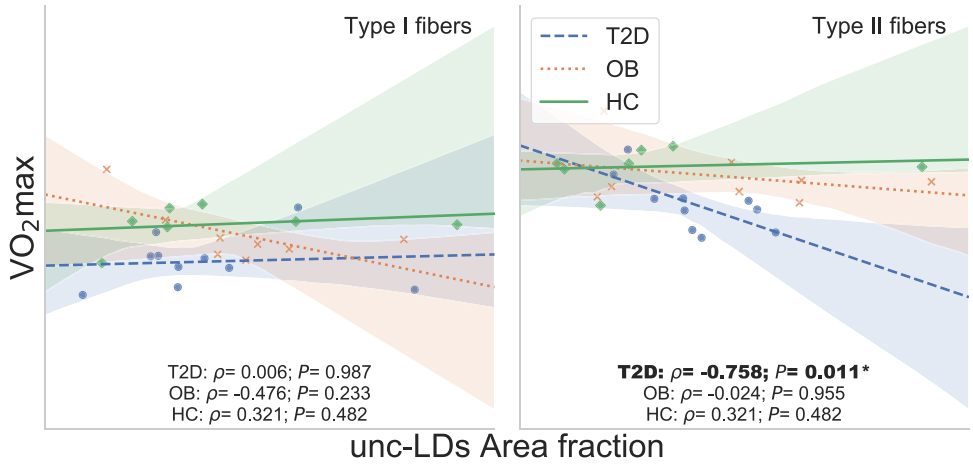

b: unc-LDs diameter vs. VO_2 max

Fig. 7. Linear association with VO_2 max. Between VO_2 max and area fraction of a) col-LDs and b) unc-LDs. Shaded areas show bootstrapped 95% confidence intervals for the fitted regressions. Bold signifies $|\rho| > 0.5$; * $P < 0.05$.

insulin resistance (Nielsen et al., 2010). Such results are not necessarily conflicting, as the aforementioned study compared type 2 diabetic with BMI matched obese individuals and endurance athletes. Furthermore, both methods have well known contrasting advantages and disadvantages regarding image resolution and total area sampled, and therefore might not be measuring the same precise physical phenomena. In this study we refrained from using terms like “subsarcolemmal" and “intramyofibrillar", as admittedly, we cannot resolve such regions with confidence. Instead, we measured every detectable LD from hundreds of cells, classified them according to their association with PLIN5 and plotted their distribution.

Despite all-LDs being closer to the membrane in HC type II fibers, subcellular localization of both col-LDs and PLIN5 pools did not differ between HC and T2D (Fig. 4d). However, just like all-LDs, unc-LDs were significantly more internalized in T2D type II fibers versus the same fiber type of HC (Fig. 4c). This led us to suspect that more and larger LDs were left uncoated of PLIN5 in inner regions of T2D type II fibers. We therefore decided to specifically investigate the size of these more internalized unc-LDs, and as suspected, T2D had an important portion of enlarged unc-LDs in inner regions of type II fibers (Fig. 5).

4.4. Conclusions

These results point to a novel characteristic in insulin resistant skeletal muscle physiology, i.e., type II fibers are abnormally flooded with large LDs unattended by PLIN5. The importance of this discovery is yet to be completely assessed, it could become paramount and should pave for future research exploring the link between this phenomenon and insulin resistance.

Together with the fact that type II fibers have poorer machinery to process and hydrolyze triacyglycerol, it becomes tempting to hypothesize that, such increased amounts of IMCL uncoated with PLIN5 in type II fibers could be mechanistically associated with skeletal muscle insulin resistance.

Moreover, we observed that larger unc-LDs correlate positively with blood glucose levels in T2D only, although weakly and with no apparent fiber type differences (Supplement A.1). As often associated to insulin resistance (Leite et al., 2009; Morinder et al., 2009), we further observed VO_2 max strongly correlate with unc-LDs area fraction in type II fibers of T2D (Fig. 7b).

Whether these forsaken large droplets are downstream or upstream the insulin resistance pathway, is something that cannot be answered with this study. While the failure of PLIN5 in coating LDs may lead to insulin resistance, such mechanism seems to require some degree triacyglycerol hydrolysis by lipases such as ATGL or HSL and presence of mitochondria (Watt, 2009; Bruce et al., 2007; Machann et al., 2004; MacPherson and Peters, 2015), most of which tend to be closer to the sarcolemma (Mason et al., 2014a, 2014b).

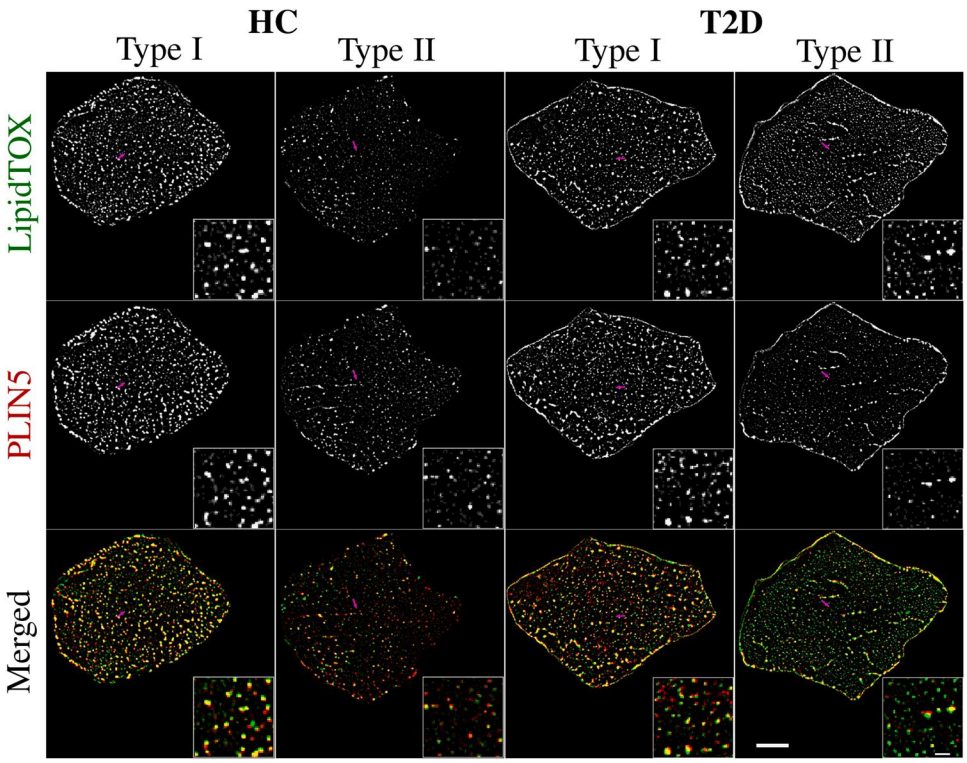

Fig. 8. Representative image of IMCL and PLIN5 in different fiber types. Note greener type II fibers in T2D, depicting increased IMCL (green) unattended by PLIN5 (red). Small boxes correspond to the area pointed by magenta arrows. Large bar = 10 μm; small bar = 2 μm.

In the future it would be interesting to repeat similar setups using additional markers, like the lipases mentioned above and the CGI-58 co-activator, which hydrolyzing activity has been shown to be inhibited upon PLIN5's presence (Granneman et al., 2009, 2011; Wang et al., 2011). It will be important to evaluate any possible interaction between such hydrolyzing agents and the sub-population of large and internalized unc-LDs identified in this study.

4.5. *Limitations, strengths and implications*

Care should be taken when interpreting light microscopy data from muscle sections. Even if the imaging equipment plus processing techniques are optimal and the known resolution limit is reached, many if not most LDs will remain undetected. Better resolution could be achieved with electron microscopy, but there would be a significant trade-off in sampling area. Another inherent limitation of such methods concerns the representability offered by a thin section, from a small biopsy of a given specific muscle, from a small number of subjects, at a given time. We believe some of our results could reveal clearer and more significant with a larger number of statistical cases. To add to the latter, we acknowledge the fact that all but one T2D subjects were medicated, which could have an impact on intramyocellular PLIN5 (Minnaard et al., 2009). Moreover, like often in literature, we made a dual classification of fiber types, which is likely too simplistic to represent the real and large spectrum of fibers present in skeletal muscle. A final note on the limitations of this study should be given to the fact that for sake of comparability, only male subjects were studied, although there are known differences between genders regarding this topic.

Nevertheless, thorough image processing techniques grant us confidence in data validity, while robust data analysis methods allowed us to measure and visualize the relationships between size, localization and association of LDs with PLIN5 between groups. Thus, we are able to report a clear and novel pattern, emerging from the increased unc-LDs in inner regions of type II fibers of T2D.

Our observations provide clues for future directions concerning the study of lipid droplets and PLIN5 in skeletal muscle insulin resistance. We believe it is important to continue investigating the physiology of different lipid droplet sub-populations, specifically, enlarged unc-LDs in inner regions of type II fibers.

Funding

This study was supported by the Academy of Finland (grant 132987 and 298875) and Fundação para a Ciência e a Tecnologia (FCT, Portugal) under grant UIDB/04111/2020 (COPELABS). The author Vasco Fachada acknowledges his FCT grant SFRH/BD/68308/2010.

Conflict of interest

The authors declare that there are no conflicts of interest associated with this manuscript.

Author contribution statement

VF interpreted the data and wrote the manuscript. HK, UK, PR and VF designed the study. NF, HK and UK contributed to writing the manuscript. Immunohistochemistry and microscopy were carried by VF and PR. Bioinformatics was carried by VF, NF and TT. All authors read and approved the final version of the manuscript.

Data Availability

Data will be made available on request.

Appendix A. Supporting information

Supplementary data associated with this article can be found in the online version at doi:10.1016/j.acthis.2022.151869.

References

Anon, 2020. T. pandas development team, pandas-dev/pandas: Pandas (Feb. 2020). 10.5281/zenodo.3509134.

Bickel, P.E., Tansey, J.T., Welte, M.A., 2009. Pat proteins, an ancient family of lipid droplet proteins that regulate cellular lipid stores. Biochim. Biophys. Acta (BBA) Mol. Cell Biol. Lipids 1791 (6), 419–440 (lipid Droplets as dynamic organelles connecting influx, efflux and storage of lipids).

Bonen, A., Luiken, J., Liu, S., Dyck, D., Kiens, B., Kristiansen, S., Turcotte, L., Van Der Vusse, G., Glatz, J., 1998. Palmitate transport and fatty acid transporters in red and white muscles. Am. J. Physiol. Endocrinol. Metab. 275 (3), E471–E478.

Bonen, A., Parolin, M.L., Steinberg, G.R., Calles-Escandon, J., Tandon, N.N., Glatz, J.F., Luiken, J.J., Heigenhauser, G.J., Dyck, D.J., 2004. Triacylglycerol accumulation in human obesity and type 2 diabetes is associated with increased rates of skeletal muscle fatty acid transport and increased sarcolemmal fat/cd36. FASEB J. 18 (10), 1144–1146.

Bruce, C.R., Brolin, C., Turner, N., Cleasby, M.E., van der Leij, F.R., Cooney, G.J., Kraegen, E.W., 2007. Overexpression of carnitine palmitoyltransferase i in skeletal muscle in vivo increases fatty acid oxidation and reduces triacylglycerol esterification. Am. J. Physiol. Endocrinol. Metab. 292 (4), E1231–E1237.

Coen, P.M., Dubé, J.J., Amati, F., Stefanovic-Racic, M., Ferrell, R.E., Toledo, F.G., Goodpaster, B.H., 2009. Insulin resistance is associated with higher intramyocellular triglycerides in type i but not type ii myocytes concomitant with higher ceramide content. Diabetes.

Costes, S.V., Daelemans, D., Cho, E.H., Dobbin, Z., Pavlakis, G., Lockett, S., 2004. Automatic and quantitative measurement of protein-protein colocalization in live cells. Biophys. J. 86 (6), 3993–4003.

Daemen, S., Gemmink, A., Brouwers, B., Meex, R.C., Huntjens, P.R., Schaart, G., Moonen-Kornips, E., Jörgensen, J., Hoeks, J., Schrauwen, P., Hesselink, M.K., 2018. Distinct lipid droplet characteristics and distribution unmask the apparent contradiction of the athlete's paradox. Mol. Metab. 17, 71–81. https://doi.org/10.1016/j.molmet.2018.08.004. ⟨https://www.sciencedirect.com/science/article/pii/S2212877818307415⟩.

Gemmink, A., Bosma, M., Kuijpers, H.J., Hoeks, J., Schaart, G., van Zandvoort, M.A., Schrauwen, P., Hesselink, M.K., 2016. Decoration of intramyocellular lipid droplets with plin5 modulates fasting-induced insulin resistance and lipotoxicity in humans. Diabetologia 59 (5), 1040–1048.

Gemmink, A., Daemen, S., Brouwers, B., Hoeks, J., Schaart, G., Knoops, K., Schrauwen, P., Hesselink, M.K., 2021. Decoration of myocellular lipid droplets with perilipins as a marker for in vivo lipid droplet dynamics: a super-resolution microscopy study in trained athletes and insulin resistant individuals. Biochim. Biophys. Acta (BBA) Mol. Cell Biol. Lipids 1866 (2), 158852. https://doi.org/10.1016/j.bbalip.2020.158852. ⟨https://www.sciencedirect.com/science/article/pii/S1388198120302444⟩.

Goodpaster, B.H., Wolf, D., 2004. Skeletal muscle lipid accumulation in obesity, insulin resistance, and type 2 diabetes. Pediatr. Diabetes 5 (4), 219–226.

Goodpaster, B.H., He, J., Watkins, S., Kelley, D.E., 2001. Skeletal muscle lipid content and insulin resistance: evidence for a paradox in endurance-trained athletes. J. Clin. Endocrinol. Metab. 86 (12), 5755–5761.

Granneman, J.G., Moore, H.-P.H., Krishnamoorthy, R., Rathod, M., 2009. Perilipin controls lipolysis by regulating the interactions of ab-hydrolase containing 5 (abhd5) and adipose triglyceride lipase (atgl). J. Biol. Chem. 284 (50), 34538–34544.

Granneman, J.G., Moore, H.-P.H., Mottillo, E.P., Zhu, Z., Zhou, L., 2011. Interactions of perilipin-5 (plin5) with adipose triglyceride lipase. J. Biol. Chem. 286 (7), 5126–5135.

Harris, C.R., Millman, K.J., van der Walt, S.J., Gommers, R., Virtanen, P., Cournapeau, D., Wieser, E., Taylor, J., Berg, S., Smith, N.J., Kern, R., Picus, M., Hoyer, S., van Kerkwijk, M.H., Brett, M., Haldane, A., FernándezdelRío, J., Wiebe, M., Peterson, P., Gérard-Marchant, P., Sheppard, K., Reddy, T., Weckesser, W., Abbasi, H., Gohlke, C., Oliphant, T.E., 2020. Array programming with NumPy. Nature 585, 357–362. https://doi.org/10.1038/s41586-020-2649-2.

Hunter, J.D., 2007. Matplotlib: a 2d graphics environment. Comput. Sci. Eng. 9 (3), 90–95. https://doi.org/10.1109/MCSE.2007.55.

Koh, H.-C.E., Ørtenblad, N., Winding, K.M., Hellsten, Y., Mortensen, S.P., Nielsen, J., 2018. High-intensity interval, but not endurance, training induces muscle fiber type-specific subsarcolemmal lipid droplet size reduction in type 2 diabetic patients. Am. J. Physiol. Endocrinol. Metab. 315 (5), E872–E884.

Leite, S.A., Monk, A.M., Upham, P.A., Chacra, A.R., Bergenstal, R.M., 2009. Low cardiorespiratory fitness in people at risk for type 2 diabetes: early marker for insulin resistance. Diabetol. Metab. Syndr. 1 (1), 1–6.

LeLay, S., Dugail, I., 2009. Connecting lipid droplet biology and the metabolic syndrome. Prog. Lipid Res. 48 (3–4), 191–195.

Machann, J., Häring, H., Schick, F., Stumvoll, M., 2004. Intramyocellular lipids and insulin resistance. Diabetes Obes. Metab. 6 (4), 239–248.

MacPherson, R.E., Peters, S.J., 2015. Piecing together the puzzle of perilipin proteins and skeletal muscle lipolysis. Appl. Physiol. Nutr. Metab. 40 (7), 641–651. https://doi.org/10.1139/apnm-2014-0485.

Malenfant, P., Joanisse, D., Theriault, R., Goodpaster, B., Kelley, D., Simoneau, J., 2001. Fat content in individual muscle fibers of lean and obese subjects. Int. J. Obes. 25 (9), 1316–1321.

Mason, R., Meex, R., Russell, A., Canny, B., Watt, M., 2014. Cellular localization and associations of the major lipolytic proteins in human skeletal muscle at rest and during exercise. PLoS One 9, e103062. https://doi.org/10.1371/journal.pone.0103062.

Mason, R.R., Watt, M.J., 2015. Unraveling the roles of plin5: linking cell biology to physiology. Trends Endocrinol. Metab. 26 (3), 144–152.

Mason, R.R., Mokhtar, R., Matzaris, M., Selathurai, A., Kowalski, G.M., Mokbel, N., Meikle, P.J., Bruce, C.R., Watt, M.J., 2014. Plin5 deletion remodels intracellular lipid composition and causes insulin resistance in muscle. Mol. Metab. 3 (6), 652–663.

Minnaard, R., Schrauwen, P., Schaart, G., Jorgensen, J.A., Lenaers, E., Mensink, M., Hesselink, M.K., 2009. Adipocyte differentiation-related protein and oxpat in rat and human skeletal muscle: involvement in lipid accumulation and type 2 diabetes mellitus. J. Clin. Endocrinol. Metab. 94 (10), 4077–4085.

Morinder, G., Larsson, U.E., Norgren, S., Marcus, C., 2009. Insulin sensitivity, vo2max and body composition in severely obese swedish children and adolescents. Acta Paediatr. 98 (1), 132–138.

Moro, C., Bajpeyi, S., Smith, S.R., 2008. Determinants of intramyocellular triglyceride turnover: implications for insulin sensitivity. Am. J. Physiol. Endocrinol. Metab. 294 (2), E203–E213.

Nielsen, J., Mogensen, M., Vind, B.F., Sahlin, K., Højlund, K., Schrøder, H.D., Ørtenblad, N., 2010. Increased subsarcolemmal lipids in type 2 diabetes: effect of training on localization of lipids, mitochondria, and glycogen in sedentary human skeletal muscle. Am. J. Physiol. Endocrinol. Metab. 298 (3), E706–E713.

Nissinen, T.A., Hentilä, J., Fachada, V., Lautaoja, J.H., Pasternack, A., Ritvos, O., Kivelä, R., Hulmi, J.J., 2021. Muscle follistatin gene delivery increases muscle protein synthesis independent of periodical physical inactivity and fasting. FASEB J. 35 (3), e21387.

Russell, A., 2004. Lipotoxicity: the obese and endurance-trained paradox. Int. J. Obes. 28 (4), S66–S71.

Schneider, C.A., Rasband, W.S., Eliceiri, K.W., 2012. Nih image to imagej: 25 years of image analysis. Nat. Methods 9 (7), 671–675.

Seabold, S., Perktold, J., 2010. statsmodels: econometric and statistical modeling with python. In: 9th Python in Science Conference, 2010.

Shaw, C.S., Jones, D.A., Wagenmakers, A.J., 2008. Network distribution of mitochondria and lipid droplets in human muscle fibres. Histochem. Cell Biol. 129 (1), 65–72.

Shaw, C.S., Sherlock, M., Stewart, P.M., Wagenmakers, A.J., 2009. Adipophilin distribution and colocalisation with lipid droplets in skeletal muscle. Histochem. Cell Biol. 131 (5), 575–581.

Shaw, C.S., Swinton, C., Morales-Scholz, M.G., McRae, N., Erftemeyer, T., Aldous, A., Murphy, R.M., Howlett, K.F., 2020. Impact of exercise training status on the fiber type-specific abundance of proteins regulating intramuscular lipid metabolism. J. Appl. Physiol. 128 (2), 379–389.

van Loon, L.J., Goodpaster, B.H., 2006. Increased intramuscular lipid storage in the insulin-resistant and endurance-trained state. Pflüg. Arch. 451 (5), 606–616.

Van Loon, L.J., Koopman, R., Manders, R., van der Weegen, W., van Kranenburg, G.P., Keizer, H.A., 2004. Intramyocellular lipid content in type 2 diabetes patients compared with overweight sedentary men and highly trained endurance athletes. Am. J. Physiol. Endocrinol. Metab. 287 (3), E558–E565.

Virtanen, P., Gommers, R., Oliphant, T.E., Haberland, M., Reddy, T., Cournapeau, D., Burovski, E., Peterson, P., Weckesser, W., Bright, J., van der Walt, S.J., Brett, M., Wilson, J., Millman, K.J., Mayorov, N., Nelson, A.R.J., Jones, E., Kern, R., Larson, E., Carey, C.J., Polat, İ., Feng, Y., Moore, E.W., VanderPlas, J., Laxalde, D., Perktold, J., Cimrman, R., Henriksen, I., Quintero, E.A., Harris, C.R., Archibald, A.M., Ribeiro, A.H., Pedregosa, F., van Mulbregt, P., 2020. SciPy 1.0 Contributors, SciPy 1.0: fundamental algorithms for scientific computing in Python. Nat. Methods 17, 261–272. https://doi.org/10.1038/s41592-019-0686-2.

Wang, H., Bell, M., Sreenevasan, U., Hu, H., Liu, J., Dalen, K., Londos, C., Yamaguchi, T., Rizzo, M.A., Coleman, R., et al., 2011. Unique regulation of adipose triglyceride lipase (atgl) by perilipin 5, a lipid droplet-associated protein. J. Biol. Chem. 286 (18), 15707–15715.

Waskom, M., 2020. The seaborn development team, mwaskom/seaborn (Sep. 2020). 10.5281/zenodo.592845.

Watt, M.J., 2009. Storing up trouble: does accumulation of intramyocellular triglyceride protect skeletal muscle from insulin resistance? Clin. Exp. Pharmacol. Physiol. 36 (1), 5–11.

Wolins, N.E., Quaynor, B.K., Skinner, J.R., Tzekov, A., Croce, M.A., Gropler, M.C., Varma, V., Yao-Borengasser, A., Rasouli, N., Kern, P.A., et al., 2006. Oxpat/pat-1 is a ppar-induced lipid droplet protein that promotes fatty acid utilization. Diabetes 55 (12), 3418–3428.

II

BRANCHED-CHAIN AMINO ACID DEPRIVATION DECREASES LIPID OXIDATION AND LIPOGENESIS IN C2C12 MYOTUBES

by

Karvinen, S.*, Fachada, V.*, Sahinaho, U.M., Pekkala, S., Lautaoja, J.H., Mäntyselkä, S., Permi, P., Hulmi, J.J., Silvennoinen, M., Kainulainen, H (2022)

Metabolites 12(4), 328.

https://doi.org/10.3390/metabo12040328

*These authors contributed equally to the paper.

metabolites

MDPI

Article

Branched-Chain Amino Acid Deprivation Decreases Lipid Oxidation and Lipogenesis in C2C12 Myotubes

Sira Karvinen [1,†], Vasco Fachada [1,†], Ulla-Maria Sahinaho [1], Satu Pekkala [1], Juulia H. Lautaoja [1], Sakari Mäntyselkä [1], Perttu Permi [2,3,4], Juha J. Hulmi [1], Mika Silvennoinen [1] and Heikki Kainulainen [1,*]

1 NeuroMuscular Research Center, Faculty of Sport and Health Sciences, University of Jyväskylä, FI-40014 Jyväskylä, Finland; sira.m.karvinen@jyu.fi (S.K.); vasco.fachada@gmail.com (V.F.); ulla-maria.u-m.sahinaho@jyu.fi (U.-M.S.); satu.p.pekkala@jyu.fi (S.P.); juulia.h.lautaoja@jyu.fi (J.H.L.); sakari.a.mantyselka@jyu.fi (S.M.); juha.hulmi@jyu.fi (J.J.H.); mmjsilvennoinen@gmail.com (M.S.)
2 Department of Biological and Environmental Science, University of Jyväskylä, FI-40014 Jyväskylä, Finland; perttu.permi@jyu.fi
3 Department of Chemistry, Nanoscience Center, University of Jyväskylä, FI-40014 Jyväskylä, Finland
4 Institute of Biotechnology, Helsinki Institute of Life Science, University of Helsinki, FI-00014 Helsinki, Finland
* Correspondence: heikki.kainulainen@jyu.fi
† These authors contributed equally to this work.

Abstract: Impaired lipid metabolism is a common risk factor underlying several metabolic diseases such as metabolic syndrome and type 2 diabetes. Branched-chain amino acids (BCAAs) that include valine, leucine and isoleucine have been proven to share a role in lipid metabolism and hence in maintaining metabolic health. We have previously introduced a hypothesis suggesting that BCAA degradation mechanistically connects to lipid oxidation and storage in skeletal muscle. To test our hypothesis, the present study examined the effects of BCAA deprivation and supplementation on lipid oxidation, lipogenesis and lipid droplet characteristics in murine C2C12 myotubes. In addition, the role of myotube contractions on cell metabolism was studied by utilizing in vitro skeletal-muscle-specific exercise-like electrical pulse stimulation (EPS). Our results showed that the deprivation of BCAAs decreased both lipid oxidation and lipogenesis in C2C12 myotubes. BCAA deprivation further diminished the number of lipid droplets in the EPS-treated myotubes. EPS decreased lipid oxidation especially when combined with high BCAA supplementation. Similar to BCAA deprivation, high BCAA supplementation also decreased lipid oxidation. The present results highlight the role of an adequate level of BCAAs in healthy lipid metabolism.

Keywords: metabolic health; protein supplementation; skeletal muscle; electrical pulse stimulation; in vitro exercise; nuclear magnetic resonance spectroscopy

Citation: Karvinen, S.; Fachada, V.; Sahinaho, U.-M.; Pekkala, S.; Lautaoja, J.H.; Mäntyselkä, S.; Permi, P.; Hulmi, J.J.; Silvennoinen, M.; Kainulainen, H. Branched-Chain Amino Acid Deprivation Decreases Lipid Oxidation and Lipogenesis in C2C12 Myotubes. *Metabolites* **2022**, *12*, 328. https://doi.org/10.3390/metabo12040328

Academic Editor: Silvia Sacchi

Received: 23 February 2022
Accepted: 2 April 2022
Published: 5 April 2022

1. Introduction

Impaired lipid metabolism and fat accumulation predispose people to several adverse health risks such as insulin resistance, metabolic syndrome and type 2 diabetes [1]. Over the last decade, branched-chain amino acids (BCAAs) that include valine, leucine and isoleucine have been proven to share a role in fat oxidation and hence in maintaining metabolic health [2,3]. More specifically, metabolomic and transcriptomic studies suggest that efficient BCAA catabolism (i.e., low serum BCAA levels) is associated with higher fat oxidation, physical activity and leanness [4,5]. On the contrary, inefficient BCAA catabolism (i.e., high serum BCAA levels) is linked to low physical activity, increased adiposity and other risk factors for metabolic diseases [6]. Nevertheless, the underlying mechanisms between BCAA utilization and lipid oxidation remain to be determined.

We have previously introduced a hypothesis suggesting that BCAA degradation mechanistically connects to lipid oxidation and storage in the skeletal muscle (Figure 1) [3]. Unlike other amino acids, BCAAs are not degraded directly by the liver but are transported into the

bloodstream and catabolized mainly in muscle cells [7,8]. Since skeletal muscle comprises around 40% of body mass, it is also the main tissue that oxidizes lipids and thus aids in the prevention of obesity [9,10]. According to our hypothesis, we propose that, especially during increased demand for BCAA catabolism (such as during exercise), transamination of BCAAs is critical for cytosolic oxaloacetate formation. In our model, oxaloacetate is further metabolized to phosphoenolpyruvate for glyceroneogenesis, which is required in skeletal muscles for the storage of fatty acids as lipid droplets (LDs) (Figure 1). We suggest that these intramyocellular LDs are then utilized to provide energy during extended exercise sessions as well as constitutively during rest. Thus, the high activity of this cycle leads to better exercise performance, leaner body composition and improved health [3]. Our hypothesis is supported by the observations that the prevention of amino acid catabolism in mice impairs exercise metabolism and reduces endurance capacity [11], whereas high expression of the genes involved in BCAA degradation and fatty acid metabolism in skeletal muscle is linked to high endurance capacity in rats [12]. Furthermore, acute exercise stimulus has proven to activate branched-chain α-ketoacid dehydrogenase (BCKD) [13,14], which is the main regulator of BCAA oxidation.

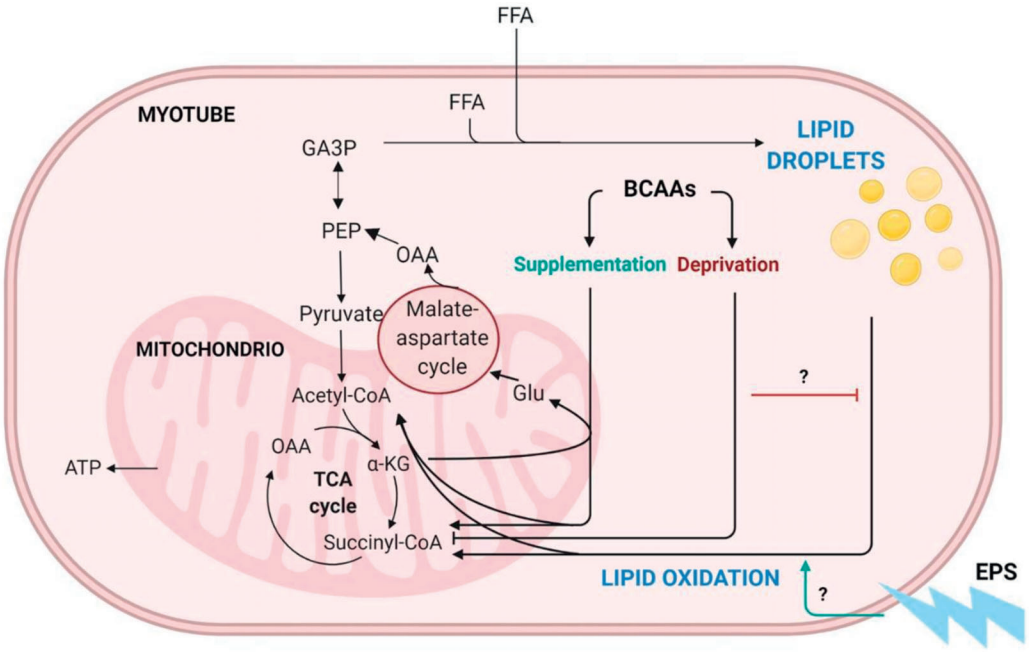

Figure 1. Schematic presentation of BCAA catabolism, lipid oxidation and lipogenesis in skeletal muscle. BCAA = branched-chain amino acid, EPS = electrical pulse stimulation, TCA = tricarboxylic acid cycle, OAA = oxaloacetate, CoA = coenzyme A, ATP = adenosine triphosphate, αKG = α-ketoglutarate, Glu = glucose, PEP = phosphoenolpyruvate, GAP3 = glyceraldehyde-3-phosphate, FFA = free fatty acid. Modified from Kainulainen et al., 2013 [3]. Figure was created with BioRender.com.

In line with our hypothesis, a growing number of both rodent and human studies suggest that BCAA-rich protein supplementation has beneficial effects on several health-and-fitness-related factors, such as body composition, exercise performance and muscle properties, as well as glucose and lipid metabolism [15–22]. On the other hand, BCAA deficiency has been shown to result in impaired growth and protein wasting, as well as changes in hormonal secretion and intracellular signaling [23,24]. In contrast, some studies have shown that diets with reduced BCAA content promote metabolic health [25,26]. Particularly, reducing isoleucine has been shown to restore the metabolic health of diet-induced obese mice [27].

Exercise acutely increases fat oxidation in the skeletal muscles [28]. Furthermore, endurance training increases the capacity of muscle to oxidize fat by increasing mitochondrial density, the activity of key enzymes involved in lipid oxidation and oxygen delivery to the

muscles [29]. It is also well-established that skeletal muscles from trained individuals have higher lipid content compared with untrained individuals, yet they have better insulin sensitivity and oxidative capacity [30,31]. This phenomenon, called "athlete's paradox", is thought to store and serve energy in the form of LDs for long-lasting exercise [30]. Some studies suggest that BCAA supplementation may further promote resistance to fatigue by increasing lipid oxidation during exercise [16].

In the present study, we examined the effects of BCAA deprivation and supplementation on lipid metabolism in murine C2C12 myotubes. In addition, we utilized an in vitro skeletal-muscle-specific exercise-like electrical pulse stimulation (EPS) to mimic and investigate the effect of exercise on myotube metabolism. According to the previous literature, we suggested two hypotheses: First, deprivation of BCAAs will lead to reduced lipid oxidation in myotubes. Second, EPS combined with BCAA supplementation further increases lipid oxidation in myotubes. In addition, we investigated how these conditions affect lipogenesis and lipid droplets (Figure 1).

2. Results

Optimal BCAA supplementation for lipid oxidation was tested with three different BCAA concentrations: 0 (no BCAA), 0.8 (normal BCAA) and 2.8 mmol/L (high BCAA) (Figure 2A). Of the three BCAA concentrations tested, the normal BCAA led to the highest lipid oxidation compared with both no BCAA and high BCAA groups (Figure 2A, $p \leq 0.001$); thus, it was chosen as the control level for the lipid oxidation experiments.

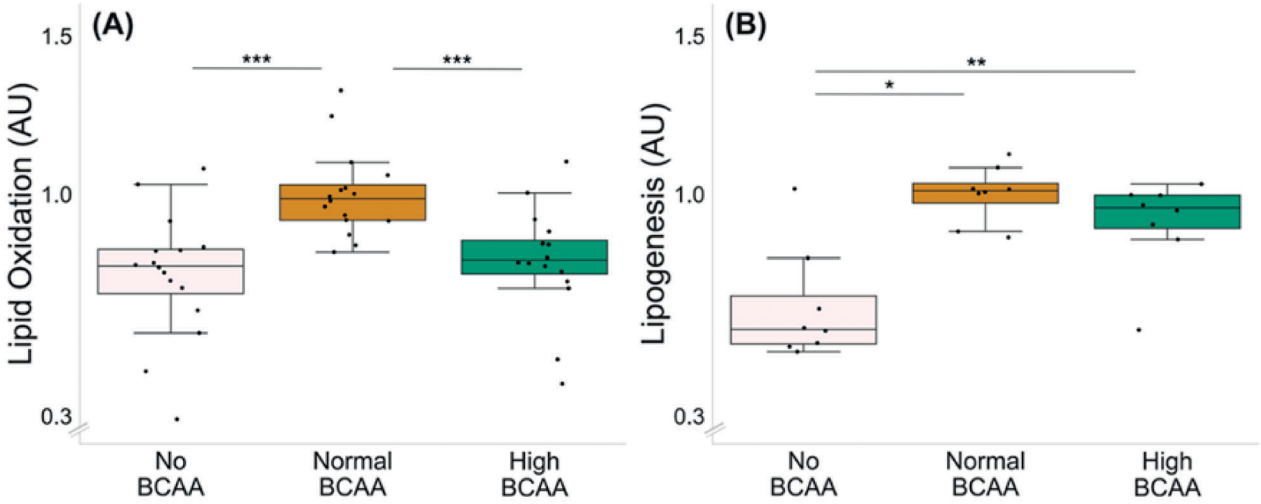

Figure 2. Lipid oxidation (**A**) and lipogenesis (**B**) in C2C12 myotubes with different BCAA levels. (**A**) Normal BCAA level (0.8 mmol/L) led to higher lipid oxidation compared with no BCAA (0 mmol/L) or high BCAA (2.8 mmol/L). n = 16/group. (**B**) Normal and high BCAA levels led to higher lipogenesis compared with no BCAA. n = 8/group. Boxes in the boxplot figures depict interquartile ranges and medians, and whiskers represent the 95% confidence interval. * $p \leq 0.050$, ** $p \leq 0.010$, *** $p \leq 0.001$. BCAA = branched-chain amino acid.

The optimal BCAA supplementation for lipogenesis was examined with the same BCAA concentrations as used for the lipid oxidation experiment (Figure 2B). Of the BCAA concentrations tested, both normal and high BCAA led to higher lipogenesis compared with no BCAA (Figure 2B, $p \leq 0.021$). Since the groups with normal and high supplementation of BCAAs did not significantly differ from each other (p = 0.093), the same concentration as chosen for the oxidation experiments was used as the control level for the lipogenesis experiments.

2.1. BCAA Deprivation Decreased Lipid Oxidation and Lipogenesis in C2C12 Myotubes

Deprivation of all BCAAs decreased lipid oxidation in murine C2C12 myotubes (normal BCAA vs. no BCAA, $p < 0.001$, Figure 3A). In addition, the deprivation of leucine ($p = 0.046$) and isoleucine ($p < 0.001$), but not valine (0 = 0.070), decreased lipid oxidation. Lipid oxidation was also lower in the isoleucine deprivation group compared with the leucine and valine deprivation groups ($p \leq 0.004$, Figure 3A). The deprivation of all BCAAs decreased lipogenesis in the myotubes (Figure 3B, normal BCAA vs. no BCAA, $p < 0.001$). In addition, the deprivation of a single BCAA at a time (valine, leucine or isoleucine) decreased lipogenesis compared with normal BCAA ($p < 0.001$), yet the decrease was not as significant as when all BCAAs were absent (no Leu, no Ile or no Val compared with no BCAA, $p \leq 0.003$).

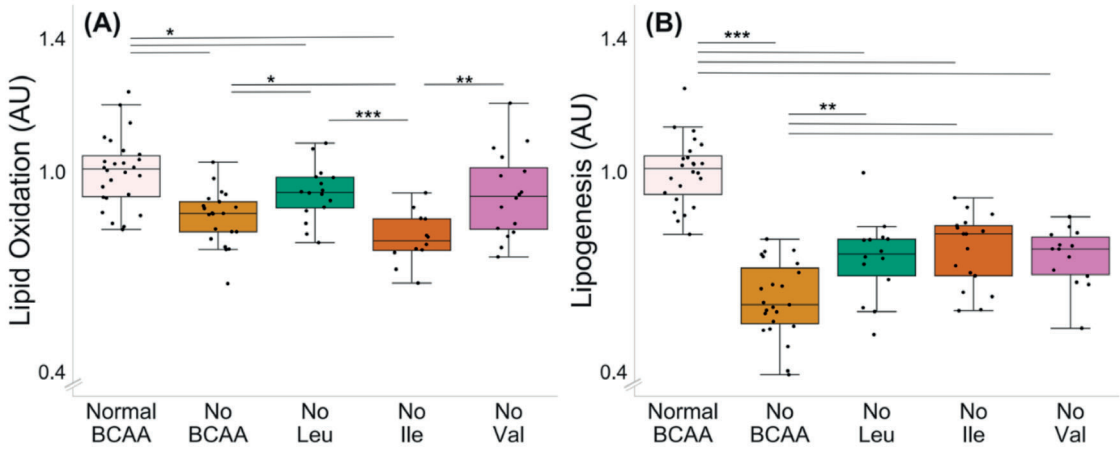

Figure 3. Lipid oxidation (**A**) and lipogenesis (**B**) with BCAA deprivation in murine C2C12 myotubes. (**A**) Deprivation of all BCAAs or deprivation of leucine or isoleucine alone reduced lipid oxidation in myotubes. Lipid oxidation was lower in isoleucine deprivation group compared with leucine and valine deprivation groups. Normal BCAA $n = 26$, no BCAA $n = 21$, no Leu $n = 16$, no Ile $n = 12$, no Val $n = 16$. (**B**) Deprivation of all BCAAs reduced lipogenesis in myotubes (normal BCAA vs. no BCAA). Deprivation of a single BCAA reduced lipogenesis compared with normal BCAA. Lipogenesis in single BCAA deprivation groups was higher compared with the no BCAA group. Normal BCAA $n = 24$, no BCAA $n = 23$, no Leu $n = 14$, no Ile $n = 17$, no Val $n = 14$. Boxes in the boxplot figures depict interquartile ranges and medians, and whiskers represent the 95% confidence interval. * $p \leq 0.050$, ** $p \leq 0.010$, *** $p \leq 0.001$. BCAA = branched-chain amino acid, Leu = leucine, Ile = isoleucine, Val = valine.

2.2. High BCAA Supplementation Combined with EPS Decreased Lipid Oxidation, whereas BCAA Deprivation but Not EPS Decreased Lipogenesis in C2C12 Myotubes

The experiments with normal (0.8 mmol/L), no (0 mmol/L) and high (2.8 mmol/L) BCAA supplementation with and without EPS are shown in Figure 4. There was a significant effect of EPS regardless of BCAA level ($p \leq 0.023$), indicating that EPS decreased lipid oxidation (Figure 4A,B). High BCAA content in cell media did not affect lipid oxidation (normal BCAA control vs. high BCAA control, $p = 0.292$), whereas high BCAA combined with EPS decreased lipid oxidation ($p = 0.032$). The deprivation of BCAAs decreased lipogenesis in both control ($p = 0.002$) and EPS-treated ($p = 0.022$) myotubes (Figure 4C).

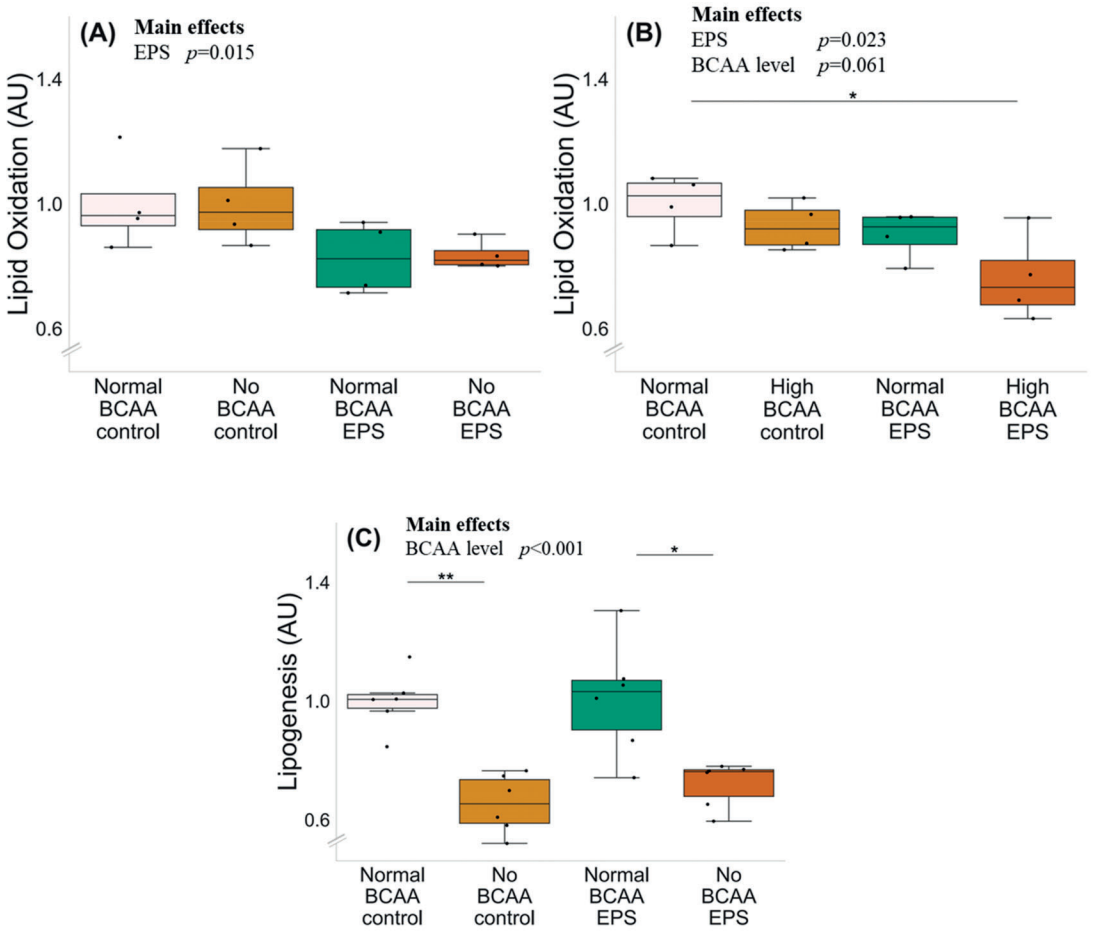

Figure 4. Lipid oxidation, BCAA deprivation and EPS in murine C2C12 myotubes with normal (**A**) and high (**B**) BCAA levels and lipogenesis with BCAA deprivation and EPS in myotubes (**C**). (**A**) Normal BCAA (0.8 mmol/L) concentration, EPS or BCAA deprivation did not affect lipid oxidation. (**B**) High BCAA (2.8 mmol/L) combined with EPS-reduced lipid oxidation. $n = 4$/group. (**C**) Deprivation of BCAAs reduced lipogenesis in myotubes during control conditions (normal BCAA vs. no BCAA) and with EPS treatment (normal BCAA EPS vs. no BCAA EPS) $n = 6$/group. Boxes in the boxplot figures depict interquartile ranges and medians, and whiskers represent the 95% confidence interval, * $p \leq 0.050$, ** $p \leq 0.010$. BCAA = branched-chain amino acid, EPS = skeletal-muscle-specific exercise-like electrical pulse stimulation.

2.3. BCAA Deprivation Diminished the Number of Lipid Droplets in the EPS-Treated C2C12 Myotubes

Microscopic examinations of lipid droplets (LD) in murine C2C12 myotubes with and without BCAA and with and without EPS are shown in Figure 5. There were no significant effects of EPS, BCAA levels or their interaction. However, the group-wise comparisons showed that in EPS-treated myotubes, BCAA deprivation led to a lower number of LDs per mm^3 ($p = 0.048$, Figure 5B,C).

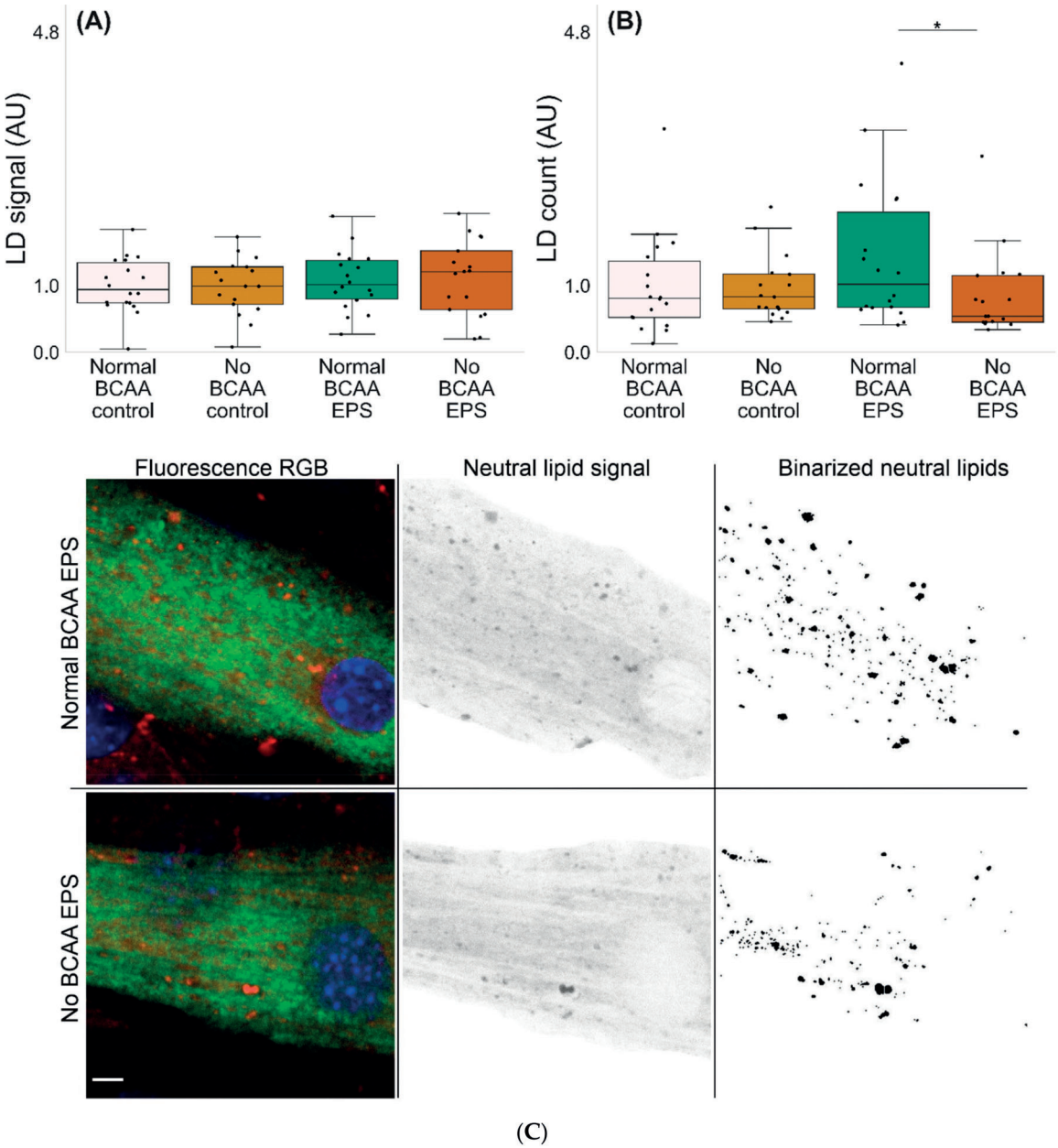

Figure 5. Lipid droplet characteristics in murine C2C12 myotubes (**A**–**C**). (**A**) In EPS-treated myotubes, there were no changes in LD signal fraction, whereas (**B**,**C**) BCAA deprivation diminished the number of LDs (EPS-treated myotubes 0.8 mmol BCAA vs. 0 mmol/L BCAA). n = 17–18/group. Boxes in the boxplot figures depict interquartile ranges and medians, and whiskers represent the 95% confidence interval, * $p \leq 0.050$. BCAA = branched-chain amino acid, EPS = skeletal-muscle-specific exercise-like electrical pulse stimulation. In (**C**), MF20 = green, DAPI = blue and LD540 = red, gray and binary. Scale bar = 5 μm.

2.4. Metabolites in C2C12 Myotubes and in Cell Culture Media

To confirm that our cell culture media with no BCAA were very low of BCAAs and that being supplemented with normal BCAA had substantially higher BCAA and BCAA degradation product contents, nuclear magnetic resonance (NMR)-based metabolomics was conducted for murine C2C12 myotubes and cell media (Supplementary Table S1). Our results confirmed that, in myotubes cultured without BCAAs (no BCAA), the levels of pooled BCAAs (isoleucine, leucine and valine) and individual BCAAs were lower than

in myotubes cultured with BCAAs (normal BCAA) ($p = 0.004$, Supplementary Table S1). Furthermore, in the cell culture media of the myotubes cultured without BCAAs, the level of pooled BCAAs, individual BCAAs as well as pooled BCAA degradation products (isobutyrate, isovalerate, 2-ketoisovalerate, 2-methylbutyrate, 3-methyl-2-oxovalerate and 2-oxoisocaproate) were lower than in myotubes cultured with BCAAs, suggesting decreased BCAA degradation in cells treated with no BCAA media ($p = 0.014$, Supplementary Table S1). All identified metabolites in myotubes and cell culture media are presented in Supplementary Table S2.

2.5. Total Protein Content, and Citrate Synthase Activity and Cell Viability Measurements

Corresponding total protein contents and citrate synthase activities of the study setups are presented in Supplementary Figures S1–S3. Overall, BCAA supplementation increased both the total protein content and CS activity of the murine C2C12 myotubes (Supplementary Figures S1–S3).

The cell viability following EPS was examined via measuring lactate dehydrogenase (LDH) level in cell medium after lipid oxidation and lipogenesis experiments (Supplementary Figure S4). Our results showed that, in lipid oxidation experiment, the LDH level was lower in the media of EPS-treated myotubes (main effect $p = 0.013$), whereas there was no effect of BCAA level (main effect $p = 0.257$, Supplementary Figure S4a). When examining the lipogenesis experiment, BCAA deprivation increased the LDH level (main effect $p = 0.003$). EPS treatment slightly but consistently increased LDH activity in all of the studied BCAA concentrations in the lipogenesis experiment (main effect $p > 0.001$).

3. Discussion

This study examined the effects of branched-chain amino acid (BCAAs = valine, leucine and isoleucine) supplementation on lipid metabolism of the murine C2C12 myotubes. In addition, the effects of muscle contractions in muscle metabolism were mimicked and studied in myotubes utilizing in vitro skeletal-muscle-specific exercise-like electrical pulse stimulation (EPS). Supporting our previous hypothesis [3], the present study showed that deprivation of the BCAAs reduced both lipid oxidation and lipogenesis in C2C12 myotubes. The BCAA deprivation further diminished the number of lipid droplets in the EPS-treated myotubes. High serum BCAA levels can act as biomarkers for some metabolic diseases [4,6]; indeed, we observed that a high BCAA level in myotube media may lead to dysregulated lipid metabolism. However, the current results together with the data from other research groups [32] suggest that also very low levels (or ingestion of) BCAAs may lead to disturbances in muscle lipid metabolism. These results thus suggest that adequate (not too high nor too low) BCAA level is important for healthy lipid metabolism in muscle. However, further studies are warranted to elucidate the dose response in BCAA ingestion and its possible connection to lipid metabolisms in vivo.

3.1. The Deprivation of BCAAs Reduced Lipid Oxidation and Lipogenesis in C2C12 Myotubes

We hypothesized that as BCAAs may feed lipid oxidation, deprivation of BCAAs would lead to reduced lipid oxidation. According to our hypothesis, deprivation of all BCAAs reduced lipid oxidation in murine C2C12 myotubes. This observation is in line with previous literature, showing that defects in muscle BCAA oxidation contribute to impaired lipid metabolism [33,34]. Interestingly, in addition to BCAA deprivation, high level of BCAAs also resulted in reduced lipid oxidation when compared to normal level of BCAAs. These results are supported by a previous study where both deprivation and excess supplementation of leucine reduced palmitate oxidation in C2C12 myotubes [35].

We observed that the deprivation of leucine or isoleucine but not valine alone reduced lipid oxidation. Lipid oxidation was also lower in the absence of isoleucine compared with the leucine or valine deprivation groups. In a previous study, upregulation of leucine catabolism together with β-oxidation was shown to protect mice from high-fat diet-induced obesity, supporting the role of leucine catabolism on lipid oxidation and

metabolic health [36]. In addition, isoleucine supplementation seems to simultaneously activate liver and skeletal muscle free fatty acid uptake and oxidation [19]. The observed prominent effect of isoleucine on lipid oxidation in our study may partly be due to the fact that, unlike valine or leucine, isoleucine can feed the tricarboxylic acid (TCA) cycle through two separate pathways: via acetyl-CoA or succinyl-CoA [3], thus, perhaps, acting as a regulator of TCA activity. In the case of valine, the α-ketoacids, intermediate products resulting from BCAA catabolism, undergo oxidative decarboxylation in the reactions catalyzed by BCKD. BCKD is a rate-limiting enzyme complex in BCAA oxidation, which is activated by increased availability of leucine and isoleucine but not valine [37]. If BCAA and lipid oxidation are interconnected, the lack of BCKD activation by valine could partly explain the smaller role of valine on lipid oxidation.

Our results also revealed that BCAA deprivation reduced lipogenesis in myotubes. Deprivation of a single BCAA at a time reduced lipogenesis compared with normal BCAA level, yet the decrease was not as significant as when all BCAAs were absent. These findings support our previous hypothesis that BCAA deprivation would not only disrupt lipid oxidation but also lipogenesis [3]. Supporting our hypothesis, studies have shown that BCAAs fuel lipogenesis in adipocytes and adipose tissue [38,39]. Furthermore, removing BCAAs from culture media prevents the ATP synthase-mediated LD formation in murine myocytes [40]. According to our hypothesis, increased BCAA catabolism is essential for cytosolic oxaloacetate production that is metabolized to phosphoenolpyruvate for glyceroneogenesis. Increased glyceroneogenesis in turn leads to the storage of fatty acids in lipid droplets in myocytes. Deprivation of BCAAs seems to disrupt this cycle, leading to reduced lipogenesis. We observed decreased BCAAs and their breakdown products using NMR spectroscopy, suggesting indeed substantially decreased BCAA degradation when BCAAs are absent from the C2C12 culture medium.

3.2. EPS Treatment Decreased Lipid Oxidation but Not Lipogenesis in C2C12 Myotubes

In the present study, we further examined the effect of EPS on lipid oxidation and lipogenesis in murine C2C12 myotubes. Our results revealed that EPS decreased lipid oxidation, especially when combined with high BCAA supplementation. Accordingly, we have previously reported that EPS reduces lipid oxidation under normal BCAA conditions [41]. This result is probably due to the very glycolytic nature of C2C12 cells in ATP production, also during low-intensity EPS [41,42]. In this setup, we did not observe a difference in lipid oxidation between BCAA deprivation and normal BCAA groups, possibly due to small n used in the EPS experiments (n = 4) compared with the BCAA-deprivation experiments (n = 21–26).

Furthermore, the high BCAA supplementation combined with EPS-reduced lipid oxidation. In previous literature, some studies have shown a decrease in intramuscular lipid content during electrically stimulated muscle contractions in situ or in vivo [43–45], while others have not observed a decrease [46]. These inconsistencies may be due to the high variability associated with the measurement of intramuscular lipid content as well as differences in the stimulation protocol and duration of the stimulation [44]. In vitro, EPS has been reported to have controversial effects on fatty acid oxidation, which may be explained, for example, by the methodological differences, cell line used or fatty acid analyzed [47–49]. In a previous study utilizing isolated soleus muscles, tetanic contractions increased palmitate oxidation [50]. However, in our setup, we were only able to successfully measure lipid oxidation. This is one limitation of our study, as lipid oxidation does not necessarily represent the whole lipid oxidation capacity of the myotubes. Furthermore, C2C12 cells normally use carbohydrates as their primary energy source [41,42]. Hence, cultured murine C2C12 myotubes with treated EPS do not necessarily fully represent muscle metabolism during human exercise in vivo.

3.3. BCAA Deprivation Diminished the Number of Lipid Droplets in the EPS-Treated C2C12 Myotubes

EPS treatment combined with BCAA deprivation diminished the number of lipid droplets in murine C2C12 myotubes. This observation is in line with previous literature showing that LDs are an important source of energy during exercise and that acute exercise as well as electrically stimulated muscle contractions reduce LDs due to increased oxidation [43–45,51]. Yet, this result is inconsistent with the findings in the present study that both BCAA deprivation and EPS led to decreased lipid oxidation. However, it is important to note that lipid oxidation directly concerns fatty acids and only indirectly LDs, which are made primarily of triacylglycerol [45].

As previously studied, a decrease in the LD number may be a reflection of fission, not only from chemical hydrolysis but from mechanical stress as well [52,53].

Nevertheless, despite the decrease in the number of detectable lipid droplets, the overall lipid signal was not affected by our experiments. This may be explained by the fact that a large part of neutral lipids (i.e., triacylglycerols) diffuse through the cytosol in the form of suboptical (<~100 nm in diameter) LDs [54]. We thus hypothesize that, when combined with myotube contractions, BCAA-driven lipogenesis could be providing fatty acids for triacylglycerol esterification and respective LD replenishment. Conversely, BCAA deprivation and consequent reduced lipogenesis would lead to lower fatty acid availability, resulting in lower esterification rates and a reduced number of LDs. An overall reduced lipid oxidation explains the unchanged neutral lipid signal.

4. Materials and Methods

Murine C2C12 myoblasts (American Type Culture Collection, ATCC, Manassas, VA, USA) were maintained in high glucose-containing Dulbecco's Modified Eagle growth medium (GM) (4.5 g/L, DMEM, #BE12-614F, Lonza, Basel, Switzerland) supplemented with 10% (*v*/*v*) fetal bovine serum (FBS, #10270, Gibco, Rockville, MD, USA), 100 U/mL penicillin, 100 µg/mL streptomycin (P/S, #15140, Gibco) and 2 mM L-Glutamine (#17-605E, Lonza). For the experiments, myoblasts were seeded on 12-well or 6-well plates (NunclonTM Delta; Thermo Fisher Scientific, Waltham, MA, USA). When the myoblasts reached 95–100% confluence, the cells were rinsed with phosphate-buffered saline (PBS, pH 7.4), and the GM was replaced by differentiation medium (DM) containing high glucose DMEM, 2% (*v*/*v*) horse serum (HS, 12449C, Sigma-Aldrich, St. Luis, MO, USA), 100 U/mL and 100 µg/mL P/S and 2 mM L-glutamine to promote differentiation into myotubes, unless stated otherwise. Fresh DM was changed every other day. The cells were screened negative for mycoplasma contaminations, following manufacturer's instructions (MycoSPY Master Mix Test Kit, M020, Biontex, München, Germany). The experiments were conducted on days 5–6 post differentiation, and samples were collected immediately after indicated time points.

4.1. Treatments

The BCAA deprivation and supplementation experiments were carried out in high-glucose BCAA-free DM, i.e., containing no L-leucine, L-isoleucine and L-valine. More specifically, DM contained high glucose BCAA-free DMEM (4.5 g/L, BioConcept, 1-26S289-I, Allschwill, Switzerland), 2% (*v*/*v*) horse serum, 100 U/mL penicillin, 100 µg/mL streptomycin and 2 mM L-Glutamine. The experimental groups were as follows: normal BCAA cells (normal BCAA) were supplemented with 0.8 mmol/L of all BCAAs, relative to which BCAA deprivation (0 mmol/L, no BCAA), and high BCAA supplementation (2.8 mmol/L, high BCAA) groups contained indicated amounts of BCAAs. In deprivation of a single BCAA at the time, the media were deficient of either L-leucine, L-isoleucine or L-valine and were supplied with 0.8 mmol/L of other BCAAs. The experiments were repeated in duplicate or triplicate.

4.1.1. Lipid Oxidation

Lipid oxidation experiments were carried out by measuring oleate oxidation as described previously [41]. Briefly, for measuring oleate oxidation, the murine C2C12 myotubes grown in normal BCAA conditions (0.8 mml/l) were first acclimatized to dissolved and albumin-complexed 0.1 mM oleic acid (#O3008, Sigma-Aldrich, St. Luis, MO, USA) and 1 mM L-carnitine (C0158, Sigma-Aldrich) in DM on the day 4 post differentiation. The following day, the myotubes were rinsed with PBS and incubated in the oxidation medium containing BCAA-free medium, 0.1 mM oleic acid, 2% (*v*/*v*) horse serum, 100 U/mL penicillin, 100 µg/mL streptomycin and 2 mM L-Glutamine, 1 mM L-carnitine and 1 µCi/mL [9,10-^{3}H(N)] oleic acid (24 Ci/mmol, NET289005MC, PerkinElmer, Boston, MA, USA). The radiolabeled oleic acid was omitted from the negative controls. The lipid oxidation experiment was carried out for 2 h at 37 °C, as previously described [41]. Target BCAA concentration (no BCAA, normal BCAA or high BCAA) was applied during the 2 h lipid oxidation experiment to investigate the effect of BCAA deprivation or supplementation on lipid oxidation. After the lipid oxidation experiment, the myotubes were washed with PBS and also PBS was collected. The myotubes were harvested into PBS-0.1% PBS-Triton X-100 for enzyme activity and total protein content analyses. The media and PBS were run through Dowex OH resin ion-exchange columns (pH 7.1 × 8^{-200}, Cat no. 217425, Sigma Aldrich). Deionized H_2O was used to elute the $^{3}H_2O$ produced and secreted by the myotubes to the media. The radioactivity was analyzed as disintegration per minute (DPM), as previously described [41]. The radioactivity that had been incorporated in $^{3}H_2O$ was determined by scintillation counting in Optiphase HiSafe 3 scintillation cocktail (Cat no. 1200.437, PerkinElmer) with Tri-Carb 2910 TR Liquid Scintillation Analyzer (PerkinElmer) and expressed as DPM/per well. The lipid oxidation results were expressed relative to normal BCAA group.

4.1.2. Skeletal-Muscle-Specific Exercise-like Electrical Pulse Stimulation (EPS) and Lipid Oxidation

The murine C2C12 myotubes on 6-well plates were acclimatized to 0.1 mM oleic acid and 1 mM L-carnitine in normal BCAA DM on the day 4 post differentiation. On the next day, the electrodes were placed directly onto the wells. The electrical stimulation (1 Hz, 2 ms, 12 V) was applied to the cells using a C-Pace pulse generator (C-Pace EM, IonOptix, Milton, MA, USA) for 24 h at 37 °C with the same protocol as described earlier [41], as it has been shown to mimic various exercise-like responses [41,48]. As described previously, EPS was paused after 22 h and lipid oxidation experiment was carried out for 2 h at 37 °C with EPS and target BCAA concentration (no BCAA, normal BCAA or high BCAA) to investigate the interactive effects of EPS and BCAA deprivation or supplementation on lipid oxidation. For the final 10 min of EPS, 10 min control myotubes were supplied with the radiolabeled medium. The 10 min controls were used as a baseline, and the control DPM was subtracted from the 2 h measurement DPMs. After the EPS, the oxidation media were collected. A 500 µL aliquot was taken from the medium, from which 20 µL input was placed on scintillation vials. The remaining 480 µL were run through Dowex OH resin ion-exchange columns and the $^{3}H_2O$ produced by the cells was eluted with deionized H_2O. The results were calculated as described above. The myotubes were harvested immediately after the EPS into PBS-0.1% PBS-Triton X-100 for enzyme activity and total protein content analyses. The lipid oxidation results were expressed relative to normal BCAA group.

4.1.3. Lipogenesis

Lipogenesis was measured by the uptake of ^{3}H-acetate into the lipids described previously [55], with minor modifications. On the day 5 post differentiation, murine C2C12 myotubes were washed with PBS and changed to DM with target BCAA concentration (no BCAA, normal BCAA or high BCAA) to investigate the effect of BCAA deprivation or supplementation on lipogenesis. In addition, DM was supplied with 10 µM sodium acetate (Cat no. 32319, Sigma-Aldrich, USA) and 0.5 µCi ^{3}H-acetate (Cat.no. NET003H005MC,

PerkinElmer, USA) per well to stimulate lipogenesis. Myotubes were incubated for 16 h at 37 °C in lipogenesis medium. After incubation, cells were washed with PBS and scraped into 0.1 M HCl. An aliquot of the lysate was reserved for analysis of total protein content. The lipids were extracted with 2:1 chloroform/methanol (v:v) [55]. The samples were centrifuged for 10 min at 3000 x g in RT. The lower phases were transferred to scintillation vials. The radioactivity that had been incorporated in the cellular lipids was determined by scintillation counting, as described above. The results were expressed relative to normal BCAA group.

4.1.4. Electrical Pulse Stimulation (EPS) and Lipogenesis

On the day 5 post differentiation, the murine C2C12 myotubes on 6-well plates were washed with PBS and fresh lipogenesis medium with target BCAA concentration (no BCAA, normal BCAA or high BCAA) as described above was added. Electrical stimulation (1 Hz, 2 ms, 12 V) was applied for 16 h. After the EPS, the cells were collected for lipid extraction. The scintillation counting was performed as described above. The lipogenesis results were expressed relative to normal BCAA group.

4.2. Histology and Image Analysis

Histology and image analysis were carried out for lipid oxidation experiments. For this purpose, the cells were cultured on 6-well plates containing coverslips. Each experimental group was measured from 18 coverslips. After the 24 h of EPS, the cells were fixed with 4% paraformaldehyde for 15 min, followed by 30 min blocking using 10% goat serum (GS) in PBS with 0.05% saponin (PBS-SAP). As a marker for differentiated murine C2C12 myotubes, MF-20 mouse monoclonal antibody (Developmental Studies Hybridoma Bank, University of Iowa, Iowa City, IA) was incubated for 1 h with a dilution 1:100 in 1% GS in PBS-SAP. The secondary antibody incubation with Alexa fluor 647 Donkey anti-Mouse IgG (H+L) (Thermo Fisher Scientific) for 1 h with a 1:150 dilution in 1% GS in PBS-SAP was followed by marking of the neutral lipids and nuclei for 30 min in PBS with 0.1 µg/mL of LD540 [56] and 0.5 µg/mL of DAPI (Thermo Fisher Scientific), respectively. The samples were mounted with Mowiol. The confocal images (voxel size = 0.1 × 0.1 × 1.3 µm) were made from three random 203.3 × 203.3 µm areas in each coverslip, using a Zeiss LSM700 microscope with a 63×/1.4 oil objective. Nuclei, myotubes and neutral lipid markers were excited with a 405, 488 and 555 laser line, respectively. The MF-20 signal was used to segment and analyze lipid droplets from differentiated myotubes only. Image analysis was performed in ImageJ 1.53c and Python 3.9.0. Cell culture, microscopy and image analysis were performed blindly from each other.

4.3. Nuclear Magnetic Resonance (NMR) Spectroscopy

The cell lysates and the experiment media were collected and prepared for the ^{1}H-NMR analysis from lipid oxidation experiment. The method and data analysis have been explained in detail previously [41]. Briefly, media from three wells were mixed with cold methanol (600 µL of sample and 1.200 µL of methanol), and cells were scraped into 200 µL of 90% (v:v) 9:1 aqueous methanol/chloroform mixture. The resulting supernatants were lyophilized and then reconstituted. All the NMR spectra were collected using a Bruker AVANCE III HD NMR spectrometer, operating at 800 MHz ^{1}H frequency (Bruker Corporation, MA, USA) equipped with a cryogenically cooled ^{1}H, ^{13}C, ^{15}N triple-resonance probe head. The obtained data were analyzed using Chenomx software 8.6 (Chenomx, Edmonton, AB, Canada).

4.4. Total Protein Content and Enzyme Activity Measurements

Total protein content (Bicinchoninic Acid Protein Assay Kit, Pierce Biotechnology, Rockford, IL, USA) and citrate synthase (CS) activity (#CS0720, Sigma-Aldrich) were analyzed according to the manufacturers' protocol with an automated Indiko analyzer (Thermo Fisher Scientific, Vantaa, Finland). To assess the cell viability, media lactate

dehydrogenase (LDH) activity was measured from the EPS experiments using an LDH assay kit following the manufacturer's instructions (#981906, Thermo Fisher Scientific, Waltham, Massachusetts, Canada) [57].

4.5. Statistical Analyses

The results in the figures are presented as interquartile ranges and medians with 95% confidence interval (CI) and in tables as mean and standard error of mean (SEM). The normal distribution of the variables was assessed using Shapiro–Wilks tests followed by Levene's test for examining the equality of the variances. First, the extreme outliers were excluded from the analysis (>3× interquartile range). In the lipogenesis and lipid oxidation experiments, the data are expressed relative to control group (normal BCAA), since the treatments significantly affected the total protein content and CS activity of the samples (Supplementary Figures S1–S3). When the normality criteria were met, the differences between the groups were examined using one-way ANOVA followed by independent samples *t*-test. When the normality criteria were not fulfilled, the differences between the groups were examined using Kruskal–Wallis test followed by Mann–Whitney U-test. In the NMR results, groups differing from BCAA level and EPS treatment were compared using Mann–Whitney U-test. Data analyses were carried out using IBM SPSS Statistics. In all analyses, p-value < 0.05 was considered to indicate statistical significance.

5. Conclusions

The present study shows that deprivation of BCAAs reduces both lipid oxidation and lipogenesis in cultured murine C2C12 myotubes. These results partially support our previous hypothesis that, in skeletal muscle, adequate BCAA catabolism increases lipid oxidation and lipogenesis when compared to BCAA deprivation. However, it appears that a higher BCAA level is not able to further increase these processes; instead, it may even affect them contrariwise. Exercise mimicking EPS decreased lipid oxidation, especially when combined with high BCAA supplementation, whereas BCAA deprivation combined with EPS diminished the number of lipid droplets in myotubes. Our results highlight the role of an adequate level of BCAAs in a healthy lipid metabolism.

Supplementary Materials: The following supporting information can be downloaded at: https://www.mdpi.com/article/10.3390/metabo12040328/s1, Table S1: Metabolites measured via ^{1}H-NMR spectroscopy in the myotubes and the cell culture media (μM); Table S2: List of all identified metabolites in the myotubes and the cell culture media via ^{1}H-NMR spectroscopy; Figure S1: The C2C12 myotube total protein content (a) and CS activity (b) in lipid oxidation experiment and total protein content in lipogenesis experiment (c) with different BCAA concentrations; Figure S2: The C2C12 myotube total protein content (a) and CS activity (b) in lipid oxidation experiment and total protein content (c) in lipogenesis experiments with BCAA deprivation; Figure S3: The C2C12 myotube total protein content (a,c) and CS activity (b,d) in lipid oxidation experiments with no and high BCAA and 24h EPS and protein content (e) in lipogenesis experiment with no BCAA and 16h EPS; Figure S4: LDH activity (U/l) in cell media with and without EPS and with different BCAA levels in lipid oxidation (a) and lipogenesis (b) experiments.

Author Contributions: Conceptualization, H.K., J.J.H., S.P. and M.S.; methodology, U.-M.S., V.F., J.H.L., S.P., P.P. and S.M.; software, S.K., V.F., S.M. and P.P.; validation, S.P., M.S., J.H.L. and S.M.; formal analysis, S.K., V.F. and S.M.; resources, H.K., P.P., S.P., V.F and M.S.; writing—original draft preparation, S.K., V.F and U.-M.S.; review and editing all authors; visualization V.F. and S.K.; supervision, H.K. and J.J.H.; funding acquisition, H.K. All authors have read and agreed to the published version of the manuscript.

Funding: This study was funded by a grant from the Academy of Finland (grant number 298875 to H.K.).

Institutional Review Board Statement: Murine C2C12 myoblasts were obtained from the American Type Culture Collection, ATCC, Manassas, VA, USA.

Informed Consent Statement: Not applicable.

Data Availability Statement: Data is contained within the article or Supplementary Materials.

Acknowledgments: We would like to thank the laboratory staff at the Faculty of Sport and Health Sciences for their valuable assistance in the laboratory analyses.

Conflicts of Interest: The authors declare no conflict of interest.

References

1. Savage, D.B.; Petersen, K.F.; Shulman, G.I. Disordered lipid metabolism and the pathogenesis of insulin resistance. *Physiol. Rev.* **2007**, *87*, 507–520. [CrossRef] [PubMed]
2. Adams, S.H. Emerging perspectives on essential amino acid metabolism in obesity and the insulin-resistant state. *Adv. Nutr.* **2011**, *2*, 445–456. [CrossRef] [PubMed]
3. Kainulainen, H.; Hulmi, J.J.; Kujala, U.M. Potential role of branched-chain amino acid catabolism in regulating fat oxidation. *Exerc. Sport Sci. Rev.* **2013**, *41*, 194–200. [CrossRef] [PubMed]
4. Kujala, U.M.; Makinen, V.P.; Heinonen, I.; Soininen, P.; Kangas, A.J.; Leskinen, T.H.; Rahkila, P.; Wurtz, P.; Kovanen, V.; Cheng, S.; et al. Long-term leisure-time physical activity and serum metabolome. *Circulation* **2013**, *127*, 340–348. [CrossRef] [PubMed]
5. Leskinen, T.; Rinnankoski-Tuikka, R.; Rintala, M.; Seppanen-Laakso, T.; Pollanen, E.; Alen, M.; Sipila, S.; Kaprio, J.; Kovanen, V.; Rahkila, P.; et al. Differences in muscle and adipose tissue gene expression and cardio-metabolic risk factors in the members of physical activity discordant twin pairs. *PLoS ONE* **2010**, *5*, e12609. [CrossRef] [PubMed]
6. Wang, T.J.; Larson, M.G.; Vasan, R.S.; Cheng, S.; Rhee, E.P.; McCabe, E.; Lewis, G.D.; Fox, C.S.; Jacques, P.F.; Fernandez, C.; et al. Metabolite profiles and the risk of developing diabetes. *Nat. Med.* **2011**, *17*, 448–453. [CrossRef]
7. Rennie, M.J. Influence of exercise on protein and amino acid metabolism. In *Handbook of Physiology*; Rowell, L.B., Shepherd, J.T., Eds.; Section 12: Exercise: Regulation and Integration of Multiple Systems; American Physiological Society: Bethesda, MD, USA, 1996; Volume 20, Chapter 22; pp. 995–1035.
8. Holecek, M. Branched-chain amino acids in health and disease: Metabolism, alterations in blood plasma, and as supplements. *Nutr. Metab.* **2018**, *15*, 1–12. [CrossRef]
9. Berggren, J.R.; Boyle, K.E.; Chapman, W.H.; Houmard, J.A. Skeletal muscle lipid oxidation and obesity: Influence of weight loss and exercise. *Am. J. Physiol. Metab.* **2008**, *294*, E726–E732. [CrossRef]
10. Argiles, J.M.; Campos, N.; Lopez-Pedrosa, J.M.; Rueda, R.; Rodriguez-Manas, L. Skeletal Muscle Regulates Metabolism via Interorgan Crosstalk: Roles in Health and Disease. *J. Am. Med. Dir. Assoc.* **2016**, *17*, 789–796. [CrossRef]
11. She, P.; Zhou, Y.; Zhang, Z.; Griffin, K.; Gowda, K.; Lynch, C.J. Disruption of BCAA metabolism in mice impairs exercise metabolism and endurance. *J. Appl. Physiol.* **2010**, *108*, 941–949. [CrossRef]
12. Kivelä, R.; Silvennoinen, M.; Lehti, M.; Rinnankoski-Tuikka, R.; Purhonen, T.; Ketola, T.; Pullinen, K.; Vuento, M.; Mutanen, N.; Sartor, M.A.; et al. Gene expression centroids that link with low intrinsic aerobic exercise capacity and complex disease risk. *FASEB J.* **2010**, *24*, 4565–4574. [CrossRef] [PubMed]
13. Xu, M.; Nagasaki, M.; Obayashi, M.; Sato, Y.; Tamura, T.; Shimomura, Y. Mechanism of activation of branched-chain alpha-keto acid dehydrogenase complex by exercise. *Biochem. Biophys. Res. Commun.* **2001**, *287*, 752–756. [CrossRef] [PubMed]
14. Kasperek, G.J.; Dohm, G.L.; Snider, R.D. Activation of branched-chain keto acid dehydrogenase by exercise. *Am. J. Physiol.-Regul. Integr. Comp. Physiol.* **1985**, *248*, R166–R171. [CrossRef] [PubMed]
15. Balage, M.; Dardevet, D. Long-term effects of leucine supplementation on body composition. *Curr. Opin. Clin. Nutr. Metab. Care* **2010**, *13*, 265–270. [CrossRef]
16. Gualano, A.B.; Bozza, T.; De Campos, P.L.; Roschel, H.; Costa, A.D.S.; Marquezi, M.L.; Benatti, F.; Junior, A.H.L. Branched-chain amino acids supplementation enhances exercise capacity and lipid oxidation during endurance exercise after muscle glycogen depletion. *J. Sports Med. Phys. Fit.* **2011**, *51*, 82–88.
17. D'Antona, G.; Ragni, M.; Cardile, A.; Tedesco, L.; Dossena, M.; Bruttini, F.; Caliaro, F.; Corsetti, G.; Bottinelli, R.; Carruba, M.O.; et al. Branched-chain amino acid supplementation promotes survival and supports cardiac and skeletal muscle mitochondrial biogenesis in middle-aged mice. *Cell Metab.* **2010**, *12*, 362–372. [CrossRef]
18. Newgard, C.B.; An, J.; Bain, J.R.; Muehlbauer, M.J.; Stevens, R.D.; Lien, L.F.; Haqq, A.M.; Shah, S.H.; Arlotto, M.; Slentz, C.A.; et al. A branched-chain amino acid-related metabolic signature that differentiates obese and lean humans and contributes to insulin resistance. *Cell Metab.* **2009**, *9*, 311–326. [CrossRef]
19. Nishimura, J.; Masaki, T.; Arakawa, M.; Seike, M.; Yoshimatsu, H. Isoleucine prevents the accumulation of tissue triglycerides and upregulates the expression of PPARalpha and uncoupling protein in diet-induced obese mice. *J. Nutr.* **2010**, *140*, 496–500. [CrossRef]
20. Ahtiainen, J.P.; Lensu, S.; Ruotsalainen, I.; Schumann, M.; Ihalainen, J.K.; Fachada, V.; Mendias, C.L.; Brook, M.S.; Smith, K.; Atherton, P.J.; et al. Physiological adaptations to resistance training in rats selectively bred for low and high response to aerobic exercise training. *Exp. Physiol.* **2018**, *103*, 1513–1523. [CrossRef]
21. Lensu, S.; Pekkala, S.P.; Mäkinen, A.; Karstunen, N.; Turpeinen, A.T.; Hulmi, J.J.; Silvennoinen, M.M.; Ma, H.; Kujala, U.M.; Karvinen, S.; et al. Beneficial effects of running and milk protein supplements on Sirtuins and risk factors of metabolic disorders in rats with low aerobic capacity. *Metab. Open* **2019**, *4*, 100019. [CrossRef]

22. Hulmi, J.J.; Laakso, M.; Mero, A.A.; Häkkinen, K.; Ahtiainen, J.P.; Peltonen, H. The effects of whey protein with or without carbohydrates on resistance training adaptations. *J. Int. Soc. Sports Nutr.* **2015**, *12*, 1–13. [CrossRef] [PubMed]
23. Nair, K.S.; Short, K.R. Hormonal and signaling role of branched-chain amino acids. *J. Nutr.* **2005**, *135*, 1547S–1552S. [CrossRef] [PubMed]
24. Watford, M. Lowered concentrations of branched-chain amino acids result in impaired growth and neurological problems: Insights from a branched-chain alpha-keto acid dehydrogenase complex kinase-deficient mouse model. *Nutr. Rev.* **2007**, *65*, 167–172. [CrossRef]
25. Fontana, L.; Cummings, N.E.; Apelo, S.I.A.; Neuman, J.C.; Kasza, I.; Schmidt, B.A.; Cava, E.; Spelta, F.; Tosti, V.; Syed, F.A.; et al. Decreased Consumption of Branched-Chain Amino Acids Improves Metabolic Health. *Cell Rep.* **2016**, *16*, 520–530. [CrossRef] [PubMed]
26. Cummings, N.E.; Williams, E.M.; Kasza, I.; Konon, E.N.; Schaid, M.D.; Schmidt, B.A.; Poudel, C.; Sherman, D.S.; Yu, D.; Apelo, S.I.A.; et al. Restoration of metabolic health by decreased consumption of branched-chain amino acids. *J. Physiol.* **2018**, *596*, 623–645. [CrossRef] [PubMed]
27. Yu, D.; Richardson, N.E.; Green, C.L.; Spicer, A.B.; Murphy, M.E.; Flores, V.; Jang, C.; Kasza, I.; Nikodemova, M.; Wakai, M.H.; et al. The adverse metabolic effects of branched-chain amino acids are mediated by isoleucine and valine. *Cell Metab.* **2021**, *33*, 905–922. [CrossRef]
28. Hargreaves, M.; Spriet, L.L. Author Correction: Skeletal muscle energy metabolism during exercise. *Nat. Metab.* **2020**, *2*, 990. [CrossRef]
29. Jeukendrup, A.E. Regulation of fat metabolism in skeletal muscle. *Ann. N. Y. Acad. Sci.* **2002**, *967*, 217–235. [CrossRef]
30. Goodpaster, B.H.; He, J.; Watkins, S.; Kelley, D.E. Skeletal muscle lipid content and insulin resistance: Evidence for a paradox in endurance-trained athletes. *J. Clin. Endocrinol. Metab.* **2001**, *86*, 5755–5761. [CrossRef]
31. Li, X.; Li, Z.; Zhao, M.; Nie, Y.; Liu, P.; Zhu, Y.; Zhang, X. Skeletal Muscle Lipid Droplets and the Athlete's Paradox. *Cells* **2019**, *8*, 249. [CrossRef]
32. Qin, L.Q.; Xun, P.; Bujnowski, D.; Daviglus, M.L.; Van Horn, L.; Stamler, J.; He, K.; Group, I.C.R. Higher branched-chain amino acid intake is associated with a lower prevalence of being overweight or obese in middle-aged East Asian and Western adults. *J. Nutr.* **2011**, *141*, 249–254. [CrossRef] [PubMed]
33. Lerin, C.; Goldfine, A.B.; Boes, T.; Liu, M.; Kasif, S.; Dreyfuss, J.M.; De Sousa-Coelho, A.L.; Daher, G.; Manoli, I.; Sysol, J.R.; et al. Defects in muscle branched-chain amino acid oxidation contribute to impaired lipid metabolism. *Mol. Metab.* **2016**, *5*, 926–936. [CrossRef] [PubMed]
34. Connor, S.C.; Hansen, M.K.; Corner, A.; Smith, R.F.; Ryan, T.E. Integration of metabolomics and transcriptomics data to aid biomarker discovery in type 2 diabetes. *Mol. Biosyst.* **2010**, *6*, 909–921. [CrossRef] [PubMed]
35. Estrada-Alcalde, I.; Tenorio-Guzman, M.R.; Tovar, A.R.; Salinas-Rubio, D.; Torre-Villalvazo, I.; Torres, N.; Noriega, L.G. Metabolic Fate of Branched-Chain Amino Acids During Adipogenesis, in Adipocytes From Obese Mice and C2C12 Myotubes. *J. Cell. Biochem.* **2017**, *118*, 808–818. [CrossRef]
36. Boulange, C.L.; Claus, S.P.; Chou, C.J.; Collino, S.; Montoliu, I.; Kochhar, S.; Holmes, E.; Rezzi, S.; Nicholson, J.K.; Dumas, M.E.; et al. Early metabolic adaptation in C57BL/6 mice resistant to high fat diet induced weight gain involves an activation of mitochondrial oxidative pathways. *J. Proteome Res.* **2013**, *12*, 1956–1968. [CrossRef]
37. Aftring, R.P.; Miller, W.J.; Buse, M.G. Effects of diabetes and starvation on skeletal muscle branched-chain alpha-keto acid dehydrogenase activity. *Am. J. Physiol.-Endocrinol. Metab.* **1988**, *254*, E292–E300. [CrossRef]
38. Wallace, M.; Green, C.R.; Roberts, L.S.; Lee, Y.M.; McCarville, J.L.; Sanchez-Gurmaches, J.; Meurs, N.; Gengatharan, J.M.; Hover, J.D.; Phillips, S.A.; et al. Enzyme promiscuity drives branched-chain fatty acid synthesis in adipose tissues. *Nat. Chem. Biol.* **2018**, *14*, 1021–1031. [CrossRef]
39. Green, C.R.; Wallace, M.; Divakaruni, A.S.; Phillips, S.A.; Murphy, A.N.; Ciaraldi, T.P.; Metallo, C.M. Branched-chain amino acid catabolism fuels adipocyte differentiation and lipogenesis. *Nat. Chem. Biol.* **2016**, *12*, 15–21. [CrossRef]
40. Sánchez-González, C.; Nuevo-Tapioles, C.; Herrero Martín, J.C.; Pereira, M.P.; Serrano Sanz, S.; Ramírez de Molina, A.; Cuezva, J.M.; Formentini, L. Dysfunctional oxidative phosphorylation shunts branched-chain amino acid catabolism onto lipogenesis in skeletal muscle. *EMBO J.* **2020**, *39*, e103812. [CrossRef]
41. Lautaoja, J.H.; O'Connell, T.M.; Mäntyselkä, S.; Peräkylä, J.; Kainulainen, H.; Pekkala, S.; Permi, P.; Hulmi, J.J. Higher glucose availability augments the metabolic responses of the C2C12 myotubes to exercise-like electrical pulse stimulation. *Am. J. Physiol. Endocrinol. Metab.* **2021**, *321*, E229–E245. [CrossRef]
42. Abdelmoez, A.M.; Sardón Puig, L.; Smith, J.A.B.; Gabriel, B.M.; Savikj, M.; Dollet, L.; Chibalin, A.V.; Krook, A.; Zierath, J.R.; Pillon, N.J. Comparative profiling of skeletal muscle models reveals heterogeneity of transcriptome and metabolism. *Am. J. Physiol. Cell Physiol.* **2020**, *318*, C615–C626. [CrossRef] [PubMed]
43. Barclay, J.K.; Stainsby, W.N. Intramuscular lipid store utilization by contracting dog skeletal muscle in situ. *Am. J. Physiol.* **1972**, *223*, 115–119. [CrossRef] [PubMed]
44. Hopp, J.F.; Palmer, W.K. Electrical stimulation alters fatty acid metabolism in isolated skeletal muscle. *J. Appl. Physiol.* **1990**, *68*, 2473–2481. [CrossRef] [PubMed]
45. Spriet, L.L.; Heigenhauser, G.J.; Jones, N.L. Endogenous triacylglycerol utilization by rat skeletal muscle during tetanic stimulation. *J. Appl. Physiol.* **1986**, *60*, 410–415. [CrossRef] [PubMed]

46. Masoro, E.J.; Rowell, L.B.; McDonald, R.M.; Steiert, B. Skeletal muscle lipids. II. Nonutilization of intracellular lipid esters as an energy source for contractile activity. *J. Biol. Chem.* **1966**, *241*, 2626–2634. [CrossRef]
47. Marš, T.; Miš, K.; Meznarič, M.; Prpar Mihevc, S.; Jan, V.; Haugen, F.; Rogelj, B.; Rustan, A.C.; Thoresen, G.H.; Pirkmajer, S.; et al. Innervation and electrical pulse stimulation—In vitro effects on human skeletal muscle cells. *Appl. Physiol. Nutr. Metab.* **2021**, *46*, 299–308. [CrossRef] [PubMed]
48. Nikolić, N.; Skaret Bakke, S.; Tranheim Kase, E.; Rudberg, I.; Flo Halle, I.; Rustan, A.C.; Thoresen, G.H.; Aas, V. Correction: Electrical Pulse Stimulation of Cultured Human Skeletal Muscle Cells as an In Vitro Model of Exercise. *PLoS ONE* **2013**, *8*. [CrossRef]
49. Li, L.-J.; Ma, J.; Li, S.-B.; Chen, X.-F.; Zhang, J. Electric pulse stimulation inhibited lipid accumulation on C2C12 myotubes incubated with oleic acid and palmitic acid. *Arch. Physiol. Biochem.* **2021**, *127*, 344–350. [CrossRef]
50. Dyck, D.J.; Bonen, A. Muscle contraction increases palmitate esterification and oxidation and triacylglycerol oxidation. *Am. J. Physiol.* **1998**, *275*, E888–E896. [CrossRef]
51. van Loon, L.J.; Greenhaff, P.L.; Constantin-Teodosiu, D.; Saris, W.H.; Wagenmakers, A.J. The effects of increasing exercise intensity on muscle fuel utilisation in humans. *J. Physiol.* **2001**, *536*, 295–304. [CrossRef]
52. Picard, M.; Gentil, B.J.; McManus, M.J.; White, K.; St Louis, K.; Gartside, S.E.; Wallace, D.C.; Turnbull, D.M. Acute exercise remodels mitochondrial membrane interactions in mouse skeletal muscle. *J. Appl. Physiol.* **2013**, *115*, 1562–1571. [CrossRef] [PubMed]
53. Prats, C.; Donsmark, M.; Qvortrup, K.; Londos, C.; Sztalryd, C.; Holm, C.; Galbo, H.; Ploug, T. Decrease in intramuscular lipid droplets and translocation of HSL in response to muscle contraction and epinephrine. *J. Lipid Res.* **2006**, *47*, 2392–2399. [CrossRef] [PubMed]
54. Fraenkel, M.; Weiss, R.; Leizerman, I.; Anaby, D.; Golomb, E.; Leibowitz, G.; Kaiser, N. Scanning electron microscopic analysis of intramyocellular lipid droplets in an animal model of type 2 diabetes. *Obesity* **2008**, *16*, 695–699. [CrossRef] [PubMed]
55. Akie, T.E.; Cooper, M.P. Determination of Fatty Acid Oxidation and Lipogenesis in Mouse Primary Hepatocytes. *JoVE* **2015**, *102*, e52982. [CrossRef]
56. Spandl, J.; White, D.J.; Peychl, J.; Thiele, C. Live cell multicolor imaging of lipid droplets with a new dye, LD540. *Traffic* **2009**, *10*, 1579–1584. [CrossRef]
57. Tamura, K.; Goto-Inoue, N.; Miyata, K.; Furuichi, Y.; Fujii, N.L.; Manabe, Y. Effect of treatment with conditioned media derived from C2C12 myotube on adipogenesis and lipolysis in 3T3-L1 adipocytes. *PLoS ONE* **2020**, *15*, e0237095. [CrossRef]

III

EFFECTS OF LONG-TERM PHYSICAL ACTIVITY AND BCAA AVAILABILITY ON THE SUBCELLULAR ASSOCIATIONS BETWEEN INTRAMYOCELLULAR LIPIDS, PERILIPINS AND PGC-1α

by

Fachada, V., Silvennoinen, M., Sahinaho, U.M., Rahkila, P., Kivelä, R., Hulmi, J.J., Kujala, U.M., Kainulainen, H (2023)

International Journal of Molecular Sciences 24(5), 4282.

https://doi.org/10.3390/ijms24054282

International Journal of
Molecular Sciences

MDPI

Article

Effects of Long-Term Physical Activity and BCAA Availability on the Subcellular Associations between Intramyocellular Lipids, Perilipins and PGC-1*α*

Vasco Fachada, Mika Silvennoinen, Ulla-Maria Sahinaho, Paavo Rahkila, Riikka Kivelä, Juha J. Hulmi *, Urho Kujala and Heikki Kainulainen

Faculty of Sport and Health Sciences, NeuroMuscular Research Center, University of Jyväskylä, FI-40014 Jyväskylä, Finland
* Correspondence: juha.hulmi@jyu.fi

Abstract: Cellular skeletal muscle lipid metabolism is of paramount importance for metabolic health, specifically through its connection to branched-chain amino acids (BCAA) metabolism and through its modulation by exercise. In this study, we aimed at better understanding intramyocellular lipids (IMCL) and their related key proteins in response to physical activity and BCAA deprivation. By means of confocal microscopy, we examined IMCL and the lipid droplet coating proteins PLIN2 and PLIN5 in human twin pairs discordant for physical activity. Additionally, in order to study IMCLs, PLINs and their association to peroxisome proliferator-activated receptor gamma coactivator 1-alpha (PGC-1*α*) in cytosolic and nuclear pools, we mimicked exercise-induced contractions in C2C12 myotubes by electrical pulse stimulation (EPS), with or without BCAA deprivation. The life-long physically active twins displayed an increased IMCL signal in type I fibers when compared to their inactive twin pair. Moreover, the inactive twins showed a decreased association between PLIN2 and IMCL. Similarly, in the C2C12 cell line, PLIN2 dissociated from IMCL when myotubes were deprived of BCAA, especially when contracting. In addition, in myotubes, EPS led to an increase in nuclear PLIN5 signal and its associations with IMCL and PGC-1*α*. This study demonstrates how physical activity and BCAA availability affects IMCL and their associated proteins, providing further and novel evidence for the link between the BCAA, energy and lipid metabolisms.

Keywords: lipid droplets; PLIN2; PLIN5; skeletal muscle; physical activity; C2C12; electrical pulse stimulation; EPS; subcellular localization

Citation: Fachada, V.; Silvennoinen, M.; Sahinaho, U.-M.; Rahkila, P.; Kivelä, R.; Hulmi, J.J.; Kujala, U.; Kainulainen, H. Effects of Long-Term Physical Activity and BCAA Availability on the Subcellular Associations between Intramyocellular Lipids, Perilipins and PGC-1*α*. *Int. J. Mol. Sci.* **2023**, *24*, 4282. https://doi.org/10.3390/ijms24054282

Academic Editor: Rasmus Kjøbsted

Received: 5 February 2023
Accepted: 9 February 2023
Published: 21 February 2023

1. Introduction

On top of being the largest organ in the human body, skeletal muscle has high energy demands, leading to elevated lipid turnover rates [1–3]. Despite being well established, the connection between skeletal muscle lipid metabolism and metabolic health is far from linear. On one hand, several metabolic diseases—such as insulin resistance—have been associated with physical inactivity and elevated intramyocellular lipids (IMCL). On the other hand, highly insulin sensitive individuals—such as endurance athletes—associate with even higher levels of IMCL [2,4]. It became ever more clear that mere levels of IMCL were not sufficient to explain skeletal muscle lipid metabolism efficiency. The perilipin protein family members (PLINs) are central agents in managing the fate of IMCL, and they are mostly known for regulating the access of lipolytic and lipogenic enzymes onto the surface of lipid droplets (LDs), thus protecting the cell against lipotoxicity and improving metabolic health [5–10].

The responses of human skeletal muscle LDs and PLINs to different exercise modalities have been well studied in a multitude of setups [11–15]. However, up to this date, the effects of long-term physical activity on IMCL and PLINs, amongst genetically similar individuals, remain largely unstudied. As a first aim of the present work, we propose

to explore this gap. Therefore, through confocal microscopy and pixel-to-pixel intensity correlation analysis (ICA) [16], we examined IMCL, PLIN2 and PLIN5 and their associations in two main fiber types of twin pairs with discordant physical activity. We hypothesize that physically discordant twins will display different patterns of IMCL-PLIN association relative to previously studied setups.

The IMCL-PLINs dynamics are complex, and the role of PLINs themselves is not limited to hydrolysis or esterification of triacylglycerol (TAG) within LDs. For instance, PLIN5 has been shown to be necessary to transport monounsaturated fatty acids (MUFAs) into nuclei, in order to activate peroxisome proliferator-activated receptor gamma coactivator 1-alpha (PGC-1α) and, consequently, induce mitochondria biogenesis and fatty acid oxidation [17,18]. Additionally, PGC-1α is also an important bridge between the skeletal muscle lipid and branched-chain amino acid (BCAA) metabolisms, as it activates the latter through multiple nuclear receptors [19,20]. Importantly, unlike other amino acids that can be processed by the liver, BCAA are mostly catabolized in skeletal muscle [21,22]. Respectively, we have previously hypothesized that the connection between IMCL and metabolic health could further extend to the BCAA metabolism [22], as one important source of TAG in muscle comes from glyceroneogenesis [23]. Furthermore, inefficient skeletal muscle BCAA metabolism has been associated with impaired lipid metabolism and insulin resistance [21]. Finally, there is a known interplay between exercise and muscle BCAA metabolism [24,25]. However, studies establishing the relationship between intramyocellular BCAA and PLINs are essentially lacking. Therefore, it is important to investigate the impacts that BCAA availability may have on LD-PLINs regulation.

As a second aim, we investigated IMCL, PLIN2, PLIN5 and PGC-1α subcellular responses to exercise and BCAA availability. By combining electrical pulse stimulation (EPS)—an exercise-mimicking method [26]—with BCAA deprivation, we measured the optical density and performed ICA in different myotube compartments. We hypothesize that skeletal muscle PLIN5 and PGC-1α signals associate in response to EPS, especially within the nuclei. Moreover, we postulate that, besides LDs, PLIN5 or PGC-1α, PLIN2 may have unreported nuclear associations, which could be affected by EPS and/or BCAA deprivation.

2. Results

2.1. Active Co-Twins Have Increased IMCL in Type I Fibers

Concerning the twin participants described in Table 1, type I fibers contained more IMCL than type II fibers, as expected ($p < 0.001$, Figure 1A–C). Interestingly, physically active twins had increased IMCL in type I fibers compared to their inactive co-twin ($p < 0.001$, Figure 1B,C), but there was no difference in type II fibers due to LTPA. The active twins demonstrated a significant difference in IMCL between fiber types ($p < 0.001$), which was not observed in the inactive co-twins ($p = 0.064$), as seen in Figure 1C.

As expected, PLIN5 associated IMCL was significantly higher in type I than in type II fibers ($p = 0.001$, Figure 2A,B), and with no differences between twin pairs (Figure 2B,C). Lastly, both *PLIN5* mRNA levels and PLIN5 confocal mean signal remained unchanged between twin pairs (Figure S7).

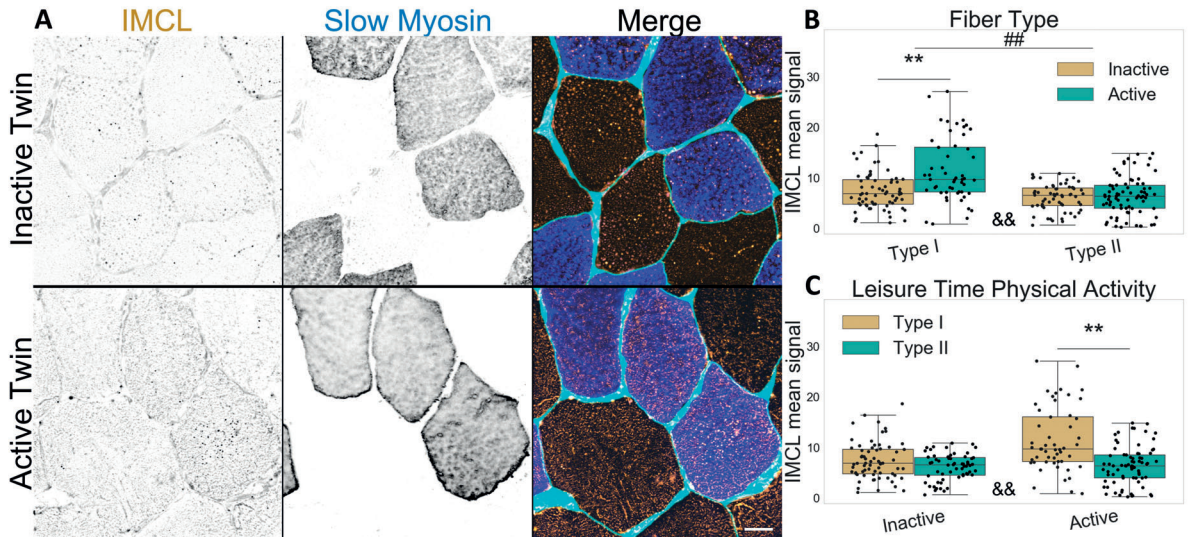

Figure 1. IMCL mean signal intensity between twin pairs. (**A**) representative image showing differences between groups. Gray level indicates signal, cyan indicates segmented sarcolemma. Note the active twin type I fibers with higher IMCL signal; Bar = 20 µm; (**B**) fiber type as main effect, with LTPA combined; (**C**) LTPA main effect, with fiber type combined; main effect differences denoted with ## ($p < 0.001$); combined group differences denoted with ** ($p < 0.001$); interacting effect between fiber type and LTPA denoted with **&&** ($p < 0.001$). Dots in (**B**,**C**) represent individual cells.

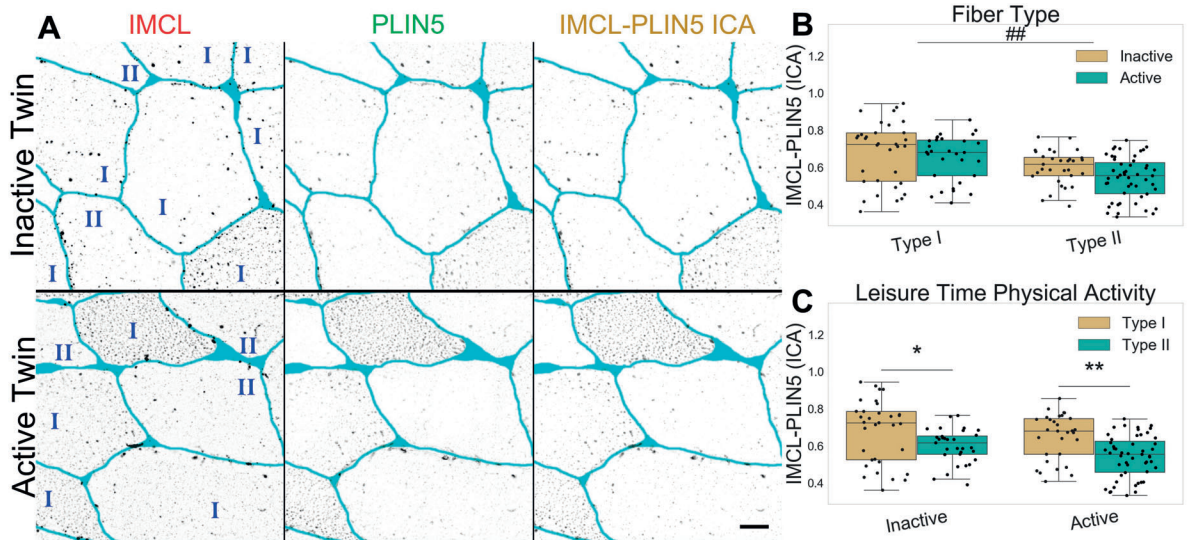

Figure 2. IMCL-PLIN5 intensity correlation analysis in twin pairs. (**A**) representative image showing differences between groups. Gray level indicates signal, cyan indicates segmented sarcolemma. Bar = 20 µm; (**B**) fiber type as main effect, with LTPA combined; (**C**) LTPA main effect, with fiber type combined. Main effect differences denoted with ## ($p < 0.001$). Combined group differences denoted with * ($p < 0.01$) and ** ($p < 0.001$). Dots in (**B**,**C**) represents individual cells.

Table 1. Characteristics of twin pairs. Mean ± SEM. ** $p < 0.001$ with *t*-test.

Number of Participants	Inactive 4	Active 4
LTPA (MET-hours ·day^{-1}) **	2.9 +/− 1.4	13.8 +/− 1.0
Age (years)	58.0 +/− 2.9	58.0 +/− 2.9
VO_2 max (mL · min^{-1} · kg^{-1})	30.2 +/− 1.4	32.8 +/− 1.8
Body weight (kg)	71.5 +/− 3.4	69.8 +/− 5.1
BMI (kg · m^{-2})	25.0 +/− 0.6	24.6 +/− 1.1
Body fat (%)	24.1 +/− 2.9	20.2 +/− 3.3
Triglycerides (mmol · L^{-1})	0.9 +/− 0.2	1.0 +/− 0.3
HOMA index	1.9 +/− 0.3	1.5 +/− 0.5

2.2. Inactive Twins Show Decreased IMCL-PLIN2 Association

The inactive twin pairs show a decreased association between IMCL and PLIN2 ($p = 0.008$), mainly through a very significant decrease in the type II fibers ($p < 0.001$, Figure 3A–C). The latter happened despite no fiber type or LTPA differences in PLIN2 mean signal (Figure S1) or *PLIN2* mRNA levels (Figure S7). Taken together, this shows that IMCL targeting by PLIN2 is clearly restrained in type II fibers of inactive twins.

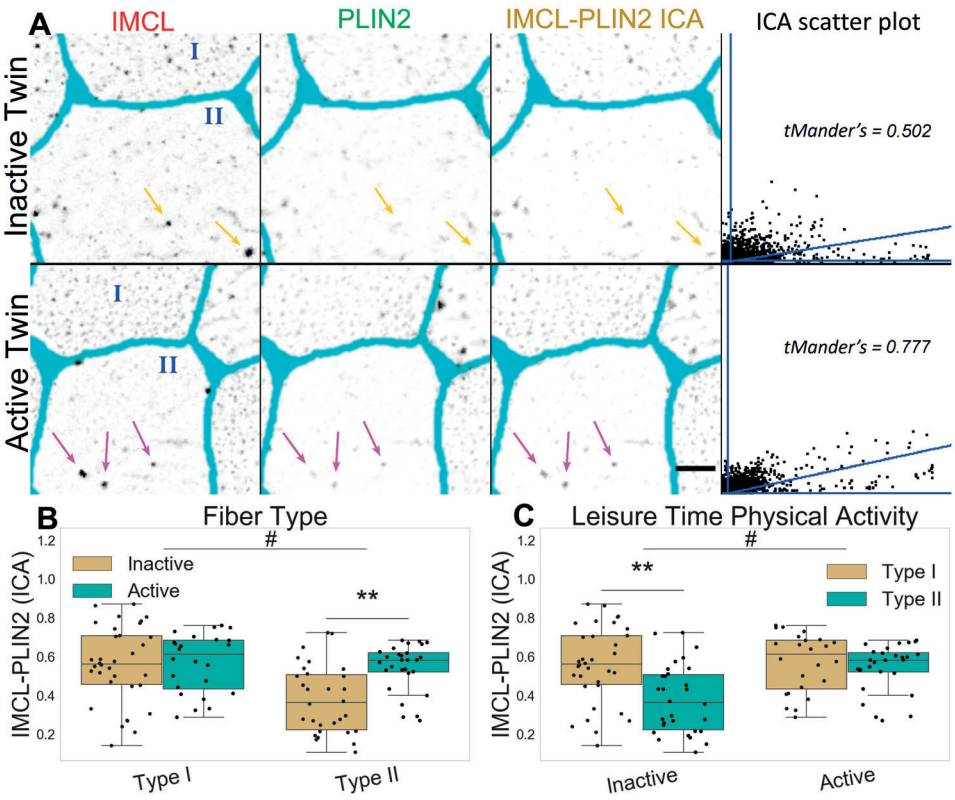

Figure 3. IMCL-PLIN2 intensity correlation analysis in twin pairs. (**A**) representative image showing differences between groups. Gray level indicates marker signal, cyan indicates segmented sarcolemma. Note active twin type II fiber with high intensity IMCL significantly colocalized by PLIN2 (magenta arrows), unlike the inactive twin (orange arrows). Bar = 10 µm. Scatter plot is relative to the arrowed type II fiber; (**B**) fiber type as main effect, with LTPA combined; (**C**) LTPA as main effect, with fiber type combined, main effect differences denoted with # ($p < 0.01$); combined group differences denoted with ** ($p < 0.001$). Dots in (**B**,**C**) represent individual cells.

2.3. PLIN5 Abounds in C2C12 Myotube Nuclei, PLIN2 Detected

Next, given the role in regulating energy metabolism and a known nuclear interaction with PLIN5, we studied PGC-1α and its association with IMCL and PLIN5 in different myotube compartments.

The compartmental analysis showed a significant contrast ($p < 0.001$) between cytosolic and nuclear signals for all markers within the myotubes. The most abundant nuclear signals were observed for IMCL and PLIN5. A much smaller proportion of PLIN2 ($p < 0.001$) was detected above the background and occasionally in a particle-like manner (Figure 4A,B).

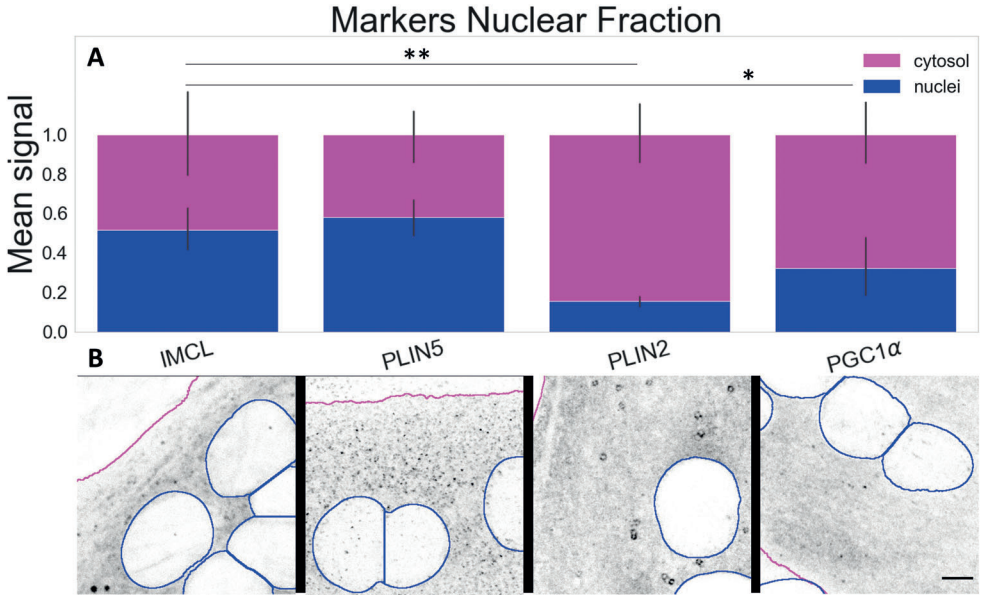

Figure 4. Marker signal comparison between compartments; (**A**) proportion of nuclear signal (blue bars) in relation to cytosolic signal (full bars). Data normalized to the cytosolic reference and measured from the control group (Normal BCAA | Rest). Differences between nuclear fractions of IMCL versus remaining markers * ($p < 0.05$) and ** ($p < 0.001$). Whiskers signify standard deviation; (**B**) representative images of respective markers. Gray is signal, blue are limits of segmented nuclei, magenta are limits of segmented myotubes. Bar = 5 µm.

2.4. PLIN2 Dissociates from IMCL upon BCAA Deprivation in Myotubes

Both IMCL and PLIN2 showed a mostly diffused signal in C2C12 myotubes. Occasionally, semi-spherical IMCL aggregates were visible as LDs (Video S1). Likewise, PLIN2 aggregates were common and often seen as dotted ring structures enveloping LDs (Figure 5A).

In addition to fiber type and exercise, BCAA can also affect IMCL metabolism, and this may interact with muscle contraction. Respectively, we observed a cytosolic decrease in the association between PLIN2 and IMCL after BCAA deprivation ($p = 0.028$, Figure S2), especially after EPS ($p = 0.048$, Figure 5B). The same combination (No BCAA | EPS) resulted in increased PLIN2 and PLIN5 association inside the nuclei ($p = 0.030$), and in a dependent manner ($p = 0.033$, Figure 5C).

Such events were independent from the overall PLIN2 signal, which remained unchanged after EPS and BCAA deprivation (Figure S2).

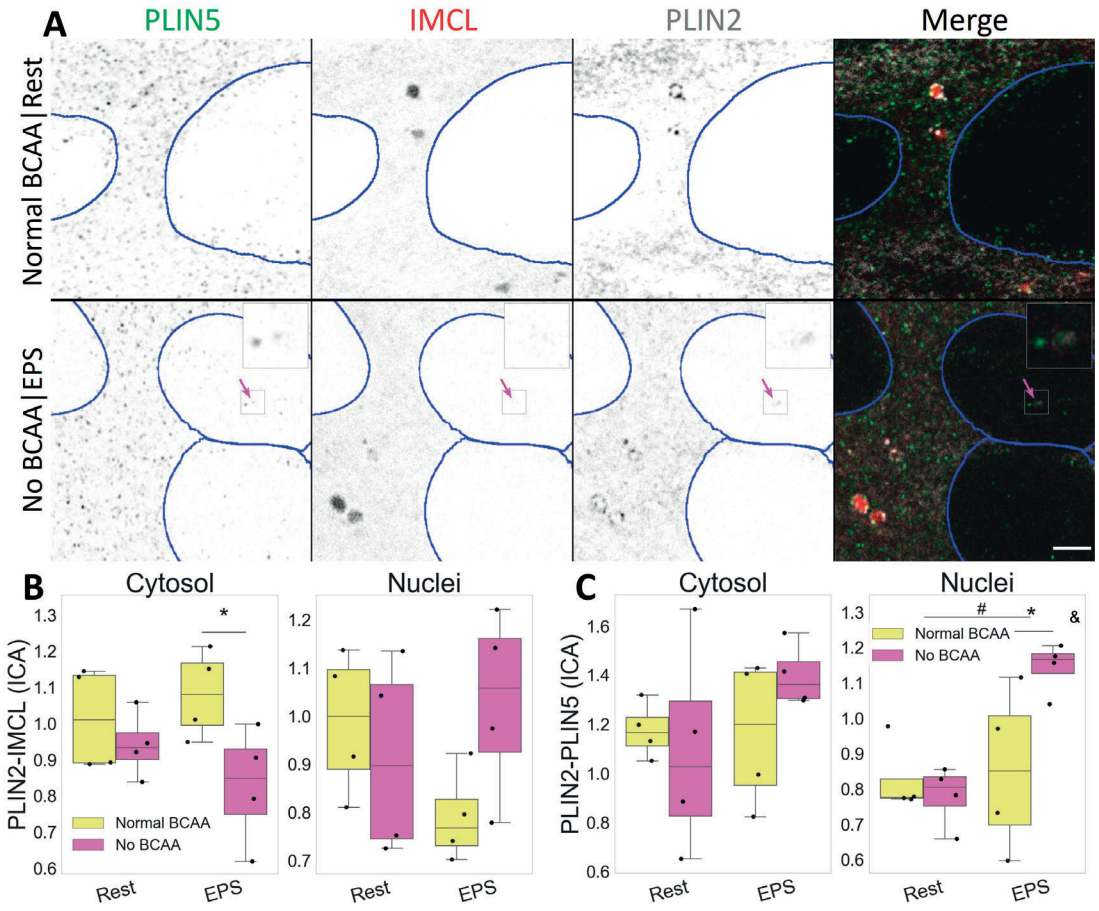

Figure 5. Compartmental PLIN2 association with IMCL and PLIN5 after EPS and BCAA deprivation. (**A**) representative image. Note a more diffused PLIN2 pattern after BCAA deprivation and PLIN2-PLIN5 association in nuclei after EPS (pink arrow). Gray is signal, blue are limits of segmented nuclei. Bar = 3 µm; (**B**) colocalization via intensity correlation analysis (ICA) between PLIN2 and IMCL; (**C**) colocalization via intensity correlation analysis (ICA) between PLIN2 and PLIN5. Main effect differences denoted with **#** ($p < 0.05$). Combined group differences denoted with * ($p < 0.05$); interacting effect between fiber type and LTPA denoted with **&** ($p < 0.05$). Dots in (**B**,**C**) represent averaged coverslip values; data normalized to the control group reference (Normal BCAA | Rest).

2.5. PLIN5 Moves to Myotube Nuclei upon Stimulation, Further Associating with IMCL and PGC-1α

The PLIN5 signal was mostly punctate and abundant, often immediately adjacent to or colocalizing with other markers. In turn, PGC-1α showed mostly a diffused signal, sometimes concentrating in differently shaped aggregates and often colocalizing with IMCL (Figure 6A).

Notably, PLIN5 signal increased in nuclei after EPS ($p = 0.033$, Figure 6B), where it associated with IMCL ($p = 0.019$, Figure 6D), especially under BCAA availability ($p = 0.002$, Figure S3). Likewise, under Normal BCAA | EPS, nuclear PLIN5 further associated with PGC-1α, and very significantly so ($p = 0.009$, Figure 6E).

Interestingly, BCAA deprivation alone was sufficient to decrease PGC-1α signal in myotube nuclei ($p = 0.009$, Figure 6C). It is worth noting that such effect was seen only in the nuclei, as neither a cytosolic confocal signal (Figure 6B) nor whole cell Western blots detected changes in PGC-1α protein concentration (Figure S8).

In the cytosol, the level of association between PLIN5 and PGC-1α was increased after BCAA deprivation ($p = 0.026$), as seen in (Figure 6E). The level of association between IMCL and PGC-1α was not altered with either EPS or BCAA deprivation (Figure S4).

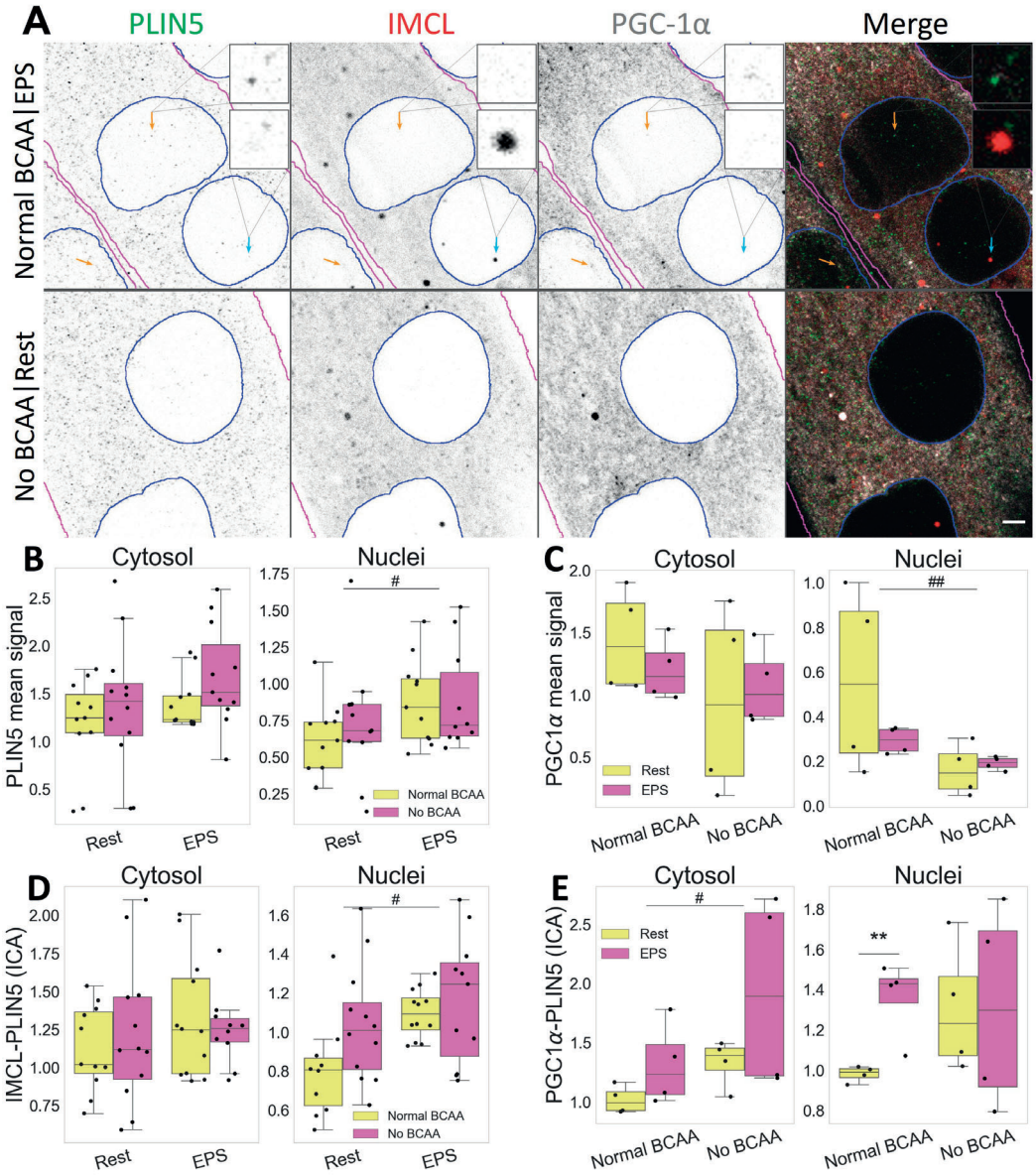

Figure 6. Compartmental association and distribution of PLIN5, IMCL and PGC-1α after EPS and BCAA deprivation. (**A**) representative image. Note more abundant PLIN5 in nuclei after EPS, with stronger association with PGC-1α (orange arrows) and IMCL (cyan arrow). Gray is signal, blue are limits of segmented nuclei, magenta are limits of segmented myotubes. Bar = 3 µm; (**B**) PLIN5 signal intensity in different compartments; (**C**) PGC-1α signal intensity in different compartments; (**D**) ICA between IMCL and PLIN5 in different compartments; (**E**) ICA between PGC-1α and PLIN5 in different compartments. Main effect differences denoted with # ($p < 0.05$) and ## ($p < 0.01$). Combined group differences denoted with ** ($p < 0.01$). Dots in (**B**–**E**) represent averaged coverslip values; data normalized to the control group reference (Normal BCAA | Rest).

3. Discussion

3.1. Overview

This study examined the effects of physical activity on intramyocellular lipids and respective coating proteins in human twin pairs discordant for life-long physical activity. We found that, in physically active twins, the intramyocellular phenotype resembles that of athletes, namely in their type I fiber elevated lipid content, together with an enhanced lipid coating by PLIN2.

Secondly, we investigated myotube inter-compartmental responses to muscle contraction induced by EPS and to BCAA deprivation. We found that BCAA deprivation leads to a cytosolic dissociation between PLIN2 and IMCL, especially when combined with EPS. Importantly, we found that EPS leads to an increased presence of PLIN5 in nuclei, with increased association to PGC-1α, IMCL and PLIN2. Finally, we found that the signal of nuclear PGC-1α is abruptly decreased after BCAA deprivation.

3.2. Active Twins Resemble Athlete Phenotype

It has been shown that a healthy elevation of IMCL can be expected from not only athletes [2,4,12], but also from sedentary individuals who underwent a 6-week training period, especially in type I fibers [13]. Although the overall IMCL content was not different between twin pairs, we did observe significantly increased IMCL in type I fibers of active twins when compared to their inactive co-twins (Section 2.1). Our results suggest that the *athlete paradox* phenotype [2] may not be genetically determined and might be reached via life-long LTPA. Concomitantly, we have previously demonstrated that the active twins have improved skeletal muscle oxidative energy and lipid metabolism [24]. It should be noted that LTPA has recently been associated with slower epigenetic aging [27], suggesting that such mechanisms may be behind the results reported in our work.

Of the muscle PLINs, PLIN5 is probably the most studied member, and it is known for positively responding to exercise and high fat diet, both at the protein level and on IMCL association [8,9,12,28–30]. Interestingly, despite an obvious fiber type difference, LTPA led to no changes in PLIN5 signal or PLIN5 associated IMCL (Section 2.3). This may reflect the fact that intramyocellular physiological responses driven by LTPA could be distinct from those of more strenuous exercise programs in previous studies.

In addition, associating with efficient TAG storage and healthier profiles, intramyocellular PLIN2 has been shown to increase with exercise [13,31]. Although we did not register changes in PLIN2 signal, we did observe a significant decrease in IMCL-PLIN2 association in type II fibers of inactive twins (Section 2.2), suggesting an unhealthier phenotype. The hypothesis that lipotoxic signaling in skeletal muscle could originate from type II fibers is not new, as this fiber type is generally ill-equipped to metabolize lipids [32], especially in innermost regions of fibers ([33], Figure S5). Future studies should further explore the signaling impact of poorly PLIN coated-IMCL in glycolytic muscle fibers.

3.3. Myotubes Resembling Type II Fibers

Beyond PLINs [31], exercise and EPS are also expected to increase PGC-1α levels in skeletal muscle, including C2C12 myotubes [34–37]. Associated with mitochondrial biogenesis and fatty acid oxidation, as well as with glucose uptake and decreased glucose oxidation, PGC-1α is a rather lipolytic and glucogenic agent [38]. However, in the current study, EPS alone did not trigger significant cytosolic responses in the signal of PLIN2, PLIN5, PGC-1α or their association. Accordingly, from previous studies using the same protocol, we have observed a sharp glycolytic response in C2C12 myotubes [25] and only a modest lipolytic one [39]. More specifically, we had shown that EPS led to unchanged IMCL content, unaffected lipogenesis and decreased lipid oxidation [39].

One study has reported increased PGC-1α protein and unchanged lactate or pyruvate levels after using EPS [40]. Contrastingly, we have observed unchanged PGC-1α signal (this study) and increased lactate and pyruvate-derived products [25]. Interestingly, pyruvate is a known inhibitor of PGC-1α [41] and could be hindering a stronger lipolytic response in

our setup. Conflicting results when studying lipid metabolism in C2C12 are not uncommon, as the generally glycolytic nature of this cell line can be increased with longer differentiation protocols [40,42]. Future research should focus on the same phenomena using different cell lines and culture parameters.

3.4. BCAA Necessary for PLIN2 Coating of IMCL

Our group has earlier demonstrated that the unhealthier profile of the inactive twins extends beyond an inefficient lipid metabolism, showing an associated downregulation of BCAA catabolism [24]. Furthermore, we have previously shown that BCAA deprivation decreases both lipid oxidation and lipogenesis in myotubes. In addition, when combined with EPS, BCAA deprivation also decreased the number of segmented LDs [39]. In the current work, the latter combination resulted in a dissociation between cytosolic IMCL and PLIN2 (Section 2.4), while the association between IMCL and PLIN5 remained unchanged (Section 2.5).

Often associating with TAG accumulation and protection against lipotoxicity derived-insulin resistance, PLIN2 is known to abound on the surface of LDs. There it can bind to both lipases and esterification enzymes, possibly having a more lipogenic role than PLIN5 [5,6,31,43]. Finally, there is evidence suggesting that BCAA facilitates TAG accumulation in muscle [44] and that EPS increases BCAA catabolism [25]. Together with our results, these data suggest that PLIN2 coating of IMCL is central to a healthy storage of lipid derivatives, which is improved by BCAA availability combined with physical activity, ultimately resulting in efficient BCAA and lipid metabolisms.

An efficient BCAA catabolism together with BCAA availability promotes ketonegenesis via several mitochondrial enzymes [45], some of which can further synthesize cholesterol for cellular needs [46]. It can be speculated that, in a scenario of impaired BCAA catabolism or BCAA deprivation, the source of ketone bodies and cholesterol could shift towards IMCL, once exposed and uncoated from PLIN2 (Figure 7A,C). It is known that C2C12 myotubes are able to produce ketone bodies, especially when contracting [25] and that cholesterol is a major constituent of IMCL [47].

3.5. Setting Transcription in Cytosol?

In this study, the individual signals from cytosolic PLIN5 and PGC-1α remained unaltered after BCAA deprivation. Nevertheless, the same experiment led to an increase in the cytosolic association between these markers (Section 2.5), often with very clearly colocalizing aggregates (Figure 7B). The same two proteins are known to interact, even if not directly binding [17]. Moreover, PGC-1α can interact with nuclear receptors, such as estrogen-related receptor α (ERRα) and sirtuin 1 (SIRT1), which have also been shown to be present in cytosolic pools [48,49] (Figure 7C). Interestingly, PGC-1α-mediated upregulation of BCAA metabolism does require ERRα [20], whose activation is dependent on cholesterol [50].

The relationship between cytosolic ERRα-PGC-1α-SIRT1-PLIN5-IMCL complexes and BCAA availability is unclear. It is possible that, through PLIN5 coordination, cytosolic IMCL could provide cholesterol and MUFAs to ERRα and SIRT1, respectively (Figure 7C), thus triggering the translocation to nuclei and consequent activation of transcription factors. In fact, we observed that, under Normal BCAA, EPS led to an increased triple association between cytosolic PGC-1α-PLIN5-IMCL (Figure S4). More research is needed to clarify the dynamics between cytosolic pools of IMCL, PLINs, and related transcription factor co-activators.

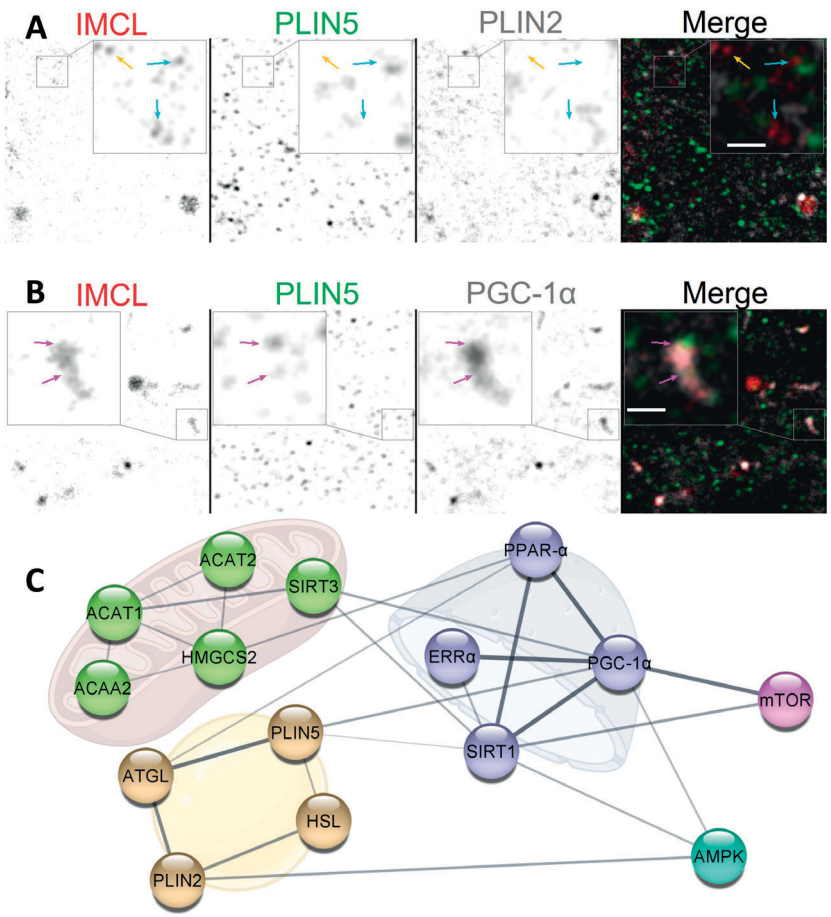

Figure 7. Potential dynamics between IMCL, PLINs and PGC-1α. (**A**) dissociating cytosolic PLIN2. Note that IMCL aggregates with no PLIN2 associated (cyan arrows) and with no PLIN association whatsoever (orange arrow); (**B**) cytosolic association of IMCL-PLIN5-PGC-1α. Note occasional but extensive association between IMCL and PGC-1α, often colocalizing with PLIN5 (magenta arrows). Gray is signal. Bars in (**A**,**B**) = 500 nm; (**C**) physical interaction network from *STRING* databases. Golden cluster are LD proteins. Green clusters are mitochondrial enzymes involved in BCAA degradation and cholesterol biosynthesis. Purple clusters are nuclear proteins involved in transcription. Cyan positively responds to exercise. Pink positively responds to BCAA availability. Line thickness indicates the strength of data support. See the end of document for abbreviations.

3.6. Nuclear Affairs

Gallardo-Montejano et al. have demonstrated that catecholamine and fasting causes phosphorylation of PLIN5 and its translocation to nuclei, promoting PGC-1α activation via SIRT1 disinhibition [17]. The same authors hypothesized that exercise would cause a similar response. Our results support this hypothesis, as we unprecedentedly showed that, in response to EPS, PLIN5 does enrich myotube nuclei, further associating with PGC-1α (Section 2.5). More recently, Natj et al. elegantly demonstrated that PLIN5's role in activating SIRT1-PGC-1α occurs via MUFAs binding and chaperoning from LDs towards the nuclei [18]. Although we observed an increase in both IMCL-PLIN5 and PGC-1α-PLIN5 associations in the nuclei, we did not observe any changes in IMCL-PGC-1α nuclear association (Figure S4). This suggests that the delivery of MUFAs by PLIN5 does not require close proximity between nuclear IMCL and PGC-1α aggregates, and that nuclear IMCL-PLIN5 association possibly has further roles to be explored.

Independent of EPS, we have observed a very sharp decline in nuclear PGC-1α after BCAA deprivation (Section 2.5). This may indicate that the function of PGC-1α as a

nuclear transcription factor co-activator becomes hampered by BCAA deprivation. This is consistent with the decreases in lipid oxidation and lipogenesis we have previously observed from the same setup and experiment [39]. The precise mechanism behind such strong effects cannot be demonstrated by our study, but BCAAs are known inducers of the mammalian target of rapamycin complex 1 (mTORC1) [51], which in turn is an important activator of PGC-1α [52] (Figure 7B).

Lastly, LDs and other PLINs have also been reported from nuclei. While nuclear PLIN3 and PLIN5 were shown abundant, nuclear PLIN2 has been reported as virtually absent and largely unresponsive [17,53]. Our results corroborate the latter observation (Section 2.3). However, we observed that, when electrically stimulated, PLIN2 increasingly associates with PLIN5 in myotube nuclei, especially if deprived from BCAA (Section 2.4). Although it is believed that PLIN2 and PLIN5 do not bind each other [17,54], their spatial correlation under such stimuli may indicate some level of indirect interaction, leading to possible changes in the metabolic status. Future research is needed on potential coordinating roles between the different PLINs within nuclei.

3.7. Limitations and Strengths

Although a strong model to study effects of physical activity even in small cohorts [24,55], the number of twins and respective fibers were relatively small, especially for studying such dynamic events which tend to be very variable between cells. Despite this limitation, concerning IMCL and PLINs, this is the first study showing the effects of life-long physical activity in genetically similar humans, bringing additional insights to the area.

While it is our strength that we have two very different models of physical activity/exercise, the C2C12 and twin models used in this study should not be directly compared. In addition, the current C2C12 experimental model may be too glycolytic for robust IMCL metabolism studies. However, knowing that undifferentiated myoblasts are too far removed from muscle biology, we were able to classify and measure the signal from myotubes exclusively (Figure S6), producing novel observations. Nevertheless, future studies should try to replicate the same observations in other cell models, such as FACS sorted myofibers or satellite cells.

One of the focuses of this work was to investigate if BCAA deprivation would affect IMCL, PLINs and PGC-1α, thus establishing this unexplored link. We have not, however, studied the effects of BCAA over-supplementation on these markers and, therefore, this should be addressed in future research.

Moreover, given the suboptical nature of diffused biomolecules, we preferred to focus on overall signal intensity rather than solely on thresholded objects—hence, for instance, the focus on the term IMCL, more inclusive and not limited to LDs or TAG. With the current instruments, we could have confidently segmented the brighter marker aggregates of about ø 1 µm, but by doing so, we would be discarding precious information coming from smaller or more diffused aggregates (Figure 7A).

In our study, we cannot strictly pertain to protein–protein or IMCL–protein binding interactions, something that could be aided by fluorescence resonance energy transfer, cell fractionation or immunoprecipitation. Instead, we conducted ICA on distinct tissue and intracellular compartments, allowing us to investigate the distribution and spatial correlation between multiple markers, some of which are not immunopercepitable. Even when two given biomolecules do not directly bind, the statistical correlation between their signals can inform us about regions where such markers could—either directly or indirectly—associate and co-act on given signaling phenomena [16,56].

4. Materials and Methods

4.1. Human Twin Pairs

A total of 8 participants from 4 same-sex twins pairs (2 male and 2 female) with discordant leisure time physical activity (LTPA) for 32 years were identified from the Finnish Twin Cohort (Table 1). Discordance was based on a series of structured questions

concerning leisure activity and physical activity during journeys to and from work. The leisure time (metabolic equivalent (MET)) index was calculated by assigning a multiple of the resting metabolic rate to each form of physical activity (intensity × duration × frequency) and expressed as a sum score of leisure time MET hours per day. It is worth noting that the active twins' average LTPA score (13.8, Table 1), roughly corresponds to 1 h of running per day, for more than three decades. On the other hand, the inactive twins are not sedentary and endured basic levels of LTPA.

The study participants were advised not to exercise vigorously during the morning and two days before both of their laboratory visits (one visit for clinical examinations including exercise tests and one visit for biopsy studies). Muscle tissue samples were taken after an overnight fast between 8:00 a.m. and 10:00 a.m. under local anesthesia after skin cooling and disinfection. Using a suction technique with a Bergström's needle (ø 5 mm), the muscle biopsy was taken from *Vastus lateralis* at the midpoint between *Trochanter major* and the lateral joint line of the knee. The sample was then mounted transversely on cork with Tissue Tek™ (Miles, Elkhart, In, USA; Sakura, Cat. # 4583), and frozen rapidly (10–15 s) in isopentane (Fluka, Cat. # 59080), precooled to −160 °C in liquid nitrogen and stored at −80 °C.

For further details on participant description and recruiting procedures, see Leskinen et al. (2009, 2010) [24,55].

4.2. Myotube Experiments

Murine C2C12 myoblasts (American Type Culture Collection, ATCC, Manassas, VA, USA) were maintained in high glucose-containing Dulbecco's Modified Eagle growth medium (GM) (4.5 g · L^{-1}, DMEM, #BE12-614F, Lonza, Basel, Switzerland) supplemented with 10% (v/v) fetal bovine serum (FBS, #10270, Gibco, Rockville, MD, USA), 100U · mL^{-1} penicillin, 100 µg · mL^{-1} streptomycin (P/S, #15140, Gibco) and 2 mM L-Glutamine (#17-605E, Lonza, Basel, Switzerland). Myoblasts were seeded on 6-well plates (NunclonTM Delta; Thermo Fisher Scientific, Waltham, MA, USA). When the myoblasts reached 95–100% confluence, the cells were rinsed with phosphate-buffered saline (PBS, pH 7.4), and the GM was replaced by differentiation medium (DM) containing high glucose DMEM, 2% (v/v) horse serum (HS, 12449C, Sigma-Aldrich, St. Louis, MO, USA), 100 U · mL^{-1} and 100 µg · mL^{-1} P/S and 2 mM L-glutamine to promote differentiation into myotubes. Fresh DM was changed every second day. The cells were screened negative for mycoplasma contaminations, following manufacturer's instructions (MycoSPY Master Mix Test Kit, M020, Biontex, München, Germany). The experiments were conducted on days 5–6 post differentiation and on a duplicated way.

The myotubes on 6-well plates were acclimatized to 0.1 mM oleic acid and 1 mM L-carnitine in normal BCAA DM on the day 4 post differentiation. On the next day, the electrodes were placed directly onto the wells. The electrical stimulation (1 Hz, 2 ms, 12 V) was applied to the cells using a C-Pace pulse generator (C-Pace EM, IonOptix, Milton, MA, USA) for 24 h at 37 °C with the same protocol as described earlier [25]. As described previously, EPS was paused after 22 h and target BCAA concentrations (no BCAA or normal BCAA) were employed to investigate the interactive effects of EPS and BCAA deprivation.

The BCAA deprivation experiments were carried out for 2 h at 37 °C in high-glucose BCAA-free DM (4.5 g · L^{-1}, BioConcept, 1-26S289-I, Allschwill, Switzerland). The experimental groups were as follows: (1) cells supplemented with 0.8 mmol · L^{-1} of all BCAAs without EPS (Normal BCAA | Rest) or (2) with EPS (Normal BCAA | EPS), and (3) cells deprived (0.0 mmol · L^{-1}) of all BCAA's without EPS (No BCAA | Rest) or (4) with EPS (No BCAA | EPS).

4.3. Protein Extraction and Western Blotting

The C2C12 cells were harvested and Western blotting was conducted as previously described [25] with minor modifications. Briefly, 10 µg of total protein per samples were

loaded on 4–20% Criterion TGX Stain-Free protein gels (#5678094, Bio-Rad Laboratories, Hercules, CA, USA) and samples were separated by SDS-PAGE.

To visualize proteins using stain-free technology, the gels were activated and the proteins were transferred to the PVDF membranes. Membranes were blocked with Intercept Blocking Buffer (#927-70001, LI-COR, Lincoln, NE, USA) followed by overnight incubation at 4 °C with primary antibody (PGC-1α, 1:10,000, ab191838, Abcam, Cambridge, UK) in Intercept Blocking Buffer diluted (*v*:*v*, 1:1) with Tris-buffered saline (TBS) with 0.1% Tween-20.

Membranes were incubated with the horseradish peroxidase-conjugated secondary IgG antibody (anti-Rabbit, 1:40,000) (Jackson ImmunoResearch Laboratories, West Grove, PA, USA) in Intercept Blocking Buffer diluted (*v*:*v*, 1:1) with TBS-0.1% Tween 20. Enhanced chemiluminescence (SuperSignal west femto maximum sensitivity substrate; Pierce Biotechnology, Rockford, IL, USA) and ChemiDoc MP device (Bio-Rad Laboratories) were together used for protein visualization.

Stain free (75-250 kDA area of the lanes) was used as a loading control and for the normalization of the results.

4.4. Gene-Expression Arrays

The RNA preparation, cRNA generation and microarray hybridization procedures were used as previously described [24]. In brief, Trizol-reagent (Invitrogen, Carlsbad, CA, USA) was used to isolate total RNA from the twin muscle biopsies, which were homogenized on FastPrep FP120 apparatus (MP Biomedicals, Illkirch, France).

An Illumina RNA amplification kit (Ambion, Austin, TX, USA) was used according to the manufacturer's instructions to obtain biotinlabeled cRNA from 500 ng of total RNA.

Hybridizations to Illumina HumanWG-6 v3.0 Expression BeadChips (Illumina Inc., San Diego, CA, USA) containing probes for *PLIN2* and *PLIN5*, were performed by the Finnish DNA Microarray Center at Turku Center for Biotechnology according to the Illumina BeadStation 500× manual.

Hybridized probes were detected with Cyanin-3-streptavidin (1 µg · mL^{-1}, Amersham Biosciences, GE Healthcare, Uppsala, Sweden) using Illumina BeadArray Reader (Illumina Inc.) and BeadStudio v3 software (Illumina Inc.).

The gene expression data and the raw data sets for skeletal muscle have been deposited in the *GEO* database (https://www.ncbi.nlm.nih.gov/geo/query/acc.cgi?acc=GSE20319, accessed on 5 January 2023).

4.5. Histology

For each twin, two 8 µm cross sections were made in a cryostat at −25 °C (Leica CM 3000, Wetzlar, Germany) and collected onto 13 mm round coverslips. For the cell culture experiments, duplicate 6-well plates were used containing three 13 mm round coverslips per well. Each experimental group was measured from 18 coverslips. After the 24 h of EPS, the plates were removed from the incubator and the medium aspirated. In both the human and C2C12 experiments, the samples were immediately fixed in 4% paraformaldehyde for 15 min at room temperature (RT). After washing for 3 × 5 min with PBS, the samples were blocked with 10% goat serum (GS) in PBS-0.05% saponin (PBSap) for 30 min and then washed briefly with PBSap. Primary antibodies were diluted in 1% GS-PBSap and incubated for 1 h at RT. A 3 × 10 min wash in PBSap ensued before incubating the secondary antibodies for 1 h at RT. Excess antibody was removed with another 3 × 10 min wash in PBSap. Finally, non-immuno stains were incubated for 30 min before 2 × 10 s washed with PBS. Thorough vial mixing and smooth rocking were ensured for every incubation step in order to grant an even stain.

For the twin studies, two different quadruple staining procedures took place, each sharing as common markers: LD540 for IMCL (0.1 µg· mL^{-1}, [57]), caveolin 3 for sarcolemma (2 µg· mL^{-1}, PA1-066, Thermo Fisher Scientific) and slow myosin heavy chain (MyHC) for type I fibers (2 µg· mL^{-1}, A4.951, DSHB, University of Iowa, IA, USA). While one section

was further incubated for PLIN2 (1:200 dilution, GP47, Progen), the second section was instead incubated for PLIN5 (1:200 dilution, GP31, Progen). Respectively, the following secondary antibodies were used in combination: Alexa Fluor 405 Goat anti-Rabbit IgG (H+L), Alexa Fluor 594 Goat anti-Mouse IgG (H+L) and Alexa Fluor 488 Goat anti-Guinea Pig IgG (H+L) (Thermo Fisher Scientific).

For the C2C12 samples, a quintuple staining was performed, using 3 antibody markers: differentiated myotubes (5 µg· mL^{-1}, MF-20, DSHB), PLIN5 (1:200 dilution, GP31, Progen), plus either PLIN2 (5 µg· mL^{-1}, ab52356, Abcam) or PGC-1α (5 µg· mL^{-1}, ab191838, Abcam). Respectively, the following secondary antibodies were used in combination: Alexa Fluor 647 Donkey anti-Mouse IgG (H+L), Alexa Fluor 488 Goat anti-Guinea Pig IgG (H+L) and Alexa Fluor 594 Donkey anti-Rabbit IgG (H+L) (Thermo Fisher Scientific). Additionally, IMCL (0.1 µg· mL^{-1}, LD540, [57]) and nuclei (5 µg· mL^{-1}, DAPI, Thermo Fisher Scientific) were stained in all coverslips. Cross reactivity was successfully ruled out by carefully controlling every antibody combination.

Every coverslip was mounted on microscopy slides using Mowiol with 2.5% DABCO (Sigma-Aldrich) and left to dry for 24 h in the dark at 4 °C. Imaging took place within 48 h after mounting.

4.6. Image Acquisition

All image data were acquired on a LSM700 confocal microscope using the *ZEN black* software (Zeiss, Germany). Twin data were collected with a Plan-Apochromat 20×/0.8 objective (Zeiss, Germany), producing 2 images per participant, each image covering an area of 320.1 × 320.1 µm (voxel size = 0.31 × 0.31 × 2.4 µm). Cell data were collected with a Plan-Apochromat 63×/1.4 oil objective (Zeiss, Germany) from 3 random 203.2 × 203.2 µm confluent areas in each coverslip, producing 9 images per well and a total of 54 images per experimental group (voxel size = 0.1 × 0.1 × 1 µm).

Multi channel acquisition was achieved through the use of 4 laser lines (405, 488, 555 and 639 nm). Bleed-through was successfully avoided in each channel by manually configuring the secondary dichroic mirror position over two different photomultiplier tubes. Control samples incubated solely with secondary antibodies were used to set background values.

4.7. Image Analyses

For C2C12, the MF-20 signal was used to segment and analyze differentiated myotubes only. The nuclei detected within the segmented myotubes were also segmented, thus allowing compartmental analyses on the cytosolic versus nucleic markers. For the human cross sections, only intact and artifact-free fibers were segmented (Active = 19.3 ± 2.5 and Inactive = 15.5 ± 4.3. Mean ± SE). Segmentation was aided by machine learning algorithms using the *Trainable Weka Segmentation* tool [58] in *Fiji* [59]. Each analyzed fiber cross section was classified into either type I or type II, according to the detected and thresholded signal of slow myosin per cell area. The optical density of each marker was determined by measuring the mean value of the respective signal within each cell. The level of association between the different markers was determined through pixel-to-pixel intensity correlation analysis (ICA), by thresholding image data according to Costes et al. [16] in *Fiji*. In order to ensure a zero valued background, prior to analyses, all images were denoised and deconvoluted in *Fiji* using a theoretical point spread function separately for each channel.

4.8. Data Cleaning and Statistics

For the twin data, given the low number of participants, statistical cases are constituted of individual muscle fibers. Concerning the C2C12 data, from each coverslip, the 2 closest values per variable were averaged, while from each well, the values from the 2 closest coverslips were further averaged. To control for inter cell batch variability, all values were normalized against the control group (Normal BCAA | Rest). Finally, for both human and C2C12 studies, outliers were identified and removed via z-score (2 standard deviations).

Boxes in the boxplot figures depict interquartile ranges and medians, while whiskers represent the 95% confidence interval, unless stated otherwise. The main effect significance is marked with **#** and combined group significance is marked with *, while interacting effects between independent variables are expressed with **&**. Normality was assessed with Shapiro–Wilk tests and group comparisons were preformed with either Mann–Whitney U tests or *t*-tests, depending on data distribution. Interacting effects were tested with a two-way ANOVA. Given the large number of human muscle fibers, significance levels were set at $p < 0.01$ and $p < 0.001$. For C2C12, the significance levels were set at $p < 0.05$ and $p < 0.01$. The ICA between the different markers were tested with a Manders split coefficent test after the thresholding step mentioned in Section 4.7.

Data crunching, statistics and boxplot visualization were performed in *Python 3.9.0*, with the packages *NumPy* [60], *pandas* [61], *SciPy* [62], *statsmodels* [63], *seaborn* [64] and *matplotlib* [65], respectively. All *Fiji* and *Python* routines can be found at https://github.com/seiryoku-zenyo/twinC2C12-studies, accessed on 1 August 2022.

Comparison and analysis of mRNA data were performed with the *GEO2R* functionality on the *GEO* database (https://www.ncbi.nlm.nih.gov/geo/geo2r/?acc=GSE20319, accessed on 5 January 2023).

Protein network analysis and visualization were performed with *STRING* [66] and *Cytoscape* [67] software.

5. Conclusions

The present study expands our basic knowledge on the known link between a functional BCAA metabolism, physical activity and an efficient lipid metabolism: specifically, via PLIN2's function in coating IMCL upon BCAA availability and long-term physical activity. Moreover, we showed that PLIN5 has an ability to translocate to nuclei and associate with PGC-1α after contractions.

Supplementary Materials: The following supporting information can be downloaded at: www.mdpi.com/xxx/s1.

Author Contributions: V.F. interpreted the data and wrote the manuscript. H.K., U.K., M.S. and V.F. designed the study experiments. U.-M.S. was responsible for cell culture, EPS-BCAA experiments and Western blots. Immunohistochemistry and microscopy were carried by V.F. and P.R. Bioinformatics was carried out by V.F., J.J.H. and R.K. supervised, and V.F. helped with writing the manuscript. All authors have read and agreed to the published version of the manuscript.

Funding: This study was supported by the Academy of Finland (grants 132987, 298875 and 114866). The author V.F. acknowledges his FCT grant SFRH/BD/68308/2010.

Institutional Review Board Statement: This study was conducted according to good clinical and scientific practice/guidelines and the Declaration of Helsinki. The ethics committee of the Central Hospital of Central Finland approved our study plan on 15 August 2006.

Informed Consent Statement: Informed written consent was obtained from all participants involved in the study.

Data Availability Statement: Data are available upon request. All *ImageJ* and *Python* routines can be found at https://github.com/seiryoku-zenyo/twinC2C12-studies, accessed on 1 August 2022.

Acknowledgments: We would like to acknowledge Juulia Lautaoja and Emilia Kettunen for their crucial instructions concerning cell culture methodologies. We would also like to thank Ma Hongqiang for the help with image acquisition. We acknowledge the use of BioRender.com, accessed on 1 August 2022 in producing the art illustrations.

Conflicts of Interest: The authors declare that there are no conflicts of interest associated with this manuscript.

Abbreviations

The following abbreviations are used in this manuscript:

ACAA2	Acetyl-Coenzyme A acyltransferase 2
ACAT1	Acetyl-CoA acetyltransferase, mitochondrial
ACAT2	Acetyl-CoA acetyltransferase, cytosolic
ATGL	Adipose triglyceride lipase
BCAA	Branched-chain amino acids
EPS	Electrical pulse stimulation
ERRα	Estrogen-related receptor alpha
HMGCS2	3-hydroxy-3-methylglutaryl-CoA synthase 2, mitochondrial
HSL	Hormone-sensitive lipase
ICA	Intensity correlation analysis
IMCL	Intramyocellular lipids
LDs	Lipid droplets
LTPA	Leisure time physical activity
mTORC1	Mammalian target of rapamycin complex 1
MUFAs	Monounsaturated fatty acids
MyHC	Myosin heavy chain
PGC-1α	Peroxisome proliferator-activated receptor gamma coactivator 1-alpha
PLIN2	Perilipin 2
PLIN3	Perilipin 3
PLIN5	Perilipin 5
PLINs	Perilipin protein family
PPAR-α	Peroxisome proliferator-activated receptor alpha
SIRT1	Sirtuin 1
SIRT3	Sirtuin 3
TAG	Triacylglycerol

References

1. Pedersen, B.K. Muscle as a Secretory Organ. In *Comprehensive Physiology*; John Wiley & Sons, Ltd.: Hoboken, NJ, USA, 2013; pp. 1337–1362. [CrossRef]
2. Goodpaster, B.H.; He, J.; Watkins, S.; Kelley, D.E. Skeletal Muscle Lipid Content and Insulin Resistance: Evidence for a Paradox in Endurance-Trained Athletes. *J. Clin. Endocrinol. Metab.* **2001**, *86*, 5755–5761. [CrossRef]
3. Moro, C.; Bajpeyi, S.; Smith, S.R. Determinants of intramyocellular triglyceride turnover: Implications for insulin sensitivity. *Am. J. Physiol. Endocrinol. Metab.* **2008**, *294*, E203–E213. [CrossRef]
4. van Loon, L.J.C.; Koopman, R.; Manders, R.; van der Weegen, W.; van Kranenburg, G.P.; Keizer, H.A. Intramyocellular lipid content in type 2 diabetes patients compared with overweight sedentary men and highly trained endurance athletes. *Am. J. Physiol. Endocrinol. Metab.* **2004**, *287*, E558–E565. [CrossRef]
5. Sztalryd, C.; Brasaemle, D.L. The perilipin family of lipid droplet proteins: Gatekeepers of intracellular lipolysis. *Biochim. Biophys. Acta Mol. Cell Biol. Lipids* **2017**, *1862*, 1221–1232. [CrossRef]
6. MacPherson, R.E.; Peters, S.J. Piecing together the puzzle of perilipin proteins and skeletal muscle lipolysis. *Appl. Physiol. Nutr. Metab.* **2015**, *40*, 641–651. [CrossRef]
7. Prats, C.; Donsmark, M.; Qvortrup, K.; Londos, C.; Sztalryd, C.; Holm, C.; Galbo, H.; Ploug, T. Decrease in intramuscular lipid droplets and translocation of HSL in response to muscle contraction and epinephrine. *J. Lipid Res.* **2006**, *47*, 2392–2399. [CrossRef]
8. Whytock, K.; Shepherd, S.; Wagenmakers, A.; Strauss, J. Hormone sensitive lipase preferentially redistributes to perilipin-5 lipid droplets in human skeletal muscle during moderate-intensity exercise. *J. Physiol.* **2018**, *596*, 2077–2090. [CrossRef]
9. Unraveling the roles of PLIN5: Linking cell biology to physiology. *Trends Endocrinol. Metab.* **2015**, *26*, 144–152. [CrossRef]
10. Gemmink, A.; Bosma, M.; Kuijpers, H.J.; Hoeks, J.; Schaart, G.; van Zandvoort, M.A.; Schrauwen, P.; Hesselink, M.K. Decoration of intramyocellular lipid droplets with PLIN5 modulates fasting-induced insulin resistance and lipotoxicity in humans. *Diabetologia* **2016**, *59*, 1040–1048. [CrossRef]
11. Gemmink, A.; Daemen, S.; Brouwers, B.; Hoeks, J.; Schaart, G.; Knoops, K.; Schrauwen, P.; Hesselink, M.K. Decoration of myocellular lipid droplets with perilipins as a marker for in vivo lipid droplet dynamics: A super-resolution microscopy study in trained athletes and insulin resistant individuals. *Biochim. Biophys. Acta Mol. Cell Biol. Lipids* **2021**, *1866*, 158852. [CrossRef]
12. Gemmink, A.; Daemen, S.; Brouwers, B.; Huntjens, P.R.; Schaart, G.; Moonen-Kornips, E.; Jörgensen, J.; Hoeks, J.; Schrauwen, P.; Hesselink, M.K.C. Dissociation of intramyocellular lipid storage and insulin resistance in trained athletes and type 2 diabetes patients; involvement of perilipin 5? *J. Physiol.* **2018**, *596*, 857–868. [CrossRef]

13. Shepherd, S.O.; Cocks, M.; Tipton, K.D.; Ranasinghe, A.M.; Barker, T.A.; Burniston, J.G.; Wagenmakers, A.J.M.; Shaw, C.S. Sprint interval and traditional endurance training increase net intramuscular triglyceride breakdown and expression of perilipin 2 and 5. *J. Physiol.* **2013**, *591*, 657–675. [CrossRef]
14. Shaw, C.S.; Sherlock, M.; Stewart, P.M.; Wagenmakers, A.J. Adipophilin distribution and colocalisation with lipid droplets in skeletal muscle. *Histochem. Cell Biol.* **2009**, *131*, 575–581. [CrossRef]
15. Koh, H.C.E.; Ørtenblad, N.; Winding, K.M.; Hellsten, Y.; Mortensen, S.P.; Nielsen, J. High-intensity interval, but not endurance, training induces muscle fiber type-specific subsarcolemmal lipid droplet size reduction in type 2 diabetic patients. *Am. J. Physiol. Endocrinol. Metab.* **2018**, *315*, E872–E884. [CrossRef]
16. Costes, S.V.; Daelemans, D.; Cho, E.H.; Dobbin, Z.; Pavlakis, G.; Lockett, S. Automatic and quantitative measurement of protein-protein colocalization in live cells. *Biophys. J.* **2004**, *86*, 3993–4003. [CrossRef]
17. Gallardo-Montejano, V.I.; Saxena, G.; Kusminski, C.M.; Yang, C.; McAfee, J.L.; Hahner, L.; Hoch, K.; Dubinsky, W.; Narkar, V.A.; Bickel, P.E. Nuclear Perilipin 5 integrates lipid droplet lipolysis with PGC-1α/SIRT1-dependent transcriptional regulation of mitochondrial function. *Nat. Commun.* **2016**, *7*, 12723. [CrossRef]
18. Najt, C.P.; Khan, S.A.; Heden, T.D.; Witthuhn, B.A.; Perez, M.; Heier, J.L.; Mead, L.E.; Franklin, M.P.; Karanja, K.K.; Graham, M.J.; et al. Lipid Droplet-Derived Monounsaturated Fatty Acids Traffic via PLIN5 to Allosterically Activate SIRT1. *Mol. Cell* **2020**, *77*, 810–824.e8. [CrossRef]
19. Hatazawa, Y.; Tadaishi, M.; Nagaike, Y.; Morita, A.; Ogawa, Y.; Ezaki, O.; Takai-Igarashi, T.; Kitaura, Y.; Shimomura, Y.; Kamei, Y.; et al. PGC-1α-Mediated Branched-Chain Amino Acid Metabolism in the Skeletal Muscle. *PLoS ONE* **2014**, *9*, e91006. [CrossRef]
20. Sjögren, R.J.; Rizo-Roca, D.; Chibalin, A.V.; Chorell, E.; Furrer, R.; Katayama, S.; Harada, J.; Karlsson, H.K.; Handschin, C.; Moritz, T.; et al. Branched-chain amino acid metabolism is regulated by ERRα in primary human myotubes and is further impaired by glucose loading in type 2 diabetes. *Diabetologia* **2021**, *64*, 2077–2091. [CrossRef]
21. Lerin, C.; Goldfine, A.B.; Boes, T.; Liu, M.; Kasif, S.; Dreyfuss, J.M.; De Sousa-Coelho, A.L.; Daher, G.; Manoli, I.; Sysol, J.R.; et al. Defects in muscle branched-chain amino acid oxidation contribute to impaired lipid metabolism. *Mol. Metab.* **2016**, *5*, 926–936. [CrossRef]
22. Kainulainen, H.; Hulmi, J.J.; Kujala, U.M. Potential role of branched-chain amino acid catabolism in regulating fat oxidation. *Exerc. Sport Sci. Rev.* **2013**, *41*, 194–200. [CrossRef]
23. Nye, C.K.; Hanson, R.W.; Kalhan, S.C. Glyceroneogenesis is the dominant pathway for triglyceride glycerol synthesis in vivo in the rat. *J. Biol. Chem.* **2008**, *283*, 27565–27574. [CrossRef]
24. Leskinen, T.; Rinnankoski-Tuikka, R.; Rintala, M.; Seppänen-Laakso, T.; Pöllänen, E.; Alen, M.; Sipilä, S.; Kaprio, J.; Kovanen, V.; Rahkila, P.; et al. Differences in Muscle and Adipose Tissue Gene Expression and Cardio-Metabolic Risk Factors in the Members of Physical Activity Discordant Twin Pairs. *PLoS ONE* **2010**, *5*, e12609. [CrossRef]
25. Lautaoja, J.H.; O'Connell, T.M.; Mäntyselkä, S.; Peräkylä, J.; Kainulainen, H.; Pekkala, S.; Permi, P.; Hulmi, J.J. Higher glucose availability augments the metabolic responses of the C2C12 myotubes to exercise-like electrical pulse stimulation. *Am. J. Physiol. Endocrinol. Metab.* **2021**, *321*, E229–E245. [CrossRef]
26. Nikolić, N.; Bakke, S.S.; Kase, E.T.; Rudberg, I.; Halle, I.F.; Rustan, A.C.; Thoresen, G.H.; Aas, V. Correction: Electrical Pulse Stimulation of Cultured Human Skeletal Muscle Cells as an In Vitro Model of Exercise. *PLoS ONE* **2013**, *8*, e33203. . [CrossRef]
27. Kankaanpää, A.; Tolvanen, A.; Bollepalli, S.; Leskinen, T.; Kujala, U.M.; Kaprio, J.; Ollikainen, M.; Sillanpää, E. Leisure-time and occupational physical activity associates differently with epigenetic aging. *Med. Sci. Sport. Exerc.* **2021**, *53*, 487. [CrossRef]
28. Ko, K.; Woo, J.; Bae, J.Y.; Roh, H.T.; Lee, Y.H.; Shin, K.O. Exercise training improves intramuscular triglyceride lipolysis sensitivity in high-fat diet induced obese mice. *Lipids Health Dis.* **2018**, *17*, 81. [CrossRef]
29. Ramos, S.V.; MacPherson, R.E.K.; Turnbull, P.C.; Bott, K.N.; LeBlanc, P.; Ward, W.E.; Peters, S.J. Higher PLIN5 but not PLIN3 content in isolated skeletal muscle mitochondria following acute in vivo contraction in rat hindlimb. *Physiol. Rep.* **2014**, *2*, e12154. [CrossRef]
30. Rinnankoski-Tuikka, R.; Hulmi, J.J.; Torvinen, S.; Silvennoinen, M.; Lehti, M.; Kivelä, R.; Reunanen, H.; Kujala, U.M.; Kainulainen, H. Lipid droplet-associated proteins in high-fat fed mice with the effects of voluntary running and diet change. *Metabolism* **2014**, *63*, 1031–1040. [CrossRef]
31. Bosma, M.; Hesselink, M.K.; Sparks, L.M.; Timmers, S.; Ferraz, M.J.; Mattijssen, F.; van Beurden, D.; Schaart, G.; de Baets, M.H.; Verheyen, F.K.; et al. Perilipin 2 improves insulin sensitivity in skeletal muscle despite elevated intramuscular lipid levels. *Diabetes* **2012**, *61*, 2679–2690. [CrossRef]
32. Bonen, A.; Luiken, J.; Liu, S.; Dyck, D.; Kiens, B.; Kristiansen, S.; Turcotte, L.; Van Der Vusse, G.; Glatz, J. Palmitate transport and fatty acid transporters in red and white muscles. *Am. J. Physiol. Endocrinol. Metab.* **1998**, *275*, E471–E478. [CrossRef]
33. Fachada, V.; Rahkila, P.; Fachada, N.; Turpeinen, T.; Kujala, U.M.; Kainulainen, H. Enlarged PLIN5-uncoated lipid droplets in inner regions of skeletal muscle type II fibers associate with type 2 diabetes. *Acta Histochem.* **2022**, *124*, 151869. [CrossRef]
34. Yang, B.; Yu, Q.; Chang, B.; Guo, Q.; Xu, S.; Yi, X.; Cao, S. MOTS-c interacts synergistically with exercise intervention to regulate PGC-1α expression, attenuate insulin resistance and enhance glucose metabolism in mice via AMPK signaling pathway. *Biochim. Biophys. Acta Mol. Basis Dis.* **2021**, *1867*, 166126. [CrossRef]
35. Philp, A.; Belew, M.Y.; Evans, A.; Pham, D.; Sivia, I.; Chen, A.; Schenk, S.; Baar, K. The PGC-1α-related coactivator promotes mitochondrial and myogenic adaptations in C2C12 myotubes. *Am. J. Physiol. Regul. Integr. Comp. Physiol.* **2011**, *301*, R864–R872. [CrossRef]

36. Melouane, A.; Yoshioka, M.; Kanzaki, M.; St-Amand, J. Sparc, an EPS-induced gene, modulates the extracellular matrix and mitochondrial function via ILK/AMPK pathways in C2C12 cells. *Life Sci.* **2019**, *229*, 277–287. . [CrossRef]
37. Lee, I.H.; Lee, Y.J.; Seo, H.; Kim, Y.S.; Nam, J.O.; Jeon, B.D.; Kwon, T.D. Study of muscle contraction induced by electrical pulse stimulation and nitric oxide in C2C12 myotube cells. *J. Exerc. Nutr. Biochem.* **2018**, *22*, 22. [CrossRef]
38. Finck, B.N.; Kelly, D.P. PGC-1 coactivators: Inducible regulators of energy metabolism in health and disease. *J. Clin. Investig.* **2006**, *116*, 615–622. [CrossRef]
39. Karvinen, S.; Fachada, V.; Sahinaho, U.M.; Pekkala, S.; Lautaoja, J.H.; Mäntyselkä, S.; Permi, P.; Hulmi, J.J.; Silvennoinen, M.; Kainulainen, H. Branched-Chain Amino Acid Deprivation Decreases Lipid Oxidation and Lipogenesis in C2C12 Myotubes. *Metabolites* **2022**, *12*, 328. [CrossRef]
40. Son, Y.H.; Lee, S.M.; Lee, S.H.; Yoon, J.H.; Kang, J.S.; Yang, Y.R.; Kwon, K.S. Comparative molecular analysis of endurance exercise in vivo with electrically stimulated in vitro myotube contraction. *J. Appl. Physiol.* **2019**, *127*, 1742–1753. [CrossRef]
41. Philp, A.; Perez-Schindler, J.; Green, C.; Hamilton, D.L.; Baar, K. Pyruvate suppresses PGC1α expression and substrate utilization despite increased respiratory chain content in C2C12 myotubes. *Am. J. Physiol. Cell Physiol.* **2010**, *299*, C240–C250. [CrossRef]
42. Brown, D.M.; Parr, T.; Brameld, J.M. Myosin heavy chain mRNA isoforms are expressed in two distinct cohorts during C2C12 myogenesis. *J. Muscle Res. Cell Motil.* **2012**, *32*, 383–390. [CrossRef] [PubMed]
43. McIntosh, A.L.; Senthivinayagam, S.; Moon, K.C.; Gupta, S.; Lwande, J.S.; Murphy, C.C.; Storey, S.M.; Atshaves, B.P. Direct interaction of Plin2 with lipids on the surface of lipid droplets: A live cell FRET analysis. *Am. J. Physiol. Cell Physiol.* **2012**, *303*, C728–C742. [CrossRef] [PubMed]
44. Zhao, H.; Zhang, F.; Sun, D.; Wang, X.; Zhang, X.; Zhang, J.; Yan, F.; Huang, C.; Xie, H.; Lin, C.; et al. Branched-chain amino acids exacerbate obesity-related hepatic glucose and lipid metabolic disorders via attenuating Akt2 signaling. *Diabetes* **2020**, *69*, 1164–1177. [CrossRef] [PubMed]
45. Kim, S.; Jeon, J.M.; Kwon, O.K.; Choe, M.S.; Yeo, H.C.; Peng, X.; Cheng, Z.; Lee, M.Y.; Lee, S. Comparative Proteomic Analysis Reveals the Upregulation of Ketogenesis in Cardiomyocytes Differentiated from Induced Pluripotent Stem Cells. *Proteomics* **2019**, *19*, 1800284. [CrossRef] [PubMed]
46. Halama, A.; Horsch, M.; Kastenmüller, G.; Möller, G.; Kumar, P.; Prehn, C.; Laumen, H.; Hauner, H.; Hrabě de Angelis, M.; Beckers, J.; et al. Metabolic switch during adipogenesis: From branched chain amino acid catabolism to lipid synthesis. *Arch. Biochem. Biophys.* **2016**, *589*, 93–107. Applications of Metabolomics. [CrossRef]
47. Itabe, H.; Yamaguchi, T.; Nimura, S.; Sasabe, N. Perilipins: A diversity of intracellular lipid droplet proteins. *Lipids Health Dis.* **2017**, *16*, 83. [CrossRef]
48. Rossi, M.; Colecchia, D.; Iavarone, C.; Strambi, A.; Piccioni, F.; Verrotti di Pianella, A.; Chiariello, M. Extracellular Signal-regulated Kinase 8 (ERK8) Controls Estrogen-related Receptor α (ERRα) Cellular Localization and Inhibits Its Transcriptional Activity. *J. Biol. Chem.* **2011**, *286*, 8507–8522. [CrossRef]
49. Nasrin, N.; Kaushik, V.K.; Fortier, E.; Wall, D.; Pearson, K.J.; De Cabo, R.; Bordone, L. JNK1 phosphorylates SIRT1 and promotes its enzymatic activity. *PLoS ONE* **2009**, *4*, e8414. [CrossRef]
50. Wei, W.; Schwaid, A.G.; Wang, X.; Wang, X.; Chen, S.; Chu, Q.; Saghatelian, A.; Wan, Y. Ligand activation of ERRα by cholesterol mediates statin and bisphosphonate effects. *Cell Metab.* **2016**, *23*, 479–491. [CrossRef]
51. Neishabouri, S.H.; Hutson, S.; Davoodi, J. Chronic activation of mTOR complex 1 by branched chain amino acids and organ hypertrophy. *Amino Acids* **2015**, *47*, 1167–1182. [CrossRef]
52. Cunningham, J.T.; Rodgers, J.T.; Arlow, D.H.; Vazquez, F.; Mootha, V.K.; Puigserver, P. mTOR controls mitochondrial oxidative function through a YY1–PGC-1α transcriptional complex. *Nature* **2007**, *450*, 736–740. [CrossRef]
53. Ohsaki, Y.; Kawai, T.; Yoshikawa, Y.; Cheng, J.; Jokitalo, E.; Fujimoto, T. PML isoform II plays a critical role in nuclear lipid droplet formation. *J. Cell Biol.* **2016**, *212*, 29–38. [CrossRef]
54. Gemmink, A.; Daemen, S.; Kuijpers, H.J.; Schaart, G.; Duimel, H.; López-Iglesias, C.; van Zandvoort, M.A.; Knoops, K.; Hesselink, M.K. Super-resolution microscopy localizes perilipin 5 at lipid droplet-mitochondria interaction sites and at lipid droplets juxtaposing to perilipin 2. *Biochim. Biophys. Acta Mol. Cell Biol. Lipids* **2018**, *1863*, 1423–1432. [CrossRef] [PubMed]
55. Leskinen, T.; Waller, K.; Mutikainen, S.; Aaltonen, S.; Ronkainen, P.H.A.; Alén, M.; Sipilä, S.; Kovanen, V.; Perhonen, M.; Pietiläinen, K.H.; et al. Effects of 32-Year Leisure Time Physical Activity Discordance in Twin Pairs on Health (TWINACTIVE Study): Aims, Design and Results for Physical Fitness. *Twin Res. Hum. Genet.* **2009**, *12*, 108–117. [CrossRef] [PubMed]
56. Tan, H.Y.; Qiu, Y.T.; Sun, H.; Yan, J.w.; Zhang, L. A lysosome-targeting dual-functional fluorescent probe for imaging intracellular viscosity and beta-amyloid. *Chem. Commun.* **2019**, *55*, 2688–2691. [CrossRef]
57. Spandl, J.; White, D.J.; Peychl, J.; Thiele, C. Live Cell Multicolor Imaging of Lipid Droplets with a New Dye, LD540. *Traffic* **2009**, *10*, 1579–1584. [CrossRef] [PubMed]
58. Arganda-Carreras, I.; Kaynig, V.; Rueden, C.; Eliceiri, K.W.; Schindelin, J.; Cardona, A.; Sebastian Seung, H. Trainable Weka Segmentation: A machine learning tool for microscopy pixel classification. *Bioinformatics* **2017**, *33*, 2424–2426. [CrossRef] [PubMed]
59. Schindelin, J.; Arganda-Carreras, I.; Frise, E.; Kaynig, V.; Longair, M.; Pietzsch, T.; Preibisch, S.; Rueden, C.; Saalfeld, S.; Schmid, B.; et al. Fiji: An open-source platform for biological-image analysis. *Nat. Methods* **2012**, *9*, 676–682. [CrossRef] [PubMed]
60. Harris, C.R.; Millman, K.J.; van der Walt, S.J.; Gommers, R.; Virtanen, P.; Cournapeau, D.; Wieser, E.; Taylor, J.; Berg, S.; Smith, N.J.; et al. Array programming with NumPy. *Nature* **2020**, *585*, 357–362. [CrossRef]

61. Pandas Development Team. pandas-dev/pandas: Pandas, 2020. Available online: https://doi.org/10.5281/zenodo.3509134 (accessed on 1 August 2022).
62. Virtanen, P.; Gommers, R.; Oliphant, T.E.; Haberland, M.; Reddy, T.; Cournapeau, D.; Burovski, E.; Peterson, P.; Weckesser, W.; Bright, J.; et al. SciPy 1.0: Fundamental Algorithms for Scientific Computing in Python. *Nat. Methods* **2020**, *17*, 261–272. [CrossRef]
63. Seabold, S.; Perktold, J. Statsmodels: Econometric and statistical modeling with python. In Proceedings of the 9th Python in Science Conference, Austin, TX, USA, 28 June–3 July 2010.
64. Waskom, M. The Seaborn Development Team. Mwaskom/Seaborn, 2020. Available online: http://dx.doi.org/10.5281/zenodo.592845 (accessed on 1 August 2022).
65. Hunter, J.D. Matplotlib: A 2D graphics environment. *Comput. Sci. Eng.* **2007**, *9*, 90–95. [CrossRef]
66. Szklarczyk, D.; Gable, A.L.; Lyon, D.; Junge, A.; Wyder, S.; Huerta-Cepas, J.; Simonovic, M.; Doncheva, N.T.; Morris, J.H.; Bork, P.; et al. STRING v11: Protein–protein association networks with increased coverage, supporting functional discovery in genome-wide experimental datasets. *Nucleic Acids Res.* **2018**, *47*, D607–D613. [CrossRef] [PubMed]
67. Shannon, P.; Markiel, A.; Ozier, O.; Baliga, N.S.; Wang, J.T.; Ramage, D.; Amin, N.; Schwikowski, B.; Ideker, T. Cytoscape: A software environment for integrated models of biomolecular interaction networks. *Genome Res.* **2003**, *13*, 2498–2504. [CrossRef] [PubMed]